

**UNIVERSITY OF NAPOLI  
“FEDERICO II”**

**Doctorate School in Molecular Medicine**

**Doctorate Program in  
Genetics and Molecular Medicine  
Coordinator: Prof. Lucio Nitsch  
XXIV Cycle**

**“Exploring the mechanisms involved in prion  
degradation and spreading from cell-to-cell in  
neuronal cell models”**

**Ludovica Marzo**



**Napoli 2011**

## Table of Content

<b>ABSTRACT</b> .....	<b>3</b>
<b>List of Figures</b> .....	<b>6</b>
<b>List of Tables</b> .....	<b>8</b>
<b>List of Abbreviations</b> .....	<b>9</b>
<b>INTRODUCTION</b> .....	<b>11</b>
<b>1. On the nature of prions: a brief overview</b> .....	<b>12</b>
1.1 The ‘protein-only’ hypothesis vs the ‘virino’ hypothesis .....	13
1.2 Prion protein gene .....	13
1.3 Biochemical properties of PrP <sup>Sc</sup> .....	16
1.4 Prion replication .....	18
1.5 Strains and transmission barrier .....	21
<b>2. Human and animal prion diseases</b> .....	<b>24</b>
2.1 Animal.....	25
2.1.1 <i>Scrapie</i> .....	26
2.1.2 <i>Bovine Spongiform encephalopathy</i> .....	27
2.1.3 <i>Transmissible mink encephalopathy</i> .....	28
2.1.4 <i>Chronic Wasting Disease</i> .....	28
2.2 Human.....	29
2.2.1 <i>Sporadic prion diseases</i> .....	29
2.2.2 <i>Inherited prion diseases</i> .....	30
2.2.3 <i>Acquired prion diseases</i> .....	31
<b>3. Cell biology of prion disease</b> .....	<b>33</b>
3.1 The cellular protein: PrP <sup>C</sup> .....	33
3.1.1 <i>Structure and Functions</i> .....	33
3.1.2 <i>Localization</i> .....	36
3.1.3 <i>Internalization</i> .....	38
3.1.4 <i>Trafficking</i> .....	39
3.2 PrP <sup>C</sup> to PrP <sup>Sc</sup> conversion site: a secret “ <i>rendez-vous</i> ” .....	41
3.2.1 Role of lipid rafts in prion conversion .....	45
3.3 From PrP <sup>C</sup> – PrP <sup>Sc</sup> conversion to neurotoxicity: what is the link? .....	47
3.3.1 <i>Gain of function through formation of PrP<sup>Sc</sup></i> .....	48
3.3.2 <i>Loss or subversion of PrP<sup>C</sup> function</i> .....	49
<b>4. Prion degradation: is autophagy an option?</b> .....	<b>51</b>
4.1 Molecular overview of the autophagic pathway .....	51
4.2 Autophagy and Neurodegenerative Diseases .....	56
4.3 Autophagy and Prion Disease: an open debate .....	58
<b>5. Invasion and Spreading: PrP<sup>Sc</sup> body tour</b> .....	<b>60</b>

5.1 From the periphery to the central nervous system: which is the route to follow? .....	61
5.2 Cell-to-cell spreading .....	66
<b>6. Tunneling Nanotubes (TNTs) .....</b>	<b>70</b>
6.1 Mechanism of TNTs formation .....	71
6.2 Signal and molecules involved in TNTs formation.....	74
6.3 TNTs-mediated transfer.....	76
6.4 TNTs and PrP <sup>Sc</sup> spreading .....	78
<b>7. MyoX: an unconventional molecular motor for an unconventional function?.....</b>	<b>81</b>
<b>AIMS OF THE STUDY .....</b>	<b>89</b>
<b>MATERIALS AND METHODS.....</b>	<b>94</b>
<b>RESULTS AND DISCUSSION .....</b>	<b>102</b>
<b>PROJECT 1:.....</b>	<b>103</b>
<b>Role of autophagy in <i>in vitro</i> models of prion disease ...</b>	<b>103</b>
1.1 Objectives.....	103
1.2 Specific Background .....	103
1.3 Summary of the results .....	105
1.4 Discussion.....	112
<b>ANNEXE 1:.....</b>	<b>117</b>
<b>PROJECT 2:.....</b>	<b>118</b>
<b>Characterization of PrP<sup>Sc</sup> spreading from cell-to-cell by Tunneling Nanotubes (TNTs) in a prion infected neuronal cell model.....</b>	<b>118</b>
2.1 Objectives.....	118
2.2 Results .....	118
2.3 Discussion.....	146
<b>CONCLUSIONS AND PERSPECTIVES .....</b>	<b>154</b>
<b>REFERENCES .....</b>	<b>158</b>
<b>ANNEXE 2:.....</b>	<b>187</b>

# ABSTRACT

---

## Abstract

Transmissible spongiform encephalopathies (TSE), also known as prion diseases, are fatal neurodegenerative disorders present both in human and animals with different aetiology as they can occur genetically, spontaneously or by infection (Prusiner, 1998). TSE are caused by the presence of proteinaceous aggregates, called 'prions', in brains of afflicted individuals. According to the 'protein-only' hypothesis, the central event of prion pathogenesis is the conformational change of the cellular protein, PrP<sup>C</sup>, into its pathological counterpart, PrP<sup>Sc</sup> in a process in which PrP<sup>Sc</sup> acts as a template (Prusiner, 1998). Differently from PrP<sup>C</sup>, mainly constitutes of  $\alpha$ -helices, PrP<sup>Sc</sup> is enriched in  $\beta$ -sheets, aggregation-prone and resistant to treatment with proteinase K. Despite the intense research, many questions in prion biology are still open related to both the physiological functions of PrP<sup>C</sup> and mechanism of the disease caused by the misfolded form PrP<sup>Sc</sup>. Thus, exploring some of these aspects at the molecular and cellular level is of fundamental importance for a better understanding of these fatal disorders and for developing potential therapeutical approaches. However, due to the lack of PrP<sup>Sc</sup>-specific antibodies, PrP<sup>Sc</sup> cellular trafficking, production and degradation are poorly defined.

In the first part of my thesis I investigated the role of autophagy in prion disease. I demonstrated that although autophagic pathway is stimulated by prion infection, it is not involved in prion degradation. Furthermore, I showed that tamoxifen and its metabolite 4-hydroxyl-tamoxifen (OHT) (previously shown to be autophagy inducers) reduce scrapie burden by redistributing cholesterol and PrP to lysosomes in an autophagy-independent manner. These data confirm the role of the lysosomal pathway in prion degradation and of cholesterol in prion formation. Furthermore, since tamoxifen is a wide-available pharmaceutical tool it might have potential application in therapy for prion disease.

Another important question in prion biology is related to the spreading of PrP<sup>Sc</sup>. At the different stages of its lethal journey to the central nervous system, PrP<sup>Sc</sup> is transferred from one cell to another and this passage can involve several mechanisms.

Recently our laboratory has shown that PrP<sup>Sc</sup> hijacks intercellular membranous channels, called tunneling nanotubes (TNT), for intercellular spread (Gousset et al., 2009; Langevin et al., 2010). Therefore, in the second part of my PhD work I have better characterized TNT-mediated trafficking of PrP<sup>Sc</sup> between neuronal cells, as model of prion infection. I also identified factors that could be involved in TNT formation and in the resulting transfer of PrP<sup>Sc</sup> between cells. These results will contribute to the characterization of both TNT formation and prion spreading and open the way to further investigations.

## List of Figures

FIGURE 1 VARIATION IN THE PRION PROTEIN GENE .....	15
FIGURE 2 SCHEMATIC REPRESENTATION OF HAMSTER PRNP GENE AND PRP ISOFORMS .....	16
FIGURE 3 SCHEMATIC REPRESENTATION OF THE STRUCTURES OF PrP <sup>C</sup> AND PrP <sup>Sc</sup>	17
FIGURE 4 MODEL OF PRION REPLICATION.....	19
FIGURE 5 <i>IN VITRO</i> GENERATION OF INFECTIOUS PRIONS.....	20
FIGURE 6 REPRESENTATION OF THE THREE GLYCOSYLATED PrP <sup>Sc</sup> MOIETIES .....	22
FIGURE 7 HISTOPATHOLOGICAL FEATURES ASSOCIATED WITH TSEs SHOWING SPONGIFORM DEGENERATION AND ASTROCYTIC GLIOSIS.....	24
FIGURE 8 SCRAPIE AND KURU .....	26
FIGURE 9 THE HUMAN PrP <sup>C</sup> PROTEIN AND ITS MUTANTS.....	30
FIGURE 10 PRIMARY SEQUENCE AND TERTIARY STRUCTURE OF PrP <sup>C</sup> .....	33
FIGURE 11 FUNCTIONAL CATEGORIZATION OF PUTATIVE PrP <sup>C</sup> BINDING PARTNERS	36
FIGURE 12 CELLULAR LOCALISATION AND TRAFFICKING OF PrP <sup>C</sup> AND PrP <sup>Sc</sup> .....	37
FIGURE 13 POSSIBLE SITES OF PrP <sup>C</sup> -PrP <sup>Sc</sup> CONVERSION .....	43
FIGURE 14 PrP-MEDIATE NEUROTOXICITY .....	48
FIGURE 15 DIFFERENT TYPES OF AUTOPHAGY PRESENT IN EUKARYOTIC CELLS. ...	52
FIGURE 16 LC3 AND AUTOPHAGIC VACUOLES ASSEMBLING.....	54
FIGURE 17 ROLE OF AUTOPHAGY IN DIFFERENT PHYSIOLOGICAL AND PATHOLOGICAL CONDITIONS.....	56
FIGURE 18 AUTOPHAGY IN NEURODEGENERATION.....	57
FIGURE 19 ULTRASTRUCTURAL SIGNS OF AUTOPHAGIC VACUOLATION AND APOPTOSIS IN SCGT1-TRK CELLS .....	58
FIGURE 20 DIFFERENT STAGES OF PRION INFECTION.....	61
FIGURE 21 POSSIBLE CELLS INVOLVED IN THE UPTAKE OF PRION FROM THE GUT TO THE LYMPHOID TISSUES. ....	62
FIGURE 22 SCHEMATIC REPRESENTATION OF THE PASSAGE OF TSE AGENT FROM THE GUT LUMEN TO THE PNC.....	64
FIGURE 23 POSSIBLE WAYS OF CELL-TO-CELL PRION SPREADING.....	66
FIGURE 24 SCHEMATIC REPRESENTATION OF CARGO TRANSPORTED ALONG A TNT- LIKE STRUCTURE.....	71
FIGURE 25 MODEL OF TNT FORMATION .....	72
FIGURE 26 TRANSPORT OF PrP <sup>Sc</sup> VIA TNTs, AN ALTERNATIVE SPREADING MECHANISM DURING NEUROINVASION.....	79
FIGURE 27 SCHEMATIC REPRESENTATION OF THE DIFFERENT DOMAINS OF MYOSIN-X .....	82
FIGURE 28 MYOSIN-X INTRAFILOPODIAL MOTILITY .....	84
FIGURE 29 EFFECT OF MYOSIN-X OVER-EXPRESSION AND KNOCK-DOWN.....	85
FIGURE 30 TF-LC3 TOOL. ....	106
FIGURE 32 IDENTIFICATION OF DIFFERENT SUB-CELLULAR COMPARTMENTS IN TNTs OF CAD CELLS. ....	121
FIGURE 33 COLOCALISATION BETWEEN PrP <sup>Sc</sup> AND DIFFERENT SUB-CELLULAR ORGANELLES IN TNT-LIKE STRUCTURES OF SCCAD CELLS.....	123

FIGURE 34 QUIA SOFTWARE INTERFACE .....	124
FIGURE 35 QUANTITATION OF THE COLOCALISATION BETWEEN PRP <sup>Sc</sup> AND THE DIFFERENT ORGANELLE MARKERS IN TNT STRUCTURES .....	125
FIGURE 36 EFFECT OF GFP-PRPWT OVER-EXPRESSION ON TNTS NUMBER IN CAD CELLS .....	127
FIGURE 37 SCHEMATIC OF THE DID-VESICLE TRANSFER ASSAY BY FLOW CYTOMETRY .....	128
FIGURE 38 FLOW CYTOMETRY ASSAY OF DID-VESICLE TRANSFER FROM GFP- VECTOR TRANSFECTED DONORS TO CFP-VECTOR TRANSFECTED ACCEPTORS .....	130
FIGURE 39 EFFECT OF GFP-PRPWT OVER-EXPRESSION ON DID-VESICLE TRANSFER TNT-MEDIATED IN CAD CELLS .....	131
FIGURE 40 PRP <sup>Sc</sup> INFECTION INDUCES TNT-FORMATION BY INCREASING THE NUMBER OF CONNECTED sCCAD CELLS.....	132
FIGURE 41 EFFECT OF GFP-MYO-X OVER-EXPRESSION ON BOTH TNT FORMATION AND TRANSFER OF DID-VESICLE IN CAD CELLS .....	135
FIGURE 42 DID-VESICLE TRANSFER MEDIATED BY GFP-MYO-X TRANSFECTED CELLS IS AN ACTIVE MECHANISM.....	137
FIGURE 43 EFFECT ON TNT FORMATION AND DID-VESICLE TRANSFER OF MYO-X DOWN-REGULATION IN CAD CELLS .....	138
FIGURE 44 EFFECT OF GFP-HMM-MYO-X AND GFP-HEADLESS-MYO-X ON BOTH TNT FORMATION AND DID-VESICLE TRANSFER IN CAD CELLS. ....	140
FIGURE 45 EFFECT OF GFP-MYO-X-ΔF2 AND GFP-MYO-X-ΔF3 ON TNT FORMATION AND DID-VESICLE TRANSFER IN CAD CELLS.....	142
FIGURE 46 TRANSFER OF PRP <sup>Sc</sup> VIA TNTS IN CAD CELLS BY FLUORESCENCE MICROSCOPY .....	144
FIGURE 47 EFFECT OF MYO-X OVER-EXPRESSION ON TRANSFER OF PRP <sup>Sc</sup> VIA TNTS IN CAD CELLS.....	144

## List of Tables

<b>TABLE 1</b> ANIMAL AND HUMAN PRION DISEASES. ....	25
<b>TABLE 2</b> DIFFERENT ORGANELLE MARKERS USED TO DETECT SPECIFIC SUB-CELLULAR ORGANELLES IN TNT STRUCTURES.....	120

## List of Abbreviations

AD: Alzheimer disease  
BAF A1: bafilomycin A1  
BMDC: Bone Marrow Dendritic cell  
BSE: Bovine spongiform encephalopathy  
CJD: Creutzfeldt-Jakob disease  
CMA: chaperon-mediated autophagy  
CNS: Central nervous system  
CWD: Chronic Wasting Disease  
FDC: Follicular dendritic cell  
DC: Dendritic cell  
DNA: deoxyribonucleic acid  
DRM: detergent resistant membrane  
EE: Early Endosome  
ER: endoplasmic reticulum  
ERC: Endosomal Recycling Compartment  
ERAD: ER-associated degradation system  
LYS: Lysosomes  
fCJD: familial Creutzfeldt-Jakob disease  
FDC: follicular dendritic cell  
FFI: Fatal familial insomnia  
FSE: feline spongiform encephalopathy  
GALT: gut associated lymphatic system  
Gnd-HCl: Guanidine hydrochloride  
GSS: Gerstmann-Sträussler-Scheinker syndrome  
GPI: glycosylphosphatidylinositol  
GTP: guanosine triphosphate  
HIV-1: human immunodeficiency virus 1  
HD: Huntington disease  
iCJD: iatrogenic Creutzfeldt-Jakob disease  
IHC: immunohistochemistry  
kDa: kilo Dalton  
KO: Knock down  
LDL: low-density lipoprotein  
M: molar  
mRNA: messenger RNA  
μ: micron

NaOH: sodium hydroxide  
NH<sub>4</sub>Cl: ammonium chloride  
nm: nanometer  
NPC: Niemann-Pick type C  
nvCJD: see vCJD  
OHT: 4-hydroxyl-tamoxifen  
PD: Parkinson disease  
PIPLC: phosphatidylinositol-specific phospholipase C  
PNC: peripheral nervous system  
PK: proteinase K  
PMCA: protein misfolding cyclic amplification  
Prion: proteinaceous infectious particles  
PrP<sup>C</sup>: cellular (i.e. wild type) prion protein  
PrP<sup>Sc</sup>: scrapie (i.e. infectious) prion protein  
ROS: reactive oxygen species  
SDS: sodium dodecyl sulfate  
sCJD: sporadic Creutzfeldt-Jakob disease  
TGN: trans-Golgi-network  
TAM: tamoxifen  
TME: transmissible mink encephalopathy  
TSE: transmissible spongiform encephalopathy  
TNT: tunneling nanotubes  
UK: United Kingdom  
USA: United States of America  
vCJD: variant Creutzfeldt-Jakob disease  
W: tryptophan  
WB: Western Blot

# INTRODUCTION

---

## 1. On the nature of prions: a brief overview

Transmissible spongiform encephalopathies (TSE), also known as prion diseases, are fatal neurodegenerative disorders present both in human and animals with different aetiology as they can occur genetically, spontaneously or by infection (Prusiner, 1998). It is now well accepted that they are caused by the presence of proteinaceous aggregates, called 'prions', in brains of afflicted individuals deriving from a conformational change of the cellular protein PrP<sup>C</sup>, into its pathological counterpart, PrP<sup>Sc</sup> (Prusiner, 1998). But initially, the nature of the agent was highly debated for many years (Collinge, 2001). Alper and Griffith developed the theory that some transmissible spongiform encephalopathies were caused by an infectious agent consisting solely of proteins (Alper et al., 1967; GRIFFITH, 1967). This hypothesis was formulated to explain the fact that the mysterious infectious agent causing scrapie in sheep and goats and Creutzfeldt-Jacob (CJD) disease in humans (see below, Section 2 of the Introduction) resisted to ionizing radiation and nucleases treatments, thus excluding the possibility that the infectious agent could have had a viral origin. As a follow up, in 1982 Stanley B. Prusiner and its team at the University of California in San Francisco purified the infectious agent claiming that it consisted only of proteins. They named it 'prions' (pronounced "pree-ons") from "*proteinaceous infectious particles*" that are "resistant to inactivation by most procedures that modify nucleic acid" (Prusiner, 1982). Prusiner was then awarded the Nobel Prize in Medicine in 1997 for his research on prions.

Despite the fact that this 'protein-only' hypothesis formulated by Prusiner is now widely accepted and supported by a great number of data presented in the literature (Aguzzi and Calella, 2009a; Aguzzi et al., 2008; Colby and Prusiner, 2011), other hypotheses across the years have been advanced on the nature of prions.

## 1.1 The 'protein-only' hypothesis vs the 'virino' hypothesis

An alternative to the 'protein-only' hypothesis, the 'virino' hypothesis has been proposed in part to protect the 'central dogma of biology' (Crick, 1970). It claims that prions could be actually a 'virino', or slow virus, formed by a prion specific nucleic acid associated or coated by proteins encoded by the host. Firstly proposed by Dickinson and Meikle in 1971, it is based on the discovery of a single autosomal gene, that they named sinc (for **s**crapie **i**ncubator) that control scrapie incubation period in mice. This hypothesis proposed that the gene products of each sinc allele contributed to a multimeric protein structure, which then formed a 'replication site' for the scrapie agent (Dickinson and Outram, 1988). This hypothesis could also explain the absence of inflammatory response in prion diseases (Eklund et al., 1967; Manuelidis, 2003). These small viruses would be able to escape inactivation by irradiation (Manuelidis, 2003). However, all experiments to purify a prion specific nucleic acid have failed to date (Caughey et al., 1997). Nevertheless some nucleic acids copurify with the infectious material, and in human brain-samples a highly infectious fraction containing little PrP<sup>Sc</sup> together with nucleic acids can be separated from a less infectious fraction containing the majority of PrP<sup>Sc</sup> (Akowitz et al., 1993; Sklaviadis et al., 1992). These results are in agreement with the observation that the rate of conversion of prions in vitro is higher in the presence of some DNA (Cordeiro et al., 2001) or RNA molecules (Deleault et al., 2003). Additionally, it has been recently shown that PrP<sup>C</sup> interacts with viral RNAs and is able to act as a chaperone (similar to the nucleocapsid proteins NCP7 of HIV-1) (Gabus et al., 2001a; b).

Some evidences support a role for nucleic acids in prion conversion but additional studies will be necessary to assess their possible function and role in the disease.

## 1.2 Prion protein gene

Purification of the protease-resistant core PrP<sup>27-30</sup> allowed the determination of its NH<sub>2</sub>-terminal amino acid sequence and the

following synthesis of an isocoding mixture of oligonucleotides that was subsequently used to identify incomplete PrP cDNA clones from hamster and mouse (Chesebro et al., 2005; Oesch et al., 1985).

The prion protein gene (*PRNP*) belongs to the *PRN* gene family that consists of *PRND*, encoding the Doppel protein (Moore et al., 1999), and *SPRN*, encoding Shadoo (Watts and Westaway, 2007). *PRNP* is located in the short arm of the chromosome 20 in humans and in a homologous region in mouse chromosome 2 (Colby and Prusiner, 2011). The open-reading frame (ORF), responsible for the transduction of the PrP<sup>C</sup> protein, resides in a single exon in all known mammalian prions and avian genes *PRNP* (Westaway et al., 1987). However, the gene itself comprises two to three exons that contain untranslated sequences including the promoter and termination sequence (Hsiao et al., 1989; Gabriel et al., 1992). The PrP promoter contains multiple copies of GC-rich repeats that represent a well-known binding site for the transcription factor Sp1 site driving expression in many different tissues (McKnight and Tjian, 1986). *PRNP* transcript is constitutively expressed in different tissues and especially within the brain of different animals but is highly regulated during development (Chesebro et al., 1985; Oesch et al., 1985). In addition, *PRNP* mRNA does not increase during the course of prion disease (Oesch et al., 1985).

Furthermore, high levels of similarities in the *PRNP* sequence have been found by aligning more than 40 translated sequences from different species (Colby and Prusiner, 2011). This highlights the importance of PrP<sup>C</sup> protein functions and explains why the gene has been conserved through evolution. However, variations in PrP sequences exist both between species and between individuals within species (Figure 1), thus affecting their susceptibility to prion.

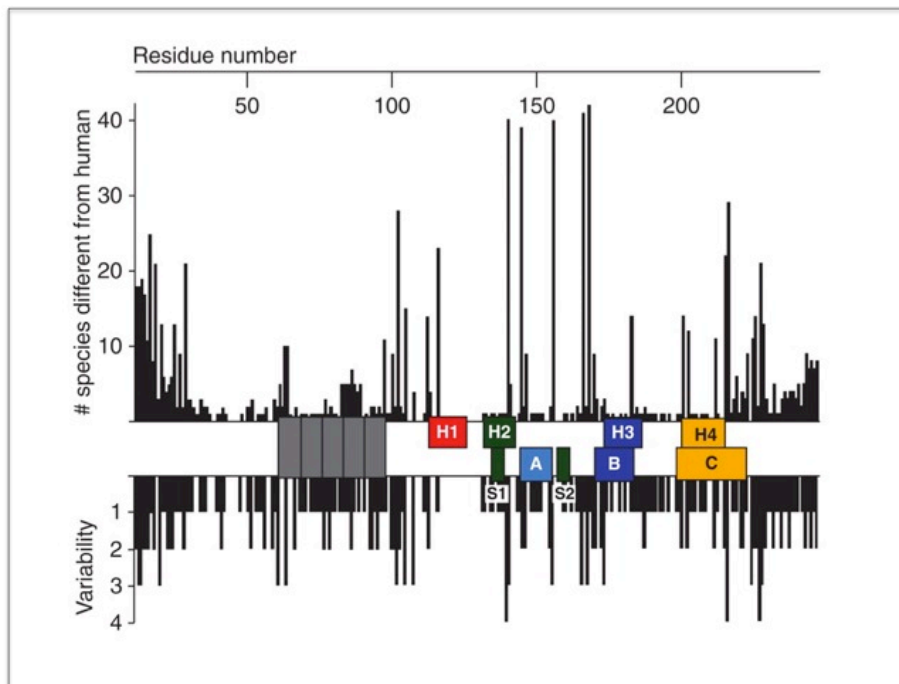


**Figure 1 Variation in the prion protein gene.** Species variations of the prion protein gene. The x-axis represents the human PrP sequence, with the five octarepeats and H1–H4 regions of the putative secondary structure shown, as well as the three  $\alpha$ -helices A, B, and C and the two  $\beta$ -strands S1 and S2 as determined by NMR. Vertical bars above the axis indicate the number of species that differ from the human sequence at each position. Below the axis, the length of the bars indicates the number of alternative amino acids at each position in the alignment. From Colby and Prusiner 2011

Besides, knock-out mice for *PRNP* gene (as *Prnp*<sup>0/0</sup>, Zürich I and *Prnp*<sup>-/-</sup>, Edinburgh) have been generated from different laboratories (Manson et al., 1994; Büeler et al., 1992). These mice are vital, do not show particular signs of alterations and develop normally. In contrast, other mice models ablated of *PRNP* did show some dysfunction, afterwards attributed to abnormal expression of Doppel and due to the technique used to engineer these mice (Moore et al., 1999; Sakaguchi et al., 1996). But, in agreement with the ‘prion-only’ hypothesis all these mice are resistant to prion infection (Aguzzi et al., 2008).

### 1.3 Biochemical properties of PrP<sup>Sc</sup>

Purified full-length PrP<sup>Sc</sup> is insoluble in non-ionic detergents and has partial protease resistance, with only the N-terminal third of the sequence being cleaved leaving a protease-resistant core, PrP<sup>27-30</sup>, which retains infectivity (Riesner, 2003). Indeed, limited protease digestion has been a convenient tool to detect PrP<sup>Sc</sup> because the same treatment fully hydrolyzes the cellular protein PrP<sup>C</sup> thus allowing the discrimination between the two forms (Figure 2).

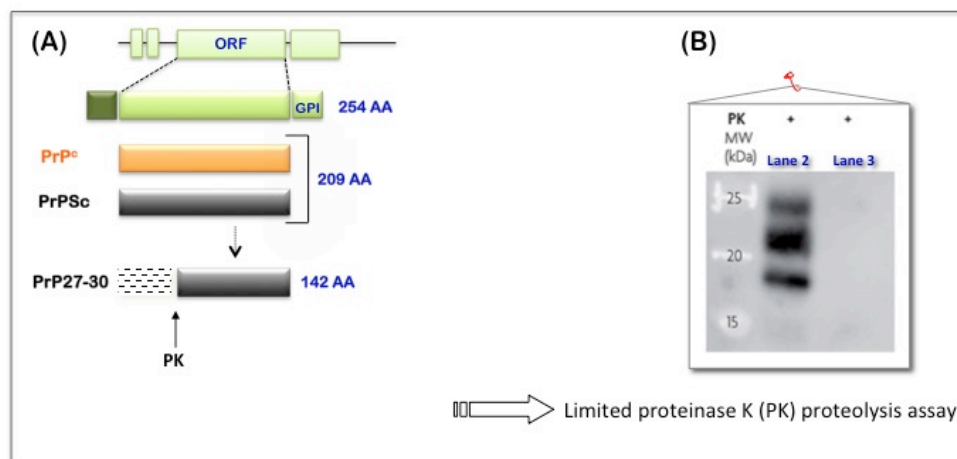


**Figure 2 Schematic representation of hamster Prnp gene and PrP isoforms.** (A) The Prnp ORF encodes a protein of 254 residues, which is shortened to 209 residues during posttranslational processing. PrP<sup>Sc</sup> is an alternate conformation of PrP<sup>C</sup> with identical primary structure. Limited proteolysis of PrP<sup>Sc</sup> cleaves the amino terminus and produces PrP 27-30, composed of approximately 142 residues. (B) Western blotting of cell lysates from prion-infected (lane 2) and uninfected (lane 3) CAD cells. Samples in lanes 2 and 3 were digested with 50 µg/µl proteinase K for 30 min at 37°C, completely hydrolyzing PrP<sup>C</sup>, thus allowing to discriminate between the two isoforms of PrP. Blot developed with anti-PrP monoclonal antibody Sha31. Modified from Prusiner 2004

Moreover, the increased propensity of PrP<sup>Sc</sup> to aggregate correlates with its resistance to PK digestion. Also, cathepsin D can digest the C-terminus of PrP<sup>Sc</sup> and liberates the glycosylphosphatidylinositol (GPI) anchor and the resulting PrP<sup>Sc</sup> fragment retains prion infectivity (Lewis et al., 2006). Besides, transgenic mice expressing PrP<sup>C</sup> lacking a GPI anchor can propagate prions (Chesebro et al., 2005), thereby suggesting that the GPI anchor - which normally attaches PrP to the

membrane (see below in section 1.4 of the Introduction) - is not a prerequisite component of the infectious prion. Unlike PrP<sup>C</sup>, which can be readily cleaved from membranes by treatment with phosphatidylinositol-specific phospholipase C (PIPLC) (Stahl et al., 1987), PrP<sup>Sc</sup> is resistant to such treatment (Caughey et al., 1990; Borchelt et al., 1993) suggesting that a conformational change prevents accessibility of PIPLC.

Structural studies by Fourier Transform Infrared Spectroscopy (FTIR) and circular dichroism have demonstrated that unlike PrP<sup>C</sup>, which is predominantly  $\alpha$ -helical, PrP<sup>Sc</sup> is highly enriched in  $\beta$ -sheets (Pan et al., 1993a; Gasset et al., 1992).  $\beta$ -sheet content in PrP<sup>Sc</sup> comprises 45% compared to 3% in PrP<sup>C</sup> (Figure 3).

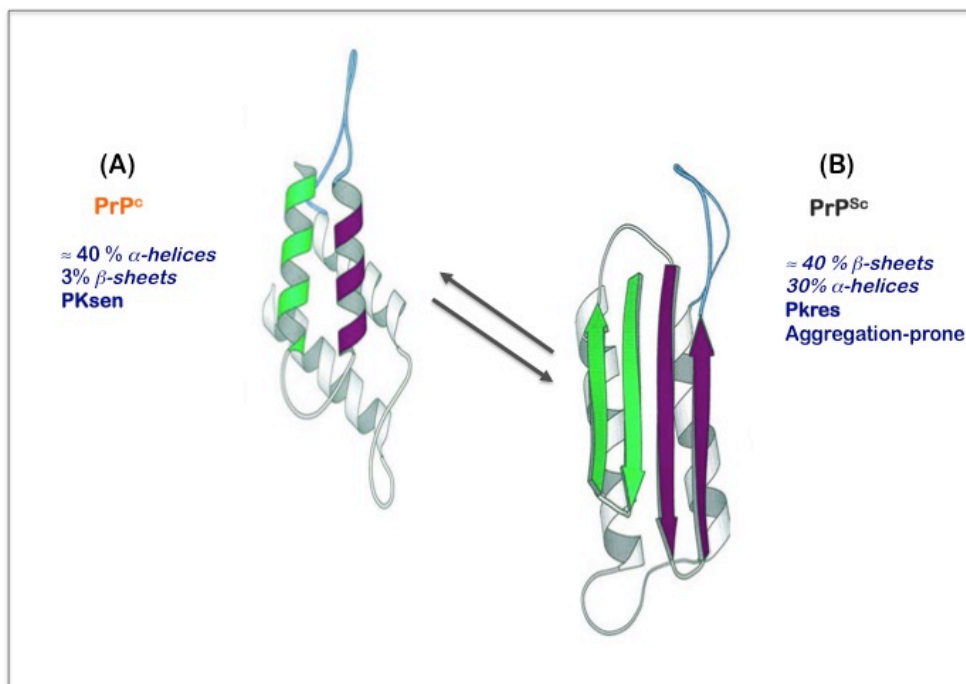


**Figure 3 Schematic representation of the structures of PrP<sup>C</sup> and PrP<sup>Sc</sup>.** Differently from PrP<sup>C</sup> (A), enriched in  $\alpha$ -helices and fully digested upon PK treatment, PrP<sup>Sc</sup> (B) is highly enriched in  $\beta$ -sheets, prone to aggregation and partially resistant to PK-digestion. (Picture from <http://www.flickr.com/photos/ajc1/with/464066753/>)

The protease-resistant core of PrP<sup>Sc</sup> has been shown to rearrange into amyloid rods, which stain with Congo red and show green-gold birefringence, typical of amyloids (Prusiner et al., 1983). Interestingly, PrP<sup>Sc</sup> deposits of varying sizes and

morphologies, including amyloid plaques, have been identified in scrapie-infected animal brain tissues (Merz et al., 1981). Nonetheless, no experimental evidence supports the presence of fibrils in human prion disease (Budka, 2003), although studies using synthetic fibrils have provided some insight into prion conformation (Tattum et al., 2006; Baskakov et al., 2002). Furthermore, although the nature of the self-propagating infectious agent is unknown, recent studies have demonstrated that small PrP oligomers of 14-28 molecules were maximally infective when compared to monomeric or fibrillar PrP (Silveira et al., 2005).

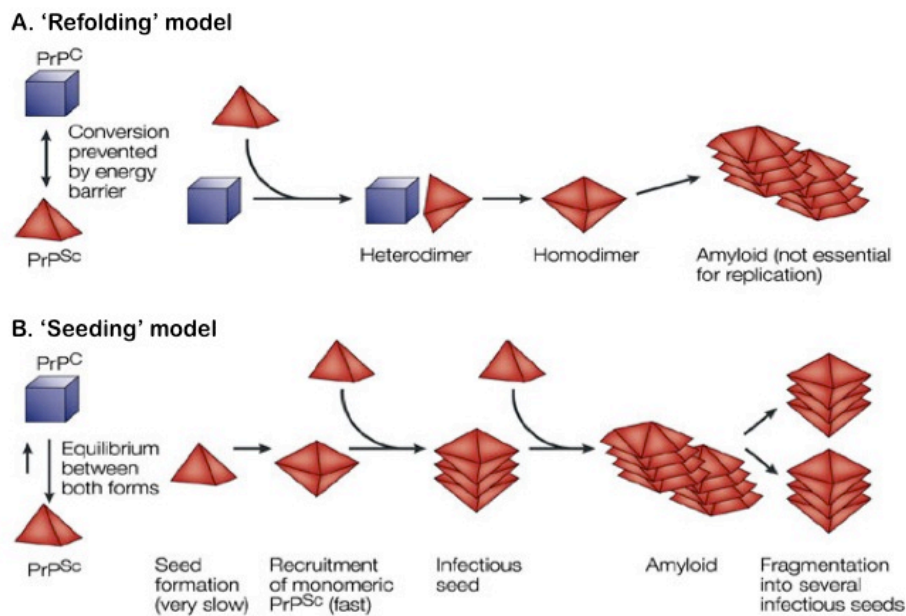
#### 1.4 Prion replication

The use of transgenic mouse models has also provided genetic and biochemical evidences that the conversion of PrP<sup>C</sup> to PrP<sup>Sc</sup> needs the formation of a PrP<sup>C</sup>-PrP<sup>Sc</sup> complex in which probably PrP<sup>C</sup> is present in a partial unfolded state, named PrP\* (PrP star) (Prusiner et al., 1990a; Meier et al., 2003). However, such a complex has never been isolated and this raises the possibility that one or more additional factors (generally termed as protein X) can be required for the conversion process (Prusiner, 1998). Indeed, supporting data towards the presence of other factors essential in prion conversion have shown that incubation of purified PrP<sup>C</sup> and PrP<sup>Sc</sup> does not allow prion replication (Soto et al., 2002). Also, addition of the bulk of cellular protein, restore the conversion process, thus providing direct evidence that other factors present in the brain are essential to catalyze prion propagation .

In addition, differences in the amino acidic sequence can influence the conversion efficiency (Scott et al., 1989) and also different levels of PrP<sup>C</sup> can be directly proportional to the rate of PrP<sup>Sc</sup> formation and this inversely to the length of the incubation time (Soto et al., 2002). In some cases, the conversion process itself is impaired, a phenomenon known as 'transmission barrier' (see below in the paragraph 1.5).

Two different conformational conversion models have been proposed to explain the phenomenon: the 'template-directed

refolding' model (Prusiner, 1998) and the 'seeded nucleation' model (Jarrett and Lansbury, 1993). In the 'template-directed refolding' PrP<sup>C</sup> to PrP<sup>Sc</sup> conversion would occur through "instructions" given by PrP<sup>Sc</sup> to PrP<sup>C</sup> in order to change the structure of the latter (Figure 4, A) in the pathological conformer of the protein.



Nature Reviews | Immunology

**Figure 4 Model of prion replication.** (A) The 'refolding' or template-directed assistance model postulates an interaction between exogenously introduced disease-associated prion protein (PrP<sup>Sc</sup>) and endogenous cellular prion protein (PrP<sup>C</sup>), which is induced to transform itself into more PrP<sup>Sc</sup>. A high-energy barrier might prevent the spontaneous conversion of PrP<sup>C</sup> to PrP<sup>Sc</sup>. (B) The 'seeding' or nucleation–polymerization model proposes that PrP<sup>C</sup> and PrP<sup>Sc</sup> are in a reversible thermodynamic equilibrium. So, only if several monomeric PrP<sup>Sc</sup> molecules are mounted in a highly ordered seed can more monomeric PrP<sup>Sc</sup> be recruited and eventually aggregate to form amyloid. In such a crystal-like seed, PrP<sup>Sc</sup> becomes stabilized. Fragmentation of PrP<sup>Sc</sup> aggregates increases the number of nuclei, which can recruit more PrP<sup>Sc</sup>, and so seems to result in replication of the agent. In sporadic prion disease, fluctuations in the local PrP<sup>C</sup> concentration might (exceptionally rarely) trigger spontaneous seeding and self-propagating prion replication. *From Aguzzi et al 2001*

On the other hand, the 'seeded nucleation' model proposes that PrP<sup>Sc</sup> could exist in equilibrium with PrP<sup>C</sup> shifted towards PrP<sup>C</sup> under physiological conditions. However the intrinsic instability of PrP<sup>Sc</sup> could lead to aggregation of this conformer in more stable 'seeds' that are prone to incorporate other monomers, thus

shifting the equilibrium towards an accumulation of the pathological isoform PrP<sup>Sc</sup> (Figure 4, B). A precise knowledge of both PrP<sup>C</sup> and PrP<sup>Sc</sup> structural features is necessary to support one or the other hypothesis. While both high-resolution nuclear magnetic resonance (NMR) and crystallographic structures are available for PrP<sup>C</sup>, a high-resolution 3D structure for PrP<sup>Sc</sup> is still missing, thus slowing down the progress in the study of the conversion mechanism (Aguzzi and Polymenidou, 2004). Recently, an *in vitro* prion conversion system called PMCA (protein misfolding cyclic amplification) in a cell-free environment has been developed to mimic PrP<sup>Sc</sup> autocatalytic replication in the presence of excess of PrP<sup>C</sup> and a minute quantity of PrP<sup>Sc</sup> (Castilla et al., 2008, 2005). In the amplification process, developed by Castilla *and colleagues*, PrP<sup>Sc</sup> aggregates formed by the conversion of PrP<sup>C</sup> are subsequently disrupted by sonication in smaller ‘seeds’ that are then reused in further cycles of conversion (Figure 5) (Soto et al., 2006).

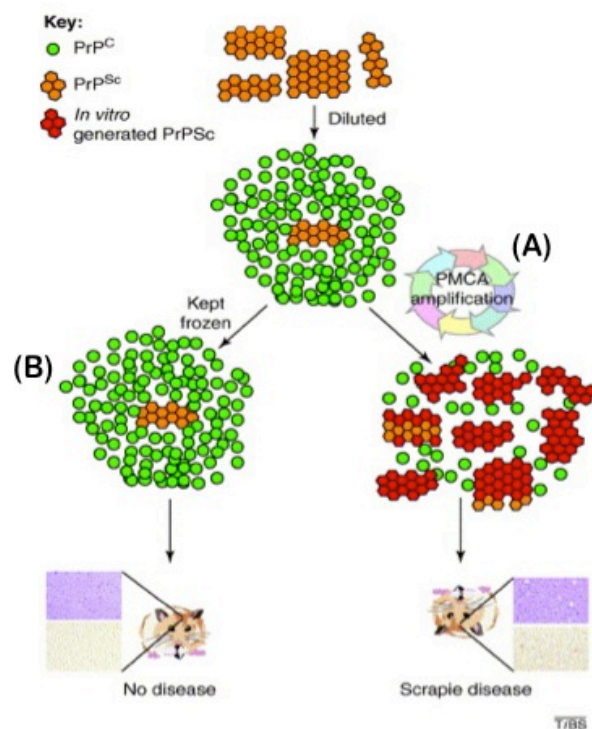


**Figure 5 *In vitro* generation of infectious prions.** Subjecting a solution of highly diluted brain-derived PrP<sup>Sc</sup> in an excess of PrP<sup>C</sup> to many cycles of protein misfolding cyclic amplification (PMCA) resulted in amplification of the amount of PrP<sup>Sc</sup> at the expense of the normal protein (A). When the *in vitro* generated PrP<sup>Sc</sup> was inoculated into wild-type hamsters, all of the hamsters developed a disease with clinical, histological and biochemical characteristics typical of scrapie.

Control hamsters inoculated with the original diluted material (B) without amplification remained free of the disease. *From Soto et al 2006*

Further experiments using PMCA have then shown that PrP<sup>Sc</sup> propagated *in vitro* led to a scrapie disease with similar pathological features than the brain-derived one, once inoculated in wild-type hamsters (Castilla et al., 2005). Moreover, Castilla and co-workers (2008) have reported that PMCA-replicated prions, derived from five different mouse and four distinct human prion strains, after injection into wild-type mice produced a disease with indistinguishable characteristics as the parental strain. Thus, confirming that PMCA could be used to replicate different types of prion. The use of PMCA reaction could be applied not only to detect prions in the brain in early pre-symptomatic cases, but also to generate a test to diagnose living animals and people (Soto et al., 2002). Therefore, taken together, these findings support the 'protein-only' hypothesis and highlight the strong identity of the different prion strains present that are directly linked with their diverse biochemical, structural and biological properties (Castilla et al., 2008).

### 1.5 Strains and transmission barrier

Prion strains represent one of the most intriguing features of prion diseases. They are defined as infectious isolates that, when transmitted to identical host, exhibit distinct prion-disease phenotypes that are maintained unaltered for several passages (Aguzzi and Calella, 2009a). Phenotypic traits associated with different strains include distinct patterns of protein aggregate deposition, incubation times, histopathological lesion profiles and specific neuronal targets. The phenomenon was first noticed when goats were inoculated with "hyper" and "drowsy" isolates from sheep. Indeed, two different phenotypic traits of the disease were observed accordingly with the inoculated isolate deriving from infected animals with characteristic disease-associated traits (PATTISON and MILLSON, 1961). Prion strains exhibit specific migration profiles of PrP<sup>Sc</sup> fragment following PK-assay on SDS-PAGE highlighting their conformational diversity

(Parchi et al., 1999). Also, they can be associated with different glycosylation patterns resulting in different ratios of the glycosylated forms (Prusiner, 1998; Collinge, 2001). Both PrP<sup>C</sup> and PrP<sup>Sc</sup> exist in three different glycosylated forms: unglycosylated, mono-glycosylated and bi-glycosylated. For example, PrP<sup>Sc</sup> fraction in immunoblots of brain extracts after digestion with PK deriving from individuals affected by variant CJD lead to a specific glycosylation pattern (type 4 pattern), similar to the one given by bovine spongiform encephalopathy-(BSE) affected brains and different to the one deriving from sporadic CJD and iatrogenic CJD (Type 1, 2 or 3 patterns) (Parchi et al., 1999; Hill et al., 1997a) (Figure 6).

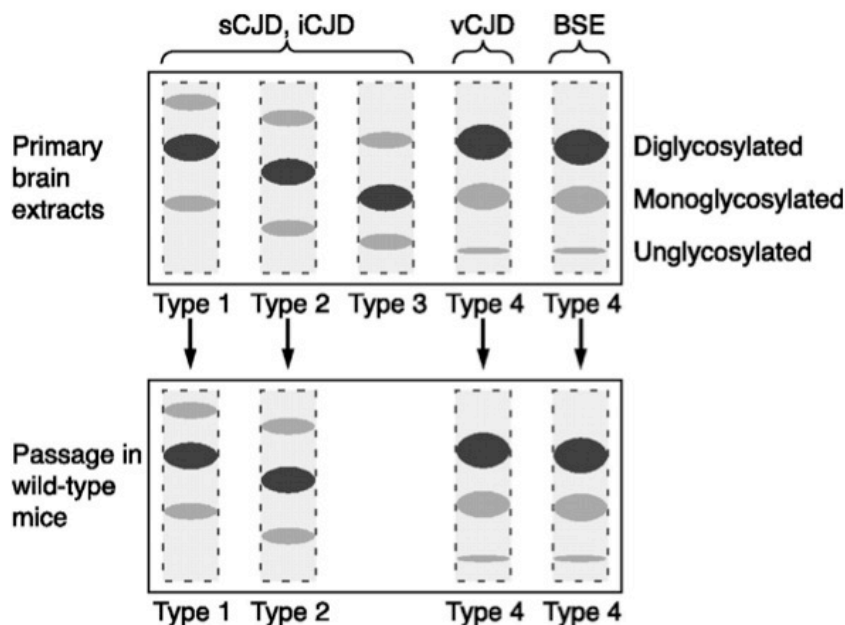


**Figure 6 Representation of the three glycosylated PrP<sup>Sc</sup> moieties** (un-, mono-, and diglycosylated PrP<sup>Sc</sup>) in immunoblots of brain extracts after digestion with proteinase K. Different inocula result in specific mobilities of the three PrP bands as well as different predominance of certain bands (*top panel*). These characteristic patterns can be retained, or changed to other predictable patterns after passage in wild-type mice (*bottom panel*). On the basis of the fragment size and the relative abundance of individual bands, three distinct patterns (PrP<sup>Sc</sup> types 1–3) were defined for sCJD and iCJD cases. In contrast, all cases of vCJD and of BSE displayed a novel pattern, designated as type 4 pattern. *From Aguzzi et al 2009*

It has been proposed that the prevalence of distinct glycoforms may determine the structure of infectious PrP seeds and thereby determine strain properties (Collinge, 2005a). These data strongly support the ‘protein-only’ hypothesis of infectivity and

suggest that strain variation is encoded by a combination of PrP conformation and glycosylation (Collinge, 2001).

Prion strains display different organ tropisms. Some of them preferentially propagate in the central nervous system, as bovine prion causing BSE and some others are also detected in secondary lymphoid organs as many scrapie and vCJD strains (Aguzzi and Calella, 2009b). Yet, this different tropism suggests that cell-specific co-factors, such as RNA species, chaperones or lipids, are required for replicating prion in different physiological environment.

'Strain mutations' are also observed upon transmission of prions to the same species carrying a different polymorphism in PrP<sup>C</sup> or to different species (Wadsworth et al., 2004; Bruce, 1993). Also, many of the inoculated animals have a delay in developing or do not develop the disease (Tateishi et al., 1996; Telling et al., 1994; Carlson et al., 1989; Telling et al., 1995). This phenomenon is referred to as the 'transmission barrier' and was first noted by Ian Pattison in 1965 (Colby and Prusiner, 2011).

It seems that the most important factor regulating the transmission barrier is the sequence homology between PrP<sup>C</sup> in the inoculum and PrP<sup>C</sup> expressed by the host. In fact, mice resistant to a different species prion strain became susceptible to the infection if artificially expressing PrP<sup>C</sup> of that species (Prusiner et al., 1990b). For example, transmission studies of human prion diseases have shown that while classical CJD prions may be efficiently transmitted to transgenic mice expressing human PrP<sup>C</sup>, they encounter a significant barrier for transmission to wild-type mice. On the other hand, vCJD prions transmit readily to wild-type mice, whereas their transmission to transgenic mice expressing human PrP<sup>C</sup> is relatively inefficient (Collinge, 2001; Collinge and Clarke, 2007).

## 2. Human and animal prion diseases

As already mentioned in the first section, transmissible spongiform encephalopathies (TSE) are fatal neurodegenerative disorders present both in human and animals that can occur genetically, spontaneously or by infection (Prusiner, 1998).

Both animal and human conditions share common histopathological features (Figure 7) that include spongiform vacuolation (affecting any part of the cerebral grey matter), neuronal loss, and astrocytic proliferation that may be accompanied by amyloid plaques (Beck et al., 1982).

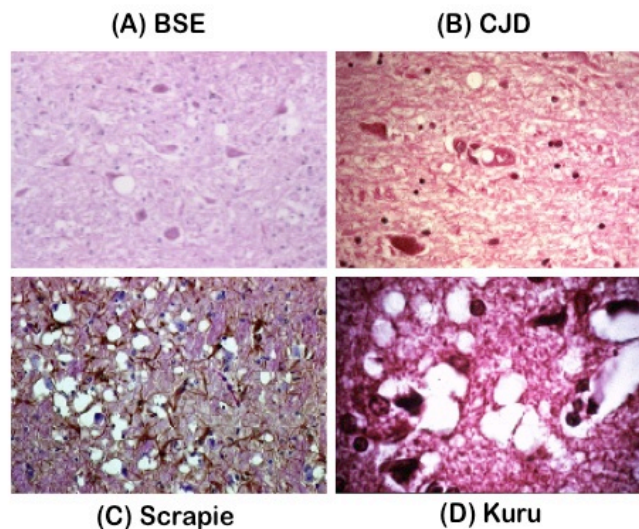


**Figure 7 Histopathological features associated with TSEs showing spongiform degeneration and astrocytic gliosis** . Analysis of grey matter from brain sections of (A) a BSE-infected cow, (B) an individual affected from CJD, (C) sheep and (D) kuru-affected individual. Modified from <http://www.biophys.uni-duesseldorf.de/research/prions/index.html>

Also, no infiltration of lymphocytes and macrophages has been detected due to the absence of the immune response (Collinge, 2001). The long pre-symptomatic period is a characteristic of TSE and is then followed by a rapid progression after the first symptoms that lead inevitably to death. Specific clinical signs are associated with each type of TSE but they include perturbations

of the locomotor and sensory system, lack of coordination and progressive dementia (Collinge, 2001).

## 2.1 Animal

Prion diseases occur in many animals and more frequently as infectious disorders (Table 1).

Disease	Host	Mechanism of pathogenesis
Kuru	Humans (Fore people)	infection through ritualistic cannibalism
Iatrogenic CJD	Humans	infection from prion-contaminated HGH
Variant CJD	Humans	infection from bovine prions
Familial CJD	Humans	germline mutations in the PRNP gene
GSS	Humans	germline mutations in the PRNP gene
FFI	Humans	germline mutations in the PRNP gene
Sporadic CJD	Humans	somatic mutation or spontaneous conversion of PrPC into PrPSc
sFI	Humans	somatic mutation or spontaneous conversion of PrPC into PrPSc
Scrapie	Sheep	Infection
BSE	Cattle	Infection or sporadic
TME	Mink	Infection with prions from sheep or cattle
CWD	Deer and elk	Infection
FSE	Cats	infection with prion-contaminated bovine tissues or MBM
Exotic ungulate encephalopathy	greater kudu, nyala, oryx	infection with prion-contaminated MBM

**Table 1 Animal and Human prion diseases.**

The most known are scrapie in sheep and goat, bovine spongiform encephalopathy (BSE) in cattle, transmissible mink encephalopathy (TME) (Marsh et al., 1991), chronic wasting disease (CWD) of mule deer and elk (Williams and Young, 1980) and the more recently described feline spongiform encephalopathy (Wyatt et al., 1991).

### 2.1.1 Scrapie

Initially thought to be a muscle disease caused by parasites, such as amoeba by Girard in 1830, scrapie is the prototypic prion disease and has been the object of studies since the 19<sup>th</sup> century because of the importance of the wool textile business in the industrial revolution and its impact on the economy (Aguzzi and Polymenidou, 2004). Its name originates from the main clinical symptom, an itching sensation caused by the disease that induces the animal to scrape its fleece off (Figure 8, A).

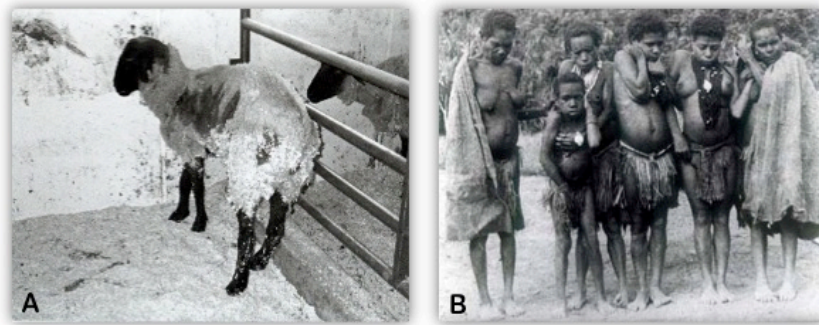


**Figure 8** Scrapie and Kuru (A) The oldest known prion disease, was described 1759 (Leopold) and is characterized by the abnormal walk and scratching of infected sheep and goats. The scrapie agent was adapted to mice and hamster, which are used as model systems in basic research. (B) Among the Fore people in Papua New Guinea the spread of kuru was caused by a ritual cannibalism. Besides the coordinative malfunctions the cerebellar deficits were often associated by uncontrollable and inappropriate episodes of laughter. *Modified from* <http://www.pipevet.com/articles/Scrapie.htm> and <http://www.biophys.uni-duesseldorf.de/research/prions/index.html>

Other symptoms include gait disorders and wool loss; death usually occurs between 6 weeks to 6 months after the onset of symptoms. Polymorphisms at codon 136 and 171 of the prion protein gene (*PRNP*) in sheep have been studied with respect to the occurrence of scrapie in sheep (Cloucard et al., 1995). At present, its routes of transmission remain unclear; however, a hereditary link has been suspected because of a strong genetic element (Parry, 1979). Initial transmissibility studies of scrapie infection were negative. The failure to recognise the long incubation times of the disease was overcome by the work of

*Cuillé and Chelle* in 1936 (“La maladie dite tremblante du mouton est-elle inocuable?” *C. R. Acad. Sci.* 203, 1552-1554) in which they demonstrated that scrapie can be transmitted into goats following injection of scrapie infected brain. The transmissibility of the infectious agent was further confirmed after scrapie was accidentally transmitted into sheep when a Scottish herd was inoculated against a virus with a brain, spleen and spinal cord extract from an infected animal (Collinge, 2001). Since then, scrapie has effectively been transmitted experimentally into other species including laboratory mice (CHANDLER, 1961), demonstrating that it can cross the ‘species barrier’ and it is currently used as model in prion research. To date, scrapie has never been shown to pose a threat to human health (Collinge, 2001).

### *2.1.2 Bovine Spongiform encephalopathy*

BSE, also known as ‘*Mad Cow disease*’, has raised the attention of the public for the first time in 1986 in Great Britain where it appeared like an epidemic disease in which nearly one million cows were infected with prions (Anderson et al., 1996). Clinical symptoms include changes in temperament and movement disorders. Since the incubation time for BSE is around 5 years, infected cattle slaughtered at 2 or 3 years of age were in a pre-symptomatic phase and therefore not recognized as afflicted by BSE (Stekel et al., 1996). The disease is caused by meat and bone meal (fed primarily to dairy cows) deriving from offal of sheep, cattle (probably affected by a rare sporadic BSE), pigs and chickens as they represent high sources of nutrients (Wilesmith et al., 1991; Nathanson et al., 1997). Changes in the feeding system eliminated the epidemic, that reached its peak in 1992 but sporadic cases can still arise occasionally (Colby and Prusiner, 2011).

Also, brain extracts deriving from prion-infected cows can transmit the disease to mice, cattle, sheep and pigs after intracerebral inoculation (Aguzzi and Calella, 2009a; Fraser et al., 1988). More importantly, and differently from scrapie, BSE can be transmitted to humans in a new variant, vCJD, by ingestion of

contaminated food (see below, paragraph 2.2). In 1994, the first cases of vCJD in teenagers and young adults occurred in Britain (Will et al., 1996a) and later one case was recognized in France (Chazot et al., 1996) presenting unusual neuropathological features that did not match with CJD cases.

### *2.1.3 Transmissible mink encephalopathy*

Transmissible mink encephalopathy (TME) was the first TSE to be identified in non-domestic animals. It rarely develops in captive mink (*Mustela vison*) and it is thought to derive from ingestion of BSE-contaminated feed (Williams and Miller, 2003). Symptoms include aggression and loss of muscle coordination; animals die within 6 weeks following the onset of symptoms. TME has been experimentally transmitted to hamsters (Kimberlin and Marsh, 1975).

### *2.1.4 Chronic Wasting Disease*

CWD is the only disease found in free-ranging animals such as mule deer, white-tailed deer and elk and it is present in the US and in Canada. It was first described in 1967 in Colorado and only in 1978 classified as a form of prion disease by histopathological exam of infected brains (Colby and Prusiner, 2011). The shedding of prions from the feces has been identified as a likely source of infection for these grazing animals (Williams and Miller, 2002) but the route of infection is still unknown. Afflicted animals develop the disease after 3-4 years from the TSE agent exposure and die very quickly in a period that goes from 2 weeks to 8 months. Symptoms include weight loss and excessive drinking (Gilch et al., 2011). Experimental evidence has confirmed neuronal vacuolation (Williams and Young, 1980), accumulation of aggregated prion protein (Spraker et al., 2002) and prion infectivity in the brain (Browning et al., 2004). Moreover, prion protein aggregates are not only found in the central nervous system (CNS), but also in lymphoid tissues, skeletal muscles and other organs. Also, up to date there is no evidence for CWD transmission to humans.

Spongiform encephalopathies of a number of zoo animals (Kirkwood et al., 1990; Jeffrey and Wells, 1988) are also recognized as animal prion diseases. Many new species—including greater kudu, nyala, Arabian oryx, Scimitar horned oryx, eland, gemsbok, bison, ankole, tiger, cheetah, ocelot, puma, and domestic cats—have developed spongiform encephalopathies coincident with or following the arrival of BSE (Collinge, 1997; Bruce et al., 1997). The majority of these subforms appear to be linked to the BSE epidemic (Sigurdson and Miller, 2003).

## 2.2 Human

Human prion diseases, traditionally classified into Creutzfeldt-Jakob disease (CJD), Gerstmann-Straüssler-Scheinker disease (GSS) and Kuru, have been subsequently divided into three etiological categories: sporadic, acquired, and inherited (Table 1).

### 2.2.1 Sporadic prion diseases

The sporadic forms (sCJD) were the first to be described by Creutzfeldt-Jakob in 1920. They are the most frequent among CJD forms, accounting for 80 to 90% of the cases, and present worldwide without sexual preference with an annual incidence of one per million. The causes of sCJD are not known and probably derive from a spontaneous misfolding of PrP<sup>C</sup> into PrP<sup>Sc</sup> (Prusiner 1989; Hsiao et al 1991). Alternatively, it has been proposed that the disease could be due to a somatic mutation of *PRNP* or infrequent amplification of low levels of PrP<sup>Sc</sup> that are part of “normal” protein homeostasis (Colby and Prusiner, 2011). Susceptibility to sCJD disease is influenced by a polymorphism at residue 129 of *PRNP* (Prusiner, 1998) and homozygosity predisposes not only to sporadic but also the acquired forms of CJD. The onset of the disease is at ~ 60 years old which quickly progresses in 4-5 months leading to death (Johnson and Gibbs, 1998). The pathology is limited to the central nervous system, where neuronal loss occurs with progressive vacuolization but in which no amyloid plaques are detected (Spero and Lazibat, 2010). Also, infected sCJD brains can transmit the disease to

experimental animals by intracerebral injection (Brown et al., 1994).

### 2.2.2 Inherited prion diseases

Around 15% of human prion disease is inherited and in all cases to date over 40 different mutations in *PRNP* are associated with genetic forms of prion disease (Colby and Prusiner, 2011). Accordingly with clinical symptoms, they have been classified as Gerstmann-Straüssler-Scheinker syndrome (GSS) (MASTERS et al., 1981), familiar (f) CJD and fatal familial insomnia (FFI) (Lugaresi et al., 1986).

The first reports of *Prnp* mutations described insertion and missense mutations in families with dominantly inherited neurodegenerative disease (Owen et al., 1989). Over 40 different types of *Prnp* mutations have been found and *Prnp* analysis allows for pre-symptomatic diagnosis of inherited prion disease (Collinge, 2005b). They include point mutations leading to amino acid substitutions or premature stop codons mostly affecting the region between the second and the third helix of the carboxy-terminus and octapeptide repeat insertions (OPRI) (Figure 9).

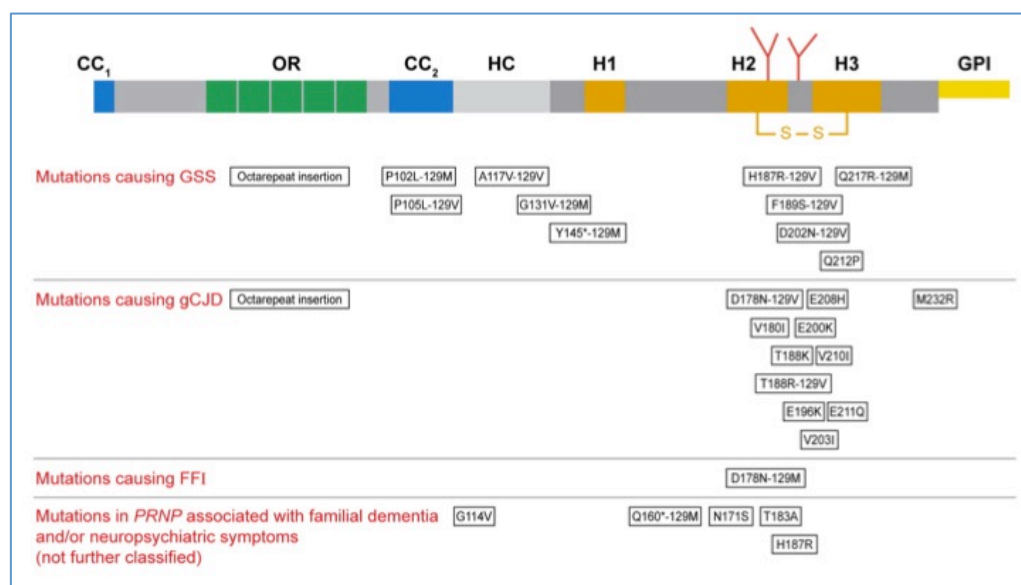


**Figure 9 The human PrP<sup>C</sup> protein and its mutants.** The mature human PrP<sup>C</sup> protein contains 208 amino acid residues. It features two positively charged amino acid clusters denoted CC<sub>1</sub>

and CC<sub>2</sub> (*blue boxes*), an octapeptide repeat region (OR) (*green boxes*), a hydrophobic core (HC) (*gray box*), three  $\alpha$ -helices (H1-H3) (*red boxes*), one disulphide bond (S–S) between cysteine residues 179 and 214, and two potential sites for N-linked glycosylation (*red forks*) at residues 181 and 197. A glycosylphosphatidylinositol anchor (GPI) (*yellow box*) is attached to the C-terminus of PrP. This figure indicates in black framed boxes point mutations and insertions found in the human *PRNP* gene in patients with prion disease. The associated polymorphisms of codon 129 (methionine M or valine V) are indicated. Amino acids are given in single-letter code. The asterisk indicates a stop codon; therefore, this mutation results in a truncated protein. From Aguzzi et al 2008

The pathology of this group of prion diseases can vary depending on the actual mutation, as well as on polymorphisms at codon 129, that also represent a key determinant of genetic susceptibility to acquired and sporadic prion diseases (Collinge, 2001). Also, given the heterogeneity in clinical signs, the importance of unidentified cellular modifiers and environmental factors should be taken into account (Kovacs and Budka, 2008).

### 2.2.3 Acquired prion diseases

Infectious forms of prion diseases include kuru, iatrogenic CJD (iCJD) and variant CJD (vCJD).

Kuru was firstly described in research in the '60 by *Gajdusek and Zigas* as an endemic disease among some tribes of New Guinea aborigines, particularly in the Fore Tribe and neighboring tribes (Figure 8, B). The route of transmission is attributed to the cannibalistic rituals through ingestion of the brains of their dead relatives in an attempt to immortalize them. The typical progression for kuru is progressive cerebellar ataxia, evolving in few months with a very broad incubation period of 4 to 40 years. With the end of cannibalism in Papua New Guinea, kuru is now eliminated (Aguzzi et al., 2008).

Iatrogenic CJD is a rare form of prion disease deriving from accidental transmission during the course of medical or surgical procedures. In 1974, the first case of iCJD caused by corneal transplantation of a graft derived from a patient suffering from sCJD was reported (Duffy et al., 1974). Later on, other routes of transmission derived from prion-tainted human growth hormones and gonadotropin, dura mater grafts and blood transfusion were also reported. The incubation period ranges between 1 and 15

years and accordingly with the origin, death occurs around 15 months from the onset of the symptoms (Prusiner, 1998; Colby and Prusiner, 2011).

Among the infectious forms of prion diseases, the variant form (vCJD) is the one that has caught the attention of the public the most. Indeed, in 1996 a major epidemic of vCJD appeared in different countries, particularly in the UK, where the number of reported cases had the highest incidence (about 150) (Will et al., 1996b). Patients are generally young at the onset of the disease (average onset is at 29 years), have a significant longer disease course, present florid plaque deposits (vacuolization) in the brain and are homozygous for methionine at position 129 in the *PRNP* gene that suggests a genetic susceptibility for vCJD. Interestingly, in experimentally infected mice, prions from patients with vCJD and prions from BSE-cattle gave similar pathological and biochemical characteristics (i.e. incubation period and localization in brain), leading researchers to conclude that the most likely cause for vCJD in humans is the consumption of BSE-contaminated beef (Hill et al., 1997b; Bruce et al., 1994). A single case of vCJD in a patient heterozygous at codon 129 has also been reported, raising the possibility of a second wave of “mad cow”-related deaths .

### 3. Cell biology of prion disease

#### 3.1 The cellular protein: PrP<sup>C</sup>

##### 3.1.1 Structure and Functions

PrP<sup>C</sup> is a ubiquitous glycoprotein expressed early in embryogenesis and present in high levels in the central nervous system in adult, particularly in neurons but also in glial cells (Manson et al., 1994; Harris, 2003). PrP<sup>C</sup> normally localizes at the extracellular site of the plasma membrane where it associates with cholesterol-enriched lipid rafts (see below, paragraph 3.2.1). In neurons, PrP<sup>C</sup> is predominant in axons and dendrites (Mironov et al., 2003). It seems to be excluded from synaptic vesicles but present within the synaptic specialization and perisynaptically, so its role at the level of the synapse is still controversial (Vassallo and Herms, 2003; Fournier et al., 1995). In addition, PrP<sup>C</sup> is widely expressed in the immune system, in hematopoietic stem cells and mature lymphoid and myeloid compartments (Isaacs et al., 2006). Also, many other tissues and organs like the spleen, intestines, the skin, muscles and the heart have been found positive for PrP<sup>C</sup> expression.

The PrP<sup>C</sup> precursor is a protein of 254 amino acids (Figure 10, A).

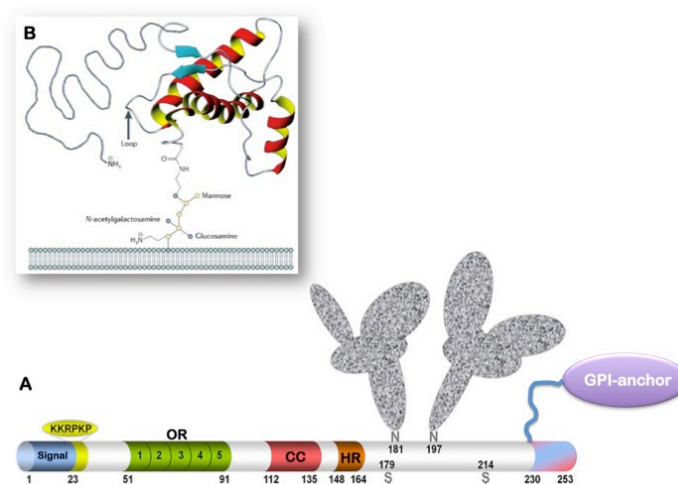


**Figure 10** (A) Primary sequence and (B) tertiary structure of PrP<sup>C</sup>. OR= Octapeptide Region; CC= Charged Region; HR= Hydrophobic Region.

After cleavage of a 23 amino acids signal peptide in the endoplasmic reticulum (ER), a glycosylphosphatidylinositol (GPI) anchor, which mediates its anchoring to the membrane, is attached to the C-terminus of the protein (Stahl et al., 1987). The two Cys residues 179 and 214 are engaged in the formation of a disulphide bond essential for the stability of the protein. The protein exists as un-, mono- or bi-glycosylated, as one or two oligosaccharidic chains can be linked to two asparagines (N) (residues 181 and 197 in humans) in the C-terminal part of PrP<sup>C</sup> in the Golgi apparatus during the journey of the protein to the plasma membrane.

At the 3D level, PrP<sup>C</sup> has a long, flexible N-terminal tail (residues 23-128); it is present in most of the animal species studied, but not in elk and deer (Prusiner, 1998). It contains an octarepeat region (OR) consisting of 5 repeats of the sequence PHGGGWGQ (major binding site for divalent cations), a basic charged region (CC) important for PrP<sup>C</sup> trafficking and an hydrophobic domain (HR) that can be used by PrP<sup>C</sup> to assume different transmembrane topologies. Indeed, PrP<sup>C</sup> presents at least three distinct topological orientations: the fully extracellular form (or (sec)PrP) and two transmembrane isoform (called Ntm-PrP and Ctm-PrP) with opposite sequence orientations with respect to the lumen of the endoplasmic reticulum (Nicolas et al., 2009). Following the unstructured N-terminus is a globular C-terminal domain consisting of three  $\alpha$ -helices interspersed with two-stranded antiparallel  $\beta$ -sheets that flank the first  $\alpha$ -helix (Figure 10, B) (Zahn *et al.*, 2000; Hornemann *et al.*, 2004). The structure of several mature PrP<sup>C</sup> proteins in mice, cattle, humans and Syrian hamsters is very similar (Colby and Prusiner, 2011), thus suggesting a relevant evolutionary conserved function for this protein.

A plethora of cellular functions have been attributed to PrP<sup>C</sup> but as already mentioned above its physiological role appears to be redundant, since PrP knock-out mice are vital and do not present severe abnormalities (Bueler et al 1992; Manson et al 1994). However, a growing number of studies implicates PrP<sup>C</sup> in diverse cellular processes (Nicolas et al., 2009) as cellular resistance to

oxidative stress (Milhavet and Lehmann, 2002), cell signalling (Mouillet-Richard et al., 2000), copper and zinc metabolism (Watt and Hooper, 2003; Pauly and Harris, 1998), synaptic transmission (Collinge et al., 1994) and cytoprotection through anti-apoptotic activity (Kuwahara et al., 1999; Bounhar et al., 2001) (see below, paragraph 3.2). Recently, Bremer and colleagues have also demonstrated that PrP<sup>C</sup> is required for the maintenance of myelin sheath around peripheral nerves (Bremer et al., 2010). In addition, a role for PrP<sup>C</sup> as cellular receptor in the toxic effect of oligomeric forms of amyloid- $\beta$ , implicated in Alzheimer's disease, has been described by Lauren and co-workers (2009). In contrast, other reports have shown that amyloid- $\beta$  toxicity is independent from PrP<sup>C</sup> (Balducci et al., 2010). Therefore, its role in Alzheimer's disease is still controversial. Besides, it has been shown that PrP<sup>C</sup> is implicated in cell adhesion (Malaga-Trillo, 2009), focal adhesion formation and filopodia extension (Schrock et al., 2008). These findings point out towards an additional role of PrP<sup>C</sup> in cytoskeleton dynamic and remodeling and cell-to-cell communication.

Furthermore, the identification of interacting partners of PrP<sup>C</sup> is of fundamental importance not only to provide new insights into its role in physiological conditions but also to better understand the basic mechanism of PrP<sup>C</sup>-PrP<sup>Sc</sup> conversion that leads to neuropathology. In a recent report, a series of interacting partners for PrP<sup>C</sup> has been found by using a proteomics approach (Zafar et al., 2011). The results have confirmed 15 interacting partners already shown to interact with both PrP<sup>C</sup> and PrP<sup>Sc</sup> but 28 new proteins were also identified. A functional categorization of these proteins (Figure 11) confirmed many of the assigned roles for PrP<sup>C</sup> in highlighting its multi-faceted functionality and involvement as a biological platform for diverse cellular processes.

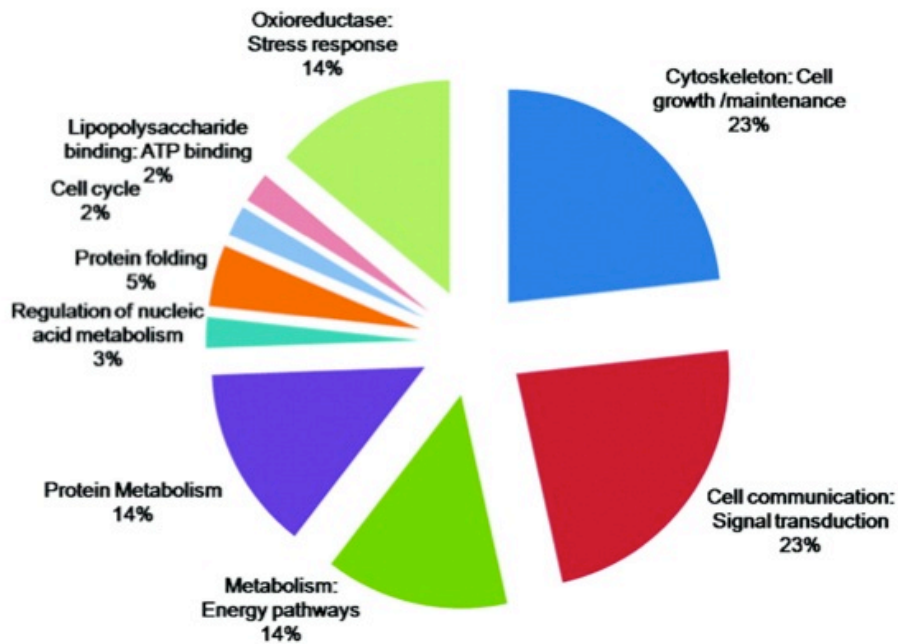
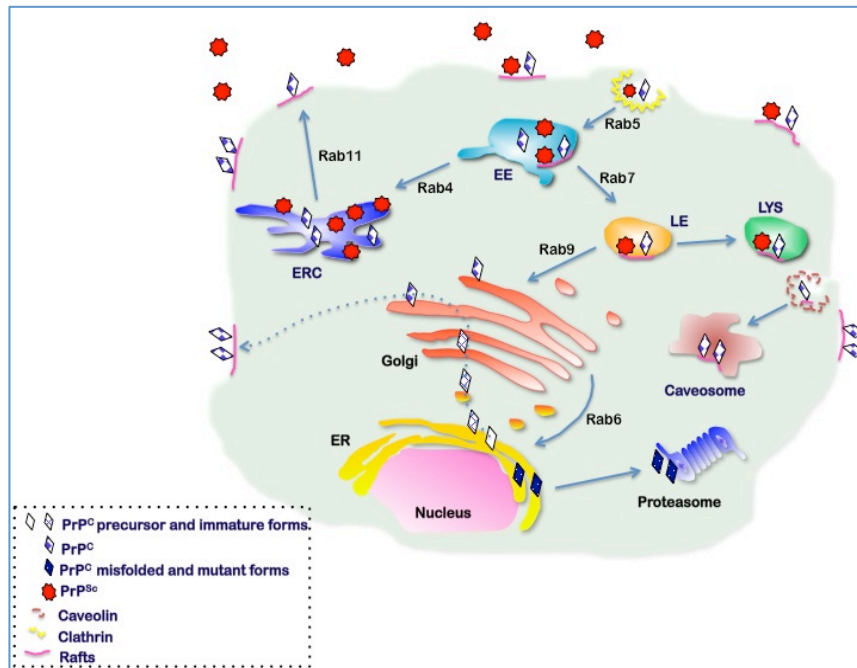


Figure 11 Functional categorization of putative PrP<sup>C</sup> binding partners. Modified from Zafar et al 2011.

### 3.1.2 Localization

After being synthesized in the rough endoplasmic reticulum (ER), immature PrP<sup>C</sup> transit in the Golgi compartment before reaching the plasma membrane similarly to other surface or secreted proteins (Harris, 2003) (Figure 12).



**Figure 12 Cellular localisation and trafficking of PrP<sup>C</sup> and PrP<sup>Sc</sup>.** Intracellular pathway of PrP<sup>C</sup> and PrP<sup>Sc</sup> is depicted together with the Rab proteins controlling different pathways.

Specifically, during its journey, PrP<sup>C</sup> undergoes a number of post-translational modifications in the endoplasmic reticulum and at the Golgi level including cleavage of the N-terminal signal peptide, addition of N-linked oligosaccharide chains, formation of a single disulphide bond, and attachment of the GPI anchor (Haraguchi et al., 1989; Turk et al., 1988). The N-linked oligosaccharide chains added in the ER are of the high-mannose type and are sensitive to digestion by endoglycosidase H. In the Golgi they are subsequently modified to more complex oligosaccharides that contain sialic acid and are resistant to endoglycosidase H (Caughey et al., 1989). PrP<sup>C</sup> is attached on the external leaflet of the plasma membrane by its GPI-anchor which mediates its segregation within specific domains of the membrane known as detergent resistant microdomains (DRMs), or lipid rafts. Association to lipid rafts is thought to occur at the level of the Golgi (Naslavsky et al., 1997a), but it has also been shown that it can take place earlier in the ER with the immature PrP<sup>C</sup>, and may be implicated in facilitating the proper folding and stability to the protein (Sarnataro et al., 2004). Additionally, PrP<sup>C</sup> has been

detected at the cell surface in caveolae and caveolae-like domains (CLDs) in cells expressing caveolin (Mouillet-Richard et al., 2000; Peters et al., 2003; Harmey). Phosphatidylinositol-specific phospholipase C (PIPLC) treatment of cells in culture has shown that with an accumulation of PrP<sup>C</sup> in the medium, due to the cleavage of the GPI-anchor by PIPLC, a progressive loss of PrP<sup>C</sup> is detected. This demonstrates that the majority of this protein is localized at the plasma membrane through its GPI-anchor (Stahl et al., 1987). Indeed, different reports have shown that the GPI-anchor mediates PrP<sup>C</sup> raft-association (Taraboulos et al., 1995a; Kaneko et al., 1997). However by using cells expressing various PrP<sup>C</sup> mutants lacking the GPI-anchor (transmembrane-anchored form of PrP<sup>C</sup>, PrP-TM) it has been shown that the N-terminal flexible domain contains a raft-target domain between amino acids 23-90 that is sufficient to confer rafts association of PrP-TM (Walmsley et al., 2003). Moreover, the highly charged region of the N-terminal consisting of residues 23-28 (-KKRPKP-) are known binding sites for glycosaminoglycans (GAGs) (Warner et al., 2002; Pan et al., 1993b). Recently it has been described that the major neuronal heparin sulphate proteoglycan GPI-anchored glypican-1 is involved in the recruitment and stabilization of PrP<sup>C</sup> in lipid rafts by interacting with the ectodomain of PrP<sup>C</sup> (Taylor et al., 2009). Also, depletion of glypican-1 significantly reduced the raft association of PrP-TM and displaced PrP<sup>C</sup> from rafts, promoting its endocytosis (Taylor et al., 2009). Altogether, these results support that both GPI-anchor and N-terminal ectodomain of PrP<sup>C</sup> mediate raft-association and stabilization (Campana et al., 2005).

### *3.1.3 Internalization*

At the cell surface, PrP<sup>C</sup> is then constitutively internalized and recycles back to the plasma membrane (Harris, 2003). Both clathrin coated pits and caveolae mediated endocytosis have been shown to be involved in PrP<sup>C</sup> internalization (Campana et al., 2005). In particular, some experimental evidences have shown that PrP<sup>C</sup> does cycle between the plasma membrane and early endosomes via clathrin coated pits dependent pathway

(Taraboulos et al., 1995a; Shyng et al., 1994). In order to be internalized by a classic clathrin-mediated manner, PrP<sup>C</sup> should translocate outside lipid raft domains and this occurs upon Cu<sup>2+</sup> binding to the protein (Taylor and Hooper, 2007). Transmembrane proteins that are internalized through clathrin-coated pits interact through their cytosolic domain with cytoplasmic clathrin-coated pits accessory proteins that mediate internalization (Bonifacino and Traub, 2003). Therefore, since PrP<sup>C</sup> is anchored on the external leaflet of the plasma membrane, its presence in these structures should involve adaptor proteins, probably interacting with the polybasic region of the N-terminus of PrP<sup>C</sup>. For example, low-density lipoprotein receptor-related protein-1 (LRP1) has been shown to mediate PrP<sup>C</sup> endocytosis in neuronal cells (Taylor and Hooper, 2007; Parkyn et al., 2008) but other proteins could be involved. Sunyach *et al.* have shown that endogenous PrP<sup>C</sup> expressed on the surface of adult sensory primary neurons recycle every few minutes via clathrin coated pits between the cell surface and recycling endosomes (Sunyach et al., 2003). Similarly, this was also shown for N2a and SH-SY5Y cells, both neural cell lines (Taylor et al., 2005; Shyng et al., 1994; Sunyach et al., 2003). Alternatively, caveolae-mediated internalization and trafficking of PrP<sup>C</sup> from late endosomes to lysosomes have been described (Peters et al., 2003). For example, PrP<sup>C</sup> has been found in caveolae, but not in clathrin-coated pits and vesicles, in Chinese hamster ovary cells, which express caveolin-1 (Peters et al., 2003). Caveolae are flask-shaped invaginations at the cell surface that are decorated by a caveolin 1 (Cav1) coat (Anderson, 1998). However, the role of caveolae in prion trafficking on neurons is irrelevant, as caveolae have not been shown to occur on adult mammalian neurons. However, caveolae-mediated PrP<sup>C</sup> endocytosis may present a distinct trafficking pattern in non-neuronal cells (Sarnataro et al., 2004).

### 3.1.4 Trafficking

Intracellular trafficking of proteins required vesicle transport between different membrane compartments (Maxfield and

McGraw, 2004). By characterizing endosomes and transport vesicles, in particular through the presence of specific Rab proteins, precise information about the traffic of a certain protein can be achieved. Rab proteins are small GTPases that regulate vesicular transport in endocytosis and exocytosis (Zerial and McBride, 2001). Different Rab proteins were found to be associated specifically with different endosomes (Figure 12). Briefly, Rab5 is associated with clathrin-coated pits and early endosomes (Bucci et al 1992; Bucci et al 1994; Stenmark et al 1994; Bucci et al 1995). Rab4 couples early in recycling compartments promoting fast recycling to the plasma membrane (van der Sluijs et al 1991; van der Sluijs et al 1992; Daro et al 1996). Rab11 is concentrated in recycling endosomes and also provide a pathway for recycling of proteins to the membrane (Ullrich et al 1996). Rab7 and Rab9 are found in late endosomes. Rab7 seems to be essential for the transport of molecules from early to late endosomes and lysosomes (Feng et al 1995; Meresse et al 1995) and Rab9 from late endosomes to *trans*-Golgi (Lombardi et al 1993). Finally, Rab6 is involved in retrograde trafficking from the Golgi to the endoplasmic reticulum (Martinez et al 1997; White et al 1999). A number of different studies have analyzed the trafficking of PrP<sup>C</sup> in cell cultures and it appears that PrP<sup>C</sup> trafficking may vary from neurons to neuroblastoma cell lines or glia cells (Prado et al 2004). Indeed, PrP<sup>C</sup> has been shown to localize to different compartments depending on the cell type. For example it has been reported that PrP<sup>C</sup> predominantly localizes in late endosomes in neuroblastoma-derived (N2a) and hypothalamic gonadotropin releasing (GT1-7) cell lines (Pimpinelli et al., 2005); other studies reported that in primary neurons and in N2a cells very little portion of PrP<sup>C</sup> resides in lysosomes (Shyng et al., 1994; Sunyach et al., 2003). Furthermore, experiments with a GFP-tagged form of PrP<sup>C</sup> (GFP-PrP<sup>C</sup>) expressed in different cell lines and studies using immunolabelling to detect endogenous PrP<sup>C</sup> have shown that PrP<sup>C</sup> is present in the Golgi (Marijanovic et al., 2009; Magalhães et al., 2002), early endosomes (EEs) and in the endosomal recycling compartment (ERC) (Magalhães et al., 2002; Marijanovic et al., 2009). Also, in hippocampal neurons, PrP<sup>C</sup> is found mainly at the plasma membrane (Galvan et al.,

2005) and on vesicles resembling early endocytic or recycling vesicles (Godsave et al., 2008).

The fate of PrP<sup>C</sup> after passage through endocytic compartments is still poorly understood. However, it has been shown that it can be degraded through the endo-lysosomal pathway after reaching the lysosomes (Campana et al., 2005; Sunyach et al., 2003; Magalhães et al., 2002). Also, approximately 10% of wild type PrP<sup>C</sup> is subject to retrograde transport through the ER-associated degradation (ERAD), probably due to incorrect processing or an excess of PrP and it is subsequently delivered to the cytosol and degraded in the proteasome (Ma et al., 2002; Parizek et al., 2001; Yedidia et al., 2001; Vetrugno et al., 2005). Additionally, PrP<sup>C</sup> shedding from the cell surface in the extracellular medium can occur, suggesting proteolysis of the GPI-anchor. Indeed, soluble PrP<sup>C</sup> has been found in conditioned media of cells in culture as well as in human cerebrospinal fluid (Parizek et al., 2001; Tagliavini et al., 1992) and within the lumen of exosomes (Fevrier et al., 2004; Vella et al., 2007).

And yet, Gilch *and colleagues* have shown that the perturbation of PrP<sup>C</sup> but also PrP<sup>Sc</sup> trafficking could result in a delay of the onset of the disease in mice, by using the chemical compound Suramin (Gilch et al., 2001). Insights from the mechanisms of internalization and trafficking of PrP<sup>C</sup> can also help in better characterizing where PrP<sup>C</sup> to PrP<sup>Sc</sup> conversion occur and how PrP<sup>Sc</sup> spread, by dissecting possible pathways and finding interacting partners for both PrP isoforms.

### 3.2 PrP<sup>C</sup> to PrP<sup>Sc</sup> conversion site: a secret “rendez-vous”

Differently from PrP<sup>C</sup> localization, PrP<sup>Sc</sup> detection is very difficult to assess because of the lack of specific antibodies. However, several studies suggest that it has a wide distribution inside cells and importantly it also appeared associated with DRMs but not necessary in the same raft domains as PrP<sup>C</sup> (Vey et al., 1996; Naslavsky et al., 1997a). Indeed, some earlier reports have shown that the majority of PrP<sup>Sc</sup> is intracellular (Taraboulos et al.,

1990), sequestered within lysosomes of prion-infected N2a cells (McKinley et al., 1991; Caughey and Raymond, 1991; Borchelt et al., 1992) with little localization at the cell surface (Vey et al 1996). In infected brains, PrP<sup>Sc</sup> has been reported to accumulate at the plasma membrane and occasionally in late endosome/lysosome-like structures (Jeffrey et al 2006). More recent reports describe accumulation of PrP<sup>Sc</sup> either in the perinuclear Golgi region of neurons in scrapie-infected transgenic mice, in the late endosomal compartment of infected GT1-7, N2a and CAD neuronal cells (Gousset et al., 2009; Pimpinelli et al., 2005; Marijanovic et al., 2009) or at the cell surface and on early endocytic and recycling vesicles in hippocampal neurons (Jeffrey et al., 1994). Also, the mechanism of internalization of PrP<sup>Sc</sup> is not well understood but a recent work suggests the possibility of clathrin-mediated endocytosis, as its cellular counterpart (Veith et al., 2009).

Due to the disparate sub-cellular localizations of both PrP<sup>C</sup> and PrP<sup>Sc</sup>, several possible sites for conversion have been postulated, but this process is still far from being fully understood. As already mentioned above, this is the process in which cellular PrP<sup>C</sup> is converted into its pathological counterpart, PrP<sup>Sc</sup>. Certainly, a better understanding of the compartments in which PrP<sup>C</sup>-PrP<sup>Sc</sup> conversion occurs is of fundamental importance to develop potential therapeutics for prion disease.

Several papers have reported that PrP<sup>C</sup> has to reach the plasma membrane before conversion (Gilch et al., 2001; Taraboulos et al., 1995a; Caughey et al., 1991; Borchelt et al., 1992) (Figure 13).

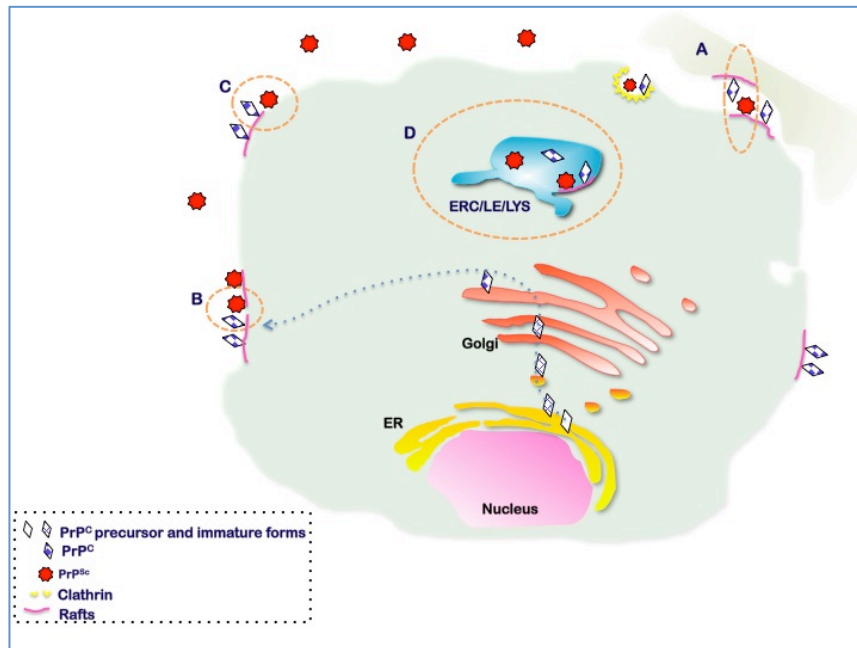


**Figure 13 Possible sites of PrP<sup>C</sup>-PrP<sup>Sc</sup> conversion.** Dotted lines and circles represent intracellular pathways and site for conversion. (A) Initiation of conversion at the cell surface after direct contact between uninfected and infected cells. (B) Lipid raft clustering, enabling interaction of otherwise separated PrP<sup>C</sup> and PrP<sup>Sc</sup>. (C) Non-raft associated PrP<sup>Sc</sup> promoting conversion of contiguous raft associated PrP<sup>C</sup>. (D) Conversion of PrP<sup>C</sup> to PrP<sup>Sc</sup> in endocytic vesicles.

Recently, Goold and co-workers (2011) have shown that the plasma membrane is an initial site of prion conversion. This could be the case of acquired forms of prion disease in which an exogenous introduced PrP<sup>Sc</sup> converts the cellular endogenous PrP<sup>C</sup>. In this work by using a neuroblastoma cell line knocked-down for endogenous PrP<sup>C</sup> and expressing an epitope-tagged PrP<sup>C</sup> the earliest events in cellular prion infection have been characterized, giving new insights on PrP<sup>Sc</sup> dynamics. In particular they found that prion conversion occurs very rapidly at the cell surface within 1 minute of prion exposure (Goold et al., 2011). This new finding does not preclude a role for intracellular compartments in prion conversion, that have already been shown to be important, and may continue and accelerate the process following PrP<sup>Sc</sup> initially synthesized at the plasma membrane. Both PrP<sup>C</sup> and PrP<sup>Sc</sup> localize to vesicles of the endosomal and lysosomal pathways. PrP<sup>Sc</sup> is trimmed at its N-terminus by endogenous proteases in acidic compartments immediately after its generation (Borchelt et al., 1992; Caughey et al., 1989)

suggesting that its conversion to a protease-resistant state occurs prior to reaching the lysosomal compartment. Moreover, inhibition of endocytosis using a temperature block or release of nascent PrP from the cell surface using PIPLC prevented PrP<sup>Sc</sup> synthesis (Borchelt et al., 1992; Campana et al., 2005). Recently, Marijanovic and colleagues (2009) selectively inhibited PrP trafficking through the different endocytic compartments using both pharmacological and reverse genetic approaches in infected cells and analyzed PrP<sup>Sc</sup> levels under the different experimental conditions. They demonstrated that early and late endosomes are not involved in PrP<sup>Sc</sup> replication. However inhibition of the trafficking from the early endosomes to the endocytic recycling compartment by over-expression of Rab22 dominant-negative would block prion conversion (Marijanovic et al 2009). Moreover, they have shown that PrP<sup>Sc</sup> accumulates in the endosomal recycling compartment (ERC) upon inhibition of PrP exit from this compartment by overexpressing a Rab11 dominant-negative mutant, which impairs recycling from the ERC back to the plasma membrane (Marijanovic et al., 2009). These data suggest that PrP<sup>C</sup> has to reach the ERC to be converted and stimulate PrP<sup>Sc</sup> production, thus pointing towards a role for the recycling compartment as an intracellular site for prion conversion. This finding is also supported by the recent evidence that PrP<sup>Sc</sup> is present in the ERC of primary hippocampal neurons derived from infected brains (Godsave et al., 2008). Also, as will be described below (paragraph 3.2.1), cholesterol has been shown to be involved in prion conversion (Taraboulos et al., 1995). Interestingly, ERC membranes are enriched in cholesterol in different cells (Hao et al., 2002; Maxfield and McGraw, 2004). Therefore, a cholesterol-dependent retention mechanism in the ERC could facilitate the efficient conversion of the native prion protein into its pathological counterpart. The involvement of the ER compartment in prion conversion is suggested by the observation that forcing the retrograde transport of PrP<sup>C</sup> to the ER by overexpressing a constitutively active form of the GTPase Rab 6, is sufficient to increase scrapie production in infected cells (Beranger et al., 2002). In the ER, high amounts of newly synthesized PrP<sup>C</sup> could be available as substrate for the conversion reaction. In addition, PrP<sup>C</sup> can be found in this

compartment in a partially unfolded state that could make it easier for PrP<sup>Sc</sup> to impress its conformation to PrP<sup>C</sup>. Furthermore, the first step in the misfolding of mutants of PrP<sup>C</sup> associated with hereditary forms of prion diseases, has been shown to occur in the ER. In addition it has been shown that dissociation of PrP<sup>C</sup> from DRMs by cholesterol depletion, induce its misfolding in the ER (Sarnataro et al., 2004). Therefore, while in the infectious diseases PrP<sup>Sc</sup> could catalyze prion amplification in this compartment even if conversion is occurring elsewhere, in the hereditary diseases the ER could represent the propitious environment where the conformational transition of mutated PrP<sup>C</sup> can take place spontaneously. More recently by inducing ER-stress or inhibiting the proteasome some researchers have found that both conditions significantly affect total PrP level resulting in accumulation of aggregated PrP forms, still able to reach the plasma membrane and be a substrate for PrP<sup>Sc</sup> conversion in other cellular sites. These results confirm a role for the ER in hereditary forms of the prion disease (Nunziante et al 2011).

### *3.2.1 Role of lipid rafts in prion conversion*

Lipid rafts are membrane microdomains enriched in cholesterol and glycosphingolipids in which lipids of specific chemistry can dynamically associate with each other to form platforms that segregate specific membrane proteins (Simons and Ikonen 2002; Lingwood and Simons 2010). One of the main methods used to prove the existence of rafts domains in cell membranes has been the extraction by non-ionic detergents such as Triton X-100, therefore detergent resistant microdomains (DRMs) represent cellular lipid rafts (Edidin 2003; Zurzolo et al 2003).

Although still quite unclear, recent studies suggest a role for lipid rafts in prion conversion (Lewis and Hooper, 2011; Taylor and Hooper, 2006; Campana et al., 2005). Interestingly both PrP<sup>C</sup> and PrP<sup>Sc</sup> localize in these particular domains but they seem to be able to associate to different DRMs. Indeed, purified DRMs containing PrP<sup>C</sup> can be biochemically separated by DRMs containing PrP<sup>Sc</sup> (Naslavsky et al., 1997a). Moreover, DRMs seem to be involved in prion uptake), like other pathogens and toxins,

and their destabilization (Sarnataro et al 2009) can induce altered PrP<sup>C</sup> exocytic trafficking in neuronal cells and a slow down of PrP<sup>C</sup> maturation in epithelial cells (Campana et al., 2005). Furthermore, insertion of PrP<sup>C</sup> in lipid rafts has an impact on its conformation stability both in vitro and in cell culture (Sarnataro et al., 2004). These data suggest a protective role for DRMs against the occurrence of prion conversion. Interestingly, it has been demonstrated that cholesterol depletion impairs PrP<sup>Sc</sup> production (Taraboulos et al 1995; Bate et al 2004) while sphingolipid depletion increase it (Naslavsky et al., 1997b). More recently, Gilch *and colleagues* have shown that inhibition of cholesterol recycling impairs cellular PrP<sup>Sc</sup> propagation. Cholesterol is one of the main components of lipid rafts (Gilch et al., 2009). The content of free cholesterol in the cell is tightly regulated by endogenous synthesis, uptake by low-density lipoprotein (LDL) and level of esterification, which allows storage of cholesterol in cytoplasmic lipid droplets (Ikonen, 2008). Recycling of cholesterol is achieved by the controlled action of two proteins, NPC-1 and NPC-2 whose loss-of-function mutations lead to Niemann-Pick type C disease (NPC), a lysosomal storage disorder associated to neurological symptoms, characterized by accumulation of cholesterol in late endosomes and lysosomes (Maxfield and Tabas, 2005). In prion-infected N2a cells, knock-down of NPC-1 led to a drastic loss of PrP<sup>Sc</sup> (Gilch et al., 2009) and treatment with the drug U18666A, producing a phenocopy of NPC disease exerts the same effect (Klingenstein et al., 2006; Hagiwara et al., 2007; Gilch et al., 2009; Marijanovic et al., 2009). These data support a role for cholesterol in prion conversion. Moreover, perturbation of cholesterol recycling and trafficking could alter intracellular trafficking of both PrP isoforms, thus slowing down the conversion process and shifting the balance of PrP<sup>Sc</sup> production/degradation towards the latter. In addition, it has been shown that impairment of prion conversion can be achieved by forcing PrP<sup>C</sup> to localize outside DRMs (i.e. substituting the GPI anchor attachment signal with a transmembrane domain in the coding sequence of PrP<sup>C</sup>) even though the anchor seems to be dispensable for the conversion process itself (Baron and Caughey, 2003; Lawson et al., 2001; Kocisko et al., 1994). These results suggest that a specific lipid

environment can be necessary for the conversion process. In this view, rafts could provide a favorable environment for conformational conversion of PrP<sup>C</sup> to PrP<sup>Sc</sup>, by concentrating proteins in specific membrane regions allowing their mutual interaction and by providing accessory molecules required for the process (Campana et al., 2005; Taylor and Hooper, 2006). Finally, rafts could be able to traffic the two isoforms to the compartments where prion conversion occur. Indeed, membrane rafts are present not only at the plasma membrane level but also in vesicles of the endocytic compartments, thus constituting a conversion-prone environment (Taylor and Hooper, 2011). Despite the fact that several advancements have been reached in understanding the mechanisms involved in PrP<sup>C</sup>-PrP<sup>Sc</sup> conversion, the role of lipid rafts, other critical factors and particular endocytic pathways participating in the process need further investigations to fully understand prion diseases at a molecular level and develop new drugs for therapy.

### 3.3 From PrP<sup>C</sup> – PrP<sup>Sc</sup> conversion to neurotoxicity: what is the link?

Understanding how PrP<sup>Sc</sup> formation actually leads to neurodegeneration following neurotoxicity is still an open question in prion biology. Despite the fact that apoptosis and oxidative stress have been shown to contribute to TSE pathology (Milhavel and Lehmann, 2002), little is known about damage causing primary events (Aguzzi et al., 2008). In principle, it is still unclear whether PrP<sup>Sc</sup> toxicity represents a gain of function or a loss of PrP<sup>C</sup> function and which is the main responsible factor for the neuropathological changes induced by prions. Some reports that have addressed this question rather support a loss of PrP<sup>C</sup> function (Nazor et al 2007). But, based on the mild phenotype of PrP<sup>C</sup> knock-out mice, other groups think that a gain of function is more conceivable (Westergard et al., 2007; Aguzzi et al., 2008). However, it is also possible that a normal neuroprotective role for PrP<sup>C</sup> needed during prion-induced brain damage could be missing due to its conversion in the pathological counterpart. A third possibility could be that in presence of PrP<sup>Sc</sup>, the cellular PrP<sup>C</sup>

could trigger toxic signals through pathways not related with its physiological function (subversion of function) (Figure 14).

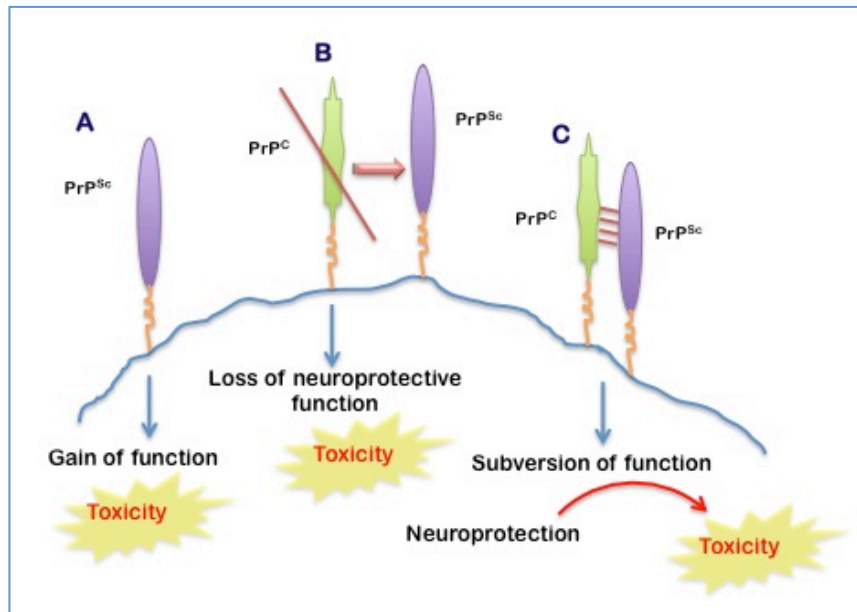


**Figure 14 PrP-mediate neurotoxicity.** (A) Toxic gain-of-function mechanism. PrP<sup>Sc</sup> possesses a novel neurotoxic activity that is independent of the normal function of PrP<sup>C</sup>. (B) Loss-of-function mechanism. PrP<sup>C</sup> possesses a normal, physiological activity, in this case neuroprotection, that is lost upon conversion to PrP<sup>Sc</sup>. (C) Subversion-of-function mechanism. The normal, neuroprotective activity of PrP<sup>C</sup> is subverted by binding to PrP<sup>Sc</sup>.

To date, several reports suggest that these three possibilities might co-exist to different extent in the diverse forms of prion diseases and they all lead to neurodegeneration.

### 3.3.1 Gain of function through formation of PrP<sup>Sc</sup>

Although the presence of PrP<sup>Sc</sup> is the hallmark of prion diseases, it is highly debated whether prion pathology could really be attributed only to a toxic gain of function. In this context, newly formed PrP<sup>Sc</sup> presents novel properties unrelated with the physiological role of PrP<sup>C</sup> and PrP<sup>Sc</sup> deposits might interfere with synaptic transmission or block of the axonal transfer (Westergard et al., 2007). Some reports have suggested that both full-length PrP<sup>Sc</sup> (Hetz et al., 2003) and shorter PrP peptides are toxic to primary neuronal cultures *in vitro* (Forloni et al., 1993), but their relevance to *in vivo* pathogenesis is under debate. Nonetheless,

from some other experimental evidences it is unlikely that accumulation of extra-neuronal PrP<sup>Sc</sup> aggregates is the only responsible factor for neurotoxicity. Indeed, when neural tissue over-expressing WT PrP<sup>C</sup> is grafted into mice lacking PrP, prion infection of the mice leads to PrP<sup>Sc</sup> levels increase and neurodegeneration only in the PrP<sup>C</sup>-expressing graft (Brandner et al., 1996). Furthermore, absence of endogenous PrP<sup>C</sup> in prion-infected mice has been demonstrated to reverse early spongiform change preventing neuronal loss and progression to clinical disease, even in presence of extra-neuronal PrP<sup>Sc</sup> (Mallucci et al., 2003).

Moreover, prion-infected transgenic mice expressing PrP<sup>C</sup> without a GPI anchor produce infectious prions, accumulate extracellular PrP amyloid plaques, but do not succumb to the disease (Chesebro et al., 2005).

Finally, it has also been described that in some cases PrP<sup>Sc</sup> accumulation does not lead to clinical symptoms (Hill and Collinge, 2003; Race et al., 2000, 2002; Hill et al., 2000).

### *3.3.2 Loss or subversion of PrP<sup>C</sup> function*

As already described (paragraph 3.1.2), PrP<sup>C</sup> seems to be implicated in diverse physiological activities even if its presence is not essential. A loss in any of these functions could theoretically lead to neurodegeneration. In particular, loss of its anti-apoptotic role could directly be related to toxicity and neuronal death. For example, neurons derived from mice lacking PrP<sup>C</sup> were originally reported to be more susceptible to apoptosis mediated by serum deprivation and this phenotype could be rescued by over-expressing either PrP<sup>C</sup> or B-cell lymphoma protein 2 (Bcl2) (Kuwahara et al., 1999). Also, overexpression of Bax, a stimulator of the apoptotic pathway, together with PrP<sup>C</sup> leads to a decrease in the rate of apoptosis in human neurons (Bounhar et al., 2001).

A third possibility is that alteration in PrP<sup>C</sup> normal function is achieved by contact with PrP<sup>Sc</sup>, thus leading to a toxic signal cascade and inducing a subversion of its normal activity. Consistent with this hypothesis, cross-linking of PrP<sup>C</sup> at the cell

surface with anti-PrP antibodies induces apoptosis of the CNS neurons *in vivo* (Solforosi et al., 2004). Additionally, binding of PrP<sup>Sc</sup> could interact with specific region of PrP<sup>C</sup> necessary for its normal function, thus stimulating altered activities. Accordingly, transgenic mice overexpressing PrP harboring a deletion in a portion in the N-terminal tail (Tg(PrP $\Delta$ 105-125)) exhibit a severe neurodegenerative illness that is lethal within one week of birth (Li et al., 2007). Indeed, this highly conserved region could be an important binding site for a putative cell-surface receptor mediating PrP<sup>C</sup> function that in presence of PrP<sup>Sc</sup> is masked (Westergard et al., 2007). Besides, abnormal topology or altered trafficking of PrP<sup>C</sup> could in part explain PrP-related neuronal toxicity in the absence of PrP<sup>Sc</sup> formation (Aguzzi and Calella, 2009). For example, targeting of PrP<sup>C</sup> to the cytosol results in rapid lethal neurodegeneration (in the absence of PrP<sup>Sc</sup>) and proteasome inhibition induces a slightly protease-resistant PrP species in cultured cells (Ma et al., 2002). Although numerous studies have provided important information about the function of PrP<sup>C</sup>, this issue has not been clarified. Until we have a clear understanding of the function of PrP<sup>C</sup> it will be difficult to understand the mechanism that leads to the pathogenesis of the disease. Therefore more studies at single cell level to understand the cell biology of PrP<sup>C</sup> and PrP<sup>Sc</sup> are needed.

## 4. Prion degradation: is autophagy an option?

PrP<sup>Sc</sup> persistence in cultured cells is thought to be maintained by a balance between its formation following the conformational change of PrP<sup>C</sup> into PrP<sup>Sc</sup> (as described in the previous section) and its degradation. A better understanding of PrP<sup>Sc</sup> metabolism and particularly how to shift the equilibrium between PrP<sup>Sc</sup> production and degradation is very important to understand the pathogenesis of the disease. Different degradation pathways might be involved in reducing intracellular PrP<sup>Sc</sup> burden. For example, a role for the lysosomal compartment in PrP<sup>Sc</sup> degradation has been described in several reports which have shown that in different infected neuronal cell lines PrP<sup>Sc</sup> is sequestered in lysosomes where can be degraded (Borchelt et al., 2002; Caughey et al., 1991; McKinley et al., 1991; Jeffrey et al., 2006; Marijanovic et al., 2009; Gousset et al., 2009; Veith et al., 2009). Furthermore, upon block of the proteasome activity significant changes in total PrP level that result in accumulation of aggregated PrP forms in the cytosol, have been observed in N2a cells (Nunziante et al., 2011). Macroautophagy (hereby referred to as autophagy) is another cellular degradation system for long-lived proteins and organelles, normally activated upon starvation for energy supply (Yang and Klionsky, 2009a). Recently, autophagy has been described to play an important role in diverse physiological and pathological processes and, in particular, in neurodegenerative diseases associated with protein aggregation (Wong and Cuervo, 2010). The role of autophagy in prion disease is controversial and it will be discussed in the paragraph 4.3 of this section.

### 4.1 Molecular overview of the autophagic pathway

Autophagy, literally “self-eating”, is a highly conserved cellular degradation system present in all tissues delivering long-lived proteins and cytoplasmic components to lysosomes and is normally induced by starvation. This process leads to the breakdown and eventual recycling of the macromolecules targeted to this pathway (Yang and Klionsky, 2009a; Ana, 2004;

Levine and Klionsky, 2004). Three different types of autophagy are present in eukaryotic cells: macroautophagy, microautophagy and chaperone-mediated autophagy (CMA) (Figure 15).

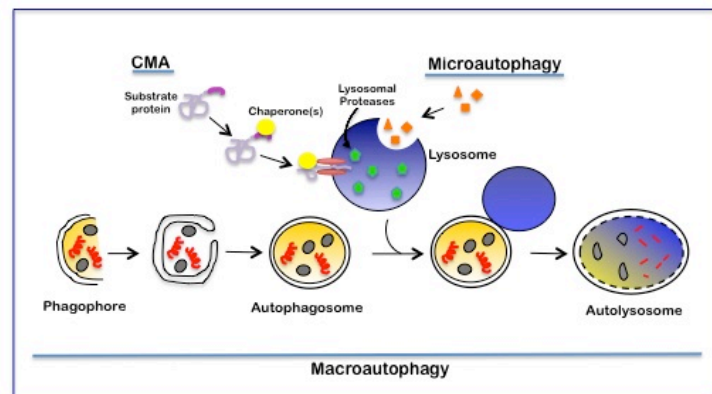


**Figure 15 Different types of autophagy present in eukaryotic cells.** During Macroautophagy, a double-membrane structure, the phagophore, arises from the cytosol and engulfs part of the cytoplasm containing different proteins and organelles; the phagophore then closes to form the autophagosome, a vacuole with a double-membrane that subsequently fuses with a lysosome, originating an autolysosome in which the content is degraded. Microautophagy involves direct sequestration of proteins and organelles by invaginations of the lysosomal membrane that pinch off into the lumen; Chaperone-mediated autophagy (CMA) targets and delivers cytosolic proteins containing a consensus peptide sequence across the lysosomal membrane via a specific receptor binding.

Microautophagy involves direct sequestration of proteins and organelles by invaginations of the lysosomal membrane that pinch off into the lumen (Mijaljica et al., 2011). CMA targets and delivers cytosolic proteins containing a consensus peptide sequence across the lysosomal membrane via a specific receptor binding. During the process, a chaperone complex mediates the substrate protein translocation in the lumen of the lysosome where degradation takes place (Li et al., 2010).

Upon stimulation of macroautophagy, hereafter simply referred to as autophagy, a double-membrane structure, the phagophore, arises from the cytosol and engulfs part of the cytoplasm containing different proteins and organelles; the phagophore then closes to form the autophagosome, a vacuole with a double-membrane (Figure 15). The origin of the phagophore, also called isolation membrane, is still debated. However, it has recently emerged that both the endoplasmic reticulum and the

mitochondria may provide the source of membranes for the autophagic vacuole (Tooze and Yoshimori, 2010). During the maturation of the autophagosome, fusion events with endosomes or multivesicular bodies (MVBs) can occur leading to the formation of amphisomes containing endocytic organelles. Their contents are then targeted to lysosomes, *via* autophagosome, for further degradation (Eskelinen, 2004). Either autophagosome or amphisome eventually fuse with lysosomes to form the autolysosome. After fusion, the inner membrane of the autophagosome is exposed to lysosomal hydrolases and its content is degraded. This final step ends with the release of degraded material into the cytosol for recycling (Figure 15) (Xie and Klionsky, 2007).

The autophagosome-lysosome fusion is a critical step for the progression of autophagy (also referred to as autophagic flux). For example, inhibition of the vacuolar ATPase (v-ATPase) with bafilomycin A1 or concanamycin A blocks the lysosomal pumping of H<sup>+</sup> and consequently inhibits lysosomal proteases activity. It has been shown that bafilomycin A1 can also block the autophagic flux (Mousavi et al., 2001; Yamamoto et al., 1998), and this can lead to both an increase in the number of autophagosomes and inhibition of degradation of the autophagic cargoes (Eskelinen, 2004; Beau et al., 2011).

To date, more than 30 Autophagy-related Genes (*Atg* genes), firstly described by Yoshinori Ohsumi's group in the early 1990s, have been identified from genetic screens in yeast model systems (Xie and Klionsky, 2007; Huang and Klionsky, 2002a). Homologues of many *Atg* genes in yeast have been found in higher eukaryotes, including humans, highlighting the fact that the molecular machinery of autophagy is evolutionally conserved among species (Mizushima and Yoshimori, 2007; Klionsky et al., 2008).

The 'core' autophagy machinery responsible for the formation of the autophagosome is composed of four main functional groups: (1) Atg12-Atg5 and Atg8-phosphatidylethanolamine conjugation systems (Ohsumi 2001); (2) the Atg1-Atg13-Atg17 kinase complex; (3) the class III phosphatidylinositol 3-kinase (PtdIns3K) complex I and, (4) Atg9 and its cycling system (Xie and Klionsky,

2007). A fifth group includes proteins needed for the last step of autophagy in which the degradation products are recycled back in the cytosol (Yang and Klionsky, 2009b).

The identification of the Atg8 mammalian homologue Microtubule-Associated Protein 1 light chain 3 (MAP1LC3, simply known as LC3) opened up a new era in the study of mammalian autophagy (Kabeya et al., 2000). LC3 was originally described as a protein that co-purified with microtubule-associated protein 1A and 1B from rat brain (Mann and Hammarback, 1994); Kabeya and co-workers (2000) have shown by subcellular fractionation and immunogold electron microscopy that LC3 localizes on autophagic vacuoles. To date, LC3 represents a widely used marker that specifically associates with these structures thus allowing the development of a series of LC3-based assay to monitor autophagy (Kimura et al., 2009; Huang and Klionsky, 2002b).

LC3 exists in two different forms: LC3-I that is cytosolic and LC3-II that is membrane bound and associated with autophagic vacuoles (Figure 16).

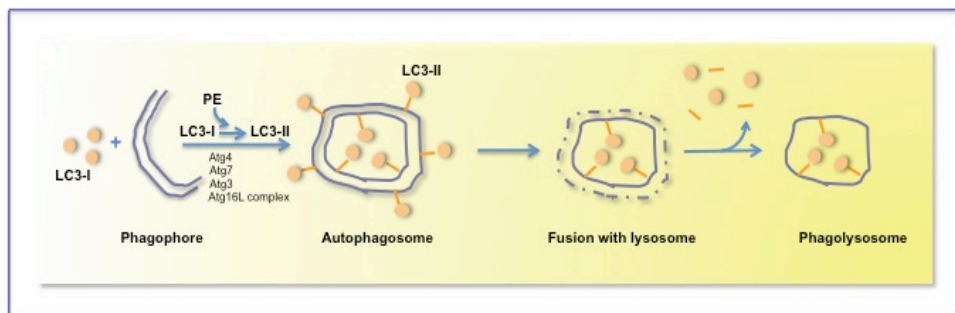


**Figure 16 LC3 and autophagic vacuoles assembling.** The protein LC3 is a known specific marker of autophagic vacuoles and it is widely used to measure autophagy. Two forms of LC3 are produced post-translationally, LC3-I (cytosolic) and LC3-II (membrane bound). LC3-II is bound on the outer face of the outer membrane and inner face of the inner membrane. When the autophagosome matures into an autolysosomes, LC3 on the outer membrane is liberated into the cytosol, whereas the one facing the lumen of the organelle is trapped inside and finally degraded by lysosomal proteases.

LC3-I results from the cleavage of the pro-LC3 form (LC3 translated from mRNA) at the level of a glycine in the C-tail.

During autophagy, LC3-I is post-translationally modified by a combination of enzymatic activities that ultimately add a phosphatidylethanolamine (PE) to the C-terminal of LC3-I, generating the LC3-II form (Kimura et al., 2009). LC3-II is bound on the outer layer of the outer membrane and inner layer of the inner membrane of the double-membrane autophagosome. When the autophagosome matures into an autolysosomes, LC3-II on the outer membrane is liberated into the cytosol as LC3-I, whereas the one facing the lumen of the organelle is trapped inside and only in the final stage of the autophagic flux is degraded by lysosomal proteases (Figure 16) (Xie and Klionsky, 2007). Therefore, the measurement of LC3-II turnover by different biochemical and microscopy approaches is a good indicator of the state of autophagy in a given condition (Kimura et al., 2009).

Regulation of autophagy is complex and a comprehensive view of regulatory mechanisms is still missing (Reggiori and Klionsky, 2002). Despite this, it is possible to identify different levels of autophagy regulation: (1) signalling pathways acting up-stream of the autophagy machinery regulating induction/inhibition of autophagy, (2) formation of autophagosome and, (3) maturation and fusion of autophagosomes with lysosomes (Esclatine et al. 2009).

Historically, mTOR (mammalian Target Of Rapamycin) has been considered the central regulator of autophagy. Indeed, the inhibition of this serine/threonine kinase (acting as a nutrients sensor) induces autophagy under starvation for energy supply and this process is an evolutionarily conserved response to stress in eukaryotes (Yang and Klionsky, 2009a). It has been shown by Blommaert and colleagues (1995) that rapamycin induces autophagy in rat hepatocytes; therefore rapamycin, by inhibiting the mTOR pathway, represents a well-known inducer of mTOR-dependent autophagy (Noda and Ohsumi, 1998). Several other mTOR-independent pathways are involved at the different levels mentioned above and their modulation with different compounds might have potential therapeutic application in disease-related autophagy de-regulation (Rubinsztein et al., 2007a).

Beyond its classical role in energy supply under starvation and turnover of organelles and proteins, autophagy plays a wide variety of roles in different physiological processes and pathological conditions as depicted in figure 17 (Beau et al., 2011; Yang and Klionsky, 2009a; Mizushima et al., 2008).

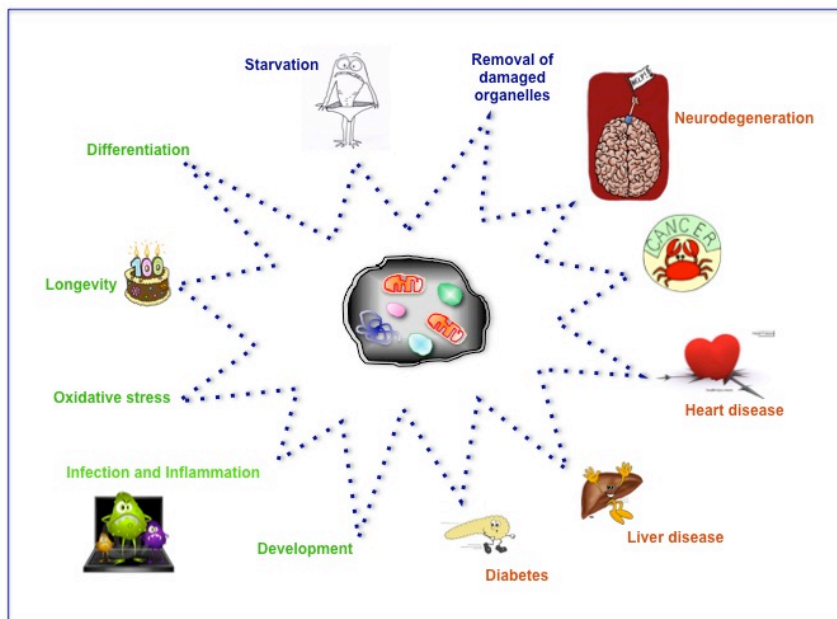


**Figure 17** Role of autophagy in different physiological (in green) and pathological (in orange) conditions.

## 4.2 Autophagy and Neurodegenerative Diseases

Recently, autophagy has been described as an important process in the pathogenesis of neurodegenerative diseases of protein aggregation such as Alzheimer's disease (AD), Parkinson's disease (PD), tauopathies and polyglutamine expansion diseases like Huntington's disease (HD) (Cherra III et al., 2010). As post-mitotic cells that must endure for the lifetime of an organism, neurons must have efficient mechanisms to avoid accumulating toxic protein aggregates that otherwise could not be diluted in the daughter cells by cell division. It has been proposed that autophagy could have a protective role in neurodegeneration

acting as a quality control system in neurons for the turnover of malfunctioning proteins and organelles. Recently it has also been shown that dysfunction in the autophagic pathway is common to numerous neurodegenerative diseases leading to the accumulation of toxic mutant aggregate-prone proteins (Figure 18) (Wong and Cuervo, 2010).

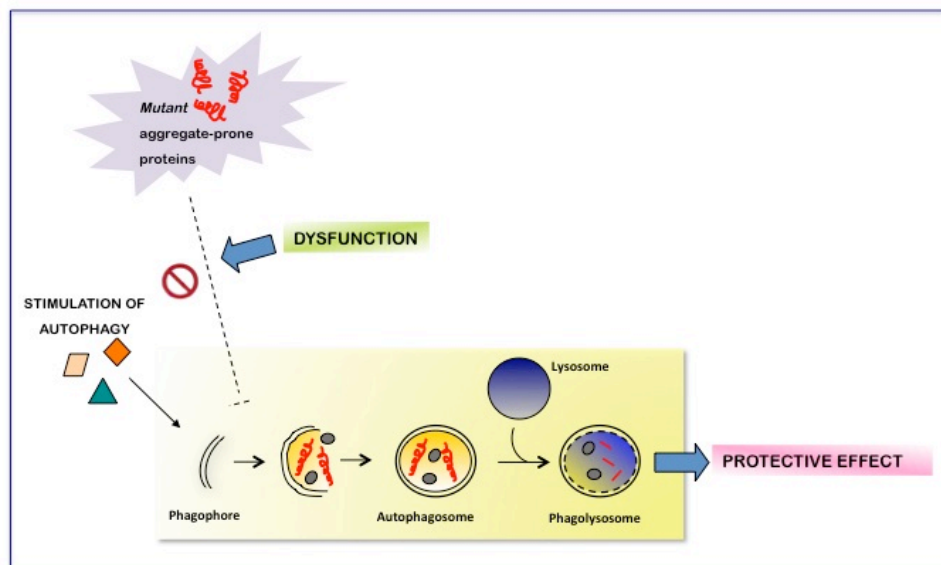


**Figure 18 Autophagy in neurodegeneration.** Mutant aggregate-prone proteins can block the autophagic pathway and lead to neurodegeneration. Alternatively, autophagy can have a protective effect against neurodegenerative disease and stimulation of the autophagic flux can enhance this effect.

For example, conditional knockout of the essential autophagy genes Atg5 or Atg7 in mouse brains, results in a neurodegenerative phenotype accompanied by massive protein aggregate accumulation that leads inexorably to death within the first few months of life (Hara et al., 2006; Komatsu et al., 2006). On the other hand, aggregate-prone proteins could also inhibit autophagy at different stages of the process. Winslow and co-workers (2010) have recently shown that  $\alpha$ -synuclein overexpression compromises autophagy via Rab1a in both mammalian cells and transgenic mice, and that this phenotype could be rescued by overexpressing Rab1a in the autophagy-defective cells. Another study, in which the status of the autophagic system was analyzed in different cell types (primary neurons and striatal cell lines) deriving from HD mouse models

and from lymphoblasts derived from HD patients, showed a defect in cargo recognition mediated by p62 resulting in a lower and inefficient clearance of substrates that led to the accumulation of toxic cytosolic aggregates (Martinez-Vicente et al., 2010).

Moreover, up-regulation of autophagy has been shown to efficiently counteract the accumulation of aggregate-prone protein deposits both in vitro and in vivo models. Therefore, an enhancement of autophagy with different compounds with the aim to reduce the produced toxic species might have a potential therapeutic use in neurodegenerative diseases because of its protective role (Figure 18) (Rubinsztein et al., 2007b).

#### 4.3 Autophagy and Prion Disease: an open debate

The role of autophagy in prion disease is still controversial and highly debated (Heiseke et al. 2010). Autophagic vacuoles were detected in cell models chronically infected with prions (Figure 19) (Schätzl et al., 1997).

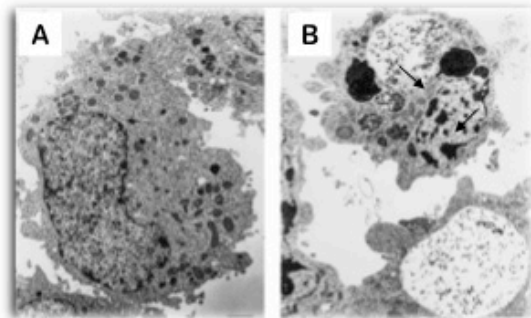


**Figure 19 Ultrastructural signs of autophagic vacuolation and apoptosis in ScGT1-trk cells.** (A) An uninfected (GT1-trk) cell showing a normal heterochromatic nucleus, well-developed Golgi system, intact mitochondria, small secretory granules, and regular-size dense lysosomes. (B) Electron micrograph demonstrates typical cytopathologic changes in ScGT1-trk cells (present in about 20% of cells). Note the cytoplasmic accumulation of autophagic vacuoles representing different stages of degeneration, giant, swollen vacuoles, and peripheral clumping of dense chromatin in the nucleus. *Modified from Schätzl et al., 1997*

More recently, it was found that autophagic vacuoles are formed in neuronal perikarya, neurites and synapses in experimentally induced scrapie, Creutzfeldt-Jakob disease (CJD) and Gerstmann-Sträussler-Scheinker (GSS) syndrome (Liberski et al., 2008) and

autophagic vacuoles were identified in synapses in various forms of human prion disease (Sikorska et al., 2004). It was then proposed that autophagy could play a disease-promoting role by contributing to the formation of spongiform changes, a pathological hallmark in prion-affected brains (Liberski and Jeffrey, 2004; Liberski et al., 2008). On the other hand, it has been demonstrated that a number of autophagy-inducing compounds such as lithium salts, trehalose and rapamycin are effective at reducing PrP<sup>Sc</sup> burden in cultured neuroblastoma cells (N2a) and delay the onset of symptoms in prion-infected mice in prophylactic treatment models (Heiseke et al., 2009; Aguib et al., 2009). Thus, the induction of autophagy has been proposed as a novel approach in the treatment of prion diseases. However, a more systematic analysis of the role of autophagy in prion infection is needed, because the molecular mechanisms by which autophagy would be protective are still not understood.

## 5. Invasion and Spreading: PrP<sup>Sc</sup> body tour

Understanding how exposure to TSE agents, present in the environment, leads to invasion and spreading to the brain of a particular host is of fundamental importance in many different aspects of prion diseases, including the control of the infection, diagnosis, prophylaxis and identification of therapeutic approaches.

From several studies, it is now well accepted that prion infection starts mainly with the uptake of prions by the alimentary tract or through scarification of gums, skin and conjunctiva (Beekes and McBride, 2007). It is interesting to note that the spreading of prions in naturally acquired prion diseases, such as scrapie, CWD, BSE and vCJD may also depend on their site of entry, strain and species, dose and PrP<sup>C</sup> genotype of the host (Kovacs and Budka, 2008). This highlights the urgency of a more systematic study of the pathogenesis at the cellular level to better characterize pathways and major players involved in prion diseases.

Despite the number of variables involved in prion spreading, from substantial data present in the literature reviewed in great detail by *Beekes and Mc Bride* (2007), it is possible to dissect the routing of TSE agents through the body in precise characteristic stages, summarized in Figure 20.

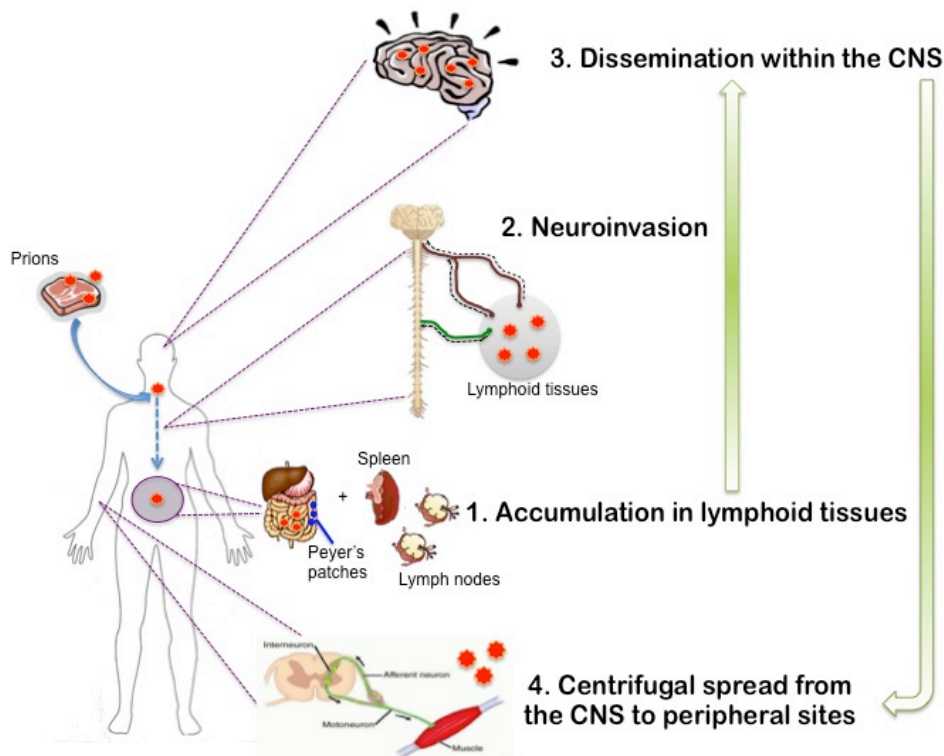


**Figure 20 Different stages of prion infection.** 1) accumulation of prions in lymphoid tissues; (2) neuroinvasion, consisting in the spread from the lymphoid tissues to the peripheral nervous system (PNS); (3) dissemination within the brain and spinal cord (central nervous system, (CNS)) and, (4) centrifugal spread from the CNS to further peripheral sites such as muscles.

Particularly: (A) accumulation of prions in lymphoid tissues; (B) neuroinvasion, consisting in the spread from the lymphoid tissues to the peripheral nervous system (PNS); (C) dissemination within the brain and spinal cord (central nervous system, (CNS)) and, (D) centrifugal spread from the CNS to further peripheral sites such as muscles (Beekes and Mc Bride, 2007).

5.1 From the periphery to the central nervous system: which is the route to follow?

Following ingestion, prion reaches the lymphoid organs. The mechanism by which prion spreads from the gastrointestinal tract after exposure to the lymphoid tissues is still not well understood but different players with specific roles has been identified.

From early studies in mice fed with scrapie or BSE agent, it was observed that the first prion deposition may occur in Peyer's patches and mesenteric lymph nodes prior to infection to other lymphoid tissues (Kimberlin and Walker, 1989) and that the spleen does not play a major role in neuroinvasion (Maignien et al., 1999). Instead, gut-associated lymphoid tissue (GALT) and GALT-draining lymph nodes appear to play a more significant role in early pathogenesis (Beekes and Mc Bride, 2007).

Once prion gets in the lymphoid follicles, its replication and transport involve different cell types such as microfold cells (M cells), follicle-associated epithelium (FAE), follicular dendritic cells (FDCs), dome and tangible body macrophages (TBMs) and dendritic cells (DCs) (Beekes and McBride, 2000). In addition, it has been shown that B cells and complement system can have a supporting role that appears not to be essential (Mabbott et al., 2001; Klein et al., 1997, 2001). Also, at later stages of infection, lympho-reticular system (LRS) components seem to accumulate the scrapie agent (McBride et al., 2001; Beekes et al., 1996). A schematic representation with the main players that are thought to be involved in the uptake of prion from the gut to the lymphoid tissues is depicted in figure 21.

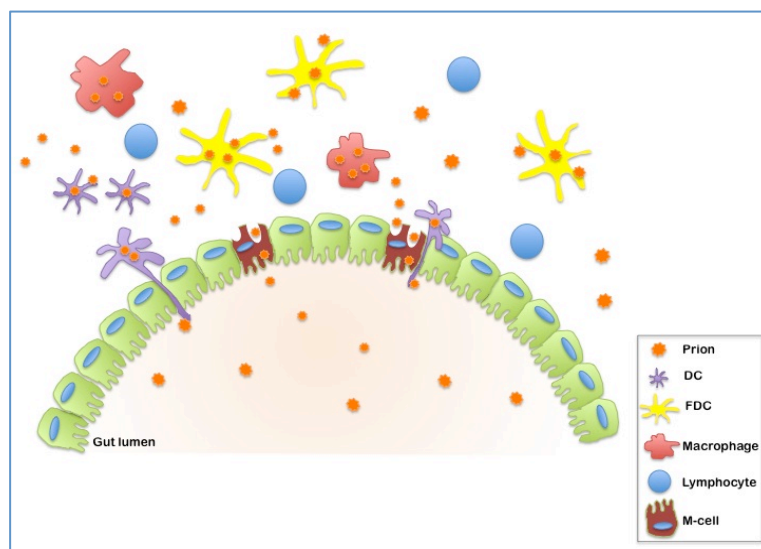


**Figure 21 Possible cells involved in the uptake of prion from the gut to the lymphoid tissues.** The intestinal epithelium is protected by a single layer of epithelial cells bound by tight junctions. How TSE agents cross this protective barrier is not known, but several mechanisms

have been proposed. Within the epithelium, microfold (M) cells are specialized for the transepithelial transport of macromolecules and particles. One study suggests that M cells are also plausible sites for the transport of TSE agents across the intestinal epithelium. TSE agent transport across the intestinal epithelium might also occur independently of M cells. Alternatively, dendritic cells (DCs) can also acquire antigens directly from the intestinal lumen by opening up the tight junctions that join the epithelial cells and inserting their dendrites between them. Once across the intestinal epithelium, current data suggest that the TSE agent might be acquired by migratory DCs and macrophages. Although DCs are plausible candidates or the delivery of TSE agents to lymphoid tissues, macrophages seem to phagocytose and sequester them (Mabbott and McPherson 2006).

A consistent number of studies have shown that mainly GALT and, in minor part, other lymphoid tissues play a pivotal role in amplifying prions and acting as a bridge towards the CNS (Aguzzi and Calella, 2009). Nevertheless a direct infection of the nervous system could also take place after oral exposure, as observed in rodent models lacking a detectable lymphoid infection (Bartz et al., 2005; Oldstone et al., 2002; Fraser et al., 1996).

Of particular interest, the involvement of FDCs, as GALT components, has been comprehensively investigated for their ability to both accumulate PrP<sup>Sc</sup>, as demonstrated by Kitamoto *and colleagues* (Kitamoto et al., 1991) and spread it to the CNS (Mabbott et al., 2003; Montrasio et al., 2000). FDCs are immobile stromal-differentiated cells that highly express PrP<sup>C</sup> (Brown et al., 1999) residing in the follicles and germinal centres (Shortman and Liu, 2002; Kapasi et al., 1993). They have many fine dendritic processes used for the trapping and retention of antigen in a native state. In the case of prion, some evidences show that FDCs capture and accumulate the infectious agent and are then able to transfer it to different cells allowing the spreading of the infection.

But how can immobile FDCs make a link between the intestinal barrier and the peripheral nerves?

Heppner *and colleagues* (2001) have shown in an *in vitro* system, consisting of a CaCo-2 epithelial cells monolayer (Heppner et al., 2001), that microfold cells (M cells) are able to actively transcytose the scrapie agent through the basolateral site of the epithelium as happens for some pathogenic microorganisms (Neutra et al., 1996). M cells are localized between the villus epithelium and the follicle-associated epithelium of the Peyer's patches and are specialized in transcytosis of macromolecules

and particles. Therefore, PrP<sup>Sc</sup> can cross the gut epithelium by this particular cell type even if not in an exclusive manner. Migratory bone-marrow dendritic cells (BMDC) can then be possible candidates for the passage of PrP<sup>Sc</sup> to FDCs and from FDCs to the PNS (Figure 22) (Gousset and Zurzolo, 2009).

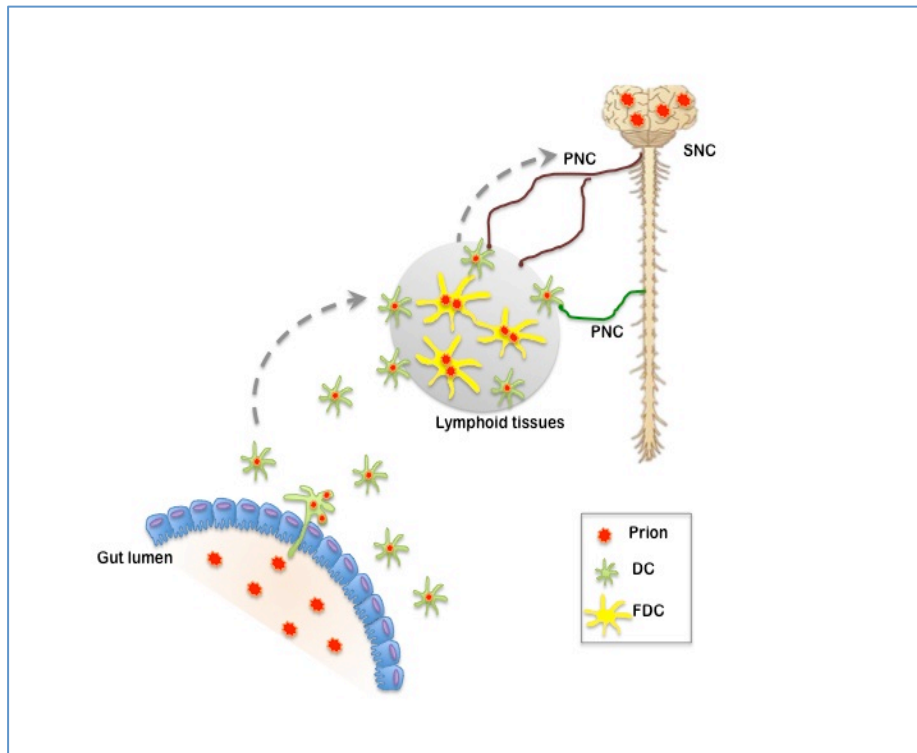


**Figure 22 Schematic representation of the passage of TSE agent from the gut lumen to the PNS.** Migratory bone-marrow dendritic cells (DC) can then be possible candidates for the passage of PrP<sup>Sc</sup> to FDCs in lymphoid tissues and from FDCs to the PNS.

Indeed, dendritic cells (DCs) are situated beneath the M cells in the intraepithelial pocket where they can uptake antigens that has been transcytosed by the M cells; therefore they are specialized in the capture of antigens in the periphery, followed by delivery to the lymphoid organs (Shortman and Liu, 2002). Alternatively, DCs can directly uptake antigens from the intestinal lumen by opening the tight junctions of the intestinal barrier (Rescigno et al., 2001). Huang *and co-workers* have shown that DCs are indeed able to transport PrP<sup>Sc</sup> from the gut to the prion-

replicative lymphoid tissue (Huang et al., 2002). Also, PrP<sup>Sc</sup> deposits have been detected in DCs from Peyer's patches, mesenteric lymph nodes or spleen (Dorban et al., 2007). Moreover, in mice lacking DCs, neuroinvasion is partially impaired because accumulation of PrP<sup>Sc</sup> does not take place following peripheral prion infection (Raymond et al., 2007; Cordier-Dirikoc and Chabry, 2008; Aucouturier et al., 2001). More recently, *Langevin* and colleagues (2010) have characterized the role of BMDCs in the transfer of prions to primary neurons using an *in vitro* system in which BMDCs were loaded with prion and then co-cultured with cerebellar primary neurons (CGNs) (Langevin et al., 2010). BMDCs deriving from both PrP<sup>C</sup>-overexpressing and knock-out mice (lacking PrP<sup>C</sup>) were able to uptake and degrade PrP<sup>Sc</sup>, demonstrating that these processes are PrP<sup>C</sup>-independent, as previously shown (Dorban et al., 2007). Moreover, a direct cell-to-cell contact, mediated by tunneling nanotubes (Langevin et al., 2010), that have been found to have a major role in prion spreading (Gousset and Zurzolo, 2009), between BMDCs and CGNs in PrP<sup>Sc</sup> transfer seems to be necessary for the process to occur similarly to what was recently shown with dorsal root ganglion neurons (Dorban et al., 2010). These results clearly point out towards a major role of dendritic cells in prion spreading from the periphery to the CNS and a further characterization of the mechanism could allow a better understanding of their role *in vivo*.

On the way to the CNS, passing mainly from the lymphoid tissues, PrP<sup>Sc</sup> get access to the peripheral nerves prior to reaching the brain.

Studies from *Mc Bride* and co-workers (1999 and 2001) suggest that efferent fibres of both sympathetic (as the splanchnic nerve) and parasympathetic nerves (as the vagus nerve) can direct prions to the CNS in a retrograde direction from the enteric nervous system. In the case of parasympathetic nerves, the entry in the CNS occurs independently from the spinal cord highlighting the fact that different routes may be responsible for prion spreading to the CNS (Baldauf et al., 1997).

Once the infection has reached the brain, it can spread along it in both anterograde and retrograde directions (Beekies et al 1996).

For example, from a study in hamsters orally challenged with scrapie, it was observed that substantial amount of PrP<sup>Sc</sup> was present in different muscles, including the tongue, providing the first evidence of a centrifugal spread of infection from the CNS to peripheral locations (Bosque et al., 2002).

## 5.2 Cell-to-cell spreading

At the different stages of its lethal journey to the CNS (Figure 20), PrP<sup>Sc</sup> is transferred from one cell to another and this passage can involve several mechanisms not mutually exclusive probably depending on cell types, strains infecting and hosts.

As depicted in figure 23, prion transmission may occur (A) by cell-to-cell contact through the conversion of recipient PrP<sup>C</sup> without internalization of donor PrP<sup>Sc</sup>; (B) in association with exosomes; (C) through the release in the medium of a C-terminal truncated form of PrP<sup>Sc</sup> followed by uptake in the recipient cell; (D) by “GPI-painting” mode and, (E) spreading through tunneling nanotubes (TNTs).

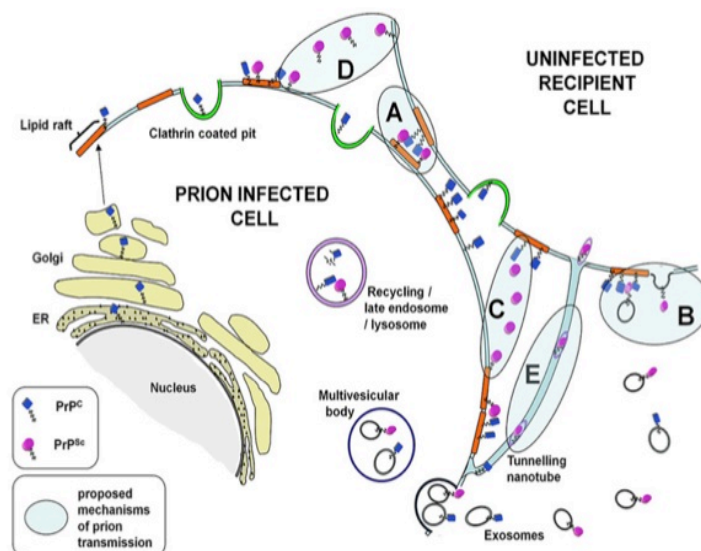


**Figure 23 Possible ways of cell-to-cell prion spreading.** Proposed mechanisms of cell-to-cell spread of prion infectivity. (A) Prion transmission through direct cell-to-cell contact (conversion of recipient PrP<sup>C</sup> without internalization of donor PrP<sup>Sc</sup>). (B) Transmission of prions through exosomal PrP<sup>Sc</sup> association; both a direct interaction of exosome-associated PrP<sup>Sc</sup> with

cell-associated PrP<sup>C</sup> and incorporation of exosomal membrane with recipient cell membrane are represented. (C) C-terminal truncation of PrP<sup>Sc</sup> allowing release from an infected cell and movement to an uninfected recipient cell. (D) "GPI-painting" mode of prion transfer. (E) PrP<sup>Sc</sup> spread through tunnelling nanotubes, in association with small vesicles of lysosomal origin. Mode (A) is represented by lipid raft associated PrP, but could involve non-raft associated PrP. Mode (D) is depicted by transfer of cell surface PrP<sup>Sc</sup>, but could potentially occur with exosomal PrP<sup>Sc</sup> (From Lewis and Hooper 2011).

A brief description of the different means of PrP<sup>Sc</sup> transmission is presented below:

- **Cell-to-cell contact**

From the works of *Kanu* and co-workers (2002) and *Paquet* and colleagues (2007), it has been shown that, in some cases, prion transmission needs a close cell-to-cell contact to occur and that contact with only the medium of infected cells or the physical separation between infected and uninfected cells abrogate infectivity (Paquet et al., 2007; Kanu et al., 2002). However, in both reports, the authors have not postulated a model of transmission. The mechanism could involve, for example, PrP<sup>C</sup> conversion *in trans* in the recipient cell by contact with PrP<sup>Sc</sup> present on the plasma membrane of an infected cell. Moreover, a transfer of infected apoptotic bodies in uninfected cells could not be totally excluded since dead infected cells are still able to pass the infectivity to naïve cells (Kanu et al., 2002).

- **Exosomes**

Exosomes are small vesicular carriers with a diameter of 40-100 nm generated within the lumen of the endosomal system and released in the extracellular space following the fusion of the endosome with the plasma membrane. These vesicles are involved in intercellular communication by transferring not only transmembrane proteins but also nucleic acids and other cytosolic components (Simons and Raposo, 2009). It has been shown that cells can release prions in association with exosomes (Fevrier et al., 2004; Vella et al., 2007); moreover, intracerebral injection of

purified prion-containing exosomal particles resulted in the infection of healthy mice (Fevrier et al., 2004).

### **Microvesicles**

- Besides vesicles of exosomal origin, a recent report describes the involvement of microvesicles (MVs) in prion spreading as well (Mattei et al., 2009). MVs are sub-micron membrane-bound vesicles released by healthy or damaged cells, whose number can increase upon injury, apoptosis or inflammation and are normally present in the blood (Ratajczak et al., 2006). *Mattei* and colleagues (2009) have shown that PrP<sup>Sc</sup> is released from infected murine neuronal cell in association with MVs, resulting in infection both *in vitro* and *in vivo*. Moreover, it has been demonstrated that blood as well as plasma of animals experimentally infected with TSEs can transmit TSE infection by transfusion (Ludlam and Turner, 2006; Cervenakova et al., 2003). In these cases, MVs could be the vehicles for prion transmission through infected blood.
- **Shedding**  
Alternatively, it has also been reported that around 15% of PrP<sup>Sc</sup> is present in a C-terminal truncated form in hamster brains (Stahl et al., 1990). This form results from the cleavage at the level of Gly228, part of sequence Gly-Arg-Arg that is a target for proteolysis and release of bioactive peptides (Stahl et al., 1990). The presence of this C-terminal truncated form of PrP<sup>Sc</sup> in the medium following the actions of a phospholipase- or protease-like activity could also allow the spreading of PrP<sup>Sc</sup> in neighboring uninfected cells (Lewis and Hooper, 2011).
- **GPI painting**  
GPI painting phenomenon consists in the transfer from one cell to another by re-insertion of a functional GPI-anchored protein in the plasma membrane of the recipient cell and seems to occur both *in vitro* and *in vivo* (Legler et al., 2005; Kooyman et al., 1995). *Baron* and co-workers (2002) have suggested that GPI-painting could be one of

the possible mechanisms of PrP<sup>Sc</sup> transfer between cells, as described for PrP<sup>C</sup> in a co-culture system using a PrP<sup>C</sup> expressing cell line (M17-PrP) and the cell line IA lacking PrP<sup>C</sup> (Liu et al., 2002).

- **Tunneling nanotubes (TNTs)**

Tunneling nanotubes (TNTs) are thin membranous bridges containing actin that serve as long-range form of intercellular communication that can easily form between different cell types in culture (Rustom et al., 2004). It has been shown that these structures can traffic both PrP<sup>C</sup> and endogenous and exogenous PrP<sup>Sc</sup> between various cell types of both neuronal and non-neuronal origins (Gousset et al., 2009). TNTs and their role in prion spreading will be described and discussed largely in the next chapter (chapter 6), as this mechanism of prion spreading is one of the subjects of my PhD work.

## 6. Tunneling Nanotubes (TNTs)

The ability of cells to communicate with each other is essential for the life of a multicellular organism and is evolutionarily conserved between species. Without cell-to-cell communication, processes such as remodeling of tissues and organs, differentiation during development, growth, cell division and responses to stimuli could not take place. Therefore, a great number of cellular genes and their products are implicated in intercellular communication and their deregulation leads to the establishment of pathological conditions associated with many diseases (Alberts, 2004).

Recently, long-range forms of intercellular communication consisting of different types of membrane bridges have been described in a wide variety of cell types in *in vitro* cell culture system. Similar connections have also been found *in vivo*. The discovery of these new types of communication highways has opened up new ways of viewing how cells interact with one another, leading to the reconsideration of the traditional view of the cell as a basic unit of structure, function and organization originally postulated by Schleiden and Schwann (1839).

Tunneling nanotubes (TNTs), initially described by *Rustom* and co-workers (2004), are long thin actin-containing bridges connecting PC12 cells in culture that do not contact the substratum, extending up to 100  $\mu\text{m}$  in length with diameters ranging from 50-200 nm. Since then, TNTs have been found in many cell types in culture, from immune to neuronal cells and primary cells, acting as conduits for cytosolic and membrane-bound molecules, organelles and spreading of pathogens (Gerdes and Carvalho, 2008) (Figure 24).

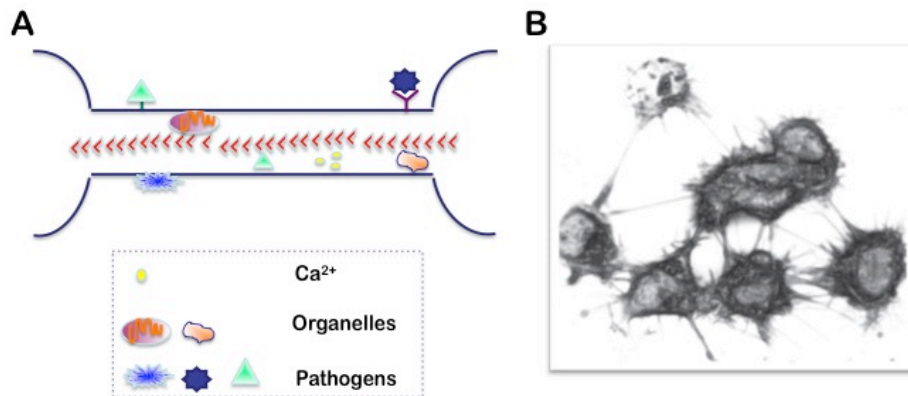


**Figure 24** (A) Schematic representation of cargo transported along a TNT-like structure. Red arrowhead correspond to F-actin cytoskeleton. Identified cargo in TNT-like structures is displayed in box drawn with dotted line. (B) Three-dimensional reconstruction of a network of TNTs in CAD cells (modified from Gousset et al 2009).

This and other examples of intercellular contacts established by different type of mammalian cells as filopodial bridges, viral cytonemes and EP bridges together with plasmodesmata found in plant cells, bacterial and parasite networks reveal a high heterogeneity in both structure and functions of these fascinating new routes of communication that need a further characterization and classification.

### 6.1 Mechanism of TNTs formation

As mentioned above, TNT-like structures were first described in PC12 neuronal cells (Rustom et al., 2004). In these cells, de novo actin-driven formation of TNTs was observed. Further examination of PC12 cells and TNT formation suggested that while the majority of tubes formed via de novo formation, from directed filopodia-like protrusions, a small subset (7%) were also able to form after cells in close contact detached from one another (Figure 25).

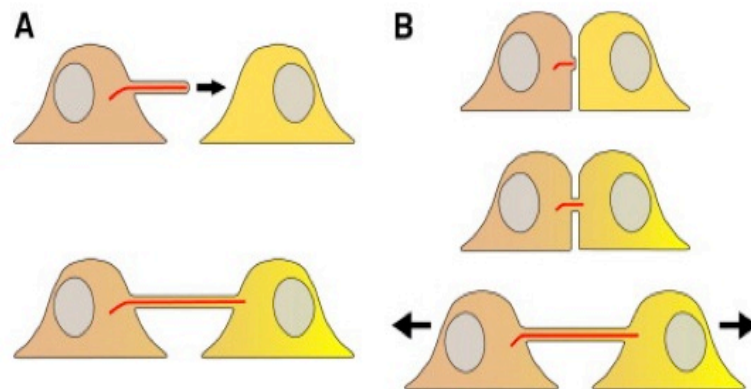


**Figure 25 Model of TNT formation.** (A) One cell forms an actin-driven protrusion directed towards the target cell (top). Fusion of the cell protrusion with the membrane of the target cell results in TNT formation (bottom). (B) TNTs may form between adjacent cells, which subsequently diverge. Red line, F-actin; arrows, direction of filopodium (A) and cell (B) movement, respectively. From Gerdes et al 2007

In the mouse neuronal CAD cell line, both types of TNT formation are observed (Gousset et al 2009). However, the significance and the differences between these various structures remain unclear. Similar to other cell types, TNT-like structures in CAD cells present a high degree of heterogeneity in the diameters (Gousset et al., 2009). Furthermore, as previously described in PC12 cells (Rustom et al., 2004), neuronal TNTs formed between CAD cells contained actin filaments but no microtubules (Gousset et al., 2009). The fact that most TNTs in neuronal cells arise from the extension of filopodia-like protrusions toward neighboring cells suggested that actin polymerization plays an important role in this type of TNT formation. Rustom and colleagues demonstrated that using the F-actin depolymerizing drug latrunculin no TNTs were detected in PC12 treated cells (Rustom et al., 2004). This type of treatment could thus be used to selectively block TNT formation and look at the effect of the presence or absence of nanotubes in various cultures. Using nanomolar concentrations of Cytochalasin D (CytoD), another actin-depolymerizing drug, Bukoretshliev *and colleagues* went further and examined the effects of this drug during the lifetime of TNTs (Bukoreshtliev et al., 2009). They showed that as expected, low levels of CytoD abrogated both filopodia formation and TNT formation. Interestingly, they also demonstrated that

once formed, CytoD had little effects neither on the stability of these tubes and their ability to transfer material from one cell to another. Thus, most neuronal TNTs arise from filopodia-like structures, detached from the substratum. Once formed however, they are no longer sensitive to low levels of actin-depolymerizing drugs, demonstrating that functional TNTs are distinct from filopodia in both structure and function. TNT-like structures have also been described in immune cells, such as B-cells, Natural killer cells and macrophages (Onfelt et al., 2004). In macrophages, two types of nanotubes were also described (Onfelt et al., 2006). The thin nanotubes were found to contain actin filament only, whereas thicker nanotubes, with diameters larger than 0.7  $\mu\text{m}$ , contained both F-actin and microtubules. These different structures also had distinct functions, with the thicker structures being able to transport in a bi-directional manner vesicles and various organelles in a microtubule dependent mechanism. Similarly, long nanotube connections between Jurkat T-cells and primary T cells were also described (Sowinski et al., 2008). Finally, numerous networks of TNT-like structures were observed between dendritic cells and THP-1 monocytes (Watkins and Salter, 2005). These connections varied greatly in length and diameter but were able to quickly transfer calcium fluxes and small dyes to interconnected cells. In Urothelial cell lines, two types of TNT-like structures were described (Veranic et al., 2008). The shorter but more dynamic structures, described as Type I nanotubes, were found to contain actin. These structures did not collapse after micromolar concentrations of CytoD. On another hand, the longer and more stable structures, or type II nanotubes, no longer had actin filaments and were composed instead of cytokeratin filaments. These examples show the disparity in the various cytoskeleton requirements and formation mechanisms in naturally occurring TNT-like structures in neuronal, immunological or epithelial cells. The type of formation however (de novo actin-driven versus cell-to-cell contact) might arise from the nature and role that these cells play in vivo.

## 6.2 Signal and molecules involved in TNTs formation

In order to better understand the role that TNTs may play in intracellular transfer of materials, a better characterization of the initiation steps of TNT formation, the signals that guide the extension of these structures toward a neighboring cell and the mechanisms of binding and fusion need to be elucidated.

Recently, the effects of stress on TNT formation have been analyzed in different cell types (Wang et al., 2011; Yasuda et al., 2011, 2010). Wang and colleagues (2010) have shown that stress induced by hydrogen peroxide ( $H_2O_2$ ) treatment led to an increase in TNT formation in both astrocyte and neurons. They also observed transfer of various organelles, such as ER, Golgi, endosomes and mitochondria via TNTs in astrocytes cultures. For both astrocytes and neurons, it was always the cells undergoing stress that developed TNTs and transferred cellular materials in a uni-directional fashion to the non-activated cell. Thus, suggesting that TNT formation might be directly induced by stress.

Interestingly these authors showed that p53 activation, which is critical in apoptosis, led to an increase in TNT formation independently of stress stimulation, and that down-regulation of p53 blocked TNT formation. Furthermore, EGF receptor up-regulation was also shown to be necessary for TNT initiation. Since the EGF receptor can activate the Akt/PI3K/mTOR pathway, they used various mutants and inhibitors to selectively block or activate each protein and found that this pathway was indeed up regulated in  $H_2O_2$  activated cells leading to an increase in TNT development. In another study, looking at a macrophage cell line and HeLa cells, it was demonstrated that the interaction between m-Sec and the Ral/exocyst complex was also critical for TNT formation (Hase et al., 2009). Thus, to see if m-Sec might also be important for TNT formation in astrocytes, Wang and colleagues looked by RT-PCR at the levels of mSec in astrocytes and found a positive relationship between  $H_2O_2$  treatment and the levels of m-Sec expression (Wang et al., 2010). They concluded that m-Sec might be regulated by p53 activation. Interestingly, in another study Yasuda and colleagues analyzed the transfer of mitotracker-labeled vesicles via TNTs between endothelial

progenitor cells (EPC) and human umbilical vein endothelial cells (HUVEC) (Yasuda et al., 2010). They observed both TNT formation between the two cell types and transfer of mitochondrial material from the EPC to the HUVEC. Upon treatment of the HUVEC with adriamycin, they observed a large increase in the transfer of mitotracker particles from the non-stressed EPC to the adriamycin-stressed HUVE in an uni-directional fashion. Further characterization in these co-cultures could determine whether the stressed cells might release some signals that might attract filopodia-like protrusions from the EPC to the HUVEC or whether the HUVEC might initiate formation and allow for a reverse transfer of material from the receptor cell to the initiator cell. This is exactly what the authors next set out to demonstrate. Indeed, in a follow-up study, they looked more precisely at the TNT formation mechanisms between these cells (Yasuda et al., 2011). First the authors showed that co-cultures of EPC with collagen I (GC)-stressed HUVEC led to a rescue of HUVEC viability. However, when the EPC were pre-treated with nanomolar levels of CytoD to block TNT formation prior to co-culture with the HUVEC, the rescue effects were almost entirely abrogated, pointing toward the importance of TNT formation from EPC to HUVEC for cell survival. Using both fluorescence microscopy and FACS analyses they showed the existence of basal levels of transfer of lysosomes between the two cell types in a bi-directional manner under non-stressed conditions. However, the transfer was much more efficient as it increased in speed and frequency and was found preferentially between non-stressed EPC and GC-stressed HUVEC, suggesting that the stressed-cells were able to signal and guide filopodia-like protrusions for the formation of *de novo* TNTs to occur. Further examinations suggested that surface-exposed phosphatidylserines (PS) in HUVEC might be able to guide TNT formation from the EPC to the stressed- HUVEC. Indeed, when PS on HUVEC were blocked by binding of Annexin V, the selective TNT formation and transfer from EPC to HUVEC was also blocked. Overall, these studies suggest that transfer of materials via TNTs in most cell types occurred from the cell type that initiated TNT formation to the receptor cell. However, while certain stress conditions might increase the formation of TNTs between cells, it

doesn't affect all cells the same way. Indeed, while in astrocytes and neurons, stress appears to increase TNT formation in the stressed cells leading to an increase in transfer of material, in endothelial cells stress increase the guidance signals from the stressed cells leading to an increased formation of TNTs from the non-stressed cells. Thus, once more the analysis of these two studies brings forward the disparities that exist in formation and nature of TNTs between different cell types. It suggests that even within an identical type of TNT formation (i.e., de novo extension of filopodia-like protrusions) the mechanisms might be very distinct from one another (activation of attractive guidance signals versus activation of initiation of filopodia-like protrusions). However, these studies open up the doors for more general signaling pathways by pointing key elements critical for TNT formation. For example, the role of m-Sec, which was found to be important in macrophages, HeLa cells and astrocytes could be of general importance in TNT formation, independently of cell type. In addition, since filopodia-like protrusions are critical for TNT formation in neuronal cells (Bukoretshliev et al., 2009), molecules that are involved in filopodia formation and dynamic have to be taken into account. In particular, in my PhD thesis I focused my attention to the role that the actin molecular motor protein, Myosin-X might play in both the formation of TNT-like structures and its function in transfer of materials in neuronal cells (described largely below, section 7). In addition, the search for guidance signals and the role that lipids might play in TNT formation might also bring up a better consensus in TNT formation in general.

### 6.3 TNTs-mediated transfer

Tunneling nanotubes have revealed a high degree of heterogeneity also from a functional point of view, as different components seems to be selectively transferred by different cell types. First, further investigation is needed to understand why some cargoes are uni-directionally or bi-directionally transported. Uni-lateral transfer occurs in the case where a donor cell transfers material to an acceptor cell, whereas bi-lateral transfer

happens when both cells mutually exchange materials. The reasons for these different transport mechanisms can depend on the structural components (actin-only versus both actin- and microtubules-containing TNTs) or on specific signals that stimulate nanotube formation and are responsible for directing the traffic in one or two ways.

Up to now several reports have shown that calcium signals could propagate between remote cells through tunneling nanotubes. This is especially important for remote cells that are unable to propagate calcium-mediated signalling to cells in close proximity using gap junctions. Initially, Watkins and Salter (2005) demonstrated that myeloid cells can respond to stimulation through soluble factors or mechanical stress and are able to amplify the cellular response by calcium signalling through membrane connections. Since then, propagation of calcium flux has been shown in many other cell types able to make connections between each other. More recently, the transfer of IP3 receptor (IP3R) and endoplasmic reticulum has been described along TNTs in SH-SY5Y neuroblastoma and HEK cell lines (Smith et al., 2011). Overall, calcium spreading through nanotubes appears to be a good option for different type of cells to quickly spread calcium signalization under physiological conditions, leading to fast responses in connected neighboring cells. Particularly fascinating and newly discovered is the spreading of death signals by nanotubes occurring in Jurkat and primary T cells (Arkwright et al., 2010). The authors have observed FasL and active caspase-3 passage from Fas-activated cells in neighboring non-activated ones was detected, thus resulting in the spreading of apoptosis through fratricide, highlighting that this might be an efficient way to shut down cellular responses (Arkwright et al., 2010). Tunneling nanotubes can be in certain cases be highways for diverse organelle transfer. Labelling with membrane-specific dyes, markers of the endo-lysosomal pathway, or other dyes specific to organelles such as mitochondria, has revealed sub-cellular organelles traveling between cells along these connections (Hurtig et al., 2010). Also, a rescue function of TNT-mediated organelle transfer might be associated with other cell types that undergo injuries as well (Plotnikov et al., 2010; Yasuda et al., 2011). Smaller particles,

named nanoparticles, have also been shown to travel within nanotubes (He et al., 2010). Tunneling nanotubes could be either actively hijacked from different pathogens or transport them as “Trojan horses”, along the membrane or inside, leading to the spreading of infection. Hijacking of these structures can be preceded by induction of TNT formation, thus optimizing pathogen transfer, as has been shown for HIV particles spreading, both surfing on or inside TNTs in primary macrophages (Eugenin et al., 2009). The HIV virus can use these highways to spread as an alternative to the other means already mentioned above. Additional investigations on the trafficking of HIV have shown that HIV specifically traffics in TNTs associated with endocytic compartments and so these organelles could be responsible for viral spread between macrophages (Kadiu and Gendelman, 2011a; b). Finally, Onfelt and colleagues (2006) have shown that *M. bovis* BCG or clusters of several bacteria can surf on thin membrane nanotubes between macrophages before being internalized by receptor-mediated endocytosis, pointing towards a possible role of these structures in bacterial infection by concentrating the pathogen on the entry site for a more efficient invasion.

#### 6.4 TNTs and PrP<sup>Sc</sup> spreading

As described in the section 6, the mechanisms of prion spreading from the periphery to the central nervous system (CNS), and subsequently within the CNS, remain questionable and a number of mechanisms, such as cell-to-cell contact, exosomes and GPI-painting, have been proposed (Kanu et al., 2002; Fevrier et al., 2004; and Baron et al., 2006). It has been shown that TNTs readily formed in neuronal CAD cells (Figure 24) (Gousset et al., 2009) were able to transfer lysosomal organelles, the cellular GPI-anchor prion protein PrP<sup>C</sup>, as well as fluorescently labeled infectious prion particles, PrP<sup>Sc</sup>. Using various co-culture conditions, Gousset and colleagues (2009) have shown that these infectious particles were efficiently transferred to non-infected cells only in the presence of TNTs. Since the prion protein is a GPI-anchored protein, it has the possibility of

traveling via TNTs either at the surface or within vesicular structures. Finally, it has also been demonstrated that the transfer *via* TNTs of infectious prion particles resulted in the transfer of infectivity to the recipient cell. This transfer was not confined to neuronal co-cultures but was also efficiently transferred between loaded Bone-Marrow dendritic cells and primary neurons (Gousset et al., 2009; Langevin et al., 2010). Altogether these studies suggested that TNTs might play a critical role *in vivo* in the spreading of prions within the central nervous system (CNS) and at the periphery (Figure 26).

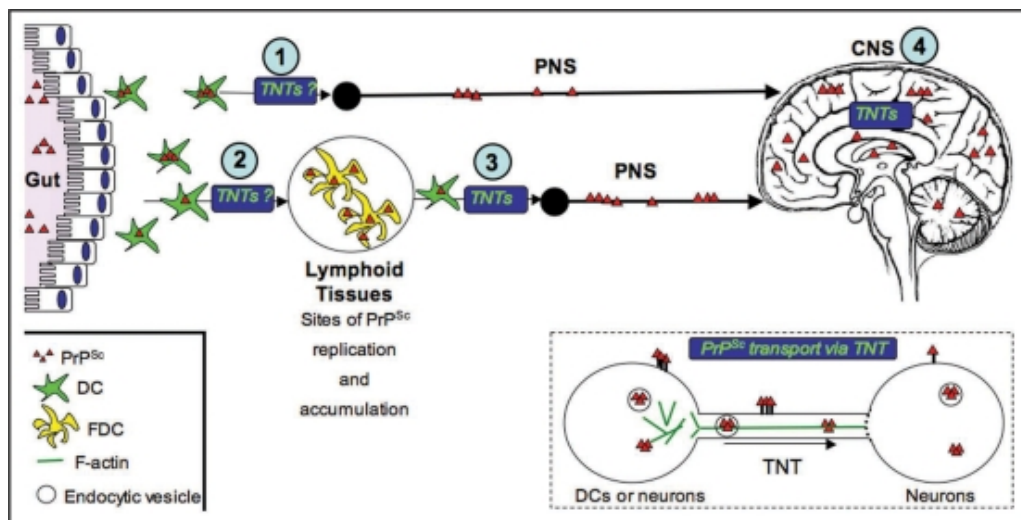


**Figure 26 Transport of PrP<sup>Sc</sup> via TNTs, an alternative spreading mechanism during neuroinvasion.** Studies in our laboratory suggest that TNTs allow for the intracellular transport of PrP<sup>Sc</sup> between dendritic cells and neurons and between neurons (see inset). The exact mechanism of transport remains to be determined. For instance, it is still not clear, whether PrP<sup>Sc</sup> is strictly transported within endocytic vesicles, or whether it can slide along the surface or be transported as aggresomes within the tubes. Similarly, the types of motors used, as well as the possible gated mechanisms to enter the recipient cells are not known. Because of the high propensity of DCs to form TNTs with different cell types, we propose that TNTs could play important roles in delivering PrP<sup>Sc</sup> to the proper cell types along the neuroinvasion route. For instance, DCs could deliver PrP<sup>Sc</sup> from the peripheral entry sites to FDCs in the secondary lymphoid tissues (2) or in a less efficient manner, they might occasionally directly transport PrP<sup>Sc</sup> to the PNS (1). They could also bridge the immobile FDC networks and the PNS (3), since we have shown that DCs can form TNTs with nerve cells. Finally, once PrP<sup>Sc</sup> has reached its final destination within the CNS, TNTs might play a final role in the spreading of PrP<sup>Sc</sup> within the brain between neurons and possibly between neuronal cells and astrocytes (4).

Like prion diseases, neurodegenerative diseases such as Alzheimer, Parkinson and Huntington appear as the result of

protein misfolding and aggregation, it is tempting to wonder whether these diseases might share some common spreading mechanisms. Recently, Wang and colleagues have analyzed whether intracellular A $\beta$  particles could spread through TNTs in astrocytes and neurons (Wang et al., 2010). Microinjection experiments demonstrated that intracellular A $\beta$ -fusion proteins were indeed able to quickly spread from cell-to-cell via TNTs. In addition, they looked at the transfer of A $\beta$  toxicity in co-cultures of infected astrocytes and neurons. They showed that increasing the number of TNTs between the cells by H<sub>2</sub>O<sub>2</sub> treatment led to an increase in neuronal cell death in co-cultures with infected astrocytes compared to the control GFP or non-stressed cells. Thus suggesting that A $\beta$  particle spreading via TNTs within the cultures resulted in an increase in neuronal toxicity leading to cell death. Such observations are very similar to what we found with PrP<sup>Sc</sup> and infectivity and suggest that prion diseases and other neurological diseases might use TNTs as a spreading mechanism. If these types of studies can be further extended to Parkinson or Huntington, they might open up new ways of looking at these diseases and could lead to new strategies to fight them.

## 7. MyoX: an unconventional molecular motor for an unconventional function?

Myosins form a large family of actin-based motor proteins implicated in diverse cell processes, such as cell locomotion, division and organelle transport (Sellers, 2000). Also, myosins mutations are linked to serious pathologies like myopathies, blindness, and hearing loss (Oliver et al., 1999; Toyoshima and Nishida, 2007). They share a general structure that consists of a head, neck and tail. The head is the motor domain that binds to actin and generate force in an ATP-dependent fashion to move along tracks of filamentous actin. The neck can interact with specific light chains or calmodulin. The tail is responsible for binding to specific targets or regulatory factors (Hartman et al., 2011). Myosins superfamily can be divided in at least 20 structurally and functionally distinct classes based on phylogenetic analysis of their conserved heads (Berg et al., 2001; Foth et al., 2006). However, a distinction between ‘conventional’ myosins, involved in muscle contraction and cytokinesis (class II), and ‘unconventional myosins’, that include all the rest, is generally accepted (Sousa and Cheney, 2005).

Myosin-X (Myo-X) is the founding member of a new class of unconventional myosins with a unique tail domain structure that includes multiple pleckstrin homology (PH) domains (Berg et al., 2001). It was initially discovered in a PCR screen to identify new myosins expressed in the inner ear. It appears to be vertebrate-specific and widespread in different tissues (Sousa et al., 2006) but not present in either *C. elegans* or *Drosophila* (Sousa and Cheney 2005). At the cellular level, Myo-X is detected in regions of dynamic actin, particularly along the leading edge of lamellipodia but more frequently at the tips of filopodia (Berg et al., 2000; Sousa and Cheney, 2005). It is also recruited to phagocytic cups in a phosphoinositide 3-kinase (PI3K)-dependent manner (Cox et al., 2002) and plays a role in spindle formation during cell division (Woolner et al., 2008; Toyoshima and Nishida, 2007; Weber et al., 2004). Full-length Myo-10 is a protein of ~ 240 kDa (Figure 25).

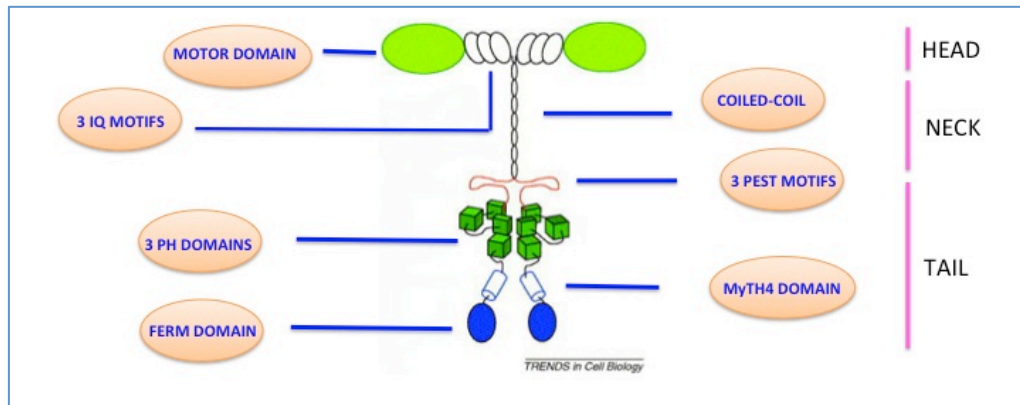


**Figure 27 Schematic representation of the different domains of Myosin-X.** See the text for a detailed description.

The head at the N-terminal is the motor domain interacting with actin bundles that binds to ATP and generates force for movement ; this region is followed by three isoleucine-glutamine (IQ) motifs that serve as calmodulin or calmodulin-like light-chain binding sites (Homma et al., 2000). After the IQ domain, there is a predicted coiled-coil of 10-20 nm probably needed for dimerization (Lupas et al., 1991). The C-terminal globular tail contains binding sites for several cytoskeletal components, plasma membrane, signaling molecules and other factors (Sousa and Cheney, 2005). It consists of different sub-domains: a PEST domain, three PH domains, a myosin tail homology 4 (MyTH4) domain and a FERM domain (Berg et al., 2000). The PEST region (enriched in proline, glutamate, serine and threonine) is often the site of proteolysis by the  $\text{Ca}^{2+}$ -dependent enzyme calpain; the cleavage of Myo-X at this site could serve to permanently ‘unhitch’ the head domain from the tail and, so, stop the activity of the protein (Berg et al., 2000; Sousa and Cheney, 2005). The presence of the three PH domains that follow the PEST domain is a unique feature of Myo-X as these domains are frequently used as binding sites for inositol phospholipids. They have an unusual organization because the first PH domain is split by the insertion of the second one (Cain and Ridley, 2009). The PH2 domain of Myo-X binds with high affinity to PIP3 (Isakoff et al., 1998) and makes it a potential direct molecular target of PI3K, a master regulator of cell motility .

Following the PH domains, there is a myosin tail homology 4 domain (MyTH4) that is a short (~150 amino acids) but well-conserved domain common to other myosins (IV, VII, X, XII and XV) (Chen et al., 2001; Liang et al., 1999) and a plant kinesin (Reddy et al 1996). It has been shown by Weber *et al* (2004) that the MyTH4 domain of Myo-X in *Xenopus* serve as a microtubules binding site, thus highlighting a possible role in bridging the actin cytoskeleton with microtubules (Weber et al., 2004) .

The tail domain of Myo-X ends with a FERM domain (band 4.1, ezrin, radixin, moesin) connected to the MyTH4 by a short linker. The FERM domain seems to require the N-term MyTH4 domain for its cellular functions (Bohil et al., 2006; Tokuo and Ikebe, 2004; Zhu et al., 2007) and it has recently been shown by crystallographic structural studies that these two domains form an integral structural supramodule (Wei et al., 2011). The FERM domain has been shown to bind to  $\beta$ -integrins (Zhang et al., 2004), Mena/VASP actin-capping proteins (Tokuo and Ikebe, 2004), axonal guidance receptor netrin-1 (Zhu et al., 2007) and VE-cadherin (Almagro et al., 2010). The capacity of Myo-X to interact with several cargo proteins allows it to participate in diverse cellular functions. FERM domains consist of three subdomains, the lobes F1, F2 and F3 (Pearson et al., 2000). It has recently been shown that both lobes F2 and F3 strongly interact with a NPXY motif in the cytoplasmic domain of integrin  $\beta_5$  but they are also required for binding to  $\beta_1$  and  $\beta_3$  (Zhang et al., 2004). The direct interaction between Myo-X and integrins is important in localizing these cargo proteins to the tip of filopodia where they can anchor the cell to the extracellular matrix.

The role of Myo-X in initiating filopodia formation and regulation is largely studied and its critical involvement has been demonstrated by many reports (Tokuo and Ikebe, 2004; Sousa and Cheney, 2005; Zhang et al., 2004; Berg et al., 2000; Bohil et al., 2006). Filopodia are cellular extensions acting as cell sensors for the extracellular environment and they are implicated in several fundamental physiological processes, mainly cell migration but also wound healing, development and cell signalling (Gupton and Gertler, 2007). These protrusive structures are thin (0.1-0.3  $\mu\text{m}$ ), finger-like and filled with tight parallel bundles of

filamentous (F)-actin (Mattila and Lappalainen, 2008). The length of filopodia is controlled by a dynamic balance between actin polymerization at the barbed ends of a filament (the rapidly growing filament end) and the retrograde flow (by which the actin filament slowly slides backwards to the cell body (Mallavarapu and Mitchison, 1999).

Myo-X is strikingly enriched at filopodial tips, a major site for signal transduction cascades regulating filopodial extension, retraction and adhesion (Berg and Cheney, 2002). It undergoes a new form of motility within filopodia named ‘intrafilopodial motility’ that consists of fast forward movements by using its motor domain (towards the tip) and slower rearward movements (towards the cell body) together with actin retrograde flow (Berg and Cheney, 2002) (Figure 26).

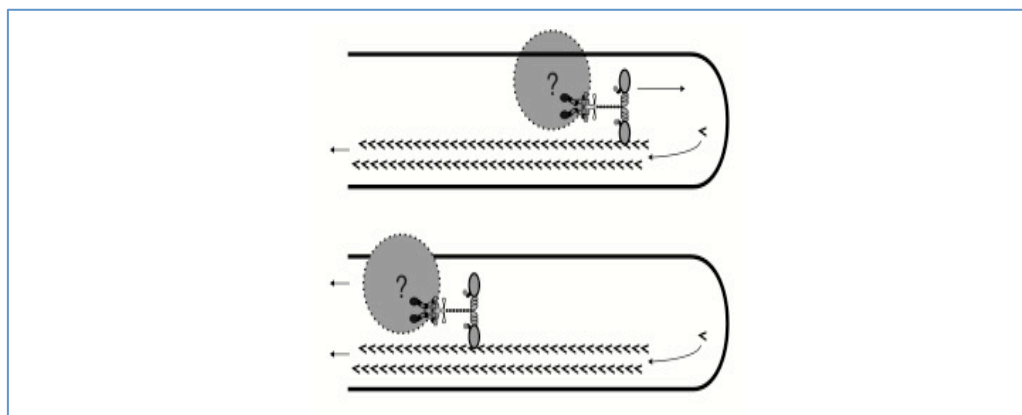


**Figure 28 Myosin-X intrafilopodial motility.** A hypothetical model of M10 function in filopodia. Actin subunits (<) (left arrow). M10 is hypothesized to transport an as yet unidentified cargo, such as cell surface molecules or cytoplasmic signalling complexes (question mark) towards the tip of the filopodium (top) and to move rearward by binding to actin filaments, which are undergoing retrograde flow (bottom).

It has been shown that a GFP-tagged heavy meromyosin (HMM)-like fragment (GFP-MyoX-HMM) consisting of only the head motor domain, neck and coiled-coil is sufficient for tip localization while GFP-MyoX-tail only or GFP-MyoX-Headless (containing neck, coiled coil and tail regions) are both diffused in the cytosol and unable to reach filopodial extremities (Berg and Cheney, 2002). Taken together these experiments show that Myo-X needs its N-

terminal actin-binding motor for filopodial tips localization. More importantly, it has been reported that Myo-X overexpression induces filopodial protrusion (Tokuo and Ibeke, 2004; Berg and Cheney, 2002; Zhang et al., 2004) and this finding raised the possibility that Myo-X could play a role in filopodia formation. Moreover, a recent work has shown that Myo-X without the tail domain can initiate filopodia upon dimer formation but these newly formed filopodia appeared to be short and unstable, differently from the over-expression of the full-length protein (Tokuo et al., 2007). This suggests that the tail domain is necessary to bring the right components to the growing site of filopodia, thus stabilizing and elongating these structures .

In addition, Bohil *and colleagues* have shown that Myo-X overexpression is a great inducer of dorsal filopodia, that do not contact the substratum, in COS-7, HEK-293 (human embryonic kidney), HUVEC (human umbilical vein endothelial cells) and CAD (mouse neuronal cell line) cells. Also, by knocking-down the Myo-X gene, they have shown that in absence of Myo-X there is a substantial loss of dorsal filopodia indicating that this protein is necessary for their formation (Figure 27).

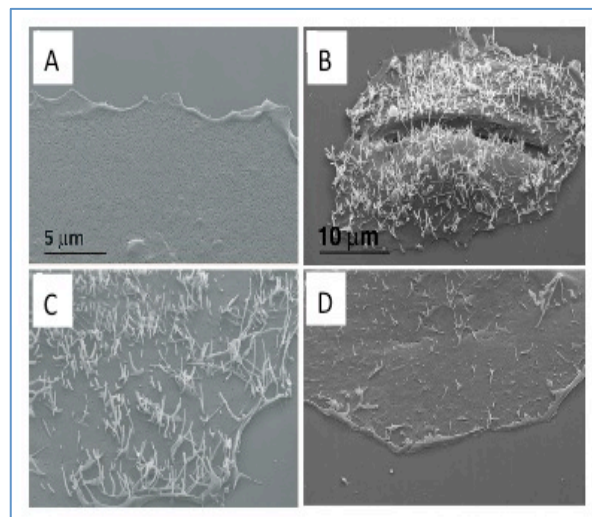


**Figure 29 Effect of Myosin-X over-expression and knock-down.** (A) The dorsal surfaces of control COS-7 cells transfected with GFP alone are smooth and lack dorsal filopodia. (C) Cells transfected with GFP-Myo10, however, exhibit a massive increase in dorsal filopodia (B) SEM of a HeLa cell treated with control siRNA showing the numerous dorsal filopodia normally present on HeLa cells. (D) SEM of a HeLa cell from the same experiment treated with Myo10

siRNA showing the loss of dorsal filopodia induced by Myo10 siRNA (Modified from Bohil et al 2006).

It is interesting to note that the implication of Myo-X in the formation of dorsal filopodia highlights the fact that the anchoring to the substratum is not necessary for Myo-X function. Accordingly, the deletion of the FERM domain did not impair the ability of Myo-X to induce filopodia (Bohil et al., 2006) even if the attachment to the substrate by integrin binding could facilitate substrate-attached filopodia formation (Zhang et al., 2004).

It has been also demonstrated that Myo-X can act downstream of Cdc42 that is a master regulator in filopodia formation (Bohil et al., 2006). However, it remains unclear how Myo-X could promote filopodia formation. Also, PIP3 has been shown to play an important role in filopodia induction by regulating Myo-X localization and function (Plantard et al., 2010). Indeed, the PH2 domain of Myo-X binds to the membrane lipid PtdIns(3,4,5)P<sub>3</sub> and no other PI and disrupting this interaction causes the redistribution of Myo-X in Rab7-positive endosomal vesicles that could be involved in trafficking and recycling of the protein (Plantard et al., 2010). Myo-X mutants lacking the PIP3 binding site do not promote induction of filopodia as the HMM-MyoX (Berg and Cheney, 2002). The mechanism of regulation is not clear but it could be possible that PIP3 binding to Myo-X is necessary to anchor the protein on the membrane; alternatively it can also be possible that PIP3 is a cargo for Myo-X that after reaching filopodial tips promote actin polymerization and thus filopodia growth (Plantard et al 2010).

Besides, it has been recently shown by using a series of truncation mutants of myosin-X that the tail domain (PH-FERM) directly interacts with the motor domain to inhibit its activity in a phospholipid-dependent and Ca<sup>2+</sup>- independent manner (Umeki et al., 2011). Based on this finding, Umeki *and co-workers* propose that this intramolecular interaction is responsible for maintaining the motor domain in an inhibited state preventing it from free movement in physiological ionic condition, thus regulating the activity of Myo-X. The binding of PIP3 to the PH domain disrupts the interaction between the head and the tail domains and this activates both the motor activity and dimer formation of Myo-X allowing the transport of its cargo complex (Umeki et al., 2011).

As already mentioned above, the distribution of Myo-X is widespread and expressed at low level in different tissues. In the brain, the function of Myo-X is still not clear but it has been shown, for example, that its mRNA increases seven-fold upon peripheral nerve crush, thus indicating that it can be involve in nerve regeneration after injury (Tanabe et al., 2003). mRNA for Myo-X protein is expressed in neurons, such as Purkinje cells, and in non-neuronal cells such as astrocytes and ependymal cells. In these cells, Myo-X localized at neuronal extensions, in neuronal filopodia, growth cones, neurites but also in the cell body (Sousa et al., 2006). Also, in undifferentiated CAD neuronal cell lines (Qi et al., 1997), Myo-X exhibits a punctuate pattern at the filopodial tips, confirming a role for this protein in filopodia dynamic (Sousa et al., 2006).

Moreover, a short form of Myo-X of ~ 165 kDa lacking the motor domain is also expressed in adult brains with the exception of the cerebellum where it is present only at early stages of development and then it disappears. This 'headless' Myo-X localizes in the cell body and is unable to undergo intrafilopodial motility (Sousa et al., 2006). Regarding its role in the brain, it could act as 'dominant negative', regulating Myo-X full-length activity in neurons or can have independent functions in other cell processes (Sousa et al., 2006). It is interesting to note that, while in the cerebrum, both Myo-X full-length and headless forms are expressed at similar levels, in the cerebellum, only the full-length form is increasing upon time and it appears to be highly regulated during development (Sousa et al., 2006). More recently, it has also been shown that Myo-X is highly expressed in the cranial neural crest (CNC) cells in embryos of *Xenopus laevis* where it is required for head and jaw cartilage development and has an essential function in migration (Hwang et al., 2009). An interesting recent report from Singh *and colleagues* (2010) have shown that Myo-X is implicated in a new model of melanin transfer named 'filopodial-phagocytosis model' in between melanocytes (MCs) to keratinocytes (KCs) crucial for the protection of the skin against UV radiations (Singh et al., 2010). Accordingly with these findings Myo-X drives filopodia formation and elongation in a Cdc42-dependent manner in MCs, creating conduits for melanosomes (specific organelles containing

melanin). Filopodial protrusions containing the melanosomes are then anchored to the membrane of KCs by integrin-binding and the help of Myo-X. In this model, the motor activity of Myo-X present at the tips could facilitate the phagocytic uptake of melanosomes by the KCs (Singh et al., 2010). In the second part of my results I have analyzed the role of Myo-X in the formation and transfer function.

# AIMS OF THE STUDY

---

## Aims of the study

Prion diseases are neurodegenerative disorders characterized by the conformational change of a cellular protein, PrP<sup>C</sup>, in its pathological counterpart, PrP<sup>Sc</sup> (Prusiner, 1998). Differently from PrP<sup>C</sup>, PrP<sup>Sc</sup> is enriched in  $\beta$ -sheets, prone to aggregation, proteinase K-resistant. It represents the main component of prions, which are the infectious particles associated with the disease (as already described in the introduction, section 1.1). Despite the intense research, many questions in prion biology are still opened related to both the physiological functions of PrP<sup>C</sup> and mechanism of the disease caused by the misfolded form PrP<sup>Sc</sup>. Thus, exploring some of these aspects at the molecular and cellular level is of fundamental importance for a better understanding of these fatal disorders and for developing potential therapeutical approaches.

My PhD work has been focused on two major projects:

- PROJECT 1 Role of autophagy in *in vitro* models of prion disease
- PROJECT 2 Characterization of PrP<sup>Sc</sup> spreading from cell-to-cell by Tunneling Nanotubes (TNTs) in a prion infected neuronal cell model

### PROJECT 1:

#### Role of autophagy in *in vitro* models of prion disease

The role of protein degradation systems in protecting cells from aberrant, misfolded proteins has been in the spotlight due to its emerging relevance to human neurodegenerative diseases (Wong and Cuervo 2010). Autophagy is a cellular process responsible for the degradation of long-lived proteins, organelles and for maintaining steady amino acid pools when the cell is starved. Indeed, autophagy has been recently described as an important process in the pathogenesis of neurodegenerative diseases of protein aggregation such as Alzheimer disease, Parkinson disease, tauopathies and Huntington disease (Cherra et al. 2010). As

already mentioned before (Introduction, section 1.4) the role of autophagy in prion disease is still controversial and highly debated (Heiseke et al. 2010). Initially, autophagic vacuoles were detected in cell models chronically infected with prions (Schatzl et al., 1997) and in neuronal perikarya, neurites and synapses in experimentally induced scrapie, Creutzfeldt-Jakob disease (CJD) and Gerstmann-Sträussler-Scheinker (GSS) syndrome (Liberski et al., 2004). It was therefore proposed that autophagy could play a disease-promoting role by contributing to the formation of the spongiform changes, a pathological hallmark in prion-affected brains (Liberski et al., 2004 and 2008). More recently, it has been demonstrated that a number of autophagy-inducing compounds such as lithium salts, trehalose and rapamycin are effective in reducing PrP<sup>Sc</sup> burden in cultured neuroblastoma cells (N2a) and delay the onset of symptoms in prion-infected mice in prophylactic treatment models (Aguib et al., 2009; Heiseke et al., 2009).

Therefore, a more systematic analysis of the role of autophagy in prion infection is needed because the molecular mechanisms by which autophagy would be either protective or co-responsible for the disease are not well understood yet.

In this context, I divided this part of my PhD work in three specific objectives:

- a. To investigate the state of the autophagic pathway in different model of prion infected cells compared to non infected cells;
- b. To examine whether induction of autophagy has a role in prion degradation by clearing PK-resistant prion protein (PrP<sup>Sc</sup>) in different infected neuronal cell models;
- c. To investigate possible drugs and alternative pathways involved in prion clearance.

This first part of my work has been submitted to Molecular Biology of the Cell as a paper in which I am the first author (See Results section 1).

## **PROJECT 2:**

### **Characterization of PrP<sup>Sc</sup> spreading from cell-to-cell by Tunneling Nanotubes (TNTs) in a prion infected neuronal cell model**

In variant Creutzfeldt-Jakob disease, prions PrP<sup>Sc</sup> enter the body with contaminated foodstuffs and can spread from the intestinal entry site to the central nervous system (CNS) by intercellular transfer from the lymphoid system to the peripheral nervous system (PNS) (Mabbott 2006). Although several means and different cell types have been proposed to have a role, the mechanism of cell-to-cell spreading remains elusive (Introduction, section 1.6).

TNTs have been identified between cells, both *in vitro* and *in vivo*, and may represent a conserved means of cell-to-cell communication (Introduction, section 1.7). Gousset *et al.* (2009) have shown that TNTs allow transfer of exogenous and endogenous PrP<sup>Sc</sup> between infected and naïve neuronal CAD cells. Significantly, transfer of endogenous PrP<sup>Sc</sup> aggregates was detected exclusively when CAD cells chronically infected with 139A mouse prion strain were connected to CAD cells by means of TNTs, thus identifying TNTs as an efficient route for PrP<sup>Sc</sup> spreading in neuronal cells (Gousset et al 2009).

Therefore, to characterize the intercellular trafficking of PrP<sup>Sc</sup> *via* TNTs and to investigate the mechanisms of TNT formation and function is of fundamental importance in prion biology and could lead to a better understanding of prion invasion and spreading to the brain of a particular host.

In this context, I divided the second part of my PhD work in the following objectives:

- a. Characterization of the sub-cellular compartments allowing the vesicular trafficking of PrP<sup>Sc</sup> inside TNTs connecting CAD cells;
- b. Role of both cellular and pathological PrP isoforms on TNT formation and transfer;
- c. Role of Myosin-X in TNT formation, TNT-mediated transfer and PrP<sup>Sc</sup> spreading from cell-to-cell.

This second part of my results has been performed in collaboration with a post-doc in the lab and will be submitted beginning of 2012 in a paper in which I will be second author.

In addition I have contributed to a review as first co-author that will be submitted by December 15 to *Frontiers in Membrane Physiology and Biophysics* (see **ANNEX 1**).

# MATERIALS AND METHODS

---

## Material and Methods

### Cell lines

GT1-1 cells (gift of Dr. Mellon P., University of California, San Diego, USA) were infected with RML prion strain (gift of Dr. Korth K., Heinrich Heine University, Dusseldorf, Germany). N2a cells and scN2a cells (infected with 22L prion strain) were provided by Dr. Korth K. Non-infected and prion-infected GT1-1 and N2a cells were maintained in Dulbecco's modified Eagle's medium (DMEM) (Invitrogen) supplemented with 10% of fetal calf serum (FCS). CAD and scCAD (infected with 139A prion strain) were both gifts of Dr. Laude H. (Institut National de la Recherche Agronomique, Jouy-en-Josas, France) and were cultured in Opti-MEM (Invitrogen) with addition of 10% FBS.

### Chemicals and antibodies

Rapamycin, Tamoxifen, HO-Tamoxifen and Bafilomycin A1 were all purchased from Sigma. Puromycin dihydrochloride used for stable selection, 25% glutaraldehyde solution and 1M HEPES solution were from Sigma.

SAF32 and Sha31 anti-prion antibodies were purchased from SpiBio. Anti-tubulin monoclonal antibodies and anti-ATG7 were from Sigma. Anti-MyosinX rabbit polyclonal antibody was purchased from Sigma. Myosin X shRNA (m) lentiviral particles, control shRNA lentiviral particles and Polybrene® reagent were from Santa Cruz Biotechnology, INC. Anti-LAMP1 antibodies were purchased from BD Pharmingen™. Anti-LC3 monoclonal antibody, used for western blotting, was from nanoTools and anti-LC3 polyclonal antibody, used for immunofluorescence, was purchased from MBL International. Anti-EEA1 and anti-Vamp1, 2, 3 antibodies were from Synaptic Systems, Germany. All the fluorescently labelled secondary antibodies as well as LysoTracker® green were purchased from Invitrogen (Molecular Probes). HCS *CellMask*™ Blue stain, Vybrant® DiD cell-labeling solution (DiD), wheat germ agglutinin tetramethylrhodamine conjugate (WGA-rhodamine) were purchased from Molecular Probes (Invitrogen). Fluorescently-labelled PrP<sup>Sc</sup> (Alexa546-PrP<sup>Sc</sup>)

was prepared as previously described (Gousset et al., 2009).

### **Plasmids, siRNAs and transfection procedures**

The tandem fluorescently- tagged (with both GFP and RFP) LC3 (Tf-LC3) and GFP-LC3 plasmids were a kind gift from Dr. Ballabio A. (Telethon Institute of Genetis and Medicine (TIGEM), Naples, Italy) and Dr. Yoshimori T. (Research Institute for Microbial Diseases, Osaka University, Osaka, Japan). The GFP-LC3 plasmid was provided from Dr. Yoshimori T. (Research Institute for Microbial Diseases, Osaka University, Osaka, Japan). ATG7 siRNA predesigned ON TARGETplus SMARTpool and siGENOME RISC-Free Control siRNA were both purchased from Dharmacon. GFP-MyoX full-length, GFP-MyoX-Headless, GFP-MyoX-HMM constructs were a kind gift from Dr. Cheney R. E. (University of North Carolina, Chapel Hill, NC, USA). GFP-MyoX- $\Delta$ F2, GFP-MyoX- $\Delta$ F3, mCherry-MyoX full-length were provided by Dr.Strömlad S. (Center for Biosciences, Department of Biosciences and Nutrition, Karolinska Institutet, 14183 Huddinge, Sweden). eGFP-vector CFP-vector and mCherry-vector were from Clontech. GFP-PML was a kind gift of Dr. Enninga J. (Dynamique des interactions hôte-pathogène, Institut Pasteur, Paris, France).

GT1-1 and scGT1 cells were transfected at 50% confluence using FuGENE6 (Roche Diagnostic) for DNA constructs according to manufacturer's protocol. To downregulate ATG7, 100 nM concentration of oligo was used with 10  $\mu$ l of HiPerFect (Qiagen) per 60 mm dish. Hyperfect reagent was mixed with siRNA in DMEM without FBS, incubated for 10 min at room temperature and added to the cells.

Transfection of both non-infected and infected CAD and N2a cells with DNA constructs was done using Lipofectamine 2000 (Invitrogen), according to producer's protocol.

When detection of PrP<sup>Sc</sup> levels was performed, downregulation and overexpression of the proteins were maintained for 5-day period. Therefore in all the experiments siRNA and plasmids, except of pEGFP were transfected twice (a second round of transfection was performed 3 days post-transfection).

## **MyoX shRNA lentiviral particles transduction and stable clones selection**

CAD cells (40000) were plated in a 12-well plate 24h prior transduction. Transduction protocol was performed accordingly to manufacturers' instructions ([lentiviral particles transduction protocol](#)). Stable clones expressing both control and MyoX shRNA were selected and maintained in culture by adding 5 µg/ml of puromycin dihydrochloride to kill non-transduced cells. Western blotting was used to evaluate the percentage of MyosinX gene downregulation after cell lysis and Bradford protein colorimetric assay to measure protein content.

## **Treatment of ScGT1, scCAD and scN2a cells with different drugs**

Rapamycin, Tamoxifen, HO-Tamoxifen were reconstituted according to manufacturer's instructions. All the drugs were used in DMEM + 10% FCS at the final concentration of 2 µM for Rapamycin, and 5 µM concentration for Tamoxifen and HO-Tamoxifen. During the 3 or 5 day-treatment, medium containing the different drugs was changed every 2 days. 5M stock concentration of NH<sub>4</sub>Cl from powder (Sigma) was prepared in sterile Ultra-pure MilliQ water.

When needed, Bafilomycin A1 or NH<sub>4</sub>Cl, respectively at 100 µM and 15 mM concentration were added to the Rapamycin, Tamoxifen or HO-Tamoxifen 5 day treatment for 2 days starting from the 4<sup>th</sup> day of the different treatments.

## **Protein analysis by western blotting**

Cells grown in 60 mm dishes after the different treatments were lysed in 500 µl of Lysis buffer (0,5% triton X-100, 0,5% DOC, 100 mM NaCl, 10 mM Tris-HCl pH 8). To analyze PrP<sup>Sc</sup> levels, 250 µg of protein/lysate were treated with 5 µg of Proteinase K (PK) for 30 min at 37°C. This step allows detecting PrP<sup>Sc</sup> content only, because of its partial resistance to PK. The protein content was then methanol-precipitated overnight at -20°C and centrifuged at 13000g for 30 minutes. After drying at 100°C, the pellet was

resuspended and denatured in Laemmli buffer before SDS-PAGE and western blot with the Sha31 anti-PrP antibody. All the other proteins, including total PrP, were analysed by western blotting from 20 or 40  $\mu\text{g}$  of total lysate. HRP-conjugated secondary antibodies and ECL™ reagents from Amersham (GE Healthcare) were used for detection.

## Immunofluorescence

For immunofluorescence analysis cells grown on coverslips into a 24 well plate or on  $\mu$ -Dish<sup>35mm, high</sup> (35 mm Petri dish with a thin bottom for high end microscopy, from Ibidi ®) were carefully washed with PBS, fixed with 2% PFA for 30 minutes and permeabilized with 0,1% of Triton X-100/PBS. A denaturation step with 6M guanidine-hydrochloride (Gnd-HCl) was performed for 10 minutes after permeabilization to detect PrP<sup>Sc</sup> in infected cells (Taraboulos et al., 1990), when needed. Cells were then blocked in 2% BSA/PBS, immunolabelled with primary and secondary antibodies and mounted with Aqua/Poly Mount (Polysciences). Additionally, CAD cells were stained for 30 minutes with HCS *CellMask*™ Blue stain (1:10000) and *rhodamine*-conjugated *WGA* (1:300) in PBS solution, when needed.

In order to label endogenous LC3, cells were differently treated as previously described (Kimura et al., 2009).

When filipin staining was used, cells were fixed with 4% PFA for 60 min and blocked with 0,2% BSA/PBS. Filipin (250  $\mu\text{g}/\text{ml}$ ) was added to blocking solution and additional 30 min incubation was performed after incubation with secondary antibodies.

## Fluorescence Microscopy

Immunofluorescences were analysed by high-resolution wide-field microscope Marianas (Intelligent Imaging Innovations) using 63x oil objective. All Z-stacks were acquired with Z-steps of 0.27  $\mu\text{m}$ . The auto-scaling (min/max) of signal detection was used to record only maximal signal intensities when PrP<sup>Sc</sup> was analyzed (Marijanovic et al., 2009). For colocalization studies of PrP<sup>Sc</sup> in different organelles in tunnelling nanotubes of CAD cells

fluorescence images were acquired with a *Perkin Elmer* (PE) UltraView® laser *spinning disk confocal imaging system* using a 63x immersion-oil objective. All Z-stacks were acquired with Z-steps of 0.3  $\mu\text{m}$ .

In the live experiments, CAD cells plated on ibidi dishes were either transfected with GFP-LC3 plasmid or incubated with LysoTracker (1:1000 dilution) for 30 min at 37 °C prior to be challenged with 1  $\mu\text{l}$ /dish of sonicated Alexa546-PrP<sup>Sc</sup>. The time-lapse movies were acquired with Biostation IM (from Nikon) and a widefield microscope (Zeiss Axiovert 200M) controlled by Axiovision software.

### **Tunneling nanotubes (TNT) detection by Fluorescence Microscopy**

To evaluate the number of TNT-connected cells TNT structures were analyzed by fluorescence microscopy. Cells were plated on  $\mu\text{-Dish}^{35\text{mm, high}}$  and maintained at 37 °C ON. Then cells were fixed for 30 minutes at room temperature (RT) with fixative solution 1 (2% PFA, 0.075% glutaraldehyde, 0.2M Hepes in PBS) and additionally for other 30 minutes at RT with fixative solution 2 (4% PFA and 0.2M Hepes in PBS). Then cells were carefully washed in PBS and labeled for 20 minutes at RT with WGA-rhodamine (1:300 in PBS solution) and 20 minutes at RT with HCS *CellMask*<sup>™</sup> Blue stain (1:10000 in PBS solution). WGA and HCS *CellMask*<sup>™</sup> cell stainings permit cell segmentation and TNT detection. Image stacks covering the whole cellular volume were acquired with a widefield microscope (Zeiss Axiovert 200M) controlled by Axiovision software.

### **Transfer of PrP<sup>Sc</sup> from scCAD to CAD through TNTs by Fluorescence Microscopy assay**

Cocultures of scCAD cells (donor cells) transfected with either pGFP-vector or GFP-MyoX full-length and GFP-PML transfected CAD cells (acceptor cells) were plated on  $\mu\text{-Dish}^{35\text{mm, high}}$  in ration 1:1 and maintained ON at 37°C. Cells were then fixed with 2% PFA for 30 minutes, permeabilized for 4 minutes with 0.1% Triton X-100 (Sigma), denatured for 10 minutes with 6 M Gnd-

HCl. After extensive washes in PBS, cells were immunostained with Sha31 (1:500 in PBS) and AlexaFluor 546-conjugated secondary antibody. Additionally, cells were stained with HCS *CellMask*<sup>™</sup> Blue stain (1:10000 in PBS solution) for 30 minutes at RT before mounting. Image stacks covering the whole cellular volume were acquired with a widefield microscope (Zeiss Axiovert 200M) controlled by Axiovision software. The auto-scaling (min/max) of signal detection was used to record only maximal signal intensities when PrPSc was analyzed (Marijanovic et al., 2009).

### **DiD-vesicle transfer in CAD cells by Flow Cytometry (FACS)**

For quantitative analyses of intercellular organelle transfer, cocultures of CFP-vector transfected CAD cells (acceptor population) and DiD-labelled CAD cells transfected with alternatively GFP- or mCherry-tagged constructs harboring proteins of interest (donor population) were plated at a ratio of 1:1 on 35 mm dishes (each experiment has been performed in triplicate). Notably, the DiD staining was performed as following. After counting, cells were centrifuged for 4 minutes at 1000 rpm and incubated with 1:3000 DiD solution in complete medium for 30 minutes at 37°C. Then, cells were centrifuged for 4 minutes at 1000 rpm and washed in complete medium 30 minutes at 37°C. Analysis of organelle transfer was performed at 16h after cell plating (overnight, ON). For this purpose, cells were scraped with 500 µl of PBS and passed through sterile 40 µm nylon cell strainers (BD Falcon<sup>™</sup>) in order to obtain single cell suspensions. Cells were then mixed with 500 µl of 4% PFA solution and let in fixation at 4°C, overnight (ON). For FACS analysis, DiD-labeled donor cells and CFP-vector transfected acceptor cells were analyzed at 633 nm and 488 nm excitation wavelengths, respectively. Flow cytometry analysis of organelle transfer (DiD-vesicle) was performed on a CyAn ADP flow cytometer (Dako Cytomation, Beckman Coulter, Inc.).

## Image processing and quantification

Raw data (both images and movies) were processed with Image J software. The constrained iterative algorithm in Slidebook 4.2 software (Intelligent Imaging Innovations) was used to deconvolve the images acquired with the high-resolution wide-field microscope Marianas. Also, in these experiments, colocalization was quantified by intensity correlation coefficient-based (ICCB) analysis using JACoP (Bolte and Cordelières, 2006). Statistical analysis of the correlation of the intensity values of both green and red pixels or blue and red pixels in dual-channel image was performed using Pearson's and Manders's coefficient and Van Steensel's approach (van Steensel et al., 1996).

To evaluate the number of TNT-connected cells, a manual analysis was performed independently by two different people and each experiment was made at least in triplicate.

To detect PrP<sup>Sc</sup> particles in CAD cells (acceptor cells) in coculture experiments and to quantify the percentage of PrP<sup>Sc</sup> particles in different organelles in TNTs of CAD cells a dedicated version of the QUIA (QUantitative Image Analysis) software (<http://www.bioimageanalysis.org/>) provided by the Quantitative Image Analysis unit (headed by J.-C. Olivo-Marin, Institut Pasteur, Paris, France) was used. FACS raw data were analysed by Kaluza® Flow Cytometry software (Beckman Coulter, Inc.).

## Statistical analysis

Standard error was used to test the *difference between the means* of two or more independent experiments. All data were statistically validated by Student's T-test. The differences were considered significant when  $p < 0.05$ .

## RESULTS AND DISCUSSION

---

## PROJECT 1:

### Role of autophagy in *in vitro* models of prion disease

*The Manuscript related to this first part of my results has been submitted to the journal "Molecular Biology of the Cell" and is appended at the end of this section.*

#### 1.1 Objectives

- a. To investigate the state of the autophagic pathway in different model of prion infected cells compared to non infected cells;
- b. To examine whether induction of autophagy has a role in prion degradation by clearing PK-resistant prion protein (PrP<sup>Sc</sup>) in different infected neuronal cell models;
- c. To investigate possible drugs and alternative pathways involved in prion clearance.

#### 1.2 Specific Background

Although PrP<sup>C</sup> and PrP<sup>Sc</sup> proteins share the same primary structure, PrP<sup>Sc</sup> diverges from PrP<sup>C</sup> insofar as it acquires a greater content of  $\beta$ -sheets compared to the predominantly  $\alpha$ -helical secondary structure of the normally folded protein. The accumulation of this protease-resistant, aggregate-prone form is associated with neuronal death and pathological features in affected individuals (Prusiner 1998). PrP<sup>Sc</sup> persistence in cultured cells is thought to be maintained by a balance between its formation following the conformational change of PrP<sup>C</sup> into PrP<sup>Sc</sup> and its degradation (as described in the Introduction, section 1.1). A better understanding of PrP<sup>Sc</sup> metabolism and particularly how to shift the equilibrium between PrP<sup>Sc</sup> production and degradation is very important to understand the pathogenesis of the disease. Furthermore it could help in developing therapeutic

strategies for prion disease. However, due to the lack of PrP<sup>Sc</sup>-specific antibodies, PrP<sup>Sc</sup> cellular trafficking, production and degradation are poorly defined. Both the plasma membrane and the endosomal recycling compartment (ERC) have been demonstrated to be sites where PrP<sup>C</sup>-PrP<sup>Sc</sup> conversion occurs (Marijanovic et al 2009; Goold et al 2011). Moreover, recent studies suggest a role for lipid rafts in prion conversion (Campana *et al.*, 2005; Taylor and Hooper, 2006; Taylor and Hooper, 2011). Indeed, it has been reported that both PrP<sup>C</sup> and PrP<sup>Sc</sup> localize in these particular domains, enriched in cholesterol and glycosphingolipids (Simons and Ikonen 2002; Lingwood and Simons 2010). Interestingly, it has been demonstrated that cholesterol depletion impairs PrP<sup>Sc</sup> production (Taraboulos et al 1995; Bate et al 2004). More recently, Gilch and colleagues (2009) have also shown that inhibition of cholesterol recycling impairs cellular PrP<sup>Sc</sup> propagation. On the other hand, different degradation pathways might be involved in reducing intracellular PrP<sup>Sc</sup> burden. For example, a role for the lysosomal compartment in PrP<sup>Sc</sup> degradation has been described in several reports which have shown that in different infected neuronal cell lines PrP<sup>Sc</sup> is sequestered in lysosomes where can be degraded (Borchelt et al 2002; Caughey et al 1991; McKinley et al 1991; Jeffrey et al 2006; Marijanovic et al 2009; Gousset et al 2009; Veith et al 2009). More recently it has been shown that macrophages, involved in early stages of prion infection, might degrade PrP<sup>Sc</sup> via the lysosomal and proteasomal pathways (Sassa et al 2010). Furthermore, upon block of the proteasome activity significant changes in total PrP levels that result in accumulation of aggregated PrP forms in the cytosol, have been observed in N2a cells (Nunziante et al 2011). Finally, several studies have shown that the ER-associated degradation pathway (ERAD) is involved in the degradation of pathogenic PrP mutants linked with familial prion diseases and is responsible for the degradation of misfolded PrP isoforms (Zanusso et al 1999; Nunziante et al 2011). Macroautophagy (hereby referred to as autophagy) is another cellular degradation system for long-lived proteins and organelles, normally activated upon starvation for energy supply (Yang and Klionsky, 2007). Recently, autophagy has been described to play an important role in diverse physiological and pathological

processes and, in particular, in neurodegenerative diseases associated with protein aggregation (Wong and Cuervo 2010). The role of autophagy in prion disease is controversial. Early works indicated the presence of autophagic vacuoles in prion-infected GT1 (scGT1) cells and in murine models of induced scrapie, Creutzfeldt-Jakob disease (CJD) and Gerstmann-Sträussler-Scheinker (GSS) syndrome as hallmarks of cytopathology upon prion infection (Schazl et al 1997; Liberski et al., 2004; Sirkosa et al 2004). This suggested that the activation of the autophagic pathway could contribute to the pathogenesis of the disease. On the contrary, more recently it has been shown that a number of autophagy-inducing compounds such as lithium salts, trehalose and rapamycin can reduce PrP<sup>Sc</sup> burden in cultured neuroblastoma (N2a) cells (Aguib et al 2009; Heiseke et al 2009), pointing towards a protective role of autophagy in prion infection. Hence, in order to shed light on this still controversial open question in prion biology we decided to further characterize of PrP<sup>Sc</sup> metabolism at cellular level and investigate the possible role of autophagy in PrP<sup>Sc</sup> clearance.

### 1.3 Summary of the results

In order to investigate the role of autophagy in prion infection, we first evaluated the autophagic flux in prion-infected cells by comparing it with uninfected cells. For this purpose, we used two well-established *in vitro* cell models, named murine neuronal hypothalamic GT1 and mouse neuroblastoma N2a cells, permissive for prion replication and widely used in prion biology (Villette 2008). As already described before (section 1.5 of the Introduction), the autophagic flux is an index of the progression of autophagy and includes the formation of the autophagosome containing organelles and proteins to degrade, and the subsequent fusion with lysosomes. This final step leads to formation of autolysosome in which the cellular components undergo degradation upon the action of lysosomal proteases in a pH-dependent manner (Yang and Klionsky 2009). Measurement of the autophagic flux is largely used to evaluate the autophagy

status in a given condition (Kimura et al 2009). In particular, we used the tandem fluorescent tagged LC3 construct (tfLC3), that encodes for LC3 linked to both GFP and RFP proteins, to monitor potential changes in the autophagic flux upon prion infection in both uninfected and prion infected GT1 and N2a cells. LC3 is a well-known autophagic marker protein and specifically associates with autophagosome membranes (Kabeya et al., 2000). This tool is based on the different sensitivity of GFP and RFP fluorophores to the acidic pH of the lysosomes (Mizushima and Yoshimori, 2007). As illustrated in Figure 30, while both GFP and RFP signals are present in autophagosomes, following the maturation process to phagolysosome only the RFP signal remains due to the quenching of the GFP-linked molecule (Kimura et al., 2009).

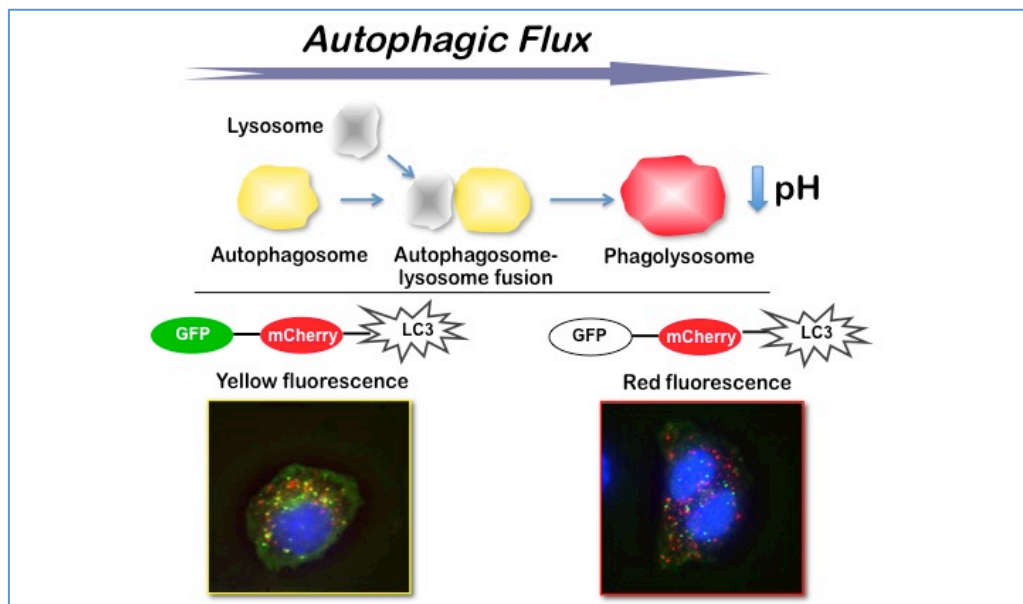


Figure 30 tf-LC3 tool.

By quantifying the number of both green and red and only-red vesicles per cell, we found that uninfected GT1 and N2a cells possess similar percentage of autophagosomes and phagolysosomes, indicating that both neuronal cell lines in culture have a basal activation of the autophagic pathway (see Figure 1, A and B, in the annex manuscript). We then assessed the autophagic flux in infected GT1 and N2a cells (scGT1 and scN2a

cells) and found a substantial increase in the number of phagolysosomes compared to uninfected cells (see Figure 1, A and B, in the annex manuscript). We concluded that chronic scrapie infection causes an increase of the autophagic flux in both scGT1 and scN2a cells, in agreement with previous findings in N2a cells (Aguib et al., 2009; Heiseke et al., 2009). We could also confirm these findings by monitoring the LC3-II levels (the post-translationally modified form of LC3 associated with autophagosome membranes) in uninfected and prion-infected GT1 and N2a cells in the presence or absence of lysosomal protease inhibitors (see Figure 1, C, in the annex manuscript). Treatment with lysosomal protease inhibitors partially inhibits the degradation of LC3-II delivered to lysosomes during organelle fusion, thus facilitates the monitoring of the state of the autophagic flux in a given condition (Mizushima and Yoshimori, 2007). Because of the combined use of these two approaches gives a good estimation of the autophagic flux (Kimura et al 2009), we could conclude that autophagy was activated upon prion infection.

However, both cell lines could still be infected and were able to replicate PrP<sup>Sc</sup> (see Supplementary Figure 2 in the annex manuscript) (Villette 2008), indicating that autophagy is not sufficient to impair the establishment of prion infection. Therefore, we asked whether further stimulation of the autophagic flux by using well-known autophagy inducers could lead to degradation of PrP<sup>Sc</sup>. In this case, scGT1 and scN2a cells were treated with rapamycin, tamoxifen and 4-hydroxyl-tamoxifen (OHT). Then by western blot with anti-PrP antibodies, we evaluated PrP<sup>Sc</sup> levels upon the different drug treatments, compared to untreated cells used as control. As already described before (section 1.1 of the Introduction), differently from PrP<sup>C</sup>, PrP<sup>Sc</sup> is resistant to proteinase K (PK) treatment (Schatzl et al 1997). This property is widely used as a tool to detect PrP<sup>Sc</sup> levels in infected cells (see Figure 2 in the annex manuscript). Interestingly, we found that tamoxifen and, its more potent derivative OHT, efficiently reduced PrP<sup>Sc</sup> levels in both scGT1 and scN2a cells (around 80-90%). Next, we evaluated the

autophagic flux upon the different drugs treatments to further analyze the involvement of the autophagy in PrP<sup>Sc</sup> clearance. For this purpose, we transfected scGT1 and scN2a cells with tf-LC3 construct and we counted the number of autophagosomes and autolysosomes upon rapamycin, tamoxifen and 4-hydroxyl-tamoxifen (OHT) treatment. Surprisingly, we found that none of the drugs used was able to increase the autophagic flux in infected cells (see Figure 3, A and B, in the annex manuscript). We could confirm these results by measuring LC3-II levels in presence or absence of lysosomal proteases inhibitors, as previously discussed (see Figure 3, C, in the annex manuscript). This led us to speculate that, due to the increased autophagic flux upon infection, further stimulation of autophagy-mediated degradation is not effective in these cells. Moreover, we analyzed PrP<sup>Sc</sup> localization in control cells and upon rapamycin, tamoxifen and OHT treatment to evaluate its presence in autophagosomes at steady state and upon stimulation of autophagy. To this aim, we used an immunofluorescence approach, in which immunolabelling with both anti-LC3 and anti-PrP antibodies were performed after treatment with Gnd-HCl to expose PrP<sup>Sc</sup> epitopes (as described in the Material and Methods section). We found that only a minor fraction of PrP<sup>Sc</sup> colocalized with endogenous LC3 in permanently infected scGT1 cells. Furthermore, the amount of PrP<sup>Sc</sup> in LC3-positive vesicles did not significantly increase upon rapamycin, tamoxifen or OHT treatments (see Figure 4 in the annex manuscript). Then to rule out the possibility that the lack of PrP<sup>Sc</sup> detection in autophagic structures was due to a fast lysosomal degradation in this compartment, we blocked the activity of lysosomal proteases using Bafilomycin A1. Also upon this treatment, we could not observe any increase in localization of PrP<sup>Sc</sup> in autophagosomes in scGT1 cells (see Figure 4 in the annex manuscript). These data indicate that the reduction in PrP<sup>Sc</sup> observed upon the different treatments is unlikely due to autophagy. Additionally, mouse catecholaminergic neuronal CAD cells (Qi et al 1997), another well-established cell line for prion-replication, was used in the same set of experiments to verify the involvement of autophagy in prion degradation. The results obtained in this cell lines corroborated our previous

findings in GT1 and N2a cells (see Supplementary Figure 3 in the annex manuscript).

To definitely rule out the role of autophagy in PrP<sup>Sc</sup> clearance, we performed an RNA interference experiment in scGT1 cells in which we down-regulated Atg7 gene, codifying for an essential autophagy protein, and then treated the cells with rapamycin, tamoxifen or OHT. After treatment with siRNA Atg7, down-regulation of ~80% was achieved and under these conditions, LC3-II could not be detected, suggesting that the autophagic pathway was efficiently inhibited (see Figure 5 in the annex manuscript). We then treated the cells with the different drugs and we compared PrP<sup>Sc</sup> levels in Atg7 down-regulated cells with control cells subjected to scrambled siRNA. Strikingly, we found that both tamoxifen and OHT treatments were still able to decrease PrP<sup>Sc</sup> levels in absence of activated autophagy (see Figure 5 in the annex manuscript).

Overall, these findings argue against a role for autophagy in prion degradation. Notwithstanding, we found that tamoxifen and (in greater extend) OHT were able to efficiently reduce PrP<sup>Sc</sup> levels in all the cell model systems used (see Figure 2 in the annex manuscript), pointing towards a potential therapeutical application of these drugs for prion disease.

Therefore we decided to analyze the possible mechanism of action of these drugs. From data presented in literature, it is known that tamoxifen and OHT modulate cholesterol metabolism by reducing its levels (de Medina et al 2004). Furthermore, these compounds disturb cholesterol trafficking by inhibiting the egress of LDL-derived cholesterol from lysosomes and causing a Niemann-Pick type C disease type phenotype (Suarez et al 2004). As already mentioned above, it is well documented that prion replication is sensitive to perturbation of lipid metabolism, and specifically, that cholesterol depletion leads to PrP<sup>Sc</sup> reduction (Taraboulos et al 1995; Campana et al 2005). Therefore we investigated whether tamoxifen- and OHT treatment had an effect on cholesterol distribution in our system. To this aim, we treated scGT1 cells with tamoxifen and OHT and evaluated cholesterol distribution compared to untreated cells by filipin staining and lysosomes immunolabelling with anti-LAMP1

antibodies. While in untreated scGT1 cells we could observe diffuse filipin staining, both tamoxifen and OHT treatments resulted in a punctate staining pattern that partially colocalizes with LAMP1 (see Figure 6 in the annex manuscript), thus suggesting an accumulation of cholesterol in late endosomal compartments upon these drugs treatment. Subsequently, we asked whether cholesterol accumulation in lysosomes could also increase PrP<sup>Sc</sup> sequestration in lysosomes, and, so, enhance PrP<sup>Sc</sup> degradation in this compartment. To test this hypothesis, we examined PrP<sup>Sc</sup> distribution in lysosomes by immunofluorescence with both anti-PrP and anti-LAMP1 antibodies in the presence of tamoxifen and OHT in comparison with untreated control. We could observe a large fraction of PrP<sup>Sc</sup> in lysosomes following OHT drug treatment. Indeed by quantify the percentage of colocalisation of PrP<sup>Sc</sup> with LAMP1, we found that upon treatment with both these drugs PrP<sup>Sc</sup> colocalisation with LAMP1 increases up to 30% compared to control cells (10%) (see Figure 7 in the annex manuscript). Finally, to demonstrate that PrP<sup>Sc</sup> rerouting to lysosomes led to degradation in this compartment, we treated scGT1 cells with OHT (in the presence or absence of lysosomal inhibitors) and we evaluated PrP<sup>Sc</sup> levels, compared to untreated control by PK assay (as already described in the Material and Methods section). We were able to demonstrate that lysosomal inhibitor treatment counteracted the effect of OHT in PrP<sup>Sc</sup> clearance and restored PrP<sup>Sc</sup> levels equal to untreated cells (see Figure 8 in the annex manuscript). These data confirmed that OHT and tamoxifen reduce PrP<sup>Sc</sup> levels by increasing prion degradation in lysosomes.

In parallel to determine whether PrP<sup>C</sup> is also relocated to lysosomes upon these drugs treatment we also evaluated PrP<sup>C</sup> distribution in lysosomes upon OHT treatment. We reasoned that in this case one of the effects of tamoxifen and OHT treatment would be also to reduce the substrate for PrP<sup>Sc</sup> production, thus impairing prions formation. Interestingly, upon OHT treatment, a major fraction of PrP<sup>C</sup> colocalised with LAMP1 (we found around 25% colocalisation compared to 9% colocalisation of the control). This suggests that OHT could increase also decrease PrP<sup>C</sup> degradation thus reducing the substrate of PrP<sup>Sc</sup> production.

In summary, in this first part of my work, by using different approaches I demonstrated that autophagy is not involved in PrP<sup>Sc</sup> degradation. Interestingly, I found that tamoxifen and OHT, two drugs used to enhance the autophagic flux, efficiently reduced PrP<sup>Sc</sup> levels in an autophagy independent manner. Then I exploited the possible mechanism of action of these drugs and I found that tamoxifen and OHT alter cholesterol trafficking and cause a redistribution of both PrP<sup>Sc</sup> and PrP<sup>C</sup> to lysosomes, thus shifting the equilibrium between prion production and degradation towards the latter.

## 1.4 Discussion

Accumulation of misfolded protein deposits in affected brain regions is a characteristic feature of many neurodegenerative diseases (Agorogiannis et al 2004; Nijholt et al 2011), suggesting that in these pathological conditions the degradative capacity of the cell fails in reducing proteins burden. Experimental evidence suggests that neuronal death may be associated with the ubiquitin-proteasome system (UPS) impairment, although whether this is a cause or consequence of neurodegeneration is still unclear. Also, UPS impairment is thought to be important in prion disease (Ma and Lindquist, 2002; Ma *et al.*, 2002; Kang *et al.*, 2004; Kristiansen *et al.*, 2005). In contrast, the role, if any, of the alternative major protein degradation pathway, autophagy, in prion disease is still unclear and highly debated (Heiseke et al 2009) (see also section 1.5 of the Introduction and paragraph 1.1 of this chapter).

Thus the aim of my study was to investigate the role of autophagy in prion disease and, so, to look more closely into the molecular interplay between autophagy, prion propagation, trafficking and clearance. In order to do so, I used both fluorescence microscopy and biochemical approaches and different neuronal cell culture models. Our results indicate that autophagy is up regulated in prion-infected cells. Indeed, as already mentioned above, in prion diseases an increased number of autophagosomes have been reported in infected neuronal cells and brain tissue (Liberski et al., 2008; Sikorska et al., 2004; Schätzl et al., 1997). Here I have confirmed and extended these findings by showing that chronic scrapie infection induces autophagic flux at higher levels but that uninfected neuronal cells already possess a basal level of autophagy. These results were in contrast with previous reports in which basal levels of autophagy could not be detected in non-infected N2a cells (Liberski et al., 2008; Sikorska et al., 2004; Schätzl et al., 1997). The most likely reason for this discrepancy was the different tool used in this study to monitor autophagy, namely, tandem fluorescent LC3 (tf-LC3) containing both GFP and RFP (Figure 1.1). This construct enables one to distinguish autophagosomes from phagolysosomes based on the presence of only red fluorescence

in the acidic phagolysosomal compartment (Aguib et al., 2009; Heiseke et al., 2009). Therefore, earlier studies reporting no basal autophagy in N2a cells were based only on observations of autophagosomes since the phagolysosomes present were essentially invisible when using GFP-LC3 alone (Heiseke et al 2009).

In addition, despite an increased autophagic flux upon infection, I found that PrP<sup>Sc</sup> is mostly absent from autophagic vesicles, even when lysosomal degradation is impaired, thus excluding a fast lysosomal degradation in this compartment. These findings raised the possibility that PrP<sup>Sc</sup> is not processed by the autophagic machinery. However if this is the case, the question arises as to why autophagy is induced by prion infection if it is not involved in PrP<sup>Sc</sup> processing. One possibility is that the presence of protein aggregates stimulates autophagic flux as a defensive response. However, prions, being membrane-bound proteins, may be able to elude recognition by the autophagic machinery by virtue of their sequestration within vesicles. In addition, it could also be that the increased autophagic flux upon prion infection is not sufficient to allow an efficient PrP<sup>Sc</sup> degradation. Therefore, in order to clarify this issue we further stimulate the autophagic flux, by using well-known autophagy inducers, namely rapamycin, tamoxifen and OHT, and examine whether there was an effect on PrP<sup>Sc</sup> clearance. I found that while a slight decrease in PrP<sup>Sc</sup> levels was achieved upon rapamycin treatment, tamoxifen and more importantly OHT reduced PrP<sup>Sc</sup> level up to 90%. Surprisingly, the measurement of the autophagic flux upon rapamycin, tamoxifen and OHT treatment showed that these drugs could not further stimulate autophagy in scrapie-infected cells. It was previously reported that rapamycin, by enhancing autophagy would lead to a moderate PrP<sup>Sc</sup> degradation (Aguib et al 2009; Heiseke et al 2009). Moreover tamoxifen and OHT were shown to stimulate autophagy (Samaddar 2008; de Medina 2009). The discrepancy with my new findings could be explained by the fact that an increase in GFP-LC3-positive vesicles (and hence autophagosomes) was previously interpreted as an increase in autophagy by these drugs. However, judging by the accumulation of both double-positive and red-only vesicles, these drugs are

likely interfering with the fusion between autophagosomes and lysosomes, thus reducing the autophagic flux.

Consistently, by using an RNA interference approach for *atg7* gene to down-regulate the autophagic pathway, I was able to rule out the involvement of autophagy in tamoxifen- and OHT-mediated PrP<sup>Sc</sup> reduction. Prevailing models in the recent literature propose that the amount of protease-resistant, aggregate-prone prion protein is maintained by a balance between PrP<sup>Sc</sup> formation by conversion of native PrP<sup>C</sup> and its destruction in lysosomes, that could be autophagy-mediated. I have rather shown here that autophagy-mediated degradation is not relevant in the regulation of PrP<sup>Sc</sup> levels in prion-infected cells, thus indicating that the mechanisms of PrP<sup>Sc</sup> clearance observed upon tamoxifen and OHT treatment are likely independent from this process.

This finding raises the question on which mechanism tamoxifen and, more efficiently OHT reduced PrP<sup>Sc</sup> levels. It was previously shown that lipids, specifically cholesterol and sphingolipids, play a crucial role in PrP<sup>Sc</sup> propagation and that changes in sub-cellular distribution of PrP by modulating lipid metabolism and trafficking, affect PrP<sup>Sc</sup> levels in infected cells (Kimura et al., 2009). Interestingly, both tamoxifen and OHT are inhibitors of cholesterol biosynthesis (Campana et al., 2005; Marijanovic et al., 2009; Lewis and Hooper, 2011; Taraboulos et al., 1995b). Interestingly, the drug concentrations at which these effects are observed are the same concentrations that were effective in reduction of PrP<sup>Sc</sup>. Tamoxifen has also been shown to inhibit the exit of cholesterol from lysosomes resulting in a lipid storage disease-like phenotype, characterized by an accumulation of cholesterol in late-lysosomal compartments (de Medina et al., 2011, 2004, 2009). By immunofluorescence I could observe a similar effect of both tamoxifen and OHT on cholesterol trafficking in prion infected neuronal cells. Importantly, I also found that these treatments induced the redistribution of both PrP<sup>Sc</sup> and PrP<sup>C</sup> towards lysosomes. This redistribution could affect both PrP<sup>Sc</sup> replication and degradation. It has been shown that the ERC is an intracellular site for PrP<sup>Sc</sup> conversion (Marijanovic et al., 2009) and it normally contain high levels of cholesterol (Suárez et al., 2004). Therefore, one possibility is that conditions

that favor endosomal degradation over endosomal recycling by re-routing PrP<sup>C</sup> from recycling endosomes to lysosomes could reduce the substrate available for its conversion. At the same time the rerouting of PrP<sup>Sc</sup> to lysosomes would facilitate the elimination of the pathological prion form by the lysosomal system. Indeed, by treating the cells with NH<sub>4</sub>Cl in presence of OHT, I was able to show that a block of lysosomal degradation counteracted the effect of OHT and restore PrP<sup>Sc</sup> levels equal to control. These data demonstrate that the rerouting of PrP<sup>Sc</sup> in lysosomes leads to its degradation in this organelle.

On the basis of these results, I propose a model in which upon OHT treatment cholesterol trafficking in the cell is altered leading to the accumulation of this lipid in lysosomes (Figure 31). This causes a reduction of the cholesterol content in the endosomal recycling compartment where can interfere with the interaction between PrP<sup>C</sup> and PrP<sup>Sc</sup> in the endocytic pathway that is necessary for PrP<sup>Sc</sup> replication. Moreover, OHT treatment leads to redirection of both PrP<sup>C</sup> and PrP<sup>Sc</sup> to lysosomes, thus shifting equilibrium between prion production and degradation towards the degradation of both PrP<sup>C</sup> (thus reducing the substrate for conversion) and PrP<sup>Sc</sup> (thus leading to its clearance of prions).

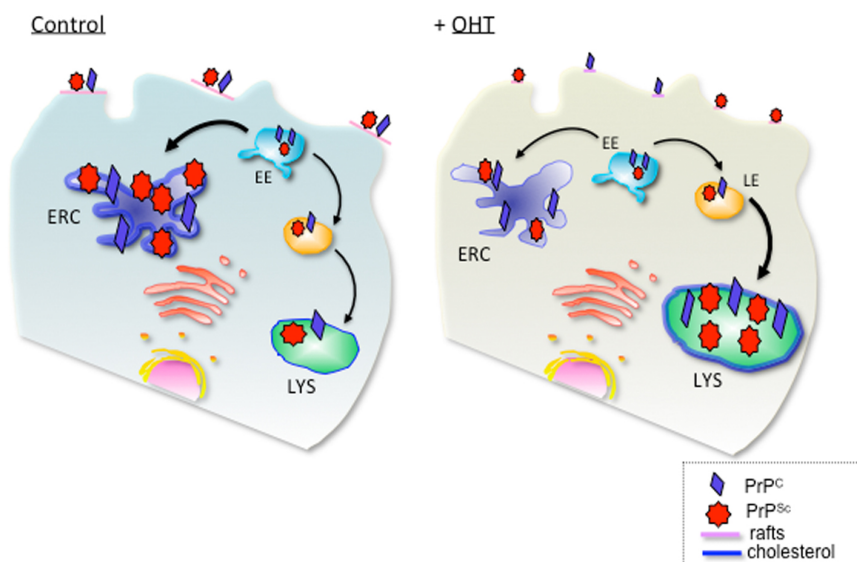


**Figure 31 Schematic presentation of PrP trafficking in infected cells and upon OHT treatment.** In infected cells PrP<sup>C</sup> and PrP<sup>Sc</sup> interact at plasma membrane in cholesterol rich lipid domains called lipid rafts. Upon internalization both PrP<sup>C</sup> and PrP<sup>Sc</sup> can recycle via endosomal

recycling compartment (ERC) or can be routed for degradation in lysosomes. Subcellular cholesterol distribution influences PrP<sup>Sc</sup> trafficking in endocytic pathway. In untreated infected cells, majority of PrP recycles through cholesterol rich ERC supporting conversion of PrP<sup>C</sup> to PrP<sup>Sc</sup>. Treatment with 4-hydroxy-tamoxifen (OHT) induces cholesterol accumulation in enlarged late endosomes PrP<sup>Sc</sup> production and degradation defines cellular load of infectious prions. We propose that OHT-induced changes in PrP<sup>Sc</sup> trafficking favor PrP<sup>Sc</sup> degradation.

Although these data clearly demonstrate a relocation of cholesterol and PrP to lysosomes, the nature of the lipids accumulating in lysosomes (reminiscent to a sphingolipids storage disease phenotype (Schulze and Sandhoff 2011) and whether lipid accumulation directly influenced PrP<sup>Sc</sup> localization in this compartment remains to be determined. While autophagy is well known as a mechanism for directing aggregated proteins into lysosomes it appears that tamoxifen and OHT induce the trafficking of prions to lysosomes in an autophagy-independent fashion. In conclusion, given its ability to both reduce infectious prions and modify cholesterol metabolism and lipid content of the cell OHT represents a well-characterized, widely available pharmaceutical that may have applications as a broad-spectrum therapy for neurodegenerative diseases of protein aggregation.

## **ANNEXE 1:**

Paper submitted to 'Molecular Biology of the Cell'

### **4-HYDROXYTAMOXIFEN TREATMENT INDUCES PrP<sup>Sc</sup> CLEARANCE IN AN AUTOPHAGY-INDEPENDENT MANNER**

Ludovica Marzo<sup>§1,2</sup>, Zrinka Marijanovic<sup>§1</sup>, Duncan Browman<sup>1</sup>, Anna Caputo<sup>1</sup> and Chiara Zurzolo<sup>1,2</sup>

1, Institut Pasteur, Unité de trafic membranaire et pathogénèse, 25 rue du docteur roux,

75015 Paris; 2, Dipartimento di Biologia e Patologia Cellulare e Molecolare, Università

Federico II, Napoli, Italy

\*Corresponding author:

Dr. Chiara Zurzolo

Unité de trafic membranaire et pathogénèse

Institut Pasteur

25, rue du docteur Roux

75724 Paris CEDEX 15, France

Phone: +33145688277

Fax: +33140613238

[chiara.zurzolo@pasteur.fr](mailto:chiara.zurzolo@pasteur.fr)

**Running Head: PrP<sup>Sc</sup> clearance induced by 4-hydroxyl-tamoxifen**

**Keywords: PrP<sup>Sc</sup>, TAM, OTH, autophagy, lysosomal degradation, cholesterol**

**§ These authors contributed equally to this work.**

## Abstract

Prion diseases are fatal neurodegenerative disorders involving the abnormal folding of a native cellular protein, named PrP<sup>C</sup>, to a malconformed aggregation-prone state, enriched in beta sheet secondary structure, denoted PrP<sup>Sc</sup>. Recently, autophagy has garnered considerable attention as a cellular process with the potential to counteract neurodegenerative diseases of protein aggregation such as Alzheimer's disease, Huntington's disease, and Parkinson's disease. Up regulation of autophagy by chemical compounds has also been shown to reduce PrP<sup>Sc</sup> in infected neuronal cells and prolong survival times in mice models. Consistent with previous reports we demonstrate that autophagic flux is increased in chronically infected cell models. However, in contrast to recent findings we show that autophagy is not causative of a reduction in scrapie burden. We report that in infected neuronal cells different compounds known to stimulate autophagy are ineffective in increasing the autophagic flux and in reducing PrP<sup>Sc</sup>. We further demonstrate that the anti-prion effect of tamoxifen and its metabolite 4-hydroxytamoxifen is not dependent on autophagy but rather depends on the ability of these drugs to alter the trafficking of both PrP and cholesterol. Because tamoxifen represents a well-characterized, widely available pharmaceutical our data indicate that it may have applications in the therapy of prion diseases.

## INTRODUCTION

Transmissible spongiform encephalopathies are infectious, neurodegenerative diseases involving the abnormal folding of the cellular prion protein PrP<sup>C</sup> into a pathologic conformer PrP<sup>Sc</sup>. This malconformed state also leads to its accumulation as aggregates in both the cytoplasm of affected neurons and the interstitial spaces within the brains of afflicted individuals (Prusiner, 1998). Recently, macroautophagy has been described as an important process in the pathogenesis of neurodegenerative diseases of protein aggregation such as Alzheimer's, Huntington's and Parkinson's

disease as well as in prion diseases (Cherra III et al., 2010). As post-mitotic cells that must endure for the lifetime of an organism, neurons require efficient mechanisms to avoid accumulating toxic protein aggregates. It has been proposed that macroautophagy, often referred to simply as "autophagy", is one such mechanism (Rubinsztein et al 2007; Wong and Cuervo, 2010). Recent evidence suggests that dysfunction in the autophagic pathway is common to numerous neurodegenerative diseases (Wong and Cuervo, 2010). Furthermore, mice engineered for neuron-specific knockout of the essential autophagy genes *atg5* or *atg7* present with a neurodegenerative phenotype accompanied by massive protein aggregate accumulation and resulting inexorably in death within the first few months of birth (Hara et al., 2006; Komatsu et al., 2006). Moreover up regulation of autophagy was shown to efficiently counteract neurodegeneration in both *in vitro* and *in vivo* models (Wong and Cuervo, 2010).

The role of autophagy in prion disease is highly debated (Heiseke et al., 2010). Autophagic vacuoles were first detected in neuronal cell models chronically infected with prions (Schätzl et al., 1997). More recently, autophagic vacuoles were identified in synapses in various forms of human prion disease (Sikorska et al., 2004) and it was found that they are formed in neuronal perikarya, neurites and synapses in experimentally induced scrapie, Creutzfeldt-Jakob disease (CJD) and Gerstmann-Sträussler-Scheinker (GSS) syndrome (Liberski et al., 2008). Therefore it was proposed that autophagy could play a disease-promoting role by contributing to the formation of spongiform (Liberski et al., 2008; Liberski and Jeffrey, 2004). On the other hand, it has been demonstrated that a number of autophagy-inducing compounds such as lithium salts, trehalose and rapamycin are effective at reducing PrP<sup>Sc</sup> burden in cultured neuroblastoma cells (N2a) and delay the onset of symptoms in prion-infected mice in prophylactic treatment models (Aguib et al., 2009; Heiseke et al., 2009). Thus, induction of autophagy was proposed as a novel approach for the treatment of prion diseases.

However, a more systematic analysis of the role of autophagy in prion infection is needed because the molecular

mechanisms by which autophagy would be protective are still not understood. In particular it has to be considered that the majority of PrP<sup>Sc</sup> resides in the endocytic pathway and not in the cytosol (Campana et al., 2005; Caughey et al., 2009). The availability of new tools and recent advances in the understanding of the dynamic process of autophagic flux, prompted us to re-examine the role of autophagy in prion propagation, trafficking and clearance. In contrast to previous studies, we observed a basal activation of autophagy in all neuronal cell models examined, independent of scrapie infection. Furthermore, chronic scrapie infection results in an increase in autophagic flux, in the absence of any significant colocalization of PrP<sup>Sc</sup> with autophagic vacuoles. We also report that autophagic flux could not be further stimulated by autophagy-inducing compounds like rapamycin, previously shown to clear prion-infection in ScN2a cells. Furthermore, tamoxifen (TAM), also described as an autophagy inducer, decreases autophagic flux in scrapie-infected cells and concomitantly reduces scrapie burden. Consistently, its active metabolite, 4-hydroxytamoxifen (OHT), is a more potent inhibitor of autophagic flux and greater inducer of prion protein clearance. We demonstrate that both TAM and OHT cause the redistribution of cholesterol and PrP<sup>Sc</sup> to lysosomes and are effective in reducing PrP<sup>Sc</sup> levels even under conditions of autophagy inhibition. Overall these data indicate that the autophagic pathway is not involved in prion degradation and that TAM and OHT stimulate clearance of PrP<sup>Sc</sup> in an autophagy-independent manner by altering both prion and lipid intracellular trafficking.

## RESULTS

### Chronic prion infection induces autophagic flux in neuronal cell culture models

To investigate the role of autophagy in PrP<sup>Sc</sup> metabolism, we analyzed whether scrapie infection could affect autophagic flux in neuronal cell lines by comparing uninfected and chronically infected GT1 and N2a cells (respectively GT1 and scGT1 and N2a and ScN2a cells), using

both fluorescent microscopy and biochemical approaches. To monitor potential changes in the autophagic flux, we analyzed LC3, a well-known autophagic marker protein specifically associated with autophagosomal membranes (Kabeya et al., 2000). Earlier work with GFP-LC3 enabled researchers to acquire a snapshot of the number of early autophagosomes forming in cells. In order to measure the dynamic flux of the autophagy pathway from early autophagosomes through to late phagolysosomes, we used the tandem fluorescently tagged LC3 construct (tfLC3, encoding for LC3 linked to both GFP and RFP proteins) combined with inhibition of lysosomal proteases.

This tool is based on the differential sensitivity of GFP and RFP fluorophores to the acidic pH of lysosomes and is specifically used to monitor the progression of autophagy (Mizushima and Yoshimori, 2007). While both GFP and RFP signals are observable in autophagosomes, following the maturation process to phagolysosomes only the RFP signal remains due to the quenching of the GFP-linked molecule (Kimura et al., 2009). Therefore, in cells in which autophagy is not activated, LC3 shows a diffuse GFP/RFP pattern; when activation of autophagy occurs, early autophagosomes can be detected in the cytosol as punctae exhibiting fluorescence in both the green and red channels (double-positive vesicles). In contrast, the punctae exhibiting fluorescence only in the red channel (red-only vesicles) indicates the progression of autophagic flux from early autophagosomes to phagolysosomes.

Quantification of labeled vesicles in control GT1 cells transfected with tfLC3 revealed that 55% of the vesicles were double-positive autophagosomes and 45% were red-only phagolysosomes. In control N2a cells 35% of the vesicles were double-positive autophagosomes, while 65% of the vesicles were red-only phagolysosomes (Figure 1A and 1B). Thus, using this improved tool to measure autophagic flux, a basal activation of the autophagic pathway was detected in both neuronal cell lines, in contrast to previous reports in which autophagy was not detected in control N2a cells (Aguib et al., 2009; Heiseke et al., 2009)(see discussion).

Next, autophagic flux in infected scGT1 and scN2a cells was assessed. Quantification of the number of red-only positive vesicles revealed a substantial increase in the number of phagolysosomes in both infected cells. Specifically, the percentage of red-only phagolysosomes in infected scGT1 and scN2a cells rose from 45% to 60% and from 65% to 90% of all LC3-decorated vesicles, respectively (Figure 1A and 1B). These data suggest that autophagic flux is increased under conditions of chronic scrapie infection in both scGT1 and scN2a cells.

These results were corroborated by western blot analysis comparing the endogenous levels of LC3-II in infected and non-infected cells, in the presence or absence of lysosomal protease inhibitors (Figure 1C). LC3-II is the post-translationally modified form of LC3, associated with autophagosome membranes, and can be distinguished from its precursor LC3-I by SDS-PAGE by its increased electrophoretic mobility (16 kDa for LC3-I, versus 14 kDa for LC3-II) (Kabeya et al., 2000). Treatment with lysosomal protease inhibitors partially inhibits the degradation of LC3-II delivered to lysosomes during organelle fusion, thus facilitating its recovery and therefore the assessment of the state of autophagic flux in a given condition (Mizushima and Yoshimori, 2007). As expected, we found a significant increase in the amount of LC3-II upon ammonium chloride treatment in both scGT1 and scN2a cells (Figure 1C). Importantly, this increase was greater in the infected cells compared to uninfected GT1 and N2a cells consistent with a higher rate of autophagic flux during prion infection (Figure 1 A, B, C).

To further corroborate our findings we analyzed autophagic flux in CAD cells, another neuronal cell line capable of propagating prions (Gousset et al., 2009; Marijanovic et al., 2009). A comparable increase in autophagic flux was observed in chronically infected scCAD cells (Supplementary Figure S1, A and B) confirming that autophagy is activated in chronically infected cells.

In order to gain some insight into the mechanism and timing of this activation, we analyzed whether *de novo* prion infection could modulate autophagy. To this aim we performed a live-cell imaging experiment in which we followed the fate

of newly up-taken PrP<sup>Sc</sup> aggregates in real-time and simultaneously monitored autophagic flux. CAD cells transfected with GFP-tagged LC3 (GFP-LC3) were challenged with Alexa546-PrP<sup>Sc</sup>, a fluorescent infectious scrapie preparation (Gousset et al., 2009), and followed by live microscopy for up to 12 hours post-infection. Similar to chronically infected cells, autophagy was induced upon the uptake of Alexa546-PrP<sup>Sc</sup> infected cells, as shown by the appearance of GFP-LC3 puncta. However, Alexa546-PrP<sup>Sc</sup>-positive vesicles were clearly distinguished from LC3-positive autophagosomes (Supplementary Movie S1), suggesting that PrP<sup>Sc</sup> was not being trafficked through the autophagic pathway.

### **Autophagy does not play a major role in PrP<sup>Sc</sup> metabolism**

The evidence indicating that autophagy was activated both in permanently and newly infected cells raised the question as to whether autophagy was involved in scrapie clearance. It was previously reported that treatment of infected scN2a cells with autophagy inducers (e.g., rapamycin, lithium or trehalose) decreased PrP<sup>Sc</sup> levels in cells and delayed the course of disease in scrapie-infected mice, although with high variability (Aguib et al., 2009; Heiseke et al., 2009).

The presence of high levels of PrP<sup>Sc</sup>, in spite of increased autophagic flux in permanently infected cells (Supplementary Figure S2), along with our observations using fluorescent microscopy in newly infected cells (Supplementary Movie S1) suggested that either PrP<sup>Sc</sup> was not being processed by the autophagic route or that this process was inefficient in reducing scrapie burden. Therefore, to directly test these hypotheses we monitored PrP<sup>Sc</sup> levels following chemical stimulation of autophagy.

Specifically, scGT1 and scN2a cells were treated with either rapamycin, TAM or OHT for 5 days and the levels of total PrP and PK-resistant PrP<sup>Sc</sup> were examined by limited proteinase K digestion assay and western blot (Schätzl et al., 1997) to test the ability of these drugs to reduce PrP<sup>Sc</sup> (Figure 2, A and C). Interestingly, we found that TAM and particularly OHT, were very efficient in PrP<sup>Sc</sup> clearance (80-90%), while rapamycin caused only a moderate and not very consistent (see also Figure 5) decrease in the PrP<sup>Sc</sup>

fraction (10-20%) in both cell lines (Figure 2, B and D).

In order to understand whether the scrapie clearance obtained by the various treatments was due to stimulation of autophagy we monitored the activation of autophagic flux in ScGT1 and scN2a cells transfected with tfLC3 after treatment with rapamycin, TAM and OHT for 5 days. Unexpectedly, quantification of the number of autophagosomes and phagolysosomes in scGT1 cells revealed that the percentage of double-positive autophagosomes and red-only phagolysosomes (approximately 40% and 60%, respectively) among the treated cells was similar to what was observed for the untreated controls (Figure 3, A). This indicated that none of the drugs were able to increase autophagic flux beyond the baseline established in infected cells. This result was confirmed independently using a biochemical approach in which LC3-II levels were measured by western blot. Indeed, no increase in LC3-II levels were observed between control and treated scGT1 cells upon inhibition of lysosomal proteolysis (Figure 3, B). In particular, it should be noted that the higher LC3-II levels found in OHT-treated cells was not significantly increased by co-treatment with lysosomal inhibitors, suggesting an inhibition of autophagic flux in this condition (Figure 3). Consistent with previous findings in scN2a cells (Heiseke et al., 2009), we observed a moderate increase in the number of autophagosomes per cell under the different drug treatments (Figure 3, A). This observation may explain why previous groups using GFP-LC3 have reported an increase in autophagy with these treatments (Aguib et al., 2009; Heiseke et al., 2009). However, similar to scGT1 cells, the percentage of phagolysosomes was unaffected or even reduced compared to the untreated cells (Figure 3A). Similar results were obtained in scCAD cells (Supplementary Figure S1, C and D). These data suggest that while the chemical treatments are capable of reducing cellular prion burden, none of these agents were able to increase autophagic flux (Figure 3, A; Supplementary Figure S1, C and D); furthermore, in the case of OHT autophagic flux was actually inhibited. In contrast with previous reports, our results indicated that rapamycin reduces scrapie

burden in infected cells modestly, while TAM and OHT are more potent prion-reducing agents. Furthermore, neither microscopy nor biochemical approaches supported a role for these chemicals in stimulating autophagic flux in prion-infected cells (Figure 3). These data suggest that the effect of the above compounds on the PrP<sup>Sc</sup> levels is independent of autophagy stimulation.

To further examine these findings we compared the subcellular localization of PrP<sup>Sc</sup> and LC3-decorated structures in infected cells both at the steady state and following the different treatments (Figure 4, A). Specifically, we performed quantitative immunofluorescence after GND treatment (Marijanovic et al., 2009) to examine the respective subcellular localizations of LC3-decorated autophagy-associated structures and PrP<sup>Sc</sup>. We found that only a minor fraction of PrP<sup>Sc</sup> (6%) colocalized with endogenous LC3 in permanently infected scGT1 cells (Figure 4, B). Furthermore, the amount of PrP<sup>Sc</sup> in LC3-positive vesicles did not significantly increase upon rapamycin, TAM or OHT treatments (Figure 4, B). Similar results were obtained in scCAD cells (Supplementary Figure S3, A and B). To rule out fast lysosomal degradation as a possible cause for the lack of PrP<sup>Sc</sup> localization in phagolysosomes we blocked the activity of lysosomal proteases using Bafilomycin A1 (Figure 4, A). However, despite this treatment, we could not observe any statistically valid increase in localization of PrP<sup>Sc</sup> in autophagosomes in scGT1 cells (Figure 4, B) supporting the hypothesis that the reduction in PrP<sup>Sc</sup> observed upon the different treatments is not due to autophagy.

To directly rule out the involvement of autophagy in PrP<sup>Sc</sup> degradation, we used an RNAi approach. To this aim, we challenged scGT1 cells with siRNA targeting Atg7, an essential autophagic gene, in two subsequent rounds of transfection in order to maintain low levels of Atg7 during a 5-day treatment with rapamycin, TAM or OHT. As depicted in Figure 5, Atg7 down-regulation was achieved (up to 90%) and under these conditions, LC3-II could not be detected, suggesting that the autophagic pathway was efficiently inhibited. Next, total PrP and PrP<sup>Sc</sup> levels were assessed in the context of Atg7 knockdown (Figure 5, A). While the rapamycin treatment did not give a consistent reduction of PrP<sup>Sc</sup>, it was

striking that both TAM and to a greater extent OHT treatments were still capable of decreasing PrP<sup>Sc</sup> levels while PrP levels remained stable. Indeed, the magnitude of the TAM- and OHT-mediated decrease of scrapie in Atg7-depleted cells was indistinguishable from that of cells co-treated with scrambled control siRNA (Figure 5, B). Further evidence from this experiment arguing against a role for autophagy in prion degradation was that no increase in PrP<sup>Sc</sup> was observed in infected cells even after prolonged treatment with anti-Atg7 siRNA alone (Figure 5, A, lanes 1 and 5 of the PK treated extracts).

### **OHT and TAM causes redistribution of both PrP<sup>Sc</sup> and cholesterol to lysosomes**

Since the data did not support a role for autophagy in reducing the PrP<sup>Sc</sup> fraction, we sought to uncover the mechanism by which TAM and OHT could exert such effects. TAM and OHT can perturb cholesterol trafficking (Suárez et al., 2004; de Medina et al., 2004, 2011). Furthermore, it is established that interference with cholesterol and sphingolipid efflux from lysosomes reduces cellular scrapie (Taraboulos et al., 1995; Baron et al., 2002). Therefore, we hypothesized that perturbation of subcellular cholesterol trafficking by TAM and OHT were responsible for their anti-prion effects.

To test this hypothesis we examined cholesterol distribution in TAM and OHT treated cells compared to untreated scGT1 cells by filipin staining. In contrast to the diffuse filipin staining observed in untreated cells, both TAM and OHT treatments resulted in a punctate staining pattern, partially colocalizing with LAMP1, a marker of late endosomes (Figure 6). These data indicate that these drugs can perturb subcellular lipid trafficking resulting in the accumulation of cholesterol in late endosomal compartments.

To determine if this treatment resulted in the rerouting of PrP<sup>Sc</sup> to lysosomes, we quantified the fraction of PrP<sup>Sc</sup> in lysosomes upon exposure to TAM and OHT. Specifically, scGT1 cells were treated with either TAM or OHT for 3 days and, after fixation, permeabilization and guanidine-hydrochloride treatment, the samples were immunostained for PrP<sup>Sc</sup>

and LAMP1 and the percentage of colocalisation between the two was evaluated (Figure 7). Quantification of the two signals revealed that PrP<sup>Sc</sup> was enriched in lysosomes in both TAM and OHT treated cells. The higher effect was observed following OHT treatment, with around 30% colocalising with LAMP1 compared to the 10% observed in the control untreated cells (Figure 7, B). This result implicated lysosomal proteases in the degradation of PrP<sup>Sc</sup>.

To address this question experimentally, lysosomal degradation was inhibited using NH<sub>4</sub>Cl and the effect on PrP<sup>Sc</sup> levels in OHT treated cells was analyzed by WB (Figure 8). We reasoned that if the observed decrease in PrP<sup>Sc</sup> levels induced by OHT treatment was due to lysosomal degradation, inhibition of this process should restore PrP<sup>Sc</sup> levels. Accordingly, we were able to show that treatment with lysosomal inhibitors counteracted the anti-prion effect of OHT (Figure 8). Indeed, this treatment led to an increase in PrP<sup>Sc</sup> fraction and prevented the clearance induced by OHT. These data indicate that OHT treatment caused the accumulation of both cholesterol and PrP<sup>Sc</sup> in lysosomes and resulted in the degradation of the latter in this compartment. Since PrP<sup>Sc</sup> failed to accumulate in LC3-positive structures even in the context of lysosomal protease inhibition (Figure 4), this indicated that scrapie was being trafficked to and degraded into lysosomes in an autophagy-independent manner.

Next, to analyze the fate of PrP<sup>Sc</sup> aggregates in real-time upon OHT-treatment a live-imaging approach was employed. To this end, CAD cells were challenged with Alexa546-PrP<sup>Sc</sup> and loaded with LysoTracker Green (to stain lysosomes) and then followed for up to 12h. It was observed that newly endocytosed PrP<sup>Sc</sup> colocalized with lysotracker-labelled lysosomes after being internalized, supporting a role for this compartment in PrP<sup>Sc</sup> degradation upon OHT treatment (Supplementary Movie S2).

Overall, these data point towards autophagy-independent involvement of the lysosomal proteolysis pathway in PrP<sup>Sc</sup> degradation upon OHT treatment. In addition, we found that upon OHT treatment a fraction of non-infectious PrP<sup>C</sup> was relocated to lysosomes (Supplementary Figure S4), suggesting

that this drug could also perturb the trafficking of the substrate of the PrP<sup>Sc</sup> conversion process. In conclusion, these results show that OHT targets PrP<sup>Sc</sup> to lysosomes where it gets degraded and support the hypothesis that the variation in the cholesterol distribution influence both the trafficking and the metabolism of PrP<sup>Sc</sup> (Lewis and Hooper, 2011; Campana et al., 2005).

## Discussion

When first observed, autophagy was considered to be only a cytopathological feature associated with cell death (Baehrecke, 2005). The field has advanced considerably with the development of new tools created to better study the phenomenon and the predominant current view is that autophagy in many contexts is cytoprotective. It has only been recently appreciated that autophagy is the most efficient mechanism by which cytosolic protein aggregates are targeted for destruction by enzymatic hydrolysis in lysosomes (Yang and Klionsky, 2009). Cellular quality control by autophagy is particularly important in neurons, where the content of aggregated proteins and damaged organelles cannot be reduced by distribution to daughter cells. Therefore, it is not surprising that various failures in the autophagic pathway are connected to neurodegenerative disorders such as Alzheimer's, Parkinson's and Huntington's disease (Wong and Cuervo, 2010). Prevailing models in the recent literature propose that the amount of protease-resistant, aggregate-prone prion protein is maintained by a balance between PrP<sup>Sc</sup> formation by conversion of native PrP<sup>C</sup> and its destruction in lysosomes, which could be mediated by the autophagic pathway. In favor of this hypothesis, the appearance of multi-vesicular bodies and autophagic vacuoles has been reported in both prion-infected, neuronal cells in culture (Schätzl et al., 1997) and in brain biopsies from prion-infected patients (Liberski et al., 2008; Sikorska et al., 2004). Furthermore, stimulation of autophagy by chemical compounds such as rapamycin, lithium salts and trehalose is able to reduce protease-resistant PrP<sup>Sc</sup> in cultured cells (Aguib et al., 2009; Heiseke et al., 2009). These observations imply a protective role for autophagy in prion infection. Alternatively, it was

proposed that autophagy may contribute to the spongiform changes that are a pathological hallmark of prion affected brains, and may be activated by apoptosis (Liberski et al., 2008; Liberski and Jeffrey, 2004; Sikorska et al., 2004). These contradictory findings raised the question of the biological role of autophagy in prion infection and disease and prompted us to look more closely into the molecular interplay between autophagy, prion propagation, trafficking and clearance.

The first clue of an altered autophagic pathway in different neurodegenerative settings is the presence of an abnormal number of autophagosomes in affected neurons (Kegel et al., 2000; Nixon et al., 2005). In prion diseases an increased number of autophagosomes have been reported in infected neuronal cells and brain tissue (Liberski et al., 2008; Sikorska et al., 2004; Schätzl et al., 1997). Here we have confirmed and extended these finding by showing elevated levels of basal autophagy in uninfected neuronal cells and demonstrated that chronic scrapie infection additionally induces autophagic flux, but not autophagy per se (Figure 1; Supplementary Figure S1, A and B). These results were in contrast with previous reports in which basal levels of autophagy could not be detected in non-infected N2a cells (Aguib et al., 2009; Heiseke et al., 2009). The most likely reason for this discrepancy was the different tool used in this study to monitor autophagy, namely, tandem fluorescent LC3 (tf-LC3) containing both GFP and RFP. This construct enables one to distinguish autophagosomes from phagolysosomes based on the presence of only red fluorescence in the acidic phagolysosomal compartment (Kimura et al., 2009). Therefore, earlier studies reporting no basal autophagy in N2a cells were based only on observations of autophagosomes since the phagolysosomes present were essentially invisible when using GFP-LC3 alone.

We also report that although chronic scrapie infection increases autophagic flux, PrP<sup>Sc</sup> is mostly absent from autophagic vesicles, even when lysosomal degradation is impaired (Figure 4). This observation raised the possibility that PrP<sup>Sc</sup> is not processed by the autophagic machinery. In fact, when Alexa546-labelled PrP<sup>Sc</sup> was added to cells transfected with GFP-LC3 and analyzed

by live imaging we could observe a clear induction of autophagy but no colocalisation of Alexa 546-PrP<sup>Sc</sup> with LC3-decorated vesicles (Supplementary Movie S1). This suggests that PrP<sup>Sc</sup> is able to escape autophagy during primary infection. Recently, similar observations were made in cells harboring mutant Htt in which cargo recognition failure by the autophagic pathway was detected (Li et al., 2010). One unanswered question from this study was: why is autophagy induced by prion infection despite its lack of involvement in its processing? It is possible that the presence of protein aggregates stimulates autophagic flux as a defensive response. However, prions, being membrane-bound proteins, may be able to elude recognition by the autophagic machinery by virtue of their sequestration within vesicles. In addition, it was found that autophagy could not be further enhanced in scrapie-infected cells with drugs like rapamycin (Figure 3; Supplementary figure S1, C and D), previously described as inducers of autophagy. Surprisingly, while screening for drugs that could modify the autophagy program we observed that in contrast to previous reports (de Medina et al., 2009) TAM and its metabolite OHT actually reduce autophagic flux. This discrepancy could be explained by the fact that an increase in GFP-LC3-positive vesicles (and hence autophagosomes) was previously interpreted as an increase in autophagy by these drugs. However, judging by the accumulation of both double-positive and red-only vesicles (Figure 3), these drugs are likely interfering with the fusion between autophagosomes and lysosomes, thus reducing the autophagic flux (Figure 3). Interestingly, while we did not detect an increase of PrP<sup>Sc</sup> in autophagosomes, we did observe increased PrP<sup>Sc</sup> clearance upon TAM and OHT treatment. This indicates that the mechanisms of PrP<sup>Sc</sup> clearance by these compounds are likely independent of autophagy (Figure 2). This hypothesis was tested directly using a gene-silencing approach. Consistent with the microscopy data, inhibition of autophagy using anti-atg7 siRNA did not affect the ability of TAM and OHT to reduce PrP<sup>Sc</sup> content in infected cells (Figure 5). Furthermore, prolonged knockdown of Atg7 did not lead to an accumulation of PrP<sup>Sc</sup> above untreated cells as would be expected if it was being

degraded by autophagy. Overall these observations argue against a major contribution of autophagy-mediated degradation in the regulation of PrP<sup>Sc</sup> levels both in *de novo* or permanent infections.

Ruling out a major involvement of autophagy in scrapie clearance raised the question as to what was the mechanism by which TAM and OHT reduced PrP<sup>Sc</sup> levels. We and others have previously shown that lipids, specifically cholesterol and sphingolipids, play a crucial role in PrP<sup>Sc</sup> propagation and that changes in sub-cellular distribution of PrP by modulating lipid metabolism and trafficking, affect PrP<sup>Sc</sup> levels in infected cells (Campana et al., 2005; Marijanovic et al., 2009; Lewis and Hooper, 2011; Taraboulos et al., 1995). Interestingly, both TAM and OHT are inhibitors of cholesterol biosynthesis (de Medina et al., 2011, 2004, 2009). Interestingly, the drug concentrations at which these effects are observed are the same concentrations that were required for reduction of PrP<sup>Sc</sup>. TAM has also been shown to inhibit the exit of cholesterol from lysosomes resulting in a lipid storage disease phenotype, characterized by the accumulation of cholesterol-laden late endosomes/lysosomes (Suárez et al., 2004). We observed a similar effect of both TAM and OHT on cholesterol trafficking in our cellular models (Figure 6). Importantly, these treatments induced the redistribution of PrP<sup>Sc</sup> and PrP<sup>C</sup> towards lysosomes (Figure 6 and Supplementary Figure S4), which could affect both PrP<sup>Sc</sup> replication and degradation. Indeed endocytic compartments, specifically the endosomal recycling compartment, normally containing high levels of cholesterol (Wüstner et al., 2002; Hao et al., 2002), was shown to be an intracellular site for PrP<sup>Sc</sup> conversion (Marijanovic et al., 2009). Therefore, conditions that favor endosomal degradation over endosomal recycling by re-routing PrP<sup>C</sup> from recycling endosomes to lysosomes could reduce its conversion and should facilitate the elimination of the pathological prion form by the lysosomal system. In this case, the prediction would be that inhibition of lysosomal degradation should counteract the effect of OHT. Indeed, when we blocked lysosomal degradation using NH<sub>4</sub>Cl in OHT-treated cells, higher levels of PrP<sup>Sc</sup> were observed (Figure 8). Thus,

by redirecting PrP<sup>Sc</sup> to lysosomes, OHT most likely interferes with the interaction between PrP<sup>C</sup> and PrP<sup>Sc</sup> in the endocytic pathway, which is necessary for PrP<sup>Sc</sup> replication thus shifting equilibrium towards PrP<sup>Sc</sup> degradation (Figure 9). PrP and cholesterol distribution suggests that TAM and OHT could trigger the accumulation of different lipids in the lysosomal pathway. Such a mechanism for reducing scrapie recalls reports on sphingolipid storage diseases (Schulze and Sandhoff, 2011). However, the nature of the lipids accumulating in lysosomes and whether lipid accumulation directly influenced PrP<sup>Sc</sup> localization in this compartment remains to be determined. While autophagy is well known as a mechanism for directing aggregated proteins into lysosomes it appears that TAM and OHT induce the trafficking of prions to lysosomes in an autophagy-independent fashion. In conclusion, given its ability to both reduce infectious prions and modify cholesterol metabolism and lipid content of the cell TAM represents a well-characterized, widely available pharmaceutical that may have applications as a broad-spectrum therapy for neurodegenerative diseases of protein aggregation.

## **MATERIALS AND METHODS**

### **Chemicals and antibodies**

Rapamycin, TAM, OHT and Bafilomycin A1 were all purchased from Sigma. SAF32 and Sha31 anti-prion antibodies were purchased from SpiBio. Anti-tubulin monoclonal antibodies and anti-ATG7 were from Sigma. All the fluorescently labelled secondary antibodies, as well as LysoTracker® green were purchased from Invitrogen (Molecular Probes). Anti-LAMP1 antibodies were purchased from BD Pharmingen™. Anti-LC3 monoclonal antibody, used for western blotting, was from nanoTools and anti-LC3 polyclonal antibody, used for immunofluorescence, was purchased from MBL International. Fluorescently labelled PrP<sup>Sc</sup> (Alexa546-PrP<sup>Sc</sup>) was prepared as previously described (Gousset et al., 2009).

### **Cell lines**

GT1-1 cells (gift of Dr. Mellon P., University of California, San Diego, USA) were infected with RML prion strain (gift of Dr. Korth K., Heinrich Heine University, Dusseldorf, Germany). N2a cells and

scN2a cells (infected with 22L prion strain) were provided by Dr. Korth K.

Non-infected and prion-infected GT1-1 and N2a cells were maintained in Dulbecco's modified Eagle's medium (DMEM) (Invitrogen) supplemented with 10% of fetal calf serum (FCS). CAD and scCAD (infected with 139A prion strain) were both gifts of Dr. Laude H. (Institut National de la Recherche Agronomique, Jouy-en-Josas, France) and were cultured in Opti-MEM (Invitrogen) with addition of 10% FBS.

### **Plasmids, siRNAs and transfection procedures**

The tandem fluorescently-tagged (with both GFP and RFP) LC3 (Tf-LC3) and GFP-LC3 plasmids were a kind gift from Dr. Ballabio A. (Telethon Institute of Genetic and Medicine (TIGEM), Naples, Italy) and Dr. Yoshimori T. (Research Institute for Microbial Diseases, Osaka University, Osaka, Japan). ATG7 siRNA pre-designed ON TARGETplus SMARTpool and siGENOME RISC-Free Control siRNA were both purchased from Dharmacon.

GT1-1 and scGT1 cells were transfected at 50% confluence using FuGENE6 (Roche Diagnostic) for DNA constructs according to manufacturer's protocol. To downregulate ATG7, 100 nM concentration of oligo was used with 10  $\mu$ l of HiPerFect (Quiagen) per 60 mm dish. Hyperfect reagent was mixed with siRNA in DMEM without FBS, incubated for 10 min at room temperature and added to the cells.

Transfection of both non-infected and infected CAD and N2a cells with DNA constructs was done using Lipofectamine 2000 (Invitrogen), according to producer's protocol.

When detection of PrP<sup>Sc</sup> levels was performed, downregulation and overexpression of the proteins were maintained for a 5-day period. Therefore in all the experiments siRNA and plasmids, except of pEGFP were transfected twice (a second round of transfection was performed 3 days post-transfection).

### **Treatment of ScGT1 and scN2a cells with different drugs**

Rapamycin, TAM, OHT were reconstituted according to manufacturer's instructions. All the drugs were used in DMEM + 10% FCS at the final concentration of 2  $\mu$ M for Rapamycin, and 5  $\mu$ M concentration for

TAM and OHT. During the 3 or 5-day treatment, medium containing the different drugs was changed every 2 days. 5M stock concentration of NH<sub>4</sub>Cl from powder (Sigma) was prepared in sterile Ultra-pure MilliQ water.

When needed, Bafilomycin A1 or NH<sub>4</sub>Cl, respectively at 100 µM and 15 mM concentration were added to the Rapamycin, TAM or OHT 5 day treatment for 2 days starting from the 4<sup>th</sup> day of the different treatments.

#### **Protein analysis by western blotting**

Cells grown in 60 mm dishes after the different treatments were lysed in 500 µl of Lysis buffer (0,5% triton X-100, 0,5% DOC, 100 mM NaCl, 10 mM Tris-HCl pH 8). To analyze PrP<sup>Sc</sup> levels, 250 µg of protein/lysate were treated with 5 µg of Proteinase K (PK) for 30 min at 37°C. This step allows detecting PrP<sup>Sc</sup> content only, because of its partial resistance to PK (Prusiner et al 1984). The protein content was then methanol-precipitated overnight at -20°C and centrifuged at 13000g for 30 minutes. After drying at 100°C, the pellet was resuspended and denatured in Laemmli buffer before SDS-PAGE and western blot with the Sha31 anti-PrP antibody. All the other proteins, including total PrP, were analysed by western blotting from 20 or 40 µg of total lysate. HRP-conjugated secondary antibodies and ECL<sup>TM</sup> reagents from Amersham (GE Healthcare) were used for detection.

#### **Immunofluorescence**

For immunofluorescence analysis cells grown on coverslips into a 24 well plate for 3 days were carefully washed with PBS, fixed with 2% PFA for 30 minutes and permeabilized with 0,1% of Triton X-100/PBS. A denaturation step with 6M guanidine-hydrochloride for 10 min was performed after permeabilization to detect PrP<sup>Sc</sup> in infected cells (Taraboulos et al., 1990), when needed. Cells were then blocked in 2% BSA/PBS, immunolabelled with primary and secondary antibodies and mounted with Aqua/Poly Mount (Polysciences).

In order to label endogenous LC3, cells were differently treated as previously described (Kimura et al., 2009).

When filipin staining was used, cells were fixed with 4% PFA for 60 min and blocked with 0,2% BSA/PBS. Filipin (250 µg/ml) was added to blocking solution and additional 30 min incubation was

performed after incubation with secondary antibodies.

#### **Fluorescence Microscopy**

Immunofluorescence micrographs were acquired by high-resolution wide-field microscope Marianas (Intelligent Imaging Innovations) using 63x oil objective. All Z-stacks were acquired with Z-steps of 0.27 µm. The auto-scaling (min/max) of signal detection was used to record only maximal signal intensities when PrP<sup>Sc</sup> was analysed (Marijanovic et al., 2009).

In the live experiments, CAD cells plated on ibidi dishes were either transfected with GFP-LC3 plasmid or incubated with LysoTracker (1:1000 dilution) for 30 min at 37°C prior to be challenged with 1 µl/dish of sonicated Alexa546-PrP<sup>Sc</sup>. The time-lapse movies were acquired with Biostation IM (from Nikon) and a wide-field microscope (Zeiss Axiovert 200M) controlled by Axiovision software.

#### **Image processing and quantification**

Raw data (both images and movies) were processed with Image J software. The constrained iterative algorithm in Slidebook 4.2 software (Intelligent Imaging Innovations) was used to deconvolve the images. Colocalization was quantified by intensity correlation coefficient-based (ICCB) analysis using JACoP (Bolte and Cordelières, 2006). Statistical analysis of the correlation of the intensity values of both green and red pixels or blue and red pixels in dual-channel image was performed using Pearson's and Menders's coefficient and Van Steensel's approach (van Steensel et al., 1996).

#### **Statistical analysis**

All data were statistically validated by Student's T-test. The differences were considered significant when p<0.05.

#### **Acknowledgements**

Priority, Pasteur Weizmann Disc

#### **References**

Aguib, Y., A. Heiseke, S. Gilch, C. Riemer, M. Baier, A. Ertmer, and H.M. Schätzl. 2009. Autophagy induction by trehalose counter-acts cellular prion-infection. *Autophagy*. 5:361-370.

Baehrecke, E.H. 2005. Autophagy: dual roles in life and death? *Nat Rev Mol Cell Biol*. 6:505-510.

- Baron, G.S., K. Wehrly, D.W. Dorward, B. Chesebro, and B. Caughey. 2002. Conversion of raft associated prion protein to the protease-resistant state requires insertion of PrP-res (PrPSc) into contiguous membranes. *EMBO J.* 21:1031-1040.
- Campana, V., D. Sarnataro, and C. Zurzolo. 2005. The highways and byways of prion protein trafficking. *Trends Cell Biol.* 15:102-111.
- Caughey, B., G.S. Baron, B. Chesebro, and M. Jeffrey. 2009. Getting a grip on prions: oligomers, amyloids, and pathological membrane interactions. *Annu. Rev. Biochem.* 78:177-204.
- Cherra III, S.J., R.K. Dagda, and C.T. Chu. 2010. Review: Autophagy and neurodegeneration: survival at a cost? *Neuropathology and Applied Neurobiology.* 36:125-132.
- Goussset, K., E. Schiff, C. Langevin, Z. Marijanovic, A. Caputo, D.T. Browman, N. Chenouard, F. de Chaumont, A. Martino, J. Enninga, J.-C. Olivo-Marin, D. Männel, and C. Zurzolo. 2009. Prions hijack tunnelling nanotubes for intercellular spread. *Nat. Cell Biol.* 11:328-336.
- Hao, M., S.X. Lin, O.J. Karylowski, D. Wüstner, T.E. McGraw, and F.R. Maxfield. 2002. Vesicular and non-vesicular sterol transport in living cells. The endocytic recycling compartment is a major sterol storage organelle. *J. Biol. Chem.* 277:609-617.
- Hara, T., K. Nakamura, M. Matsui, A. Yamamoto, Y. Nakahara, R. Suzuki-Migishima, M. Yokoyama, K. Mishima, I. Saito, H. Okano, and N. Mizushima. 2006. Suppression of basal autophagy in neural cells causes neurodegenerative disease in mice. *Nature.* 441:885-889.
- Heiseke, A., Y. Aguib, and H.M. Schatzl. 2010. Autophagy, prion infection and their mutual interactions. *Curr Issues Mol Biol.* 12:87-97.
- Heiseke, A., Y. Aguib, C. Riemer, M. Baier, and H.M. Schätzl. 2009. Lithium induces clearance of protease resistant prion protein in prion-infected cells by induction of autophagy. *Journal of Neurochemistry.* 109:25-34.
- Kabeya, Y., N. Mizushima, T. Ueno, A. Yamamoto, T. Kirisako, T. Noda, E. Kominami, Y. Ohsumi, and T. Yoshimori. 2000. LC3, a mammalian homologue of yeast Apg8p, is localized in autophagosome membranes after processing. *EMBO J.* 19:5720-5728.
- Kimura, S., N. Fujita, T. Noda, and T. Yoshimori. 2009. Monitoring autophagy in mammalian cultured cells through the dynamics of LC3. *Meth. Enzymol.* 452:1-12.
- Komatsu, M., S. Waguri, T. Chiba, S. Murata, J.-ichi Iwata, I. Tanida, T. Ueno, M. Koike, Y. Uchiyama, E. Kominami, and K. Tanaka. 2006. Loss of autophagy in the central nervous system causes neurodegeneration in mice. *Nature.* 441:880-884.
- Lewis, V., and N.M. Hooper. 2011. The role of lipid rafts in prion protein biology. *Front. Biosci.* 16:151-168.
- Li, X., C.-E. Wang, S. Huang, X. Xu, X.-J. Li, H. Li, and S. Li. 2010. Inhibiting the ubiquitin-proteasome system leads to preferential accumulation of toxic N-terminal mutant huntingtin fragments. *Human Molecular Genetics.* 19:2445 - 2455.
- Liberski, P.P., and M. Jeffrey. 2004. Tubulovesicular structures--the ultrastructural hallmark for transmissible spongiform encephalopathies or prion diseases. *Folia Neuropathol.* 42 Suppl B:96-108.
- Liberski, P.P., D.R. Brown, B. Sikorska, B. Caughey, and P. Brown. 2008. Cell death and autophagy in prion diseases (transmissible spongiform encephalopathies). *Folia Neuropathol.* 46:1-25.
- Marijanovic, Z., A. Caputo, V. Campana, and C. Zurzolo. 2009. Identification of an intracellular site of prion conversion. *PLoS Pathog.* 5:e1000426.
- de Medina, P., M.R. Paillasse, G. Ségala, F. Khallouki, S. Brillouet, F. Dalenc, F. Courbon, M. Record, M. Poirot, and S. Silvente-Poirot. 2011. Importance of cholesterol and oxysterols metabolism in the pharmacology of tamoxifen and other

AEBS ligands. *Chem. Phys. Lipids*. 164:432-437.

de Medina, P., B.L. Payré, J. Bernad, I. Bossier, B. Pipy, S. Silvente-Poirot, G. Favre, J.-C. Faye, and M. Poirot. 2004. Tamoxifen Is a Potent Inhibitor of Cholesterol Esterification and Prevents the Formation of Foam Cells. *Journal of Pharmacology and Experimental Therapeutics*. 308:1165 -1173.

de Medina, P., S. Silvente-Poirot, and M. Poirot. 2009. Tamoxifen and AEBS ligands induced apoptosis and autophagy in breast cancer cells through the stimulation of sterol accumulation. *Autophagy*. 5:1066-1067.

Mizushima, N., and T. Yoshimori. 2007. How to interpret LC3 immunoblotting. *Autophagy*. 3:542-545.

Prusiner, S.B. 1998. Prions. *Proc Natl Acad Sci U S A*. 95:13363-13383.

Schätzl, H.M., L. Laszlo, D.M. Holtzman, J. Tatzelt, S.J. DeArmond, R.I. Weiner, W.C. Mobley, and S.B. Prusiner. 1997. A hypothalamic neuronal cell line persistently infected with scrapie prions exhibits apoptosis. *J Virol*. 71:8821-8831.

Schulze, H., and K. Sandhoff. 2011. Lysosomal lipid storage diseases. *Cold Spring Harb Perspect Biol*. 3.

Sikorska, B., P.P. Liberski, P. Giraud, N. Kopp, and P. Brown. 2004. Autophagy is a part of ultrastructural synaptic pathology in Creutzfeldtâ€“Jakob disease: a brain biopsy study. *The International Journal of Biochemistry & Cell Biology*. 36:2563-2573.

Suárez, Y., C. Fernández, D. Gómez-Coronado, A.J. Ferruelo, A. Dávalos, J. Martínez-Botas, and M.A. Lasunción. 2004. Synergistic upregulation of low-density lipoprotein receptor activity by tamoxifen and lovastatin. *Cardiovasc. Res*. 64:346-355.

Taraboulos, A., M. Scott, A. Semenov, D. Avrahami, L. Laszlo, S.B. Prusiner, and D. Avraham. 1995. Cholesterol depletion and modification of COOH-terminal targeting sequence of the prion protein inhibit formation of the scrapie isoform. *J. Cell Biol*. 129:121-132.

Wong, E., and A.M. Cuervo. 2010. Autophagy gone awry in neurodegenerative diseases. *Nat Neurosci*. 13:805-811.

Wüstner, D., A. Herrmann, M. Hao, and F.R. Maxfield. 2002. Rapid nonvesicular transport of sterol between the plasma membrane domains of polarized hepatic cells. *J. Biol. Chem*. 277:30325-30336.

Yang, Z., and D.J. Klionsky. 2009. An overview of the molecular mechanism of autophagy. *Curr. Top. Microbiol. Immunol*. 335:1-32.

## FIGURES LEGEND

### Figure 1. Autophagic flux in non infected and prion-infected GT1 and N2a cells

(A) Both non infected and infected GT1 and N2a cells were transfected with Tf-LC3 construct and analysed by fluorescence microscopy. Activation of autophagy is signalled by LC3-positive vesicles (both green and red labelled); appearance of red puncta-only indicate progression of autophagic flux. Scale bars 10  $\mu$ m (B) The quantification results are presented as % of both green and red (autophagosomes) and only-red vesicles (phagolysosomes) per cell (mean  $\pm$  s.e.m, n=3). (C) Endogenous levels of LC3-II in infected and non infected cells either treated (+) or not (-) with lysosomal inhibitors revealed by monoclonal anti-LC3 antibody (clone 2G6) on western blot (mean  $\pm$  s.e.m, n=3). Quantified results were normalized for tubulin. Note that both fluorescence microscopy and biochemical approach confirmed an activation of autophagic flux during prion infection in both cell lines.

### Figure 2. TAM and OHT treatment are able to reduce PrP<sup>Sc</sup> levels in both scGT1 and scN2a cells

(A-C) ScGT1 and scN2a cells were treated with the different compounds for 5 days and levels of PrP<sup>Sc</sup> (PK+) and total PrP (PK-) were detected on western blot by using Sha31 anti-PrP antibody. Tubulin levels represent control for equal loading. (B-D) Quantification results of PrP<sup>Sc</sup> levels upon different treatments are presented as % of untreated cells where PrP<sup>Sc</sup> levels are considered to be 100% (mean  $\pm$  s.e.m, n=3).

**Figure 3. Effect of rapamycin, TAM and OHT treatment on autophagic flux in scGT1 and scN2a cells**

(A) scGT1 and scN2a cells transfected with Tf-LC3 were subjected to a 4h treatment with the different drugs and then analysed by fluorescence microscopy. The quantification results are presented as % of both green and red and only-red vesicles per cell (mean  $\pm$  s.e.m, n=3). Scale bar 10  $\mu$ m (B) Endogenous levels of LC3-II (normalized for tubulin) were compared in between scGT1 cells untreated and treated for 5 days with either rapamycin, tamoxifen and HO-tamoxifen in presence (+) or absence (-) of lysosomal proteases inhibitors (mean  $\pm$  s.e.m, n=3). The lysosomal proteases treatment clearly shows an inhibition of the autophagic flux when HO-tamoxifen was added to the cells.

**Figure 4. PrP<sup>Sc</sup> found in autophagosomes do not change upon different treatments in scGT1 cells**

(A) scGT1 cells were treated for 3 days with either rapamycin, TAM and OHT in presence (+) or absence (-) of 100  $\mu$ M concentration of Bafilomycin A1 and then subjected to a double immunofluorescence with a polyclonal anti-LC3 antibody and Saf32 anti-prion mAb. 6M guanidine-hydrochloride treatment prior immunolabelling was used to reveal PrP<sup>Sc</sup> epitopes. Yellow color shows colocalization between PrP<sup>Sc</sup> and LC3-positive vesicles. Scale bars 10  $\mu$ m. (B) The quantification results (mean  $\pm$  s.e.m, n=50) are presented as % of total signal of PrP<sup>Sc</sup> (in red) colocalizing with autophagosomes (green). Insets represent magnification of the boxed areas. Note that only a minor fraction of PrP<sup>Sc</sup> has been found in LC3-positive vesicles and both different treatments and lysosomal proteases inhibition do not increase its presence in these organelles.

**Figure 5. ATG7 down-regulation in scGT1 cells does not block PrP<sup>Sc</sup> clearance upon rapamycin, TAM and OHT treatment**

(A) scGT1 cells transfected with either control oligo (ctr oligo) or siRNA for ATG7 were treated for 5 days with rapamycin, TAM and OHT and then subjected to lysis. ATG7, LC3-II and total PrP (PK-) levels were analyzed by western blot. To measure PrP<sup>Sc</sup> levels (PK+), lysed were

additionally subjected to proteinase K limited proteolysis assay prion analysis. Tubulin has been used as a control for equal loading. (B) The quantification results (mean  $\pm$  s.e.m, n=3) are presented as % of total PrP<sup>Sc</sup> signal in untreated cells transfected with ctr oligo.

**Figure 6. Cholesterol redistributes to lysosomes upon TAM and OHT treatment in scGT1 cells**

scGT1 cells were treated with either rapamycin, TAM and OHT for 5 days and distribution of cholesterol was examined by filipin staining (in blue). Immunofluorescence with LAMP1 Ab (in green) was used to evaluate the presence of cholesterol in lysosomes. Note that upon TAM and OHT treatment cholesterol partially accumulates in lysosomes as depicted by arrowheads in the inset showing the colocalisation between filipin and LAMP1.

**Figure 7. PrP<sup>Sc</sup> localisation in lysosomes increases upon OHT treatment**

(A) Differences in PrP<sup>Sc</sup> fraction in lysosomes were examined. scGT1 cells were treated for 3 days with either rapamycin, TAM and OHT and then subjected to a double immunofluorescence with anti-LAMP1 Ab (to stain lysosomes) and Saf32 anti-prion mAb (after 6M Gnd-HCl treatment to reveal PrP<sup>Sc</sup>). (B) The quantification results (mean  $\pm$  s.e.m, n=50) are presented as % of total signal of PrP<sup>Sc</sup> (in red) colocalizing with lysosomes (green). Insets represent magnification of the boxed areas. Scale bars 10  $\mu$ m.

**Figure 8. PrP<sup>Sc</sup> is degraded in lysosomes upon OHT treatment**

scGT1 cells were treated for 5 days with OHT in presence (+) or absence (-) of NH<sub>4</sub>Cl. PrP<sup>Sc</sup> (PK+) and total PrP (PK-) were analysed by western blot. Tubulin levels represent control from equal loading. Quantification results of PrP<sup>Sc</sup> levels are presented as % of untreated cells where PrP<sup>Sc</sup> levels are considered to be 100% (mean  $\pm$  s.e.m, n=3). Note that lysosomal proteases inhibition counteracts the effect of OHT treatment restoring PrP<sup>Sc</sup> levels.

**Figure 9. Schematic presentation of PrP trafficking in infected cells and upon OHT treatment**

In infected cells PrP<sup>C</sup> and PrP<sup>Sc</sup> interact at plasma membrane in cholesterol rich lipid domains called lipid rafts. Upon internalization both PrP<sup>C</sup> and PrP<sup>Sc</sup> can recycle via endosomal recycling compartment (ERC) or can be routed for degradation in lysosomes. Subcellular cholesterol distribution influences PrP<sup>Sc</sup> trafficking in endocytic pathway. In untreated infected cells, majority of PrP recycles through cholesterol-enriched ERC supporting conversion of PrP<sup>C</sup> to PrP<sup>Sc</sup>. Treatment with 4-hydroxy-tamoxifen (OHT) induces cholesterol accumulation in enlarged late endosomes. PrP<sup>Sc</sup> production and degradation define cellular load of infectious prions. We propose that 4-hydroxy-tamoxifen-induced changes in PrP<sup>Sc</sup> trafficking favor PrP<sup>Sc</sup> degradation.

## **SUPPLEMENTARY INFORMATIONS**

### **Supplementary Figure S1. Autophagic flux in uninfected and prion-infected CAD cells and effect of rapamycin, TAM and OHT treatment on autophagic flux in scCAD cells**

(A) Both non infected and infected CAD cells were transfected with Tf-LC3 construct and analysed by fluorescence microscopy. Scale bars 10  $\mu$ m. (B) The quantification results are presented as % of both green and red (autophagosomes) and only-red vesicles (phagolysosomes) per cell (mean  $\pm$  s.e.m, n=30). As observed for GT1 and N2a cells, the autophagic flux increases upon infection. (C) scCAD cells transfected with Tf-LC3 were subjected to a 4h treatment with the different drugs and then analysed by fluorescence microscopy. (D) The quantification results are presented as % of both green and red (autophagosomes) and only-red vesicles (phagolysosomes) per cell (mean  $\pm$  s.e.m, n=30). Scale bars 10  $\mu$ m. Note that the autophagic flux is not further increased by autophagy inducers.

### **Supplementary Figure S2. Proteinase K limited proteolysis assay on uninfected and infected GT1 and N2a cells**

Both infected and non infected GT1 and N2a cells were lysed and subjected to proteinase K limited proteolysis assay. PrP<sup>Sc</sup> levels (PK+) were detected on western blotting by using Sha31 anti-PrP antibody.

### **Supplementary figure S3. PrP<sup>Sc</sup> localisation in autophagosomes by**

### **immunofluorescence and its clearance upon rapamycin, TAM and OHT treatment in scCAD cells**

(A) scCAD cells were treated for 3 days with either rapamycin, TAM and OHT and then subjected to a double immunofluorescence with a polyclonal anti-LC3 antibody and Sha31 anti-prion mAb. 6M guanidine-hydrochloride treatment prior immunolabelling was used to reveal PrP<sup>Sc</sup> epitopes. Yellow color shows colocalization between PrP<sup>Sc</sup> and LC3-positive vesicles. Scale bars 10  $\mu$ m. (B) The quantification results (mean  $\pm$  s.e.m, n=50) are presented as % of total signal of PrP<sup>Sc</sup> (in red) colocalizing with autophagosomes (green). Insets represent magnification of the boxed areas. Scale bars 10  $\mu$ m. Note that only a minor fraction of PrP<sup>Sc</sup> has been found in LC3-positive vesicles in untreated control and upon different treatments. (C) scCAD cells were treated with the different compounds for 5 days and levels of PrP<sup>Sc</sup> (PK+) and total PrP (PK-) were detected on western blot by using Sha31 anti-PrP antibody. Tubulin levels represent control for equal loading. (D) Quantification results of PrP<sup>Sc</sup> levels upon different treatments are presented as % of untreated cells where PrP<sup>Sc</sup> levels are considered to be 100% (mean  $\pm$  s.e.m, n=3).

### **Supplementary figure S4. Upon OHT treatment also a fraction of PrP<sup>C</sup> relocates to lysosomes in scGT1 cells**

Presence of PrP<sup>C</sup> in lysosomes was evaluated. scGT1 cells were treated for 3 days with OHT and then subjected to a double immunofluorescence with anti-LAMP1 Ab (to stain lysosomes) and Sha31 anti-PrP mAb (after Gnd-HCl treatment to reveal PrP<sup>Sc</sup> epitopes). Note that while in control untreated cells PrP<sup>C</sup> is mainly distributed at the level of the golgi compartment, upon OHT treatment it partially relocated to lysosomes as suggested by a more scattered signal and the quantitative colocalisation analysis. Quantification results (mean  $\pm$  s.e.m, n=50) are presented as % of total signal of PrP<sup>C</sup> (in red) colocalising with lysosomes (green). Scale bars 10  $\mu$ m.

### **Supplementary Movie S1. Alexa546-PrP<sup>Sc</sup> newly up-taken does not colocalises with GFP-LC3 in CAD cells**

The fate of newly up-taken fluorescently-labelled PrP<sup>Sc</sup> was followed in real-time up to 12h post-infection. CAD cells

transfected with GFP-LC3 plasmid were challenged with Alexa546-PrP<sup>Sc</sup> and time-lapse movies were acquired with Time-lapse imaging Biostation IM system from Nikon (temperature, humidity and CO<sub>2</sub> controlled). Single Z-stacks were taken for each time point every 5 minutes up to 12h. Note that despite activation of autophagy upon infection (as shown by the punctuate LC3 signal) Alex546-PrP<sup>Sc</sup> particles were clearly distinguished from LC3-positive autophagosomes.

**Supplementary Movie S2. Alexa546-PrP<sup>Sc</sup> newly up-taken colocalises with lysotracker labelled lysosomes in OHT treated scCAD cells**

Analysis of the fate of PrP<sup>Sc</sup> aggregates in real-time upon OHT treatment by a live-imaging approach. CAD cells were challenged with Alexa546-PrP<sup>Sc</sup> and loaded with Lysotracker green (to stain lysosomes). Movies were recorded in a microscope chamber using a wide-field Axiovert microscope for live imaging (with temperature control and supplemented with CO<sub>2</sub>); Z-stacks of 1  $\mu$ m were taken for each time point every 5 minutes up to 12h. Newly uptaken PrP<sup>Sc</sup> colocalises with lysosomal compartment after being internalized where it undergoes degradation.

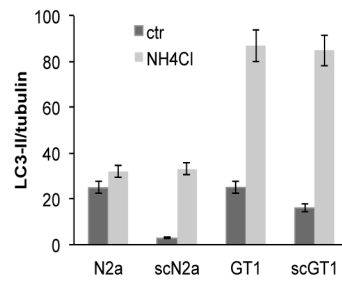
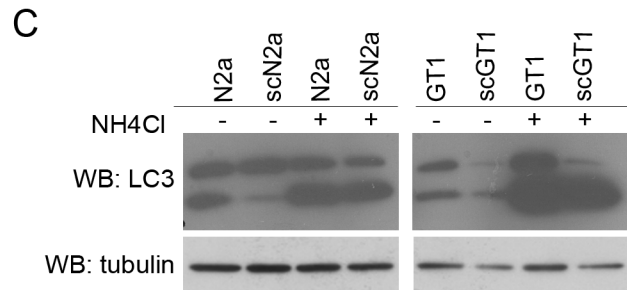
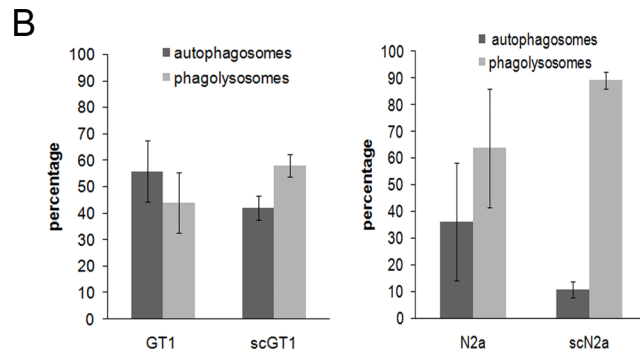
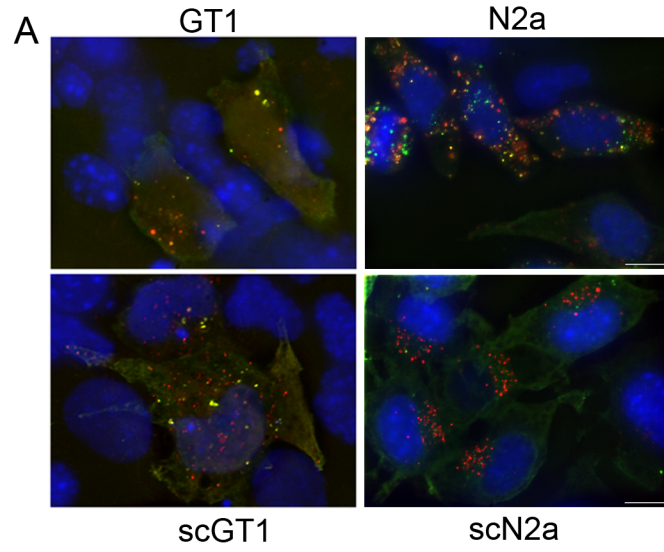


Figure 1

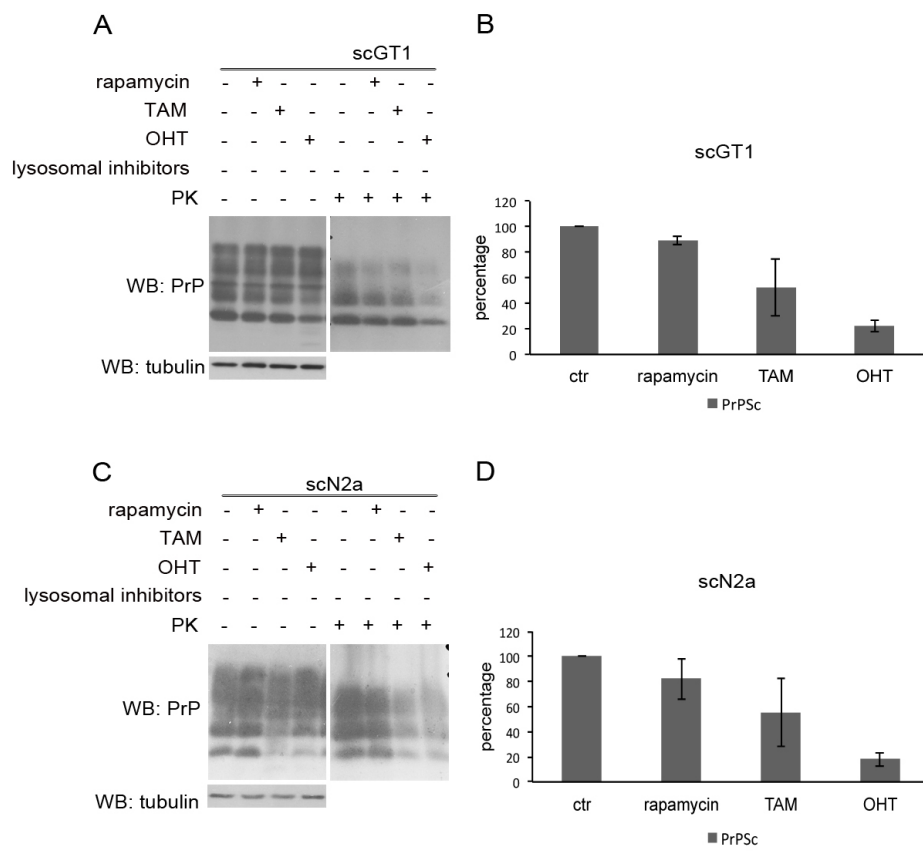


Figure 2

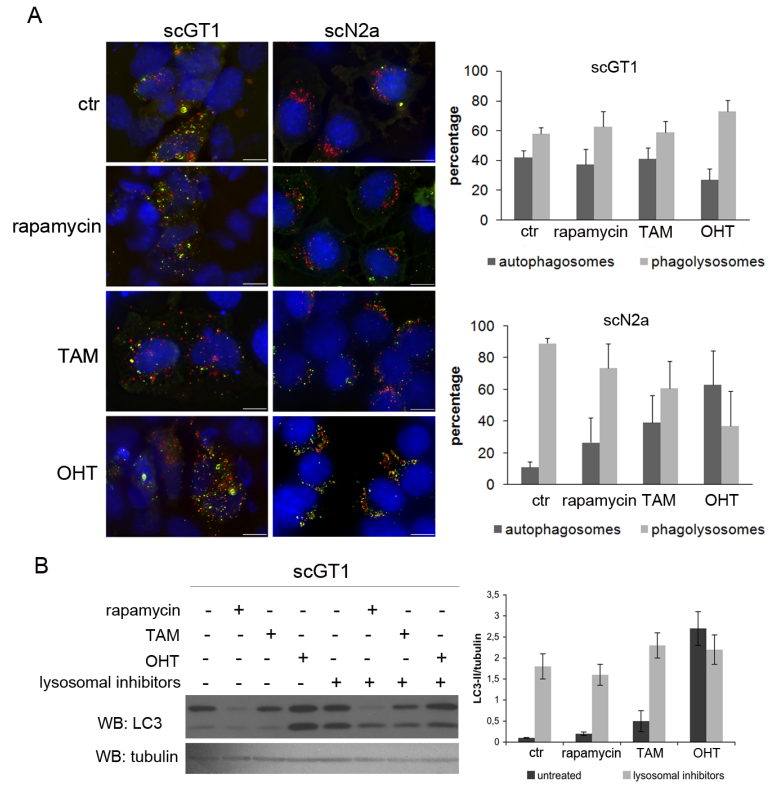


Figure 3

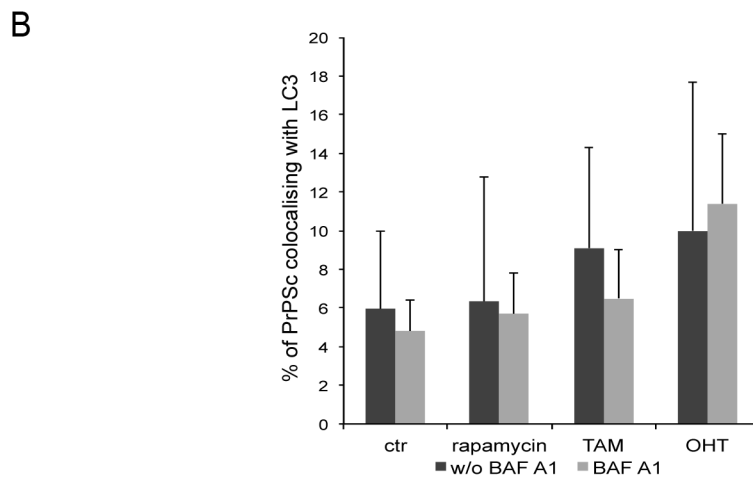
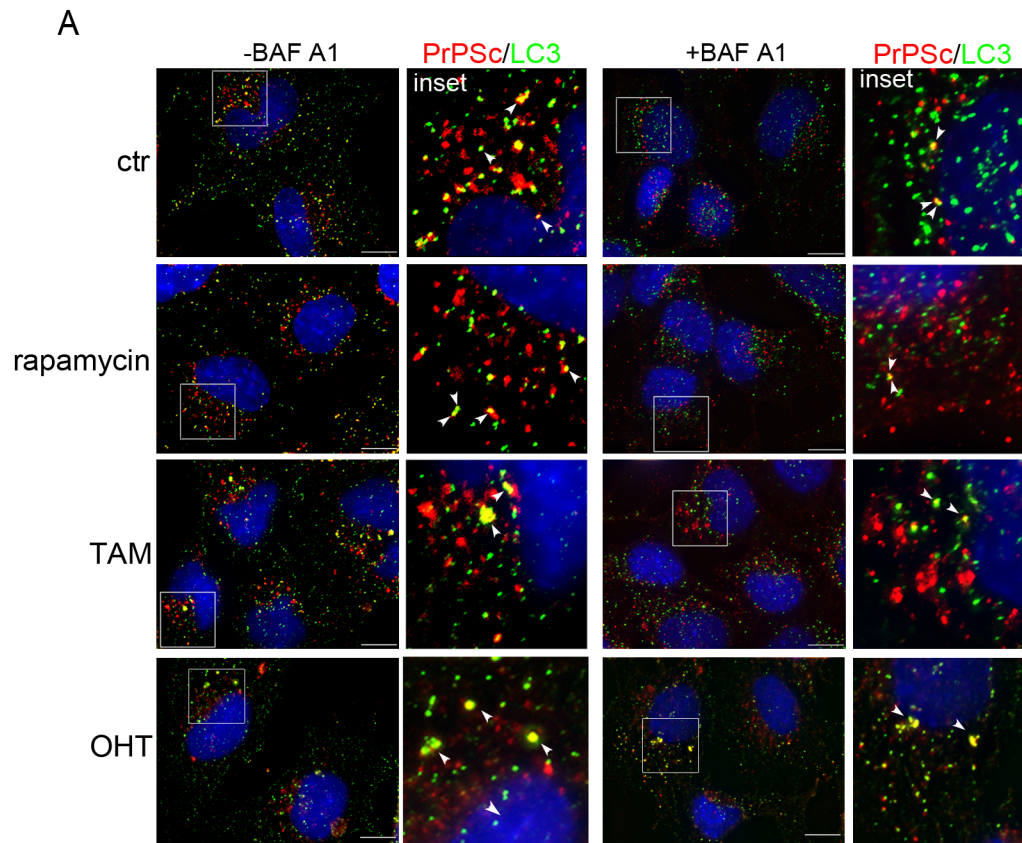


Figure 4

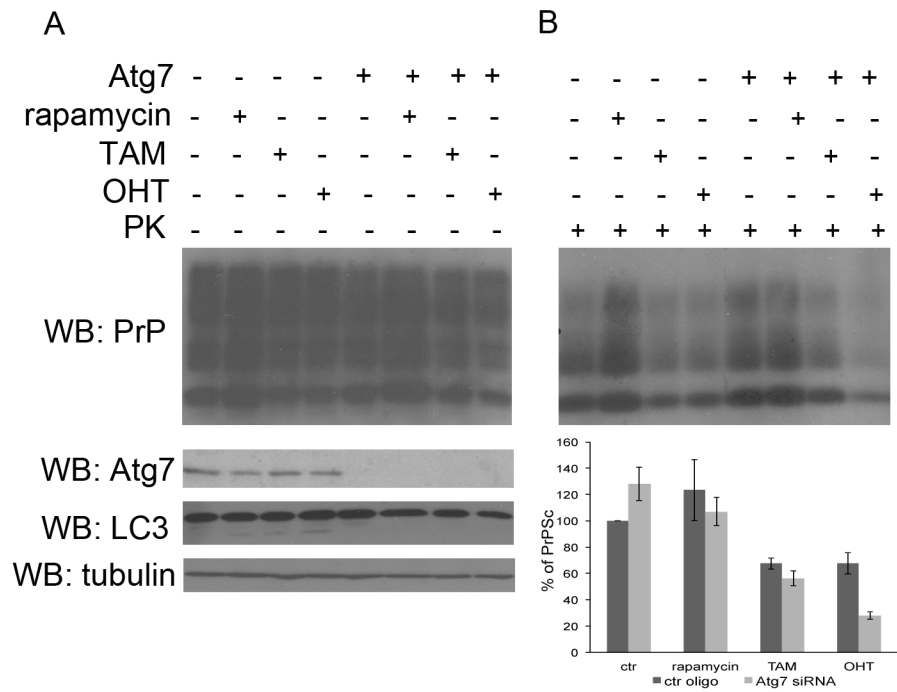


Figure 5

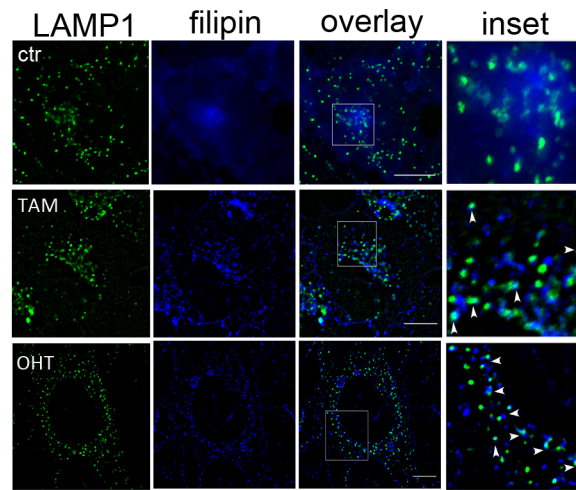


Figure 6

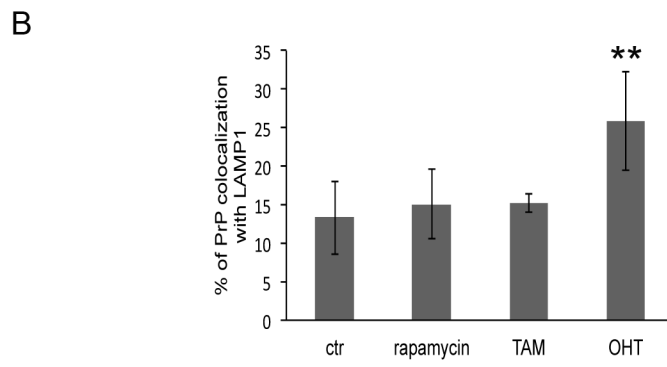
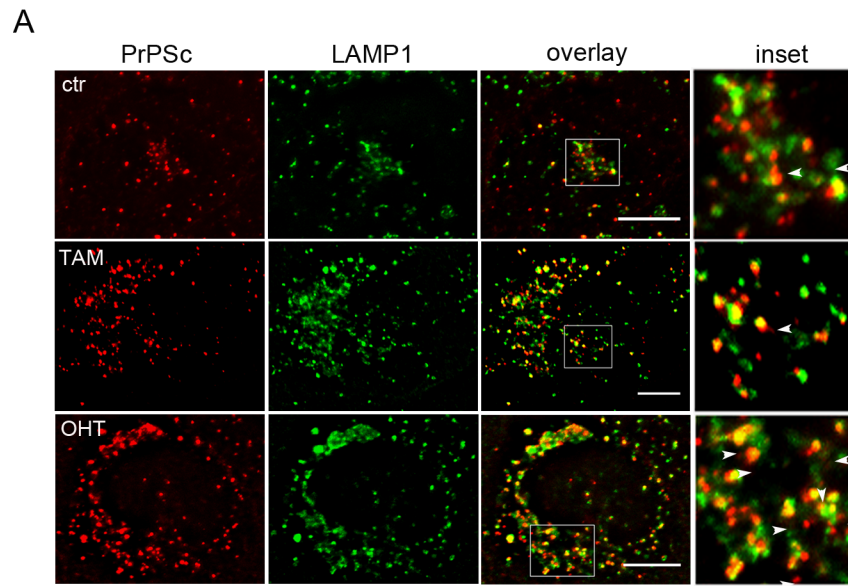


Figure 7

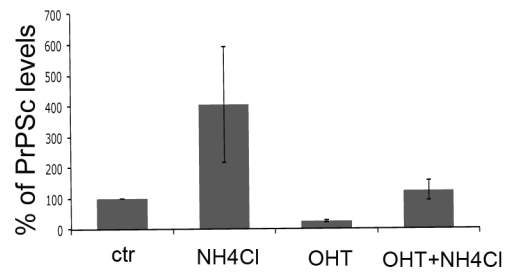
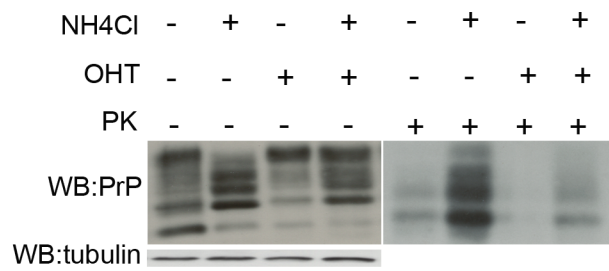


Figure 8

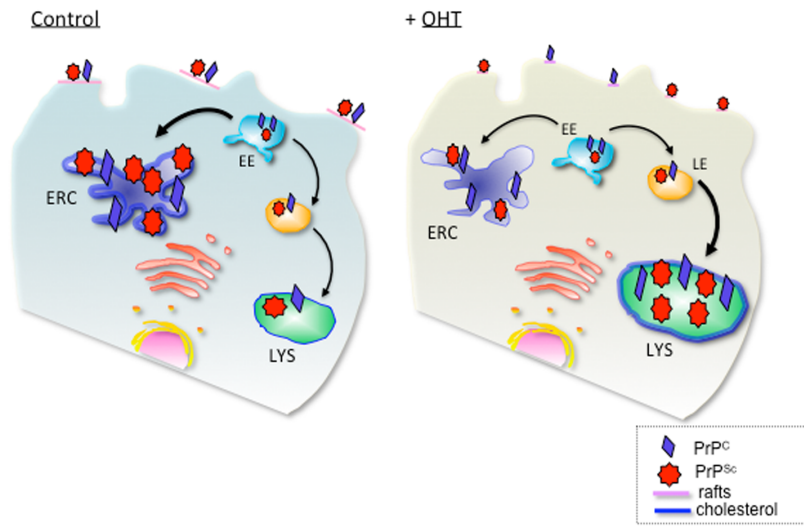
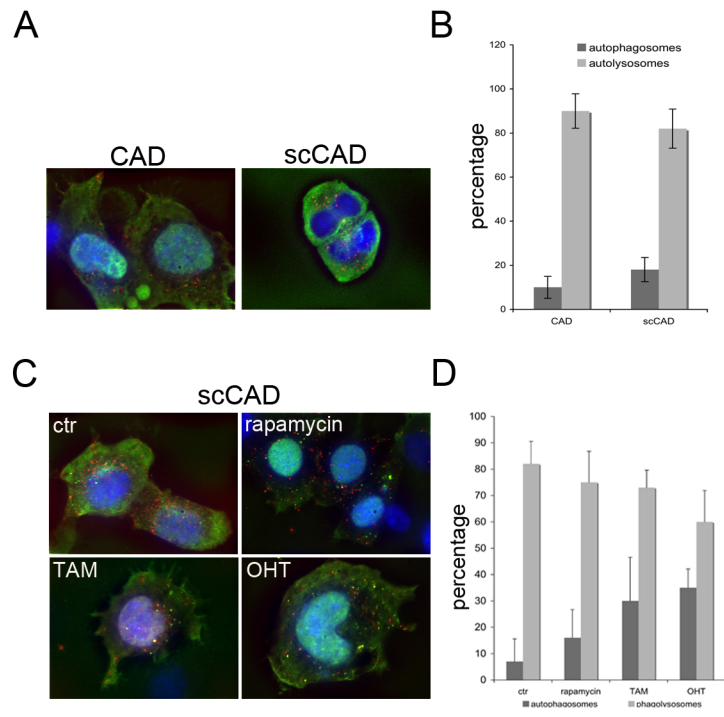
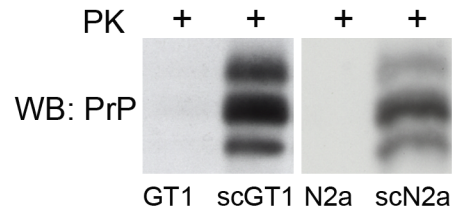


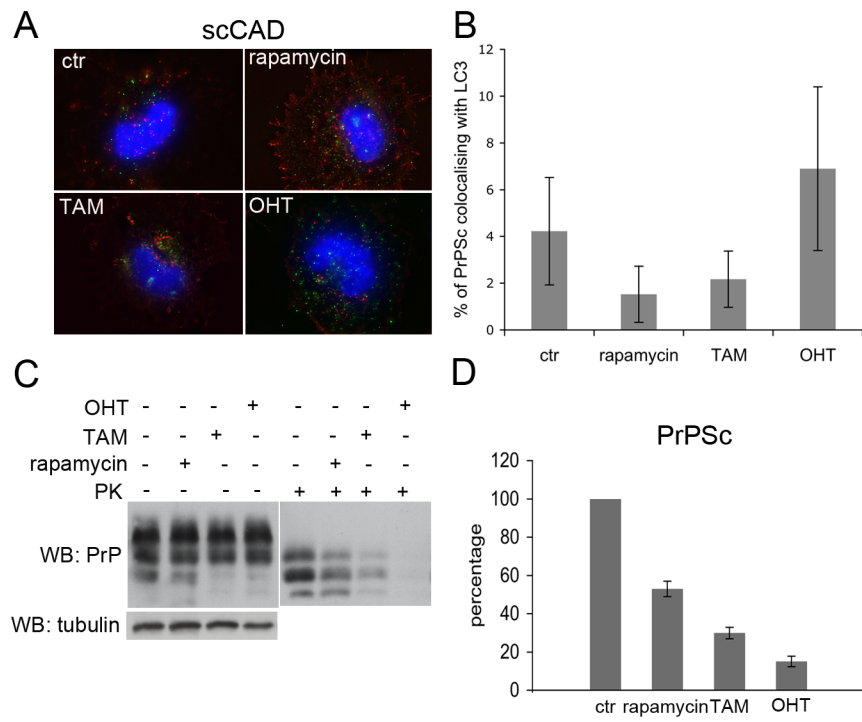
Figure 9



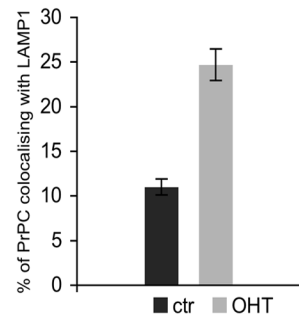
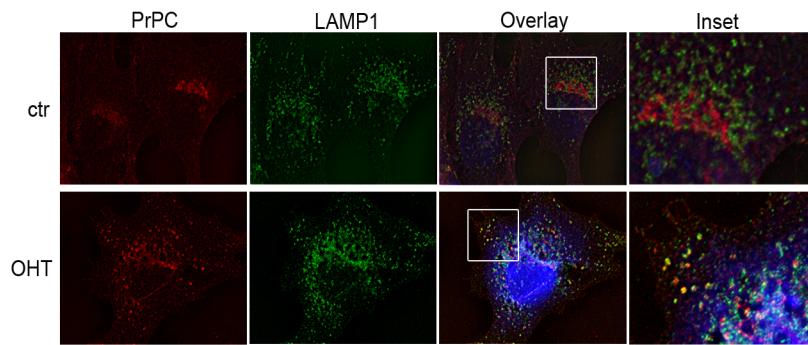
Supplementary figure 1



Supplementary Figure 2



Supplementary figure 3



Supplementary figure 4

## PROJECT 2:

### Characterization of PrP<sup>Sc</sup> spreading from cell-to-cell by Tunneling Nanotubes (TNTs) in a prion infected neuronal cell model

#### 2.1 Objectives

- a) Characterization of the sub-cellular compartments allowing the vesicular trafficking of PrP<sup>Sc</sup> inside TNTs connecting CAD cells;
- b) Role of both cellular and pathological PrP isoforms on TNT formation and transfer;
- c) Role of Myosin-X in TNT formation, TNT-mediated transfer and PrP<sup>Sc</sup> spreading from cell-to-cell.

#### 2.2 Results

##### Objective a:

##### Characterization of the sub-cellular compartments responsible of the vesicular trafficking of PrP<sup>Sc</sup> in TNT formed between CAD cells

- Specific background

Tunneling nanotubes are long thin actin-containing bridges that do not contact the substratum while connecting remote cells. They have been found in many cell types in culture acting as conduits for cytosolic and membrane-bound molecules, organelles and spreading of pathogens (Hurtig et al 2010). As already mentioned above (section 1.7), membrane-specific dyes, markers of endo-lysosomal pathway or specific intra-cellular organelle dyes have observed traveling between cells along these tubular connections (Gurke et al 2008). In addition, the TNT-mediated transfer seems to be selective, as different components seem to be selectively transferred by different cell types (Gerdes et al

2007). Particularly, PrP<sup>Sc</sup> has been found to hijack these intercellular structures to spread from cell to cell (Gousset et al 2009; Langevin et al 2010). However one of the major questions that needs to be addressed is through which mechanism PrP<sup>Sc</sup> is transferred through TNTs. Specifically is not known whether PrP<sup>Sc</sup> is transferred as cytosolic aggregate or within vesicles of a specific origin. PrP<sup>Sc</sup> appears to have a wide distribution inside the cells. Some earlier reports have shown that the majority of PrP<sup>Sc</sup> is intracellular (Taraboulos et al 1990), sequestered within lysosomes of prion-infected N2a cells (Borchelt et al 2002; Caughey et al 1991; McKinley et al 1991) with little localization at the cell surface (Vey et al 1996). More recent reports describe accumulation of PrP<sup>Sc</sup> either in the perinuclear Golgi region of neurons in scrapie-infected transgenic mice (Barmada et al 2005), in the late endosomal compartment of infected GT1-7, N2a and CAD neuronal cells (Pimpinelli et al 2005; Marijanovic et al 2009; Veith et al 2009; Arnold et al 1995; Gousset et al 2009), at the cell surface and on early endocytic and recycling vesicles of hippocampal neurons (Caughey and Raymond 1991; Jeffrey et al 1992). Interestingly, prion accumulation in the endosomal recycling compartment (ERC) can stimulate PrP<sup>Sc</sup> production, thus pointing towards a role for the recycling endosomes as an intracellular site for prion conversion. These and other evidences from our laboratory contributed to show that the ERC is one preferential site of prion conversion (Marijanovic et al 2009). Of interest, by using fluorescence video-microscopy to follow the transfer of fluorescently labelled PrP<sup>Sc</sup>, Gousset *et al.* (2009) referred that after internalization Alexa- PrP<sup>Sc</sup> was found moving inside TNTs towards a connected cell. Along with other observations this may indicate that a significant portion of PrP<sup>Sc</sup> is conveyed in transport vesicles. Given that a fraction of PrP<sup>c</sup> cycles between the plasma membrane and the endosomal system, these vesicles may be of endocytic origin. This is in agreement with the idea that the endosome is an important compartment for the conversion of PrP<sup>c</sup> to PrP<sup>Sc</sup>. Therefore, given the importance of intracellular organelles in the trafficking of PrP<sup>Sc</sup>, in the second part of my thesis I have investigated which types of vesicles/organelles are present in TNTs connecting CAD cells and whether any of those was responsible of the trafficking

of PrP<sup>Sc</sup> from one cell to another. This information is necessary to better understand the mechanism of prion spreading and will allow eventually the development of new therapeutic approaches for prion diseases.

- Results

In order to characterize the sub-cellular organelles that traffic via TNTs formed between CAD cells, a catecholaminergic mouse neuronal cell line (Qi et al 1997), we first used a fluorescence microscopy approach to detect the presence of different sub-cellular organelles in TNT structures by using different organelle specific markers. For this purpose we plated CAD cells on Ibidi dishes (ready to use supports for microscopy) in a well-spaced manner that favor the formation of TNT, as previously shown (Gousset et al 2009). As already mentioned in the section 2.1.1 of this chapter, PrP<sup>Sc</sup> has been found inside the cell along the endocytic pathway and in the Golgi in different cell systems. Therefore we decided to look specifically at the presence of these organelles in TNTs (Table 2).

Sub-cellular Organelle	Organelle marker and tool used for detection	Presence in TNT
ENDOCTIC RECYCLING COMPARTMENT (ERC) AND RECYCLING VESICLES	Anti-Vamp1,2,3 Ab; pGFP-Rab11; pGFP-Vamp3	YES
LYSOSOMES	Anti-LAMP1 Ab	YES
EARLY ENDOSOMES	Anti-EEA1 Ab	YES
Cis- and medial Golgi	Anti-Giantin Ab	NO
Trans-Golgi Network	Anti-Furin Convertase Ab	NO
Trans-Golgi Carriers	pRFP-Rab6	NO

**Table 2 Different organelle markers used to detect specific sub-cellular organelles in TNT structures.** Tools used (either antibodies or fluorescently labeled protein markers) are indicated in the central column. In the third one, presence/absence of these sub-cellular compartments in TNTs is reported.

Therefore we examined the presence of early endosome, ERC, lysosomes, Golgi and Golgi-associated carriers by immunofluorescence after labelling the cells with specific antibodies or transfection with fluorescently labelled proteins (as described in the Material and Methods section). As depicted in Figure 32, (panels A, B and C, red signal), Golgi markers used to detect cis- and medial- Golgi, Trans-Golgi network or Trans-Golgi carriers were detected inside the cell body of CAD cells but were not present in TNT structures. On the other hand, we were able to detect vesicles of endo-lysosomal origin in TNTs. Particularly, the presence of ERC was assessed by both immunolabelling and transfection with GFP-tagged versions of Rab11 and Vamp3, two specific markers of this compartment (Maxfield and Mc Graw 2004) (Figure 32, D and H).

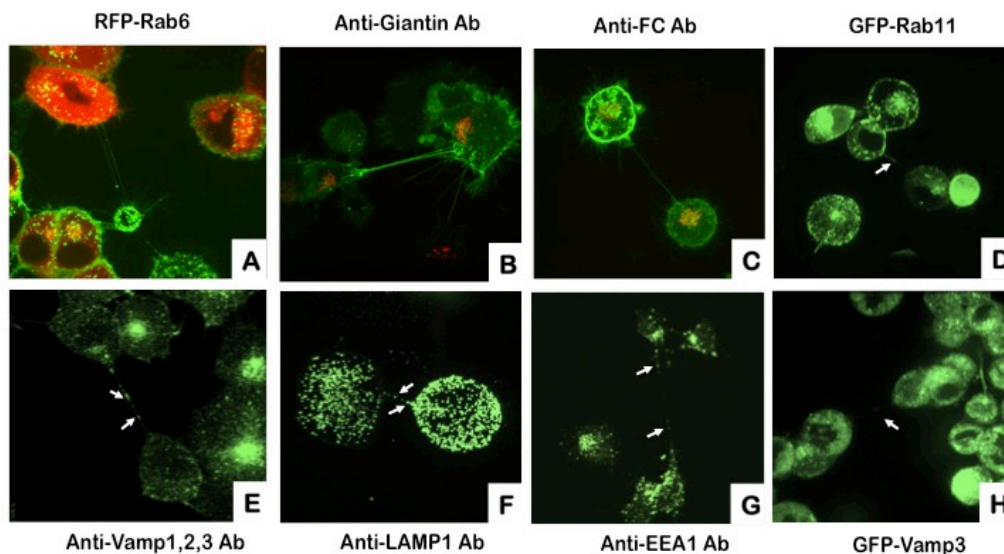


**Figure 31 Identification of different sub-cellular compartments in TNTs of CAD cells.** CAD cells were either transfected with plasmids harboring fluorescently labelled specific proteins or processed for immunofluorescence with specific antibodies as indicated in the different panels. Arrowheads indicate the presence of signals in TNTs. Red signals in the panel A, B and C correspond to RFP-Rab6, Anti-Giantin and Anti-Furin Convertase (FC) antibodies. Images indicate transfer respectively of ERC (D, E and H), Lysosomes (F) and Early Endosomes (G) via TNTs.

This finding suggests that TNTs formed in between CAD cells are able to transport different types of endocytic vesicles, particularly recycling endosomes (Figure 32, E) and early endosomes (Figure 32, G). Additionally, we could confirm the presence of lysosomes in TNT structures (Figure 2.1, F), by using LysoTracker® probe as previously shown (Gousset et al 2009). The Golgi compartment has been found to travel in between TNTs of astrocytes (Wang et al 2011) and in bridging conduits of macrophages (Kadiu and Gendelman 2011). We could not detect this compartment in the TNTs of CAD cells, thus highlighting the fact that these intercellular structures are functionally heterogeneous as different components seem to be selectively transferred by different cell types (Gerdes et al 2007).

The next step was to analyze the presence of PrP<sup>Sc</sup> in ERC, early endosomes and lysosomes that we had observed travelling in TNTs. In order to determine the involvement of these compartments in PrP<sup>Sc</sup> intercellular trafficking, we have analyzed by quantitative immunofluorescence the nature of the organelles transferring PrP<sup>Sc</sup> in TNTs in infected CAD (scCAD) cells. By using QUIA (Figure 33), a specifically designed software (for reference see the Material and Methods section), we measured the degree of colocalisation between a specific organelle marker and PrP<sup>Sc</sup> in TNT. Specifically, we performed a double immunolabelling with either anti-LAMP1, anti-Vamp1,2,3 and anti-EEA1 together with anti-PrP Sha31 antibodies after a denaturing step with Gnd-HCl 6M to expose PrP<sup>Sc</sup> epitopes for the antibody binding (as described in the Material and Methods section) (Figure 33).

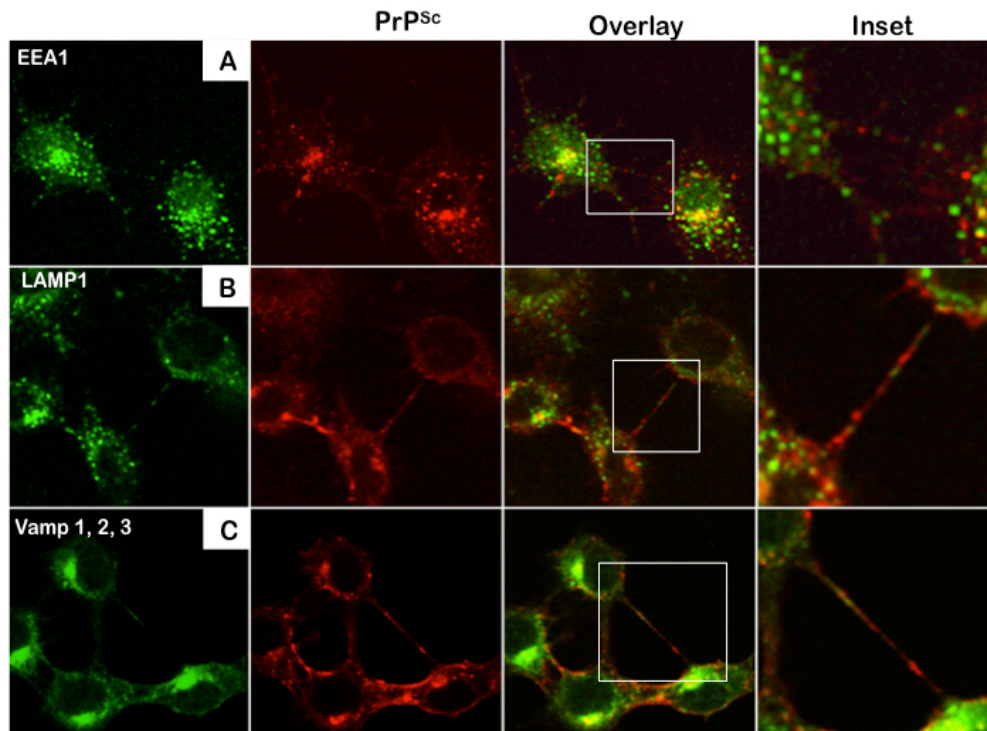


**Figure 32 Colocalisation between PrP<sup>Sc</sup> and different sub-cellular organelles in TNT-like structures of scCAD cells.** Immunofluorescence was performed after a denaturing step with Gnd-HCl to expose PrP<sup>Sc</sup> epitopes to Sha31 anti-PrP antibody. Anti-EEA1 Ab for early endosomes (A), anti-LAMP1 Ab for lysosomes (B) and anti-Vamp1, 2,3 for ERC (C) were used to specifically label these sub-cellular compartments. White square in Overlay column indicate the enlargement (Inset).

Z-stacks of 0.27  $\mu\text{m}$  were taken with a Perkin-Elmer fast confocal spinning-disk microscope from the top to the bottom of the dish in order to acquire the entire volume of TNT-connected cells with a short time of acquisition in order to protect thin TNT structures. After processing, the images were analysed with QUIA software and the percentage of colocalisation of PrP<sup>Sc</sup> with the different organelle markers was evaluated. Figure 2.3 shows an example of the analysis performed with the QUIA software. In brief, the image file is loaded into the software and a Region Of Interest (ROI) containing the TNT structure is manually selected. A “Spot detection” function is then used to select signals on both channels (red for PrP<sup>Sc</sup> signal and green for the specific organelle marker) (Figure 34, A) followed by the colocalisation step (Figure 34, B) and the output (Figure 34, C) consisting of

an excel file with the number of spots in each channel and the percentage of colocalisation in the ROI.

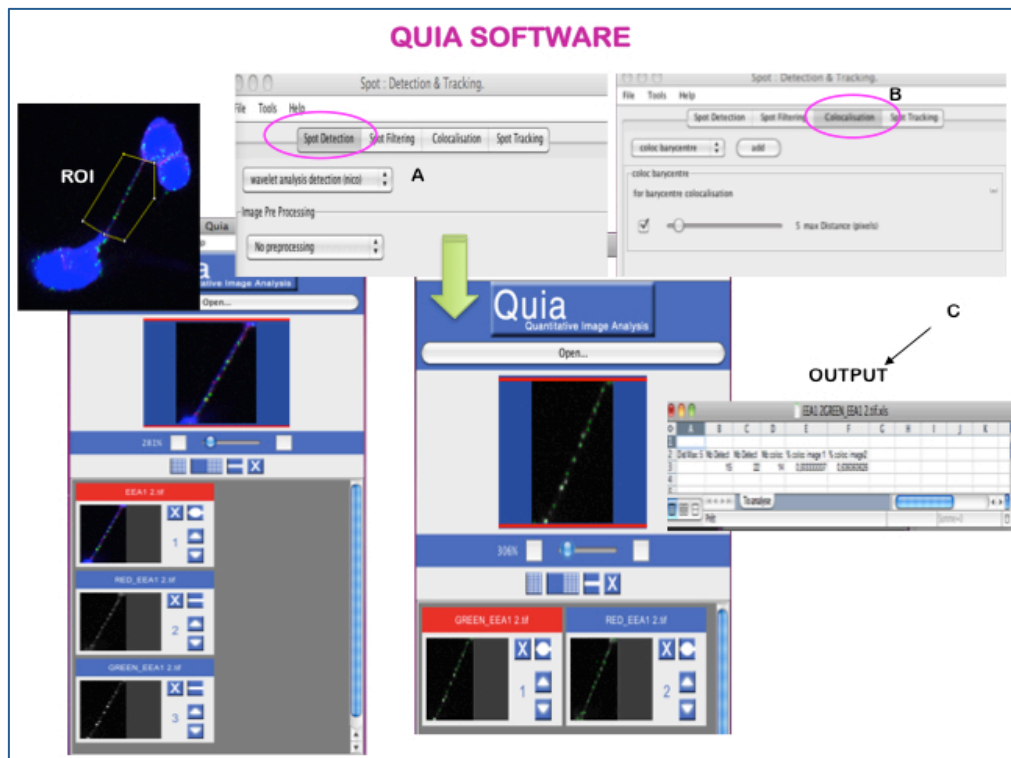


**Figure 33 QUIA Software interface.** A Region Of Interest (ROI) is manually selected on a given image and within it spots on both channels are detected (A) and then colocalised (B). An excel file gives the output of the analysis containing the total number of vesicles in both channels and the % of colocalisation between the two (C).

Given the peculiarity of the ROI and the high sensitivity requested for this analysis QUIA software has been a fundamental tool to precisely detect and quantitate signals deriving from both PrP<sup>Sc</sup> particles and different sub-cellular compartments in TNT structures.

Indeed, as shown in Figure 35, by quantitative colocalisation analysis we found that the percentage of PrP<sup>Sc</sup> colocalising with early endosomes and lysosomes in TNT is respectively around 22% and 32%, while a major fraction (around 50%) seems to colocalise with the recycling compartment. As described before the ERC is one of the intracellular compartments for PrP<sup>Sc</sup> production (Marijanovic et al 2009). Therefore, taken together these results show that PrP<sup>Sc</sup> particles travel *via* TNT mainly in the organelle in which they are produced. However different

'elements' of the endocytic pathway are important for the trafficking of PrP<sup>Sc</sup> inside the cell where it can either meet PrP<sup>C</sup> for further conversion (ERC) or been degraded in acidic compartments (lysosomes). This new finding that PrP<sup>Sc</sup> can be transported in endocytic vesicles (ERC, early endosomes and lysosomes) in TNT structures of CAD cells attributes an important role of these organelles as vehicle for the spreading of PrP<sup>Sc</sup> from cell-to-cell.

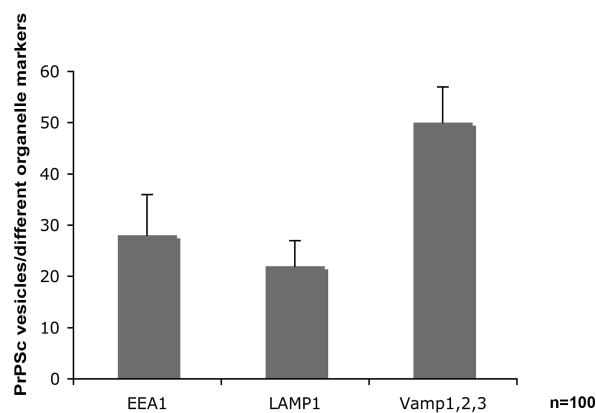


**Figure 34 Quantitation of the colocalisation between PrP<sup>Sc</sup> and the different organelle markers in TNT structures.** The percentage of PrP<sup>Sc</sup> particles colocalising respectively with EEA1 (for early endosomes), LAMP1 (for lysosomes) and Vamp1, 2, 3 (for recycling compartment) was evaluated. n represents the number of total vesicles counted deriving from three independent experiments.

Therefore, exploring the mechanisms by which cells are induced to form TNTs and specifically how the transfer of vesicles is regulated, within these structures, is essential for a better understanding the mechanism of PrP<sup>Sc</sup> spreading. These informations would also contribute to the development of novel therapeutical approaches for prion disease.

## **Objective b:**

### **Role of both cellular and pathological PrP isoforms on TNT formation and transfer**

Since TNTs have been shown to transfer selective components dependently on the cell line, we then asked whether the cellular prion protein itself, PrP<sup>C</sup>, could somehow play a role in TNT formation and transfer of endocytic vesicles or the presence of its pathological counterpart, PrP<sup>Sc</sup>, leads to a stimulation of TNT formation.

- Specific background

A plethora of cellular functions have been attributed to PrP<sup>C</sup> but as already mentioned in the introduction (section 1.4) its physiological role appears to be redundant and is not yet fully understood (Westergard 2007). Of particular interest the recent findings showing that PrP<sup>C</sup> is implicated in cell adhesion (Málaga-Trillo et al., 2009), focal adhesion formation and filopodial extensions (Málaga-Trillo et al., 2009). These findings point towards an additional role of PrP<sup>C</sup> in cytoskeleton dynamics and remodeling, and in cell-to-cell communication. Therefore, by using cell culture models of prion infection we have investigated the potential role of PrP<sup>Sc</sup> in TNTs formation and transfer of vesicles. Interestingly, it has been reported that cells undergo a rapid increase in intracellular reactive oxygen species (ROS) following exposure to infectious brain homogenates, in a prion protein (PrP) dependent manner. Furthermore, ROS production correlated with internalization and increased levels of intracellular PrP<sup>Sc</sup> (Haigh et al 2011). It is important to note that Wang and colleagues (2010) have shown that stress induced by hydrogen peroxide (H<sub>2</sub>O<sub>2</sub>) treatment led to an increase in TNT formation in both astrocytes and neurons suggesting that TNT formation might be directly induced by stress. Finally, as already mentioned above (section 7 of the introduction) TNT-mediated HIV spreading led to an increase in the number of connections both in macrophages (Kadiu et al 2011a) and T-cells (Sowinski et al 2008). As these data suggested a role for PrP in TNT formation

which might be induced either by stress activation or by its putative role in actin remodeling and cell adhesion (Malaga-Trillo 2009; Schoch et al 2009), we attempted to explore the effect that prions could have on TNTs number.

- Results

To analyse the effect of PrP<sup>C</sup> on the number of TNTs we transfected a fluorescent version of PrP<sup>C</sup> full-length (GFP-PrPWT) in CAD cells and used cells transfected with GFP-vector as control. After fixation, CAD cells were stained with WGA-rhodamine in order to visualize and manually count TNT structures. By fluorescence microscopy it appeared that GFP-PrPWT transfected cells have an increased number of protrusions and in several of them PrP<sup>C</sup> was decorating the membranes (Figure 36, A).

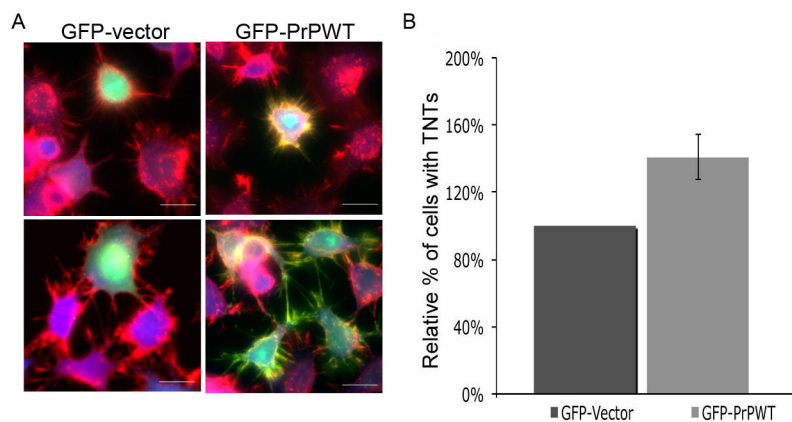


**Figure 35 Effect of GFP-PrPWT over-expression on TNTs number in CAD cells.** (A) CAD cells either transfected with GFP-vector or GFP-PrPWT were fixed and labelled with WGA-rhodamine (in red) and HCS cell mask (in blue) in order to detect both TNT structures and cell body. Scale bar 10  $\mu$ m. Note that GFP-PrPWT over-expressing cells are more enriched in cellular protrusion compared to control. (B) The relative percentage of TNT-connected cells upon GFP-PrPWT over-expression compared to GFP-vector transfected cells was evaluated. (mean  $\pm$  s.e.m, n=3).

By counting the number of cells connected by TNTs in GFP-PrPWT transfected CAD cells we could quantitatively evaluate whether over-expression of PrP<sup>C</sup> was affecting TNT formation between CAD cells, compared to control cells. Interestingly, we

found that over-expression of GFP-PrPWT on average increased the relative percentage of cells connected by TNTs by around 40% (Figure 36, B).

These networks of TNT structures observed between cells could potentially increase the frequency of transfer of different cellular components. Hence, to determine whether TNT structures formed in CAD cells upon over-expression of GFP-PrPWT were functional and therefore were able to support vesicular transfer, we analyzed the transfer of endocytic vesicles (section 2.1). In order to assess this, we set up a flow cytometry assay that would allow us to detect the transfer of DiD-labelled vesicles TNT-mediated in CAD cells (as detailed in the Material and Methods section). In Figure 37, a schematic containing the experimental design is illustrated.

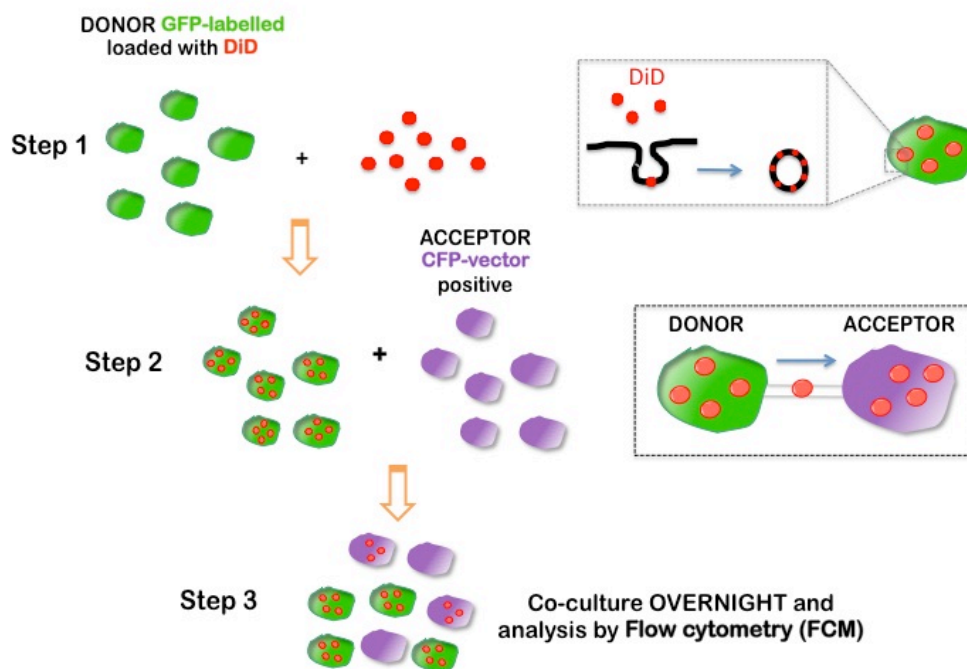


**Figure 36 Schematic of the DiD-vesicle transfer assay by Flow cytometry.** The three main steps are summarized. Step 1 represents the loading step of donor cells (that can be also transfected with different GFP-tagged proteins of interest); in the step2, donor cells are co-cultured with CFP-vector transfected cells, in order to discriminate in between the two populations. After co-culture overnight the cells are the passage of DiD-vesicle from the donor to the acceptor cells is evaluated (Step3).

In brief, donor cells were loaded with the lipid dye DiD that binds to the plasma membrane and, after internalization, allows staining of intracellular vesicles of different origin (Figure 37, Step 1). Finally, donor cells are mixed over-night with acceptor cells transfected with CFP-vector (Figure 37, Step 2). Then the amount of DiD labeled vesicles transferred from the donor cells to the recipient CFP-transfected cells is quantified by Flow cytometry (Figure 37, Step 3).

As already shown, CAD cells transfected with GFP-vector (e.g. control cells) can form functional TNTs (panel A of Figure 36). Indeed we were able to detect and quantify the transfer of DiD vesicles from the donor to the acceptor cells by flow cytometry in this condition (Figure 38, A and E), similar to what was already described (Bukoreshtliev et al 2009).

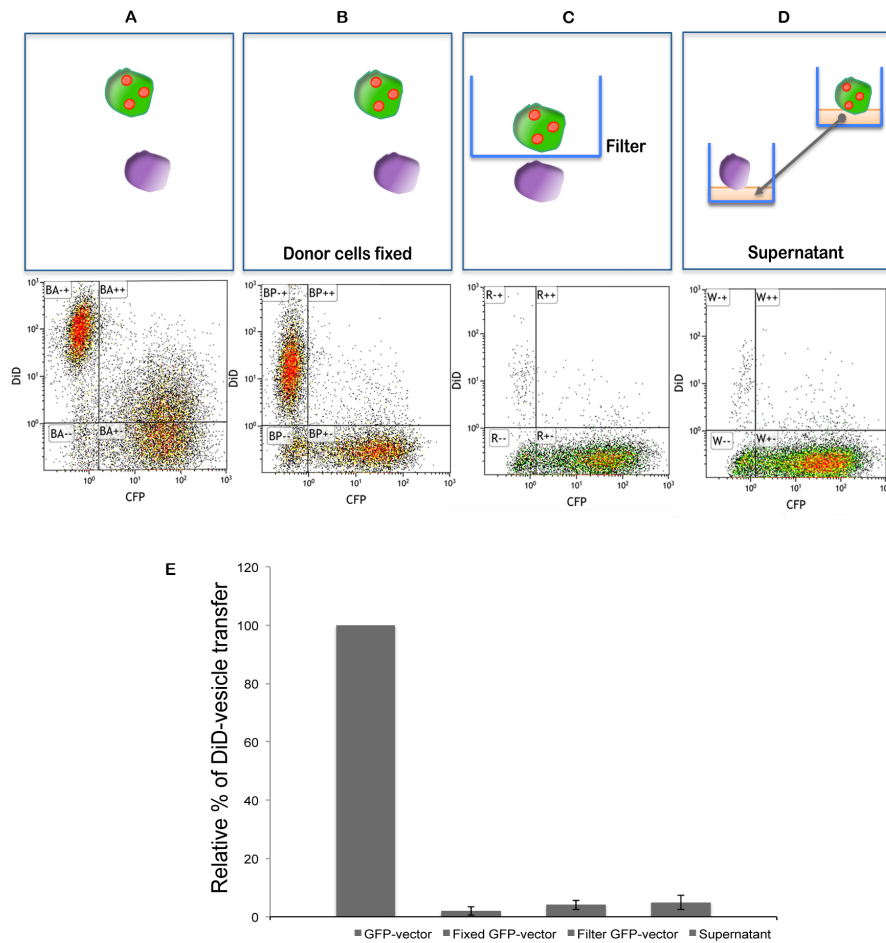


**Figure 37 Flow Cytometry assay of DiD-vesicle transfer from GFP-vector transfected donors to CFP-vector transfected acceptors.** Different co-culture systems are schematized. (A) DiD-labelled, GFP-vector positive (in green) are mixed with CFP-vector recipient CAD cells (in violet), (B) DiD-labelled, GFP-vector positive (in green) are fixed prior mixing, (C) a filter separate DiD-labelled, GFP-vector positive (in green) cells from CFP-vector recipient CAD cells and (D) supernatant deriving from a DiD-labelled, GFP-vector positive (in green) overnight culture is used to feed CFP-vector recipient CAD cells. In (E), the percentage of DiD-vesicle transfer in (B), (C) and (D) conditions has been quantified as relative transfer compared with condition in (A) corresponding to the first histogram. (mean  $\pm$  s.e.m, n=3).

Additional controls were made to demonstrate that the DiD transfer detected is an active mechanism, driven by TNT and, thus, involving cell-to-cell contact (Gousset et al., 2009 and Langevin et al., 2010). In order to verify this, we co-cultured DiD-vesicle loaded donor cells with CFP-vector transfected cells in different co-culture conditions, as illustrated in Figure 38 and described below.

- Co-culture 1 (B): fixed DiD-vesicle loaded donor CAD cells (dead cells) + CFP-vector transfected CAD cells (live cells). This control has been made to exclude any transfer of vesicles deriving from cells debris up-taken by acceptor cells.
- Co-culture 2 (C): DiD-vesicle loaded donor CAD cells + CFP-vector transfected CADs separated by a filter. This control has been made to reveal whether cell-to-cell contact was required.
- Co-culture 3 (D): CFP-vector transfected CAD cultured overnight in the culture medium of DiD-vesicle loaded donor CAD cells. This control has been made to exclude transfer mediated by secretion or exosomes.

By quantifying the percentage of transfer of DiD-vesicles from GFP-vector transfected donor cells to CFP-vector positive cells, we found that when donor cells are either fixed (Figure 38, B), separated by a filter (Figure 38, C) or when the recipient cells are in contact only with the supernatant of the donor cells (Figure 38, C), the relative transfer of DiD-vesicle compared to control is between 2% and 7% and therefore not significant (Figure 38, E).

We next determined the effect that over-expression of GFP-PrP in donor cells might play in the transfer of DiD-labelled vesicle. As depicted in Figure 39, we found that GFP-PrPWT transfected in donor cells did not increase DiD-vesicle transfer, as the percentage of relative transfer is equal to control condition with an average of 104.2%.

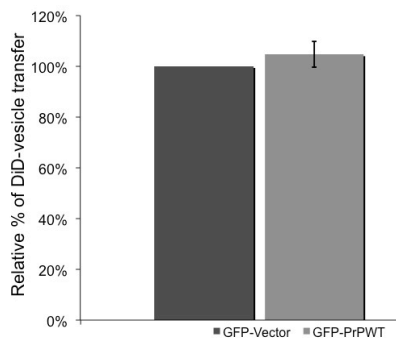


**Figure 38 Effect of GFP-PrPWT over-expression on DiD-vesicle transfer TNT-mediated in CAD cells.** The relative percentage of DiD-vesicle transfer upon GFP-PrPWT over-expression compared to GFP-vector transfected cells was evaluated (mean ± s.e.m, n=3).

Taken together these results show that the increase in TNTs number mediated by over-expression of PrP<sup>C</sup> (Figure 39, A and B) did not lead to an increase in the trafficking of endocytic vesicle in CAD cells through TNTs. This result highlighted the fact that possible candidate factors might be implicated in TNT-mediated transfer and can have different roles in the process, either structural (e.g., building up the membrane structure) or functional (e.g., as part of the machinery that allows and drives the transfer of material within the membrane). PrP<sup>C</sup> seems to have a structural function, which we are currently trying to address (see discussion, paragraph 2.3).

The next step was to evaluate the effect of prion infection on TNTs formation. To test whether PrP<sup>Sc</sup> infection could induce TNT formation in order to increase its spreading the proportion of cells having TNT structures in control or infection conditions was quantified (Figure 40).

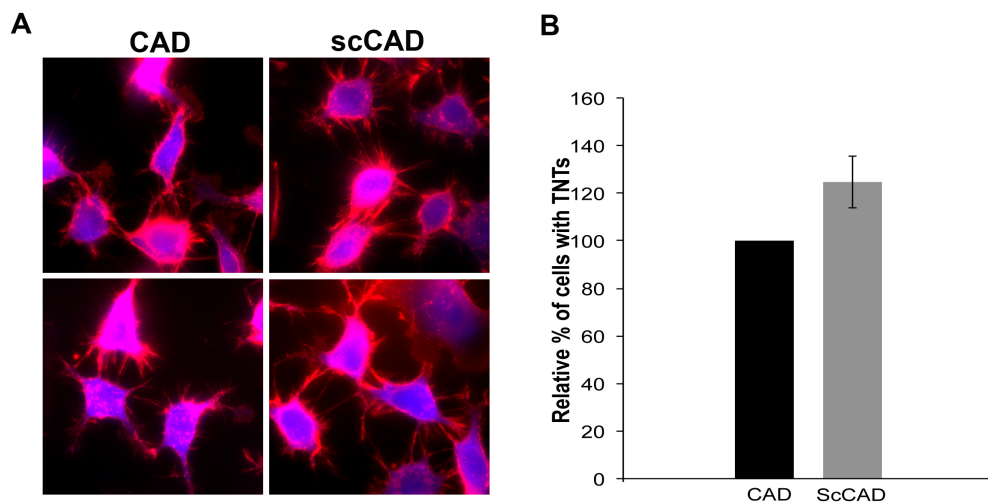


**Figure 39 PrP<sup>Sc</sup> infection induces TNT-formation by increasing the number of connected scCAD cells.** (A) CAD cells chronically infected with the prion strain 139A (ScCAD,) or uninfected CAD cells were labeled with WGA-rhodamine (in red) and HCS cell mask (blue) after fixation and images were acquired to evaluate the number of TNT-connected cells. (B) Quantitation of TNT-connected scCAD cells compared to non infected CAD cells (mean  $\pm$  S.E.M., n=3).

Thus, we compared the number cells connected via TNTs in the case of non-infected CAD with chronically infected CAD (ScCAD) cells. We found that the number of TNT-connected cells was increased of about 28% in the case of prion infection, Those data indicate that, at least in vitro, PrP<sup>Sc</sup> could potentially accelerate its spreading through direct induction of TNT formation.

Overall, these results show that both cellular prion protein PrP<sup>C</sup> and PrP<sup>Sc</sup> infection can lead to increased number of TNT structures in CAD cells. In addition, PrP<sup>C</sup> over-expression does not increase DiD-vesicle transfer, thus indicating that its function is either structural or not sufficient to drive transfer of cellular components in between cells. Further investigations in order to unravel the role of PrP<sup>C</sup> and the mechanism by which PrP<sup>Sc</sup> infection can possibly increase TNT-formation are required and will be examined in the discussion section of this chapter (paragraph 2.4).

#### **Objective c:**

#### **Role of Myosin-X in TNT formation, TNT-mediated transfer and PrP<sup>Sc</sup> spreading from cell-to-cell**

Understanding both the mechanism of TNT formation and of vesicular transfer is fundamental for unraveling and hamper prion spreading, thus, in the last part of my thesis I focused on the potential role of specific molecules in TNT formation and TNT-mediated transfer. Specifically I analyzed the possible involvement of the unconventional actin-binding motor Myosin-X in these processes.

- Specific Background

The fact that most TNTs in neuronal cells arise from the extension of filopodia-like protrusions toward neighboring cells suggested that actin polymerization plays an important role in TNT formation. In addition, since filopodia-like protrusions are critical for TNT formation in neuronal cells (Bukoretshliev et al., 2009), it is likely that factors involved in filopodia formation also

play a role in TNT biogenesis. In particular we have analyzed the role that the unconventional actin-binding protein Myosin-X might play in both the formation of TNT-like structures and its function in transfer of materials in neuronal cells. Indeed Myo-X and its effects on filopodia formation have been well studied (Berg and Cheney, 2002). In particular, over-expression of full length Myo-X in a number of cell types, including CAD cells, has led to an increase in both the number and the length of filopodia (Sousa and Cheney 2005). Also, it was shown that over-expression of Myo-X specifically increased dorsal filopodia (Bohil et al 2006), suggesting that it could play a role in *de novo* formation of TNT-like structures because it would lead to the extensions of filopodia, unattached to the substratum, toward recipient cells. Hence, in the last part of my work I wanted to understand whether this protein could play a role in TNT formation and the spreading of PrP<sup>Sc</sup> from cell-to-cell. This part of my work has been done in collaboration with Dr Karine Gousset (*Unité de trafic membranaire & pathogénèse, Institut Pasteur, Paris*).

- Results

First, to analyze the effect of Myo-X on TNT formation, we transfected a GFP-tagged version of the full-length protein (GFP-Myo-X) in CAD cells and by fluorescence microscopy we analyzed TNT structures, as previously described. Upon over-expression of GFP-MyoX, numerous TNT-like structures were observed (Figure 2.41, A).

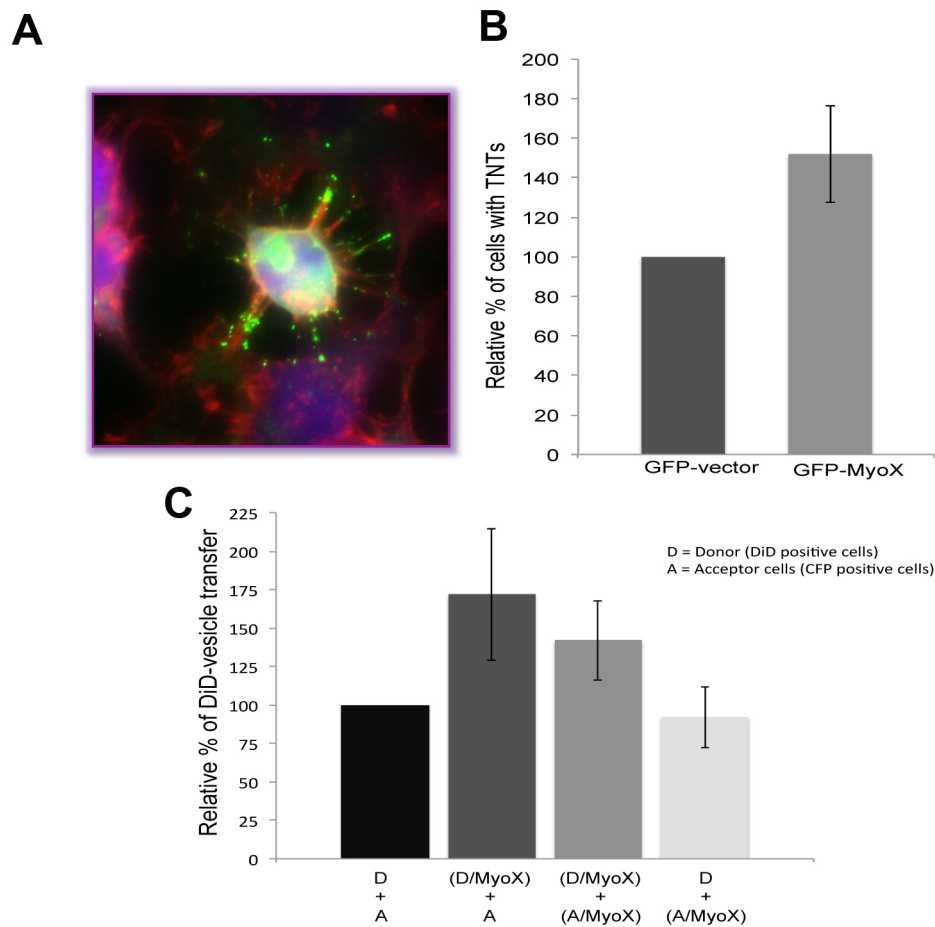


**Figure 40 Effect of GFP-Myo-X over-expression on both TNT formation and transfer of DiD-vesicle in CAD cells.** (A) CAD cells either transfected with GFP-vector or GFP-Myo-X were fixed and labelled with WGA-rhodamine (in red) and HCS cell mask (in blue) in order to detect both TNT structures and cell body. Scale bar 10  $\mu$ m. Note that GFP-Myo-X over-expressing cells are more enriched in cellular protrusion compared to control. (B) The relative percentage of TNT-connected cells upon GFP-Myo-X over-expression compared to GFP-vector transfected cells was evaluated. (mean  $\pm$  s.e.m, n=3) (C) The relative percentage of DiD-vesicle transfer upon GFP-Myo-X over-expression compared to GFP-vector transfected cells was evaluated (mean  $\pm$  s.e.m, n=3).

To quantify this result, we compared the number of TNT-like structures observed in CAD cells over-expressing GFP-Myo-X with cells over-expressing GFP vector as a control. We determined that over-expression of GFP-Myo-X on average increased the relative percent of cells with TNT-like structures by over 50% (Figure 41, B). Also, as shown in Figure 41 (panel A) GFP-Myo-X is predominantly present within these structures and can move back and forth over time in live-imaging experiments (data not

shown). We then asked whether these networks of tubes observed between cells could potentially increase the frequency of transfer in between cells. Thus, in order to determine whether TNT-like structures formed upon over-expression of GFP-Myo-X are functional TNTs (e.g., allow the intercellular transfer of vesicles), we quantify the transfer of DiD-labeled vesicles in our neuronal cell system by using the flow cytometry assay previously set up (as schematized in Figure 37). For these experiments, donor cells were loaded with the lipid dye DiD and mixed with CFP-transfected acceptor cells overnight. As expected from our previous studies, normal CAD cells transfected with GFP-vector (e.g., control cell) formed functional TNTs and transferred DiD vesicles from the donor cells to the acceptor cells (Figure 41, C, column 1). Interestingly, when we over-expressed GFP-Myo-X in donor cells we observed a relatively large increase (around 72%) in the transfer of DiD-labeled vesicles compared to the control (Figure 41, C, column 2). It is important to note that in these experiments, on average, the transfection rate efficiency of GFP-Myo-X is much lower (about 1/6) compared to the control GFP-vector. This means that by flow cytometry, the transfer efficiency of the cells over-expressing GFP-Myo-X is largely underestimated. To demonstrate that the transfer detected upon GFP-MyoX over-expression was the results of an active intercellular transfer mechanism and did not come from DiD-labeled vesicles in the supernatant, we repeated the flow cytometry assays with either fixed donor cells or in co-cultures separated by filters (Figure 38, Gousset et al., 2009 and Langevin et al., 2010). As shown in Figure 42, no significant transfer of DiD-labeled vesicles could be detected in either fixed cells or in co-cultures separated by a filter in either GFP-vector or GFP-Myo-X transfected cells.

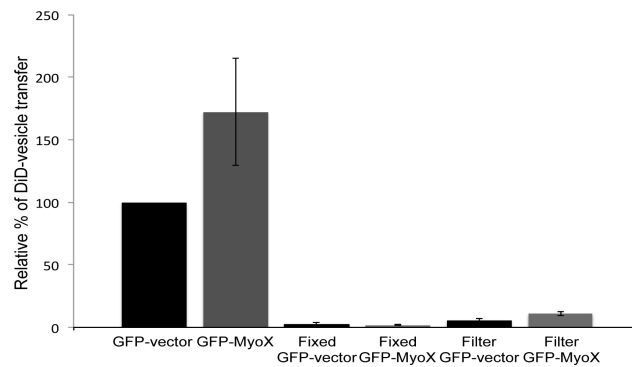


**Figure 41 DiD-vesicle transfer mediated by GFP-Myo-X transfected cells is an active mechanism.** The relative percentage of DiD-vesicle transfer upon GFP-Myo-X over-expression compared to GFP-vector transfected cells was evaluated (column 1 and 2). Additional controls with either fixed donor CAD cells (transfected with GFP-vector or GFP-Myo-X) prior mixing with acceptor CAD cells (column 3 and 4) and mixed population separated by a filter (mean  $\pm$  s.e.m, n=3). Note that the last two cases DiD-vesicle transfer is not considerable.

These results suggest that the transfer of vesicles observed by flow cytometry is an active mechanism that correlates with the number of TNT-connected cells present in culture. To further characterize the role of Myo-X over-expression on the formation and functionality of TNTs, we next determined whether its expression in donor cells or in acceptor cells would affect vesicle transfer. Thus, we repeated these experiments using co-cultures where both the donor cells and the acceptor cells were transfected with GFP-Myo-X (Figure 41, C, column 3) or in co-cultures where only the acceptor cells were transfected with GFP-Myo-X (Figure 41, C, column 4) and compared the results with control cells (Figure 41, C, column 1) or donor cells transfected with GFP-Myo-X (Figure 41, C, column 2). The results clearly demonstrate that over-expression of GFP-Myo-X in the acceptor cells had little effect in the transfer of vesicles from donor cells (Figure 41, C, columns 3 and 4). These experiments suggest that in CAD cells, the transfer of vesicles is uni-directional, going from the cell that extend the filopodial protrusion towards a recipient cells establishing the connection. Overall, they demonstrate that over-expression of GFP-Myo-X in donor cells leads to an increase in functional TNTs, thus resulting in the enhancement of the transfer of DiD-labeled vesicles to the recipient cells.

Since CAD cells already have endogenous levels of Myo-X in order to better characterize the effects of Myo-X expression on TNT formation and transfer we then attempted to knock-down Myo-X.

Using Myo-X shRNA lentiviral particles (as described in the Material and Methods section) we were able to reduce Myo-X expression levels up to 83% (Figure 43, A). Next, we analyzed the effect of Myo-X down regulation on the number of TNT-connected CAD cells. We found that while the relative number of cells with TNTs decreased in Myo-X down-regulated cells compared to the control CAD cells (Figure 43, B), TNTs were still present in the down-regulated cultures. This could be because (1) we were unable to efficiently silence Myo-X gene expression, (2) CAD cells are able to form TNTs cell dislodgement (Gousset et al 2009), a process that might not require Myo-X or (3) Myo-X can enhance *de novo* TNT formation but is not a limiting factor.

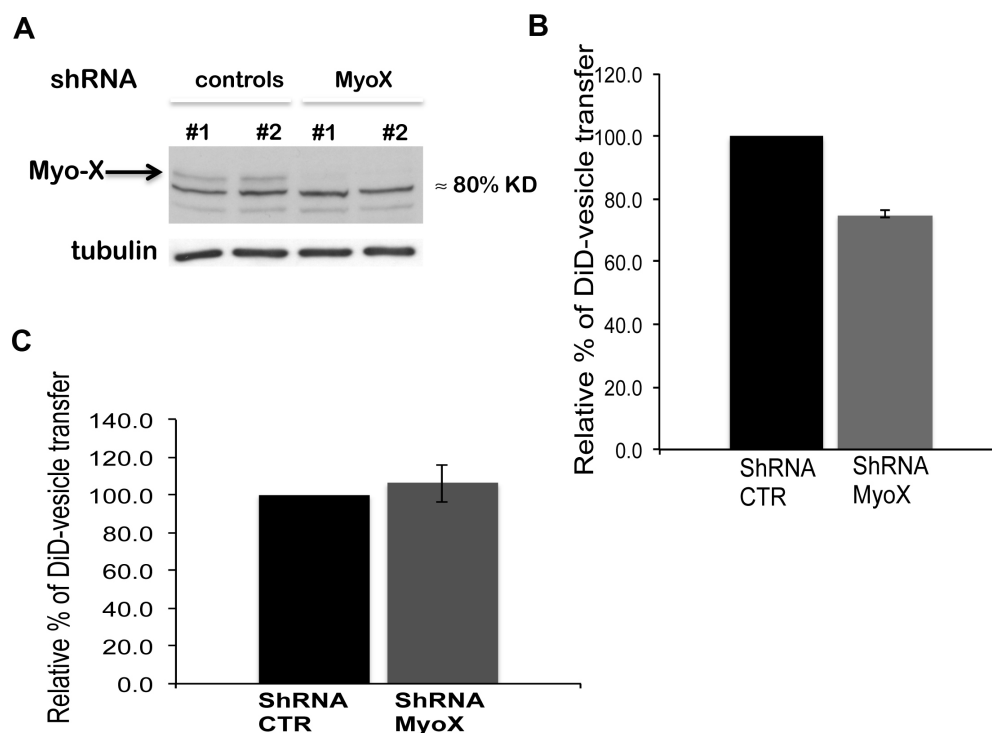


**Figure 42 Effect on TNT formation and DiD-vesicle transfer of Myo-X down-regulation in CAD cells.** (A) Western blot with anti-Myo-X antibodies in CAD cells down-regulated for Myo-X gene with Myo-X shLentiviral particles (B) The relative percentage of DiD-vesicle transfer in Myo-X downregulated cells (shRNA Myo-X) compared to CAD cells treated with scramble shRNA lentiviral particles as control (shTNA CTR) was evaluated (mean  $\pm$  s.e.m, n=3) (C) Myo-X rescue experiment. The relative percentage of DiD-vesicle transfer upon GFP-Myo-X over-expression in shRNA Myo-X CAD cells compared to GFP-vector transfected shRNA CTR cells was evaluated (mean  $\pm$  s.e.m, n=3).

Next, we analyzed the effects of down-regulation of Myo-X on the transfer of DiD-vesicles by flow cytometry to determine what types of structures were affected. By quantifying the relative percentage of vesicle transfer in Myo-X down regulated cells compared to control cells, we found a decrease of over 20 % in the transfer of DiD-labeled vesicles when Myo-X was down-regulated (Figure 43, C, column 1 and 2). In addition, when GFP-MyoX was transfected in Myo-X down-regulated cells, the transfer of vesicles could not only be rescued but also increased by almost 17% compared to control cells GFP-vector positive (Figure 43, C, column 3 and 4). This demonstrates that Myo-X expression allowed the formation of efficient functional TNTs. As stated above, GFP-Myo-X is enriched within TNTs and is able to move back and forth along the tubes. The forward movement of Myo-X to the tips of filopodia was shown to be dependent upon its molecular motor activity, while its rearward transport take advantage of actin retrograde flow (Berg and Cheney, 2002). To determine the role that either the motor domain or tail domain of Myo-X might play in both TNT formation and function we used two Myo-X mutants: (1) GFP-HMM consisting of the head motor domain, neck and coiled-coil regions or (2) GFP-Headless containing the neck, coiled coil and tail regions of Myo-X (Berg and Cheney 2002). Thus, we first expressed both mutants in CAD cells and compared them to GFP-Myo-X over-expression (Figure 44).

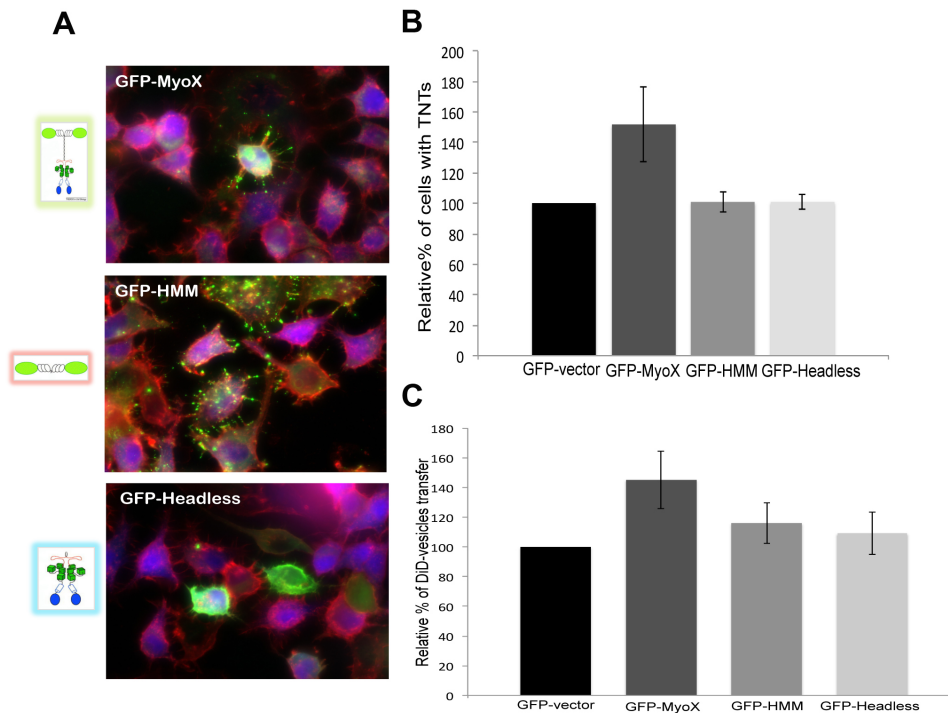


**Figure 43 Effect of GFP-HMM-Myo-X and GFP-Headless-Myo-X on both TNT formation and DiD-vesicle transfer in CAD cells.** (A) CAD cells either transfected with either GFP-Myo-X, GFP-HMM-Myo-X or GFP-Headless-Myo-X were fixed and labelled with WGA-rhodamine (in red) and HCS cell mask (in blue) in order to detect both TNT structures and cell body. Scale bar 10  $\mu$ m. (B) The relative percentage of TNT-connected cells upon GFP-Myo-X, GFP-HMM-Myo-X or GFP-Headless-Myo-X over-expression compared to GFP-vector transfected cells was evaluated (mean  $\pm$  s.e.m, n=3) (C) The relative percentage of DiD-vesicle transfer upon GFP-Myo-X, GFP-HMM-Myo-X or GFP-Headless-Myo-X over-expression compared to GFP-vector transfected cells was evaluated (mean  $\pm$  s.e.m, n=3).

As previously described (Berg and Cheney, 2002), both GFP-Myo-X and GFP-HMM are able to localize at the tips of filopodia, whereas GFP-Headless is cytosolic (Figure 44, A). Since both mutants could be transfected in CAD cells and behaved as expected (Berg and Cheney, 2002), we next determined the effects of over-expression of these constructs on TNT formation. Interestingly, even though GFP-HMM is able to behave in filopodia in a similar fashion to the full length GFP-Myo-X construct, its over-expression in CAD cells is not sufficient to increase the relative number of cells with TNTs (Figure 44, B, column 3). Similarly, the over-expression of the tail domain alone GFP-Headless, did not increase TNT formation in CAD cells (Figure 44, B, column 4). These experiments suggest that the motor and the tail domains of Myo-X are both necessary for TNT formation.

Next, to further characterize the effect of over-expression of these mutants on TNT function we analyzed the transfer of DiD-vesicles by flow cytometry (Figure 44, C). In agreement with the fact that the TNTs number was not increased, we found that neither constructs were able to increase the transfer of DiD-vesicles, to the levels observed with GFP-Myo-X (Figure 44, C).

It is of interest to note that these constructs did not have the same rate of transfection efficiency in CAD cells. On average, GFP-Headless and GFP-HMM were 2 and 4.5 times more efficiently expressed compared to GFP-Myo-X, suggesting that the effect of full length GFP-Myo-X might have been under-estimated by its lower transfection efficiency. Overall, these experiments suggest that while the motor domain might play a role in bringing Myo-X to the tip of filopodia and thus to the point of attachment with an adjacent cell, the tail domain of Myo-X might play a critical role in the binding and/or fusion of the tubes, possibly by binding to necessary components.

Therefore, to further narrow down which part of the tail domain of Myo-X might be critical for the formation of TNTs, we next decided to analyze mutations within the FERM domain located at the end of the Myo-X tail (Berg and Cheney 2002). As already described in the introduction (section 1.8) FERM domains are thought to serve as a link between cytoskeletal components and integral membrane proteins (Chishti et al., 1998). In the case of Myo-X, the FERM domain was shown to bind to integrins (Zhang et al., 2004). In their study, Zhang and colleagues demonstrated that both F2 and F3 subdomains of the FERM domain were necessary for the binding of integrins to Myo-X. Thus, we decided to analyze the effects of over-expression of the deletion mutants GFP-Myo-X- $\Delta$ F2 and GFP-Myo-X- $\Delta$ F3 lacking either the F2 or F3 lobes respectively (Zhang et al., 2004). We first analyze the localization of these mutants in transfected CAD cells (Figure 45, A).

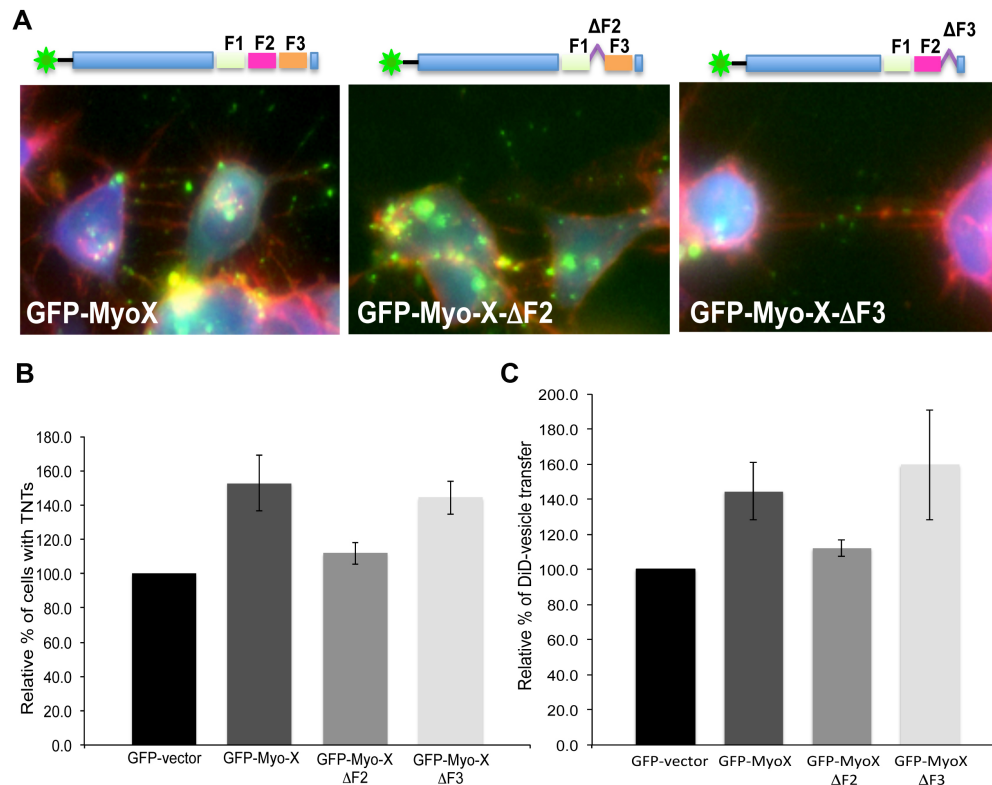


**Figure 44** Effect of GFP-Myo-X- $\Delta$ F2 and GFP-Myo-X- $\Delta$ F3 on TNT formation and DiD-vesicle transfer in CAD cells. (A) CAD cells either transfected with either GFP-Myo-X, GFP-Myo-X  $\Delta$ F2 or GFP-Myo-X  $\Delta$ F3 were fixed and labelled with WGA-rhodamine (in red) and HCS cell mask (in blue) in order to detect both TNT structures and cell body. Scale bar 10  $\mu$ m. (B) The relative percentage of TNT-connected cells upon GFP-Myo-X, GFP-Myo-X  $\Delta$ F2 or GFP-Myo-X  $\Delta$ F3 over-expression compared to GFP-vector transfected cells was evaluated (mean  $\pm$  s.e.m, n=3) (C) The relative percentage of DiD-vesicle transfer upon GFP-Myo-X, GFP-Myo-X  $\Delta$ F2 or GFP-Myo-X  $\Delta$ F3 over-expression compared to GFP-vector transfected cells was evaluated (mean  $\pm$  s.e.m, n=3).

We found that similar to Myo-X full-length both mutants could be found at the tips of filopodia or within TNTs (Figure 45, A). However, while GFP-Myo-X and GFP-Myo-X- $\Delta$ F3 were both able to increase the number of CAD cells with TNTs (Figure 45, B, column 2 and 3), GFP-Myo-X- $\Delta$ F2 was not (Figure 45, B, column 4). We then studied at the effects of these mutations in the transfer of DiD-labeled vesicles by flow cytometry. As can be seen in the panel C in Figure 45, we determined that both full length and GFP-Myo-X- $\Delta$ F3 enhanced the transfer of DiD-labeled vesicles but not GFP-Myo-X- $\Delta$ F2 in agreement with the quantification of TNT-connected cells. Since both lobes are simultaneously necessary for the binding of Myo-X to integrins,

our results suggest that integrins are not necessary for TNT formation and function. While integrins are important for attached filopodia extension, they are not necessary for the formation of dorsal filopodia (Bohil et al., 2006). Thus, this further suggests that dorsal filopodia could potentially be the precursor of TNT structures. Importantly, our data specifically identify the F2 lobe of the FERM domain as a necessary subdomain of Myo-X for both TNT formation and function, likely by binding to critical cargo proteins. Thus, it will be important to identify the binding partner(s) of F2 critical for TNT formation. So far, our data suggest that Myo-X expression is able to enhanced TNT formation and improve the intercellular transfer of vesicles. The question I wanted to answer next was if Myo-X was involved in the transfer of PrP<sup>Sc</sup> between cells. Indeed I have shown that PrP<sup>Sc</sup> travels within TNTs in endocytic vesicles (section 2.1 of this chapter). Therefore, we decided to analyze whether Myo-X expression in chronically prion infected CAD (scCAD) cells could also affect the transfer of PrP<sup>Sc</sup> particles to recipient CAD cells. Thus, we set up a microscopy experiment, in which we quantified the transfer of PrP<sup>Sc</sup> aggregates, (revealed by the anti-PrP antibody Sha31 after Gnd-HCl treatment), from ScCAD donor cells transfected with GFP-vector or GFP-Myo-X, to recipient CAD cells transfected with GFP-PML, a nuclear marker (Figure 46).

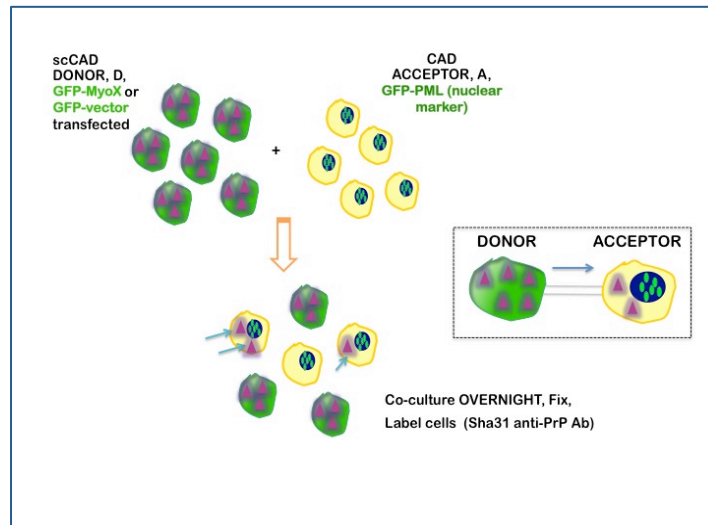


**Figure 45 Transfer of PrP<sup>Sc</sup> via TNTs in CAD cells by fluorescence microscopy.** scCAD donor cells were transfected either with GFP-vector as control or GFP-Myo-X (in green). CAD recipient cells were transfected with GFP-PML (a nuclear marker) in order to discriminate them from scCAD. Both population were mixed overnight and the transfer of PrP<sup>Sc</sup> was evaluated by immunolabelling with Sha31 anti-PrP antibody after Gnd-HCl treatment (to expose PrP<sup>Sc</sup> epitopes).

In these experiments, GFP-PML was used as a tool to identify the acceptor cells and the PrP<sup>Sc</sup> particles were quantified using the QUIA Software for spot detection (as described in the Material and Methods section). Analysis of the data clearly demonstrated that over-expression of GFP-Myo-X led to a drastic increase in the transfer PrP<sup>Sc</sup> particles from scCAD cells to naïve CAD cells (Figure 47).

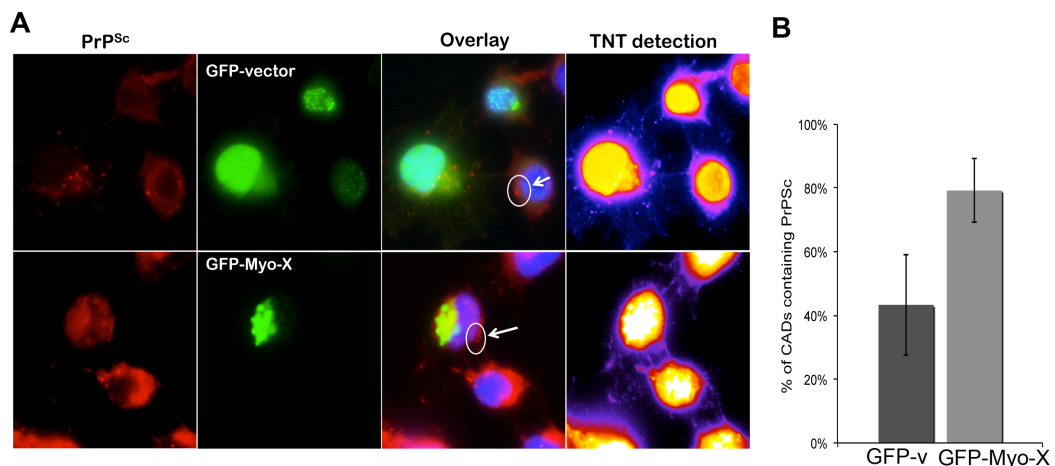


**Figure 46 Effect of Myo-X over-expression on transfer of PrP<sup>Sc</sup> via TNTs in CAD cells.** (A) Detection of the transfer of PrP<sup>Sc</sup> particles (by using Sha31 antibody) via TNTs in control

condition (scCAD donor cells transfected with GFP-vector) and after over-expression of GFP-MyoX. CAD recipient cells are transfected with GFP-PML (a nuclear marker). White circles and arrowheads indicate obtained PrP<sup>Sc</sup> passage from the donors scCAD cells to the acceptor CAD cells. (B) Quantification of the percentage of transfer by Count Spots with QUIA software. (mean  $\pm$  s.e.m, n=3).

In conclusion these data show that Myo-X is able to induce TNT formation and to regulate the transfer of vesicle and, more interestingly, the transfer of PrP<sup>Sc</sup> particles.

## 2.3 Discussion

Prion diseases are characterized by the presence of prions, proteinaceous aggregates, mainly constituted by a misfolded protein, PrP<sup>Sc</sup>. The central event in prion pathogenesis is the conformational change of the cellular protein, PrP<sup>C</sup>, in its pathological counterpart, PrP<sup>Sc</sup> (Prusiner, 1998). As discussed above (in the section 1.6 of the Introduction), at the different stages of its lethal journey to the central nervous system, PrP<sup>Sc</sup> is transferred from one cell to another and this passage can involve several mechanisms, not mutually exclusive, probably depending on cell type, the infectious strain and the host. These mechanisms include cell-to-cell contact, exosomes and GPI-painting (Kanu et al., 2002; Fevrier et al., 2004; and Baron et al., 2006). More recently it has been shown that intercellular membranous channels, called tunneling nanotubes (TNT), are hijacked by PrP<sup>Sc</sup> for intercellular spread (Gousset et al., 2009; Langevin et al 2009). In this context, in the second part of my PhD work I focused on better characterizing TNT-mediated trafficking of PrP<sup>Sc</sup> in between neuronal CAD cells, as a model of prion infection. I also tried to individuate potential factors that could be involved in TNT formation and resulting transfer of PrP<sup>Sc</sup> in particular.

PrP<sup>Sc</sup> has been found mainly intracellular, and particularly all along the endocytic pathway (Campana et al 2005). Moreover, like PrP<sup>C</sup>, PrP<sup>Sc</sup> is a GPI-anchored protein. Both proteins could travel *via* TNTs surfing the surface or inside the channel, as cytosolic aggregates or within vesicular structures. In particular, I investigated the presence of PrP<sup>Sc</sup> in different sub-cellular organelles in TNTs. To this aim, by fluorescence microscopy, I first evaluated the presence of different subcellular compartments in TNTs, namely early endosomes, lysosomes, recycling vesicles, Golgi apparatus and trans-Golgi carriers. While I could not detect Golgi and Golgi-associated vesicles in these structures, I found that early endosomes, lysosomes and recycling vesicles were trafficked in TNTs. I then further analyzed the presence of PrP<sup>Sc</sup> in early endosomes, lysosomes and recycling vesicles inside TNTs. By a specifically designed quantitative localization analysis (QUIA software, Figure 34), I

found that similar to what can be found in the cell body, PrP<sup>Sc</sup> can travel in TNTs in early endosomes and lysosomes but it is preferentially enriched in the endocytic recycling compartment (Figure 33 and Figure 35). This is particularly interesting as the ERC is also an intracellular site for prion conversion (Marijanovic et al 2009). Therefore my data suggest that PrP<sup>Sc</sup> exploits endocytic traffic through tunneling nanotubes for its intercellular spread. Similar to PrP<sup>Sc</sup>, it has also been recently reported that HIV particles can spread, both surfing on or inside TNTs in primary macrophages (Eugenin et al 2009). Recently, a more detailed characterization of HIV-carriers mediating the transfer of the virus along TNTs bridging macrophages has been made (Kadiu et al 2011a). The authors also identified the composition of TNTs by proteomic analysis following isolation from cell bodies. Interestingly they found several organelle markers, including endo-lysosomal and recycling compartments, inside TNTs and some of them colocalizing with the viral proteins Env and Gag, thus confirming a role for these intracellular organelles in HIV intercellular trafficking (Kadiu et al 2011a). Comparing intra- and inter-cellular trafficking of PrP<sup>Sc</sup> with the current knowledge in the HIV field could improve our understanding and help in characterizing intercellular spreading of prions.

Moreover, these new findings showing that PrP<sup>Sc</sup> trafficking in tunneling nanotubes could be associated with vesicles of endosomal origin, lead to some speculations and open up a series of new questions that could be a basis for further investigations. In particular, the fact that TNT structures contain F-actin as backbone suggests that the movement of organelles along TNTs is facilitated by an acto-myosin-dependent mechanism. Besides, it has been reported that the acto-myosin machinery used by the cell to move virus-containing cargoes within TNTs is 25 times faster than the surfing process seen for HIV and other retroviruses on filopodial protrusions (Sherer et al 2007), thus suggesting that intercellular vesicular trafficking is a more efficient mechanism of pathogens spreading. This leads to the question, which are the actin-associated motors involved in endocytic vesicles traffic through TNTs and, so, leading to the spread of PrP<sup>Sc</sup>? It has been shown that Myosin Va is present in TNTs and partially localizes with endocytic organelles (Rustom et

al 2004; Gerder 2007). It is known that Myosin Va is recruited on to diverse organelles, such as melanosomes and secretory vesicles, by a mechanism involving Rab GTPase (Desnos et al 2007). So, it would be interesting to assess the role of this molecular motor in driving PrP<sup>Sc</sup>-containing vesicles transfer *via* TNTs in neuronal cells.

Another intriguing question raised by these results regard the implication of the vesicular intercellular transport of PrP<sup>Sc</sup> in prion infectivity. I found that PrP<sup>Sc</sup> travel *via* TNT mainly with the recycling endosomes representing the apparatus for prion replication (Marijanovic et al 2009). Whether PrP<sup>Sc</sup> particles spreading in vesicles through tunneling nanotubes results in a productive infection of a recipient cell and how the flow of these carriers is regulated and intersects with the intracellular pathway of the 'host' remain to be investigated. In particular, what would be the fate of PrP<sup>Sc</sup>-enriched recycling endosomes once they get in a neighboring cell? To travel in different organelles can be a mean for PrP<sup>Sc</sup> to meet, by organelle fusion, with PrP<sup>C</sup>-containing early or recycling endosomes from another cell and continue to spread by further replication by transconformation. One way to explore this possibility could be by following the intercellular trafficking of specific markers of recycling endosomes, as Rab11 and Vamp3 (that I showed travelling *via* TNT, see paragraph 1.1 of this chapter) deriving from two cells population transfected with either GFP- and RFP-tagged proteins by using double color live-imaging fluorescence technique. Subsequently, by recording in real-time the organelles fusion events between vesicles deriving from one cell population with the other, it would be possible to understand whether there is interaction between the endocytic systems of two connected cell and the fate of the newly obtained endocytic vesicles.

Also, in order to evaluate the infectivity of PrP<sup>Sc</sup>-enriched endosomes it would be interesting to purify TNTs deriving from co-culture between prion-infected and uninfected cells, in a similar way on what was recently shown for HIV virus (Kadiu et al 2010). In addition, this could possibly allow the isolation of factors that are specifically present upon prion infection in TNT and could be potentially associated with PrP<sup>Sc</sup> trafficking in these structures.

Moreover, I set up a flow cytometry assay (Figure 37) to quantitate DiD- vesicles TNT-mediated transfer in CAD cells specifically to study the effect of PrP<sup>C</sup> and Myo-X on vesicular trafficking in TNT (as described in paragraphs 2.2 and 2.3 of this chapter and further discussed below). Thus, one could imagine using this assay to analyze the effect of selective blocking of different endocytic pathways on DiD-vesicles transfer. The identification and subsequent dissection of the pathways that are implicated in intercellular- vesicular trafficking could help to find possible therapeutic approaches to limit PrP<sup>Sc</sup> spreading by controlling its exit from an host cell or by impairing its trafficking to the neighboring cells.

Next I have analyzed factors that could be involved in formation of TNTs and in the spreading of prions through these channels. Because TNTs formed in between CAD cells can derive from filopodia-like protrusions (Gousset et al 2009), it is likely that TNT formation could be driven by factors that are important for filopodia formation and their maintenance.

Interestingly PrP<sup>C</sup> itself has been recently involved in cytoskeleton dynamic and remodeling and in cell-to-cell adhesion (Malaga-Trillo 2009; Chiesa and Harris 2009; Schrock et al 2009). Therefore, we have investigated its potential role on TNTs formation and transfer of vesicles. Interestingly I observed that GFP-PrPWT transfected cells seem to extend more filopodial protrusions that could fuse with the ones present on remote cells leading to formation of TNT. By quantitate the number of TNT-connected cells I indeed found an increase in TNTs number in cells over-expressing GFP-PrPWT (Figure 36). Surprisingly, this increase was not related to an increase in trafficking of endocytic vesicles in CAD cells, as I could not detect more DiD-vesicle transfer in this condition compared to control (Figure 39).

This could be explained by the fact that different molecules are involved in TNT formation. Indeed some of them can have a structural role where some others a functional property (e.g., building up the membrane structure or be part of the machinery that allows and drives the transfer of material within the TNT membrane). In this view, one could speculate that even in presence of an increased number of TNT structures PrP<sup>C</sup> over-

expression is not sufficient to increase the transfer of vesicles because other components that are fundamental for the process or a limiting step. On the other hand, the role of PrP<sup>C</sup> could be related more to TNT structure. For example, it has been shown that in zebrafish, PrP-1, an homologue of the mammalian PrP<sup>C</sup>, might directly mediate homophilic interactions or indirectly by regulating the trafficking of E-cadherins and  $\beta$ -catenin to the plasma membrane, thus promoting adherents junctions (Malaga-Trillo, 2009). This is in agreement with previous observations made for mammalian PrP<sup>C</sup> in which a role for this protein in neurite outgrowth and cell-cell interaction, respectively in hippocampal neurons and neuroblastoma cells has been reported (Monge et al 2002; Santuccione et al 2005). On the other hand it has been observed that VE-Cad, an endothelium-specific cadherin, can be transported to the tips of filopodia in association to the motor protein Myosin-X in order to develop primary cell-cell contacts by promoting homophilic cell-cell junction formation (Almagro et al 2010). Accordingly, one could hypothesize that PrP<sup>C</sup> can be involved in this event and participate in the anchoring and establishment of cell-to-cell contact with a neighboring cell, thus interacting with different partners.

Along the same line of thinking, in the last part of my thesis work (paragraph 2.3 of this chapter) I explored the role of Myo-X molecular motor in TNT-formation and TNT-mediated transfer. Indeed this protein is fundamental in initiating filopodia formation and transporting specific cargo to its tip, that is an active site for actin polymerization (Berg and Cheney, 2002; Sousa and Cheney 2005). By using both fluorescence microscopy and flow cytometry I found that over-expression of a fluorescently labelled version of Myo-X (GFP-Myo-X) increases the number of TNT-connected cells (of around 40% more compared to control). Furthermore it doubles the transfer of DiD-vesicles in CAD cells (Figure 41). Consistently, by knocking-down Myo-X gene I observed an inhibitory effect on both these processes (Figure 43). It is interesting to note that the transfer of vesicles was unidirectional (e.g., occurring from the cells over-expressing Myo-X to the acceptor cells) (Figure 41), thus highlighting that critical intracellular signals in the TNT-sending cell can stimulate and

drive TNT-formation and lead to transfer of different components.

These data clearly showed that Myo-X might play a pivotal role on TNT-mediate intercellular communication between cells. To further dissect the mechanism of action of Myo-X I analyzed the effect of the different Myo-X domains. To this aim I used different GFP-tagged construct mutants of the protein containing mutations or deletions of the different Myo-X domains (Figure 44) and by similar experimental approaches I was able to show that both motor domain (that binds to actin) and tail domain (containing cargo-binding sites) need to be present for TNT formation and transfer (Figure 44). This highlights the fact that the tip localization of Myo-X, given by its motor domain, is not sufficient to drive TNT-formation and mediated-transfer and that binding to specific cargo proteins, as critical components of TNT formation machinery, is required.

Furthermore it has been shown that both lobe 2 and 3 of the FERM domain of Myo-X (present in the tail) are crucial for binding to  $\beta$ -integrins (Zhang et al 2004). We hypothesized that this interaction might be implicated in TNT-formation mechanism. To verify this hypothesis, by using mutants of Myo-X lacking of lobe 2 or 3 of FERM domain (F2 or F3), respectively GFP-Myo-X- $\Delta$ F2 and GFP-Myo-X- $\Delta$ F3 mutants, I evaluated both the number of TNT-connected cells and DiD-vesicle transfer upon their over-expression. Interestingly, I found that, while cells over-expressing GFP-Myo-X- $\Delta$ F3 showed similar properties to GFP-Myo-X wild-type, no increase of TNT number or transfer of DiD-vesicle was detected in GFP-Myo-X- $\Delta$ F2 transfected cells (Figure 45). This clearly suggests that proteins that specifically bind to lobe 2 of the FERM domain of Myo-X, but not  $\beta$ -integrins, are necessary for both TNT formation and function. In agreement with this finding, it was recently shown that Myo-X over-expression is a greater inducer of dorsal filopodia and knock-down of Myo-X leads to a substantial loss of these structures (Bohil et al 2006). Dorsal filopodia do not contact the substratum and are independent for their function from integrins. Besides, Myo-X FERM mutants over-expression do not impair the ability of Myo-X to induce dorsal filopodia (Bohil et al 2006), thus suggesting that this type of filopodia could potentially be TNT precursors. Therefore further

investigations are needed to identify the binding partner(s) of F2 and, so, unravel the mechanism by which Myo-X and cooperative partners induce TNT-formation and transfer. In particular, it would be interesting to explore the possible role of VASP/Mena proteins in this process, as Myo-X is responsible of their localization to the tip of filopodia where they promote actin filament elongation by interacting with the plus ends and shielding them from the capping protein (Tokuo et al 2004). In this view, it could be that the actin-binding motor protein Myo-X is critical for delivering important factors that would subsequently drive elongation of the filopodial protrusions and/or establishment of cell-to-cell contact and passage of molecules through newly formed tunneling nanotubes.

Having established that Myo-X is involved in both the formation and the transfer through TNTs, the question that I addressed next was to explore the effect that over-expression of Myo-X had on PrP<sup>Sc</sup> transfer. Interestingly, I found that over-expression of Myo-X not only increases TNT numbers and vesicle transfer but it also almost doubles the transfer of PrP<sup>Sc</sup> from prion infected CAD (scCAD) to naïve CAD cells (Figure 46). Consequently, understanding the role of Myo-X in TNT-mediated transfer could also allow a better characterization of the mechanism of PrP<sup>Sc</sup> trafficking and its invasive properties in a specific host.

In addition, I also found that PrP<sup>Sc</sup> itself could increase the number of TNT-connected cells in scCAD cells (around 28% compared to uninfected cells) (Figure 40). Hijacking of TNT structures can be preceded by induction of TNT formation, thus optimizing pathogen transfer, as it has been observed for HIV spreading in macrophages (Sowinski et al 2008; Kadiu et al 2011). In these reports, the authors first observed an increase in the number of connections in macrophages, following HIV infection. Therefore, together with these findings, the increase in TNT number upon prion infection can reflect the possibility that TNT induction is also a general host-response mechanism against pathogens that can mediate transfer of 'protective' factors or other specific signals in neighboring cells. Especially, it has been shown that following PrP<sup>Sc</sup> infection, an early burst of reactive oxygen species (ROS) occurs in the brain of prion infected mice (Yun et al., 2006; Pamplona et al., 2008) and in *in vitro* cell

culture systems (Haigh et al 2011). It has been recently reported that TNTs are induced by  $H_2O_2$  in rat astrocytes and neurons in a p53-dependent manner (Wang et al 2011). Therefore, a possible link between prion infection and TNT-induction could be envisaged. Moreover, upon  $H_2O_2$ -stimulation, phosphoinositide 3-kinase (PI3-K) gene among the others is up-regulated by p53 signalling. Curiously, Myo-X is a downstream effector of PI3-K during phagocytosis (Cox et al 2002) and  $PtdIns(3,4,5)P_3$  is a regulator of Myo-X localization to the tip of filopodia (Plantard et al 2010). From the data present in literature and from the findings presented here regarding both a role for Myo-X in TNT-formation and an induction of TNT structures upon prion infection, one could be intrigued to pursue this direction and uncover a possible relationship in between the two. Particularly, would be interesting to understand how prion infection leads finally to TNT-induction and what is the biological meaning of this process, since an increase of  $PrP^{Sc}$  spreading is also observed when induction of TNT formation occurs? Further investigations are needed in order to address this important question in order to be able to explore my results towards both the understanding of the disease as well as the development of efficacious therapies.

## CONCLUSIONS AND PERSPECTIVES

---

## Conclusions and Perspectives

- In the first part of my PhD work I investigated the role of autophagy in prion disease in order to better clarify the mechanisms by which PrP<sup>Sc</sup> is degraded. This was performed by using *in vitro* cell models of prion infection and combined fluorescence microscopy and biochemical approaches.

In these experiments I found that:

- a) autophagy is not involved in PrP<sup>Sc</sup> degradation;
- b) tamoxifen and 4-hydroxyl-tamoxifen (OHT), two drugs used to enhance the autophagic flux, efficiently reduced PrP<sup>Sc</sup> levels in autophagy independent manner;
- c) tamoxifen and OHT alter cholesterol trafficking and cause a redistribution of both PrP<sup>Sc</sup> and PrP<sup>C</sup> to lysosomes, thus shifting the equilibrium between prion production and degradation towards the latter.

While autophagy has been recently shown to have a role in other neurodegenerative diseases (by directing aggregated proteins into lysosomes), my data exclude a role of autophagy in prion degradation. On the other hand, I demonstrated that tamoxifen and OHT increase PrP<sup>Sc</sup> degradation by re-routing the trafficking of prions to lysosomes independently from the autophagic pathway. Moreover, upon OHT treatment cholesterol trafficking in the cell is altered leading to the accumulation of this lipid in lysosomes. This is accompanied by a reduction of the cholesterol content in the endosomal recycling compartment that represents a favorable environment for PrP<sup>C</sup>-PrP<sup>Sc</sup> conversion, thus shifting the equilibrium between prion production and degradation towards degradation.

These results highlight the importance of the endosomal recycling compartment in prion conversion and the lipid environment as key elements necessary for prion replication. This suggests that development of new drugs able to selectively diverge the trafficking of both PrP<sup>C</sup> and PrP<sup>Sc</sup> from the recycling endosomes or interfere with their mutual interaction by changing

cholesterol distribution could be used in experimental search for treatments of prion infections. Therefore, given its ability to both reduce infectious prions and modify cholesterol metabolism OHT represents a well-characterized, widely available pharmaceutical that may have applications as broad-spectrum therapy for neurodegenerative diseases of protein aggregation.

In this view, additional experiments are needed to assess OHT therapeutic anti-prion efficacy in *in vivo* experiments. For example, it would be possible to deliver OHT by oral administration, in order to mimic a pre-clinical therapeutic situation, and evaluate both the reduction of PrP<sup>Sc</sup> burden and survival times compared to control mice.

- In the second part of my thesis I focused on characterizing the intercellular trafficking of PrP<sup>Sc</sup> *via* Tunneling Nanotubes (TNTs) and on the mechanisms of TNT formation and function in neuronal CAD cell as a model of prion infection.

By using fluorescence microscopy and flow cytometry techniques, I could show that:

- a) PrP<sup>Sc</sup> particles travel *via* TNTs in different sub-cellular compartments, as early endosomes and lysosomes, and mainly in the endocytic recycling compartment that is also an intracellular site for prion conversion;
- b) PrP<sup>C</sup> over-expression increases the number of TNT structures but does not increase vesicle transfer;
- c) PrP<sup>Sc</sup> infection can lead to an increase in TNT-like structures;
- d) Myo-X molecular motor is able to induce TNT formation, to increase the transfer of vesicle and, more interestingly, to increase the transfer of PrP<sup>Sc</sup> particles.

The identification and subsequent dissection of the pathways and the molecules that are implicated in intercellular vesicular trafficking of PrP<sup>Sc</sup> could help to find possible therapeutic approaches to limit PrP<sup>Sc</sup> spreading by controlling its exit from a host cell or by impairing its trafficking to the neighboring cells. Therefore, a better understanding of this process, together with

the study of structural and functional factors (as PrP<sup>C</sup> and Myo-X) involved in TNT formation and transfer of cellular components is of fundamental importance in prion biology.

Moreover, an increasing number of papers have reported the involvement of TNTs in normal cellular functions as well as in diseases. Indeed our findings are not confined to prion disease but could also be extended to other pathological conditions associated for example with the spreading of different aggregate proteins (e.g.,  $\beta$ -Amyloid), signals (e.g., death signals) and pathogens (e.g., HIV virus, bacteria) between different cells through TNTs. These data also highlight the need of multidisciplinary synergistic research between different fields in which TNTs have been shown to play a role, thus bringing a new way of looking at diseases and allowing the development of new strategies to fight them. Therefore a more accurate characterization of this type of long distance form of intercellular communication together with a better understanding of their physiological role is an intriguing and challenging still open question in biology.

## REFERENCES

---

Aguib, Y., A. Heiseke, S. Gilch, C. Riemer, M. Baier, A. Ertmer, and H.M. Schätzl. 2009. Autophagy induction by trehalose counter-acts cellular prion-infection. *Autophagy*. 5:361-370.

Aguzzi, A., and A.M. Calella. 2009a. Prions: Protein Aggregation and Infectious Diseases. *Physiological Reviews*. 89:1105 -1152.

Aguzzi, A., and A.M. Calella. 2009b. Prions: Protein Aggregation and Infectious Diseases. *Physiological Reviews*. 89:1105 -1152.

Aguzzi, A., and M. Polymenidou. 2004. Mammalian prion biology: one century of evolving concepts. *Cell*. 116:313-327.

Aguzzi, A., F. Baumann, and J. Bremer. 2008. The prion's elusive reason for being. *Annu. Rev. Neurosci.* 31:439-477.

Akowitz, A., E.E. Manuelidis, and L. Manuelidis. 1993. Protected endogenous retroviral sequences copurify with infectivity in experimental Creutzfeldt-Jakob disease. *Arch. Virol.* 130:301-316.

Almagro, S., C. Durmort, A. Chervin-Petinot, S. Heyraud, M. Dubois, O. Lambert, C. Mallefaud, E. Hewat, J.P. Schaal, P. Huber, and D. Gulino-Debrac. 2010. The Motor Protein Myosin-X Transports VE-Cadherin along Filopodia To Allow the Formation of Early Endothelial Cell-Cell Contacts. *Mol. Cell. Biol.* 30:1703-1717.

Alper, T., W.A. Cramp, D.A. Haig, and M.C. Clarke. 1967. Does the agent of scrapie replicate without nucleic acid? *Nature*. 214:764-766.

Ana, M.C. 2004. Autophagy: in sickness and in health. *Trends in Cell Biology*. 14:70-77.

Anderson, R.G. 1998. The caveolae membrane system. *Annu. Rev. Biochem.* 67:199-225.

Anderson, R.M., C.A. Donnelly, N.M. Ferguson, M.E. Woolhouse, C.J. Watt, H.J. Udy, S. MaWhinney, S.P. Dunstan, T.R. Southwood, J.W. Wilesmith, J.B. Ryan, L.J. Hoinville, J.E. Hillerton, A.R. Austin, and G.A. Wells. 1996. Transmission dynamics and epidemiology of BSE in British cattle. *Nature*. 382:779-788.

Arkwright, P.D., F. Luchetti, J. Tour, C. Roberts, R. Ayub, A.P. Morales, J.J. Rodríguez, A. Gilmore, B. Canonico, S. Papa, and M.D. Esposti. 2010. Fas stimulation of T lymphocytes promotes rapid intercellular exchange of death signals via membrane nanotubes. *Cell Res*. 20:72-88.

Aucouturier, P., F. Geissmann, D. Damotte, G.P. Saborio, H.C. Meeker, R. Kascsak, R. Kascsak, R.I. Carp, and T. Wisniewski. 2001. Infected splenic

dendritic cells are sufficient for prion transmission to the CNS in mouse scrapie. *J. Clin. Invest.* 108:703-708.

Baldauf, E., M. Beekes, and H. Diringer. 1997. Evidence for an alternative direct route of access for the scrapie agent to the brain bypassing the spinal cord. *J. Gen. Virol.* 78 ( Pt 5):1187-1197.

Balducci, C., M. Beeg, M. Stravalaci, A. Bastone, A. Scip, E. Biasini, L. Tapella, L. Colombo, C. Manzoni, T. Borsello, R. Chiesa, M. Gobbi, M. Salmona, and G. Forloni. 2010. Synthetic amyloid-beta oligomers impair long-term memory independently of cellular prion protein. *Proc. Natl. Acad. Sci. U.S.A.* 107:2295-2300.

Baron, G.S., and B. Caughey. 2003. Effect of glycosylphosphatidylinositol anchor-dependent and -independent prion protein association with model raft membranes on conversion to the protease-resistant isoform. *J. Biol. Chem.* 278:14883-14892.

Bartz, J.C., C. Dejoia, T. Tucker, A.E. Kincaid, and R.A. Bessen. 2005. Extraneural prion neuroinvasion without lymphoreticular system infection. *J. Virol.* 79:11858-11863.

Baskakov, I.V., G. Legname, M.A. Baldwin, S.B. Prusiner, and F.E. Cohen. 2002. Pathway complexity of prion protein assembly into amyloid. *J. Biol. Chem.* 277:21140-21148.

Beau, I., M. Mehrpour, and P. Codogno. 2011. Autophagosomes and human diseases. *The International Journal of Biochemistry & Cell Biology.* 43:460-464.

Beck, E., P.M. Daniel, A.J. Davey, D.C. Gajdusek, and C.J. Gibbs Jr. 1982. The pathogenesis of transmissible spongiform encephalopathy: an ultrastructural study. *Brain.* 105 (Pt 4):755-786.

Beekes, M., and P.A. McBride. 2000. Early accumulation of pathological PrP in the enteric nervous system and gut-associated lymphoid tissue of hamsters orally infected with scrapie. *Neuroscience Letters.* 278:181-184.

Beekes, M., and P.A. McBride. 2007. The spread of prions through the body in naturally acquired transmissible spongiform encephalopathies. *FEBS J.* 274:588-605.

Beekes, M., E. Baldauf, and H. Diringer. 1996. Sequential appearance and accumulation of pathognomonic markers in the central nervous system of hamsters orally infected with scrapie. *J. Gen. Virol.* 77 ( Pt 8):1925-1934.

Berg, J.S., and R.E. Cheney. 2002. Myosin-X is an unconventional myosin that undergoes intrafilopodial motility. *Nat. Cell Biol.* 4:246-250.

Berg, J.S., B.C. Powell, and R.E. Cheney. 2001. A millennial myosin census. *Mol. Biol. Cell.* 12:780-794.

Bohil, A.B., B.W. Robertson, and R.E. Cheney. 2006. Myosin-X is a molecular motor that functions in filopodia formation. *Proc. Natl. Acad. Sci. U.S.A.* 103:12411-12416.

Bonifacino, J.S., and L.M. Traub. 2003. Signals for sorting of transmembrane proteins to endosomes and lysosomes. *Annu. Rev. Biochem.* 72:395-447.

Borchelt, D.R., M. Rogers, N. Stahl, G. Telling, and S.B. Prusiner. 1993. Release of the cellular prion protein from cultured cells after loss of its glycoinositol phospholipid anchor. *Glycobiology.* 3:319-329.

Borchelt, D.R., A. Taraboulos, and S.B. Prusiner. 1992. Evidence for synthesis of scrapie prion proteins in the endocytic pathway. *Journal of Biological Chemistry.* 267:16188 -16199.

Bosque, P.J., C. Ryou, G. Telling, D. Peretz, G. Legname, S.J. DeArmond, and S.B. Prusiner. 2002. Prions in skeletal muscle. *Proc. Natl. Acad. Sci. U.S.A.* 99:3812-3817.

Bounhar, Y., Y. Zhang, C.G. Goodyer, and A. LeBlanc. 2001. Prion Protein Protects Human Neurons against Bax-mediated Apoptosis. *Journal of Biological Chemistry.* 276:39145 -39149.

Brandner, S., A. Raeber, A. Sailer, T. Blättler, M. Fischer, C. Weissmann, and A. Aguzzi. 1996. Normal host prion protein (PrPC) is required for scrapie spread within the central nervous system. *Proc Natl Acad Sci U S A.* 93:13148-13151.

Bremer, J., F. Baumann, C. Tiberi, C. Wessig, H. Fischer, P. Schwarz, A.D. Steele, K.V. Toyka, K.-A. Nave, J. Weis, and A. Aguzzi. 2010. Axonal prion protein is required for peripheral myelin maintenance. *Nat Neurosci.* 13:310-318.

Brown, K.L., K. Stewart, D.L. Ritchie, N.A. Mabbott, A. Williams, H. Fraser, W.I. Morrison, and M.E. Bruce. 1999. Scrapie replication in lymphoid tissues depends on prion protein-expressing follicular dendritic cells. *Nat. Med.* 5:1308-1312.

Brown, P., C.J. Gibbs Jr, P. Rodgers-Johnson, D.M. Asher, M.P. Sulima, A. Bacote, L.G. Goldfarb, and D.C. Gajdusek. 1994. Human spongiform encephalopathy: the National Institutes of Health series of 300 cases of experimentally transmitted disease. *Ann. Neurol.* 35:513-529.

Browning, S.R., G.L. Mason, T. Seward, M. Green, G.A.J. Eliason, C. Mathiason, M.W. Miller, E.S. Williams, E. Hoover, and G.C. Telling. 2004. Transmission of

prions from mule deer and elk with chronic wasting disease to transgenic mice expressing cervid PrP. *J. Virol.* 78:13345-13350.

Bruce, M., A. Chree, I. McConnell, J. Foster, G. Pearson, and H. Fraser. 1994. Transmission of bovine spongiform encephalopathy and scrapie to mice: strain variation and the species barrier. *Philos. Trans. R. Soc. Lond., B, Biol. Sci.* 343:405-411.

Bruce, M.E. 1993. Scrapie strain variation and mutation. *British Medical Bulletin.* 49:822 -838.

Bruce, M.E., R.G. Will, J.W. Ironside, I. McConnell, D. Drummond, A. Suttie, L. McCardle, A. Chree, J. Hope, C. Birkett, S. Cousens, H. Fraser, and C.J. Bostock. 1997. Transmissions to mice indicate that 'new variant' CJD is caused by the BSE agent. *Nature.* 389:498-501.

Budka, H. 2003. Neuropathology of prion diseases. *British Medical Bulletin.* 66:121 -130.

Büeler, H., M. Fischer, Y. Lang, H. Bluethmann, H.P. Lipp, S.J. DeArmond, S.B. Prusiner, M. Aguet, and C. Weissmann. 1992. Normal development and behaviour of mice lacking the neuronal cell-surface PrP protein. *Nature.* 356:577-582.

Bukoreshtliev, N.V., X. Wang, E. Hodneland, S. Gurke, J.F.V. Barroso, and H.-H. Gerdes. 2009. Selective block of tunneling nanotube (TNT) formation inhibits intercellular organelle transfer between PC12 cells. *FEBS Lett.* 583:1481-1488.

Cain, R.J., and A.J. Ridley. 2009. Phosphoinositide 3-kinases in cell migration. *Biol. Cell.* 101:13-29.

Campana, V., D. Sarnataro, and C. Zurzolo. 2005. The highways and byways of prion protein trafficking. *Trends Cell Biol.* 15:102-111.

Carlson, G.A., D. Westaway, S.J. DeArmond, M. Peterson-Torchia, and S.B. Prusiner. 1989. Primary structure of prion protein may modify scrapie isolate properties. *Proceedings of the National Academy of Sciences.* 86:7475 -7479.

Castilla, J., D. Gonzalez-Romero, P. Saá, R. Morales, J. De Castro, and C. Soto. 2008. Crossing the species barrier by PrP(Sc) replication in vitro generates unique infectious prions. *Cell.* 134:757-768.

Castilla, J., P. Saá, C. Hetz, and C. Soto. 2005. In vitro generation of infectious scrapie prions. *Cell.* 121:195-206.

Caughey, B., and G.J. Raymond. 1991. The scrapie-associated form of PrP is made from a cell surface precursor that is both protease- and phospholipase-sensitive. *J. Biol. Chem.* 266:18217-18223.

Caughey, B., K. Neary, R. Buller, D. Ernst, L.L. Perry, B. Chesebro, and R.E. Race. 1990. Normal and scrapie-associated forms of prion protein differ in their sensitivities to phospholipase and proteases in intact neuroblastoma cells. *J Virol.* 64:1093-1101.

Caughey, B., R.E. Race, D. Ernst, M.J. Buchmeier, and B. Chesebro. 1989. Prion protein biosynthesis in scrapie-infected and uninfected neuroblastoma cells. *J Virol.* 63:175-181.

Caughey, B., G.J. Raymond, D. Ernst, and R.E. Race. 1991. N-terminal truncation of the scrapie-associated form of PrP by lysosomal protease(s): implications regarding the site of conversion of PrP to the protease-resistant state. *J Virol.* 65:6597-6603.

Caughey, B., G.J. Raymond, D.A. Kocisko, and P.T. Lansbury. 1997. Scrapie infectivity correlates with converting activity, protease resistance, and aggregation of scrapie-associated prion protein in guanidine denaturation studies. *J Virol.* 71:4107-4110.

Cervenakova, L., O. Yakovleva, C. McKenzie, S. Kolchinsky, L. McShane, W.N. Drohan, and P. Brown. 2003. Similar levels of infectivity in the blood of mice infected with human-derived vCJD and GSS strains of transmissible spongiform encephalopathy. *Transfusion.* 43:1687-1694.

CHANDLER, R.L. 1961. Encephalopathy in mice produced by inoculation with scrapie brain material. *Lancet.* 1:1378-1379.

Chazot, G., E. Broussolle, C. I Lapras, T. Blättler, A. Aguzzi, and N. Kopp. 1996. New variant of Creutzfeldt-Jakob disease in a 26-year-old French man. *Lancet.* 347:1181.

Chen, Z.Y., T. Hasson, D.S. Zhang, B.J. Schwender, B.H. Derfler, M.S. Mooseker, and D.P. Corey. 2001. Myosin-VIIIb, a novel unconventional myosin, is a constituent of microvilli in transporting epithelia. *Genomics.* 72:285-296.

Cherra III, S.J., R.K. Dagda, and C.T. Chu. 2010. Review: Autophagy and neurodegeneration: survival at a cost? *Neuropathology and Applied Neurobiology.* 36:125-132.

Chesebro, B., R. Race, K. Wehrly, J. Nishio, M. Bloom, D. Lechner, S. Bergstrom, K. Robbins, L. Mayer, and J.M. Keith. 1985. Identification of scrapie prion protein-specific mRNA in scrapie-infected and uninfected brain. *Nature.* 315:331-333.

Chesebro, B., M. Trifilo, R. Race, K. Meade-White, C. Teng, R. LaCasse, L. Raymond, C. Favara, G. Baron, S. Priola, B. Caughey, E. Masliah, and M. Oldstone. 2005. Anchorless Prion Protein Results in Infectious Amyloid Disease Without Clinical Scrapie. *Science*. 308:1435 -1439.

Cloucard, C., P. Beaudry, J.M. Elsen, D. Milan, M. Dussaucy, C. Bounneau, F. Schelcher, J. Chatelain, J.M. Launay, and J.L. Laplanche. 1995. Different allelic effects of the codons 136 and 171 of the prion protein gene in sheep with natural scrapie. *Journal of General Virology*. 76:2097 -2101.

Colby, D.W., and S.B. Prusiner. 2011. Prions. *Cold Spring Harb Perspect Biol*. 3:a006833.

Collinge, J. 1997. Human Prion Diseases and Bovine Spongiform Encephalopathy (BSE). *Human Molecular Genetics*. 6:1699 -1705.

Collinge, J. 2001. PRION DISEASES OF HUMANS AND ANIMALS : Their Causes and Molecular Basis. *Annual Review of Neuroscience*. 24:519-550.

Collinge, J. 2005a. Molecular neurology of prion disease. *J. Neurol. Neurosurg. Psychiatr*. 76:906-919.

Collinge, J. 2005b. Molecular neurology of prion disease. *Journal of Neurology, Neurosurgery & Psychiatry*. 76:906 -919.

Collinge, J., and A.R. Clarke. 2007. A general model of prion strains and their pathogenicity. *Science*. 318:930-936.

Collinge, J., M.A. Whittington, K.C.L. Sidle, C.J. Smith, M.S. Palmer, A.R. Clarke, and J.G.R. Jefferys. 1994. Prion protein is necessary for normal synaptic function. *Nature*. 370:295-297.

Cordeiro, Y., F. Machado, L. Juliano, M.A. Juliano, R.R. Brentani, D. Foguel, and J.L. Silva. 2001. DNA converts cellular prion protein into the beta-sheet conformation and inhibits prion peptide aggregation. *J. Biol. Chem*. 276:49400-49409.

Cordier-Dirikoc, S., and J. Chabry. 2008. Temporary depletion of CD11c+ dendritic cells delays lymphoinvasion after intraperitoneal scrapie infection. *J. Virol*. 82:8933-8936.

Cox, D., J.S. Berg, M. Cammer, J.O. Chinegwundoh, B.M. Dale, R.E. Cheney, and S. Greenberg. 2002. Myosin X is a downstream effector of PI(3)K during phagocytosis. *Nat. Cell Biol*. 4:469-477.

Crick, F. 1970. Central dogma of molecular biology. *Nature*. 227:561-563.

- Deleault, N.R., R.W. Lucassen, and S. Supattapone. 2003. RNA molecules stimulate prion protein conversion. *Nature*. 425:717-720.
- Dickinson, A.G., and G.W. Outram. 1988. Genetic aspects of unconventional virus infections: the basis of the virino hypothesis. *Ciba Found. Symp.* 135:63-83.
- Dorban, G., V. Defaweux, C. Demonceau, S. Flandroy, P.-B. Van Lerberghe, N. Falisse-Poirrier, J. Piret, E. Heinen, and N. Antoine. 2007. Interaction between dendritic cells and nerve fibres in lymphoid organs after oral scrapie exposure. *Virchows Arch.* 451:1057-1065.
- Duffy, P., J. Wolf, G. Collins, A.G. DeVoe, B. Streeten, and D. Cowen. 1974. Letter: Possible person-to-person transmission of Creutzfeldt-Jakob disease. *N. Engl. J. Med.* 290:692-693.
- Eklund, C.M., R.C. Kennedy, and W.J. Hadlow. 1967. Pathogenesis of Scrapie Virus Infection in the Mouse. *The Journal of Infectious Diseases.* 117:15-22.
- Eskelinen, E.-L. 2004. Maturation of Autophagic Vacuoles in Mammalian Cells. *Autophagy.* 1:1-11.
- Eugenin, E.A., P.J. Gaskill, and J.W. Berman. 2009. Tunneling nanotubes (TNT) are induced by HIV-infection of macrophages: a potential mechanism for intercellular HIV trafficking. *Cell. Immunol.* 254:142-148.
- Fevrier, B., D. Vilette, F. Archer, D. Loew, W. Faigle, M. Vidal, H. Laude, and G. Raposo. 2004. Cells release prions in association with exosomes. *Proc. Natl. Acad. Sci. U.S.A.* 101:9683-9688.
- Forloni, G., N. Angeretti, R. Chiesa, E. Monzani, M. Salmona, O. Bugiani, and F. Tagliavini. 1993. Neurotoxicity of a prion protein fragment. *Nature.* 362:543-546.
- Foth, B.J., M.C. Goedecke, and D. Soldati. 2006. New insights into myosin evolution and classification. *Proc. Natl. Acad. Sci. U.S.A.* 103:3681-3686.
- Fournier, J.G., F. Escaig-Haye, T. Billette de Villemeur, and O. Robain. 1995. Ultrastructural localization of cellular prion protein (PrPc) in synaptic boutons of normal hamster hippocampus. *C. R. Acad. Sci. III, Sci. Vie.* 318:339-344.
- Fraser, H., K.L. Brown, K. Stewart, I. McConnell, P. McBride, and A. Williams. 1996. Replication of scrapie in spleens of SCID mice follows reconstitution with wild-type mouse bone marrow. *J. Gen. Virol.* 77 ( Pt 8):1935-1940.
- Fraser, H., I. McConnell, G.A. Wells, and M. Dawson. 1988. Transmission of bovine spongiform encephalopathy to mice. *Vet. Rec.* 123:472.

Gabriel, J.M., B. Oesch, H. Kretzschmar, M. Scott, and S.B. Prusiner. 1992. Molecular cloning of a candidate chicken prion protein. *Proceedings of the National Academy of Sciences*. 89:9097 -9101.

Gabus, C., S. Auxilien, C. P echoux, D. Dormont, W. Swietnicki, M. Morillas, W. Surewicz, P. Nandi, and J.L. Darlix. 2001a. The prion protein has DNA strand transfer properties similar to retroviral nucleocapsid protein. *J. Mol. Biol.* 307:1011-1021.

Gabus, C., E. Derrington, P. Leblanc, J. Chnaiderman, D. Dormont, W. Swietnicki, M. Morillas, W.K. Surewicz, D. Marc, P. Nandi, and J.L. Darlix. 2001b. The prion protein has RNA binding and chaperoning properties characteristic of nucleocapsid protein NCP7 of HIV-1. *J. Biol. Chem.* 276:19301-19309.

Galvan, C., P.G. Camoletto, C.G. Dotti, A. Aguzzi, and M. Dolores Ledesma. 2005. Proper axonal distribution of PrPC depends on cholesterol-sphingomyelin-enriched membrane domains and is developmentally regulated in hippocampal neurons. *Molecular and Cellular Neuroscience*. 30:304-315.

Gasset, M., M.A. Baldwin, D.H. Lloyd, J.M. Gabriel, D.M. Holtzman, F. Cohen, R. Fletterick, and S.B. Prusiner. 1992. Predicted alpha-helical regions of the prion protein when synthesized as peptides form amyloid. *Proc. Natl. Acad. Sci. U.S.A.* 89:10940-10944.

Gerdes, H.-H., and R.N. Carvalho. 2008. Intercellular transfer mediated by tunneling nanotubes. *Curr. Opin. Cell Biol.* 20:470-475.

Gilch, S., C. Bach, G. Lutzny, I. Vorberg, and H.M. Sch atzl. 2009. Inhibition of cholesterol recycling impairs cellular PrP(Sc) propagation. *Cell. Mol. Life Sci.* 66:3979-3991.

Gilch, S., N. Chitoor, Y. Taguchi, M. Stuart, J.E. Jewell, and H.M. Sch atzl. 2011. Chronic Wasting Disease. In *Prion Proteins*. J. Tatzelt, editor. Springer Berlin Heidelberg, Berlin, Heidelberg. 51-77.

Gilch, S., K.F. Winklhofer, M.H. Groschup, M. Nunziante, R. Lucassen, C. Spielhauer, W. Muranyi, D. Riesner, J. Tatzelt, and H.M. Sch atzl. 2001. Intracellular re-routing of prion protein prevents propagation of PrPSc and delays onset of prion disease. *EMBO J.* 20:3957-3966.

Godsave, S.F., H. Wille, P. Kujala, D. Latawiec, S.J. DeArmond, A. Serban, S.B. Prusiner, and P.J. Peters. 2008. Cryo-Immunogold Electron Microscopy for Prions: Toward Identification of a Conversion Site. *The Journal of Neuroscience*. 28:12489 -12499.

Goold, R., S. Rabbanian, L. Sutton, R. Andre, P. Arora, J. Moonga, A.R. Clarke, G. Schiavo, P. Jat, J. Collinge, and S.J. Tabrizi. 2011. Rapid cell-surface prion protein conversion revealed using a novel cell system. *Nat Commun.* 2:281.

Gousset, K., and C. Zurzolo. 2009. Tunnelling nanotubes: a highway for prion spreading? *Prion*. 3:94-98.

Gousset, K., E. Schiff, C. Langevin, Z. Marijanovic, A. Caputo, D.T. Browman, N. Chenouard, F. de Chaumont, A. Martino, J. Enninga, J.-C. Olivo-Marin, D. Männel, and C. Zurzolo. 2009. Prions hijack tunnelling nanotubes for intercellular spread. *Nat. Cell Biol.* 11:328-336.

GRIFFITH, J.S. 1967. Nature of the Scrapie Agent: Self-replication and Scrapie. *Nature*. 215:1043-1044.

Gupton, S.L., and F.B. Gertler. 2007. Filopodia: the fingers that do the walking. *Sci. STKE*. 2007:re5.

Hagiwara, K., Y. Nakamura, M. Nishijima, and Y. Yamakawa. 2007. Prevention of prion propagation by dehydrocholesterol reductase inhibitors in cultured cells and a therapeutic trial in mice. *Biol. Pharm. Bull.* 30:835-838.

Hao, M., S.X. Lin, O.J. Karylowski, D. Wüstner, T.E. McGraw, and F.R. Maxfield. 2002. Vesicular and non-vesicular sterol transport in living cells. The endocytic recycling compartment is a major sterol storage organelle. *J. Biol. Chem.* 277:609-617.

Hara, T., K. Nakamura, M. Matsui, A. Yamamoto, Y. Nakahara, R. Suzuki-Migishima, M. Yokoyama, K. Mishima, I. Saito, H. Okano, and N. Mizushima. 2006. Suppression of basal autophagy in neural cells causes neurodegenerative disease in mice. *Nature*. 441:885-889.

Haraguchi, T., S. Fisher, S. Olofsson, T. Endo, D. Groth, A. Tarentino, D.R. Borchelt, D. Teplow, L. Hood, and A. Burlingame. 1989. Asparagine-linked glycosylation of the scrapie and cellular prion proteins. *Arch. Biochem. Biophys.* 274:1-13.

Harmey, J.H. The Cellular Isoform of the Prion Protein, PRPC, Is Associated with Caveolae in Mouse Neuroblastoma (N2a) Cells. *Biochemical and Biophysical Research Communications*. 210:753-759.

Harris, D.A. 2003. Trafficking, turnover and membrane topology of PrP. *British Medical Bulletin*. 66:71 -85.

Hartman, M.A., D. Finan, S. Sivaramakrishnan, and J.A. Spudich. 2011. Principles of unconventional Myosin function and targeting. *Annu. Rev. Cell Dev. Biol.* 27:133-155.

Hase, K., S. Kimura, H. Takatsu, M. Ohmae, S. Kawano, H. Kitamura, M. Ito, H. Watarai, C.C. Hazelett, C. Yeaman, and H. Ohno. 2009. M-Sec promotes membrane nanotube formation by interacting with Ral and the exocyst complex. *Nat. Cell Biol.* 11:1427-1432.

- He, K., W. Luo, Y. Zhang, F. Liu, D. Liu, L. Xu, L. Qin, C. Xiong, Z. Lu, X. Fang, and Y. Zhang. 2010. Intercellular transportation of quantum dots mediated by membrane nanotubes. *ACS Nano*. 4:3015-3022.
- Heiseke, A., Y. Aguib, C. Riemer, M. Baier, and H.M. Schätzl. 2009. Lithium induces clearance of protease resistant prion protein in prion-infected cells by induction of autophagy. *Journal of Neurochemistry*. 109:25-34.
- Heppner, F.L., A.D. Christ, M.A. Klein, M. Prinz, M. Fried, J.-P. Kraehenbuhl, and A. Aguzzi. 2001. Transepithelial prion transport by M cells. *Nat Med*. 7:976-977.
- Hetz, C., M. Russelakis-Carneiro, K. Maundrell, J. Castilla, and C. Soto. 2003. Caspase-12 and endoplasmic reticulum stress mediate neurotoxicity of pathological prion protein. *EMBO J*. 22:5435-5445.
- Hill, A.F., and J. Collinge. 2003. Subclinical prion infection in humans and animals. *British Medical Bulletin*. 66:161 -170.
- Hill, A.F., M. Desbruslais, S. Joiner, K.C. Sidle, I. Gowland, J. Collinge, L.J. Doey, and P. Lantos. 1997a. The same prion strain causes vCJD and BSE. *Nature*. 389:448-450, 526.
- Hill, A.F., M. Desbruslais, S. Joiner, K.C. Sidle, I. Gowland, J. Collinge, L.J. Doey, and P. Lantos. 1997b. The same prion strain causes vCJD and BSE. *Nature*. 389:448-450, 526.
- Hill, A.F., S. Joiner, J. Linehan, M. Desbruslais, P.L. Lantos, and J. Collinge. 2000. Species-barrier-independent prion replication in apparently resistant species. *Proceedings of the National Academy of Sciences*. 97:10248 -10253.
- Homma, K., J. Saito, R. Ikebe, and M. Ikebe. 2000. Ca<sup>2+</sup>-dependent Regulation of the Motor Activity of Myosin V. *Journal of Biological Chemistry*. 275:34766 -34771.
- Hsiao, K., H.F. Baker, T.J. Crow, M. Poulter, F. Owen, J.D. Terwilliger, D. Westaway, J. Ott, and S.B. Prusiner. 1989. Linkage of a prion protein missense variant to Gerstmann-Sträussler syndrome. *Nature*. 338:342-345.
- Huang, F.-P., C.F. Farquhar, N.A. Mabbott, M.E. Bruce, and G.G. MacPherson. 2002. Migrating intestinal dendritic cells transport PrP(Sc) from the gut. *J. Gen. Virol*. 83:267-271.
- Huang, W.-P., and D.J. Klionsky. 2002a. *Cell Structure and Function*. 27:409-420.
- Huang, W.-P., and D.J. Klionsky. 2002b. Autophagy in yeast: a review of the molecular machinery. *Cell Struct. Funct*. 27:409-420.

- Hurtig, J., D.T. Chiu, and B. Onfelt. 2010. Intercellular nanotubes: insights from imaging studies and beyond. *Wiley Interdiscip Rev Nanomed Nanobiotechnol.* 2:260-276.
- Hwang, Y.-S., T. Luo, Y. Xu, and T.D. Sargent. 2009. Myosin-X is required for cranial neural crest cell migration in *Xenopus laevis*. *Dev. Dyn.* 238:2522-2529.
- Ikonen, E. 2008. Cellular cholesterol trafficking and compartmentalization. *Nat. Rev. Mol. Cell Biol.* 9:125-138.
- Isaacs, J.D., G.S. Jackson, and D.M. Altmann. 2006. The role of the cellular prion protein in the immune system. *Clin Exp Immunol.* 146:1-8.
- Isakoff, S.J., T. Cardozo, J. Andreev, Z. Li, K.M. Ferguson, R. Abagyan, M.A. Lemmon, A. Aronheim, and E.Y. Skolnik. 1998. Identification and analysis of PH domain-containing targets of phosphatidylinositol 3-kinase using a novel in vivo assay in yeast. *EMBO J.* 17:5374-5387.
- Jarrett, J.T., and P.T. Lansbury Jr. 1993. Seeding "one-dimensional crystallization" of amyloid: a pathogenic mechanism in Alzheimer's disease and scrapie? *Cell.* 73:1055-1058.
- Jeffrey, M., and G.A. Wells. 1988. Spongiform encephalopathy in a nyala (*Tragelaphus angasi*). *Vet. Pathol.* 25:398-399.
- Jeffrey, M., C.M. Goodsir, M.E. Bruce, P.A. McBRIDE, and J.R. Scott. 1994. Infection-specific Prion Protein (PrP) Accumulates on Neuronal Plasmalemma in Scrapie-infected Mice. *Annals of the New York Academy of Sciences.* 724:327-330.
- Johnson, R.T., and C.J. Gibbs Jr. 1998. Creutzfeldt-Jakob disease and related transmissible spongiform encephalopathies. *N. Engl. J. Med.* 339:1994-2004.
- Kabeya, Y., N. Mizushima, T. Ueno, A. Yamamoto, T. Kirisako, T. Noda, E. Kominami, Y. Ohsumi, and T. Yoshimori. 2000. LC3, a mammalian homologue of yeast Apg8p, is localized in autophagosome membranes after processing. *EMBO J.* 19:5720-5728.
- Kadiu, I., and H.E. Gendelman. 2011a. Macrophage bridging conduit trafficking of HIV-1 through the endoplasmic reticulum and Golgi network. *J. Proteome Res.* 10:3225-3238.
- Kadiu, I., and H.E. Gendelman. 2011b. Human Immunodeficiency Virus type 1 Endocytic Trafficking Through Macrophage Bridging Conduits Facilitates Spread of Infection. *J Neuroimmune Pharmacol.* 6:658-675.

- Kaneko, K., M. Vey, M. Scott, S. Pilkuhn, F.E. Cohen, and S.B. Prusiner. 1997. COOH-terminal sequence of the cellular prion protein directs subcellular trafficking and controls conversion into the scrapie isoform. *Proceedings of the National Academy of Sciences*. 94:2333 -2338.
- Kanu, N., Y. Imokawa, D.N. Drechsel, R.A. Williamson, C.R. Birkett, C.J. Bostock, and J.P. Brockes. 2002. Transfer of Scrapie Prion Infectivity by Cell Contact in Culture. *Current Biology*. 12:523-530.
- Kapasi, Z.F., G.F. Burton, L.D. Shultz, J.G. Tew, and A.K. Szakal. 1993. Induction of functional follicular dendritic cell development in severe combined immunodeficiency mice. Influence of B and T cells. *J. Immunol*. 150:2648-2658.
- Kimberlin, R.H., and R.F. Marsh. 1975. Comparison of scrapie and transmissible mink encephalopathy in hamsters. I. Biochemical studies of brain during development of disease. *J. Infect. Dis*. 131:97-103.
- Kimberlin, R.H., and C.A. Walker. 1989. Pathogenesis of scrapie in mice after intragastric infection. *Virus Res*. 12:213-220.
- Kimura, S., N. Fujita, T. Noda, and T. Yoshimori. 2009. Monitoring autophagy in mammalian cultured cells through the dynamics of LC3. *Meth. Enzymol*. 452:1-12.
- Kirkwood, J.K., G.A. Wells, J.W. Wilesmith, A.A. Cunningham, and S.I. Jackson. 1990. Spongiform encephalopathy in an arabian oryx (*Oryx leucoryx*) and a greater kudu (*Tragelaphus strepsiceros*). *Vet. Rec*. 127:418-420.
- Kitamoto, T., T. Muramoto, S. Mohri, K. Doh-Ura, and J. Tateishi. 1991. Abnormal isoform of prion protein accumulates in follicular dendritic cells in mice with Creutzfeldt-Jakob disease. *J. Virol*. 65:6292-6295.
- Klein, M.A., R. Frigg, E. Flechsig, A.J. Raeber, U. Kalinke, H. Bluethmann, F. Bootz, M. Suter, R.M. Zinkernagel, and A. Aguzzi. 1997. A crucial role for B cells in neuroinvasive scrapie. *Nature*. 390:687-690.
- Klein, M.A., P.S. Kaeser, P. Schwarz, H. Weyd, I. Xenarios, R.M. Zinkernagel, M.C. Carroll, J.S. Verbeek, M. Botto, M.J. Walport, H. Molina, U. Kalinke, H. Acha-Orbea, and A. Aguzzi. 2001. Complement facilitates early prion pathogenesis. *Nat. Med*. 7:488-492.
- Klingenstein, R., S. Löber, P. Kujala, S. Godsave, S.R. Leliveld, P. Gmeiner, P.J. Peters, and C. Korth. 2006. Tricyclic antidepressants, quinacrine and a novel, synthetic chimera thereof clear prions by destabilizing detergent-resistant membrane compartments. *J. Neurochem*. 98:748-759.

Klionsky, D.J., H. Abeliovich, P. Agostinis, D.K. Agrawal, G. Aliev, D.S. Askew, M. Baba, E.H. Baehrecke, B.A. Bahr, A. Ballabio, et al. 2008. Guidelines for the use and interpretation of assays for monitoring autophagy in higher eukaryotes. *Autophagy*. 4:151-175.

Kocisko, D.A., J.H. Come, S.A. Priola, B. Chesebro, G.J. Raymond, P.T. Lansbury, and B. Caughey. 1994. Cell-free formation of protease-resistant prion protein. *Nature*. 370:471-474.

Komatsu, M., S. Waguri, T. Chiba, S. Murata, J.-ichi Iwata, I. Tanida, T. Ueno, M. Koike, Y. Uchiyama, E. Kominami, and K. Tanaka. 2006. Loss of autophagy in the central nervous system causes neurodegeneration in mice. *Nature*. 441:880-884.

Kooyman, D.L., G.W. Byrne, S. McClellan, D. Nielsen, M. Tone, H. Waldmann, T.M. Coffman, K.R. McCurry, J.L. Platt, and J.S. Logan. 1995. In vivo transfer of GPI-linked complement restriction factors from erythrocytes to the endothelium. *Science*. 269:89-92.

Kovacs, G.G., and H. Budka. 2008. Prion diseases: from protein to cell pathology. *Am. J. Pathol.* 172:555-565.

Kuwahara, C., A.M. Takeuchi, T. Nishimura, K. Haraguchi, A. Kubosaki, Y. Matsumoto, K. Saeki, Y. Matsumoto, T. Yokoyama, S. Itohara, and T. Onodera. 1999. Prions prevent neuronal cell-line death. *Nature*. 400:225-226.

Langevin, C., K. Gousset, M. Costanzo, O. Richard-Le Goff, and C. Zurzolo. 2010. Characterization of the role of dendritic cells in prion transfer to primary neurons. *Biochemical Journal*. 431:189-198.

Lawson, V.A., S.A. Priola, K. Wehrly, and B. Chesebro. 2001. N-terminal Truncation of Prion Protein Affects Both Formation and Conformation of Abnormal Protease-resistant Prion Protein Generated in Vitro. *Journal of Biological Chemistry*. 276:35265 -35271.

Legler, D.F., M.-A. Doucey, P. Schneider, L. Chapatte, F.C. Bender, and C. Bron. 2005. Differential insertion of GPI-anchored GFPs into lipid rafts of live cells. *FASEB J*. 19:73-75.

Levine, B., and D.J. Klionsky. 2004. Development by Self-Digestion Molecular Mechanisms and Biological Functions of Autophagy. *Developmental Cell*. 6:463-477.

Lewis, P.A., F. Properzi, K. Prodromidou, A.R. Clarke, J. Collinge, and G.S. Jackson. 2006. Removal of the glycosylphosphatidylinositol anchor from PrP<sup>Sc</sup> by cathepsin D does not reduce prion infectivity. *Biochem J*. 395:443-448.

- Lewis, V., and N.M. Hooper. 2011. The role of lipid rafts in prion protein biology. *Front. Biosci.* 16:151-168.
- Li, A., H.M. Christensen, L.R. Stewart, K.A. Roth, R. Chiesa, and D.A. Harris. 2007. Neonatal lethality in transgenic mice expressing prion protein with a deletion of residues 105-125. *EMBO J.* 26:548-558.
- Li, X., C.-E. Wang, S. Huang, X. Xu, X.-J. Li, H. Li, and S. Li. 2010. Inhibiting the ubiquitin-proteasome system leads to preferential accumulation of toxic N-terminal mutant huntingtin fragments. *Human Molecular Genetics.* 19:2445 - 2455.
- Liang, Y., A. Wang, I.A. Belyantseva, D.W. Anderson, F.J. Probst, T.D. Barber, W. Miller, J.W. Touchman, L. Jin, S.L. Sullivan, J.R. Sellers, S.A. Camper, R.V. Lloyd, B. Kachar, T.B. Friedman, and R.A. Fridell. 1999. Characterization of the human and mouse unconventional myosin XV genes responsible for hereditary deafness DFNB3 and shaker 2. *Genomics.* 61:243-258.
- Liberski, P.P., and M. Jeffrey. 2004. Tubulovesicular structures--the ultrastructural hallmark for transmissible spongiform encephalopathies or prion diseases. *Folia Neuropathol.* 42 Suppl B:96-108.
- Liberski, P.P., D.R. Brown, B. Sikorska, B. Caughey, and P. Brown. 2008. Cell death and autophagy in prion diseases (transmissible spongiform encephalopathies). *Folia Neuropathol.* 46:1-25.
- Liu, T., R. Li, T. Pan, D. Liu, R.B. Petersen, B.-S. Wong, P. Gambetti, and M.S. Sy. 2002. Intercellular transfer of the cellular prion protein. *J. Biol. Chem.* 277:47671-47678.
- Ludlam, C.A., and M.L. Turner. 2006. Managing the risk of transmission of variant Creutzfeldt Jakob disease by blood products. *Br. J. Haematol.* 132:13-24.
- Lugaresi, E., R. Medori, P. Montagna, A. Baruzzi, P. Cortelli, A. Lugaresi, P. Tinuper, M. Zucconi, and P. Gambetti. 1986. Fatal familial insomnia and dysautonomia with selective degeneration of thalamic nuclei. *N. Engl. J. Med.* 315:997-1003.
- Lupas, A., M. Van Dyke, and J. Stock. 1991. Predicting coiled coils from protein sequences. *Science.* 252:1162-1164.
- Ma, J., R. Wollmann, and S. Lindquist. 2002. Neurotoxicity and Neurodegeneration When PrP Accumulates in the Cytosol. *Science.* 298:1781 - 1785.

Mabbott, N.A., M.E. Bruce, M. Botto, M.J. Walport, and M.B. Pepys. 2001. Temporary depletion of complement component C3 or genetic deficiency of C1q significantly delays onset of scrapie. *Nat. Med.* 7:485-487.

Mabbott, N.A., J. Young, I. McConnell, and M.E. Bruce. 2003. Follicular dendritic cell dedifferentiation by treatment with an inhibitor of the lymphotoxin pathway dramatically reduces scrapie susceptibility. *J. Virol.* 77:6845-6854.

Magalhães, A.C., J.A. Silva, K.S. Lee, V.R. Martins, V.F. Prado, S.S.G. Ferguson, M.V. Gomez, R.R. Brentani, and M.A.M. Prado. 2002. Endocytic Intermediates Involved with the Intracellular Trafficking of a Fluorescent Cellular Prion Protein. *Journal of Biological Chemistry.* 277:33311 -33318.

Maignien, T., C.I. Lasmézas, V. Beringue, D. Dormont, and J.P. Deslys. 1999. Pathogenesis of the oral route of infection of mice with scrapie and bovine spongiform encephalopathy agents. *J. Gen. Virol.* 80 ( Pt 11):3035-3042.

Málaga-Trillo, E., G.P. Solis, Y. Schrock, C. Geiss, L. Luncz, V. Thomanetz, and C.A.O. Stuermer. 2009. Regulation of Embryonic Cell Adhesion by the Prion Protein. *PLoS Biol.* 7:e1000055.

Mallavarapu, A., and T. Mitchison. 1999. Regulated Actin Cytoskeleton Assembly at Filopodium Tips Controls Their Extension and Retraction. *The Journal of Cell Biology.* 146:1097 -1106.

Mallucci, G., A. Dickinson, J. Linehan, P.-C. Klöhn, S. Brandner, and J. Collinge. 2003. Depleting Neuronal PrP in Prion Infection Prevents Disease and Reverses Spongiosis. *Science.* 302:871 -874.

Mann, S.S., and J.A. Hammarback. 1994. Molecular characterization of light chain 3. A microtubule binding subunit of MAP1A and MAP1B. *Journal of Biological Chemistry.* 269:11492 -11497.

Manson, J.C., A.R. Clarke, M.L. Hooper, L. Aitchison, I. McConnell, and J. Hope. 1994. 129/Ola mice carrying a null mutation in PrP that abolishes mRNA production are developmentally normal. *Mol. Neurobiol.* 8:121-127.

Manuelidis, L. 2003. Transmissible Encephalopathies: Speculations and Realities. *Viral Immunology.* 16:123-139.

Marijanovic, Z., A. Caputo, V. Campana, and C. Zurzolo. 2009. Identification of an intracellular site of prion conversion. *PLoS Pathog.* 5:e1000426.

Marsh, R.F., R.A. Bessen, S. Lehmann, and G.R. Hartsough. 1991. Epidemiological and experimental studies on a new incident of transmissible mink encephalopathy. *J. Gen. Virol.* 72 ( Pt 3):589-594.

Martinez-Vicente, M., Z. Tallochy, E. Wong, G. Tang, H. Koga, S. Kaushik, R. de Vries, E. Arias, S. Harris, D. Sulzer, and A.M. Cuervo. 2010. Cargo recognition failure is responsible for inefficient autophagy in Huntington's disease. *Nat Neurosci.* 13:567-576.

MASTERS, C.L., D.C. GAJDUSEK, and C.J. GIBBS. 1981. CREUTZFELDT-JAKOB DISEASE VIRUS ISOLATIONS FROM THE GERSTMANN-STRÄUSSLER SYNDROME. *Brain.* 104:559 -588.

Mattei, V., M.G. Barenco, V. Tasciotti, T. Garofalo, A. Longo, K. Boller, J. Löwer, R. Misasi, F. Montrasio, and M. Sorice. 2009. Paracrine diffusion of PrP(C) and propagation of prion infectivity by plasma membrane-derived microvesicles. *PLoS ONE.* 4:e5057.

Mattila, P.K., and P. Lappalainen. 2008. Filopodia: molecular architecture and cellular functions. *Nat. Rev. Mol. Cell Biol.* 9:446-454.

Maxfield, F.R., and T.E. McGraw. 2004. Endocytic recycling. *Nat. Rev. Mol. Cell Biol.* 5:121-132.

Maxfield, F.R., and I. Tabas. 2005. Role of cholesterol and lipid organization in disease. *Nature.* 438:612-621.

McBride, P.A., W.J. Schulz-Schaeffer, M. Donaldson, M. Bruce, H. Diringer, H.A. Kretzschmar, and M. Beekes. 2001. Early Spread of Scrapie from the Gastrointestinal Tract to the Central Nervous System Involves Autonomic Fibers of the Splanchnic and Vagus Nerves. *J. Virol.* 75:9320-9327.

McKinley, M.P., A. Taraboulos, L. Kenaga, D. Serban, A. Stieber, S.J. DeArmond, S.B. Prusiner, and N. Gonatas. 1991. Ultrastructural localization of scrapie prion proteins in cytoplasmic vesicles of infected cultured cells. *Lab. Invest.* 65:622-630.

McKnight, S., and R. Tjian. 1986. Transcriptional selectivity of viral genes in mammalian cells. *Cell.* 46:795-805.

de Medina, P., M.R. Paillasse, G. Ségala, F. Khallouki, S. Brillouet, F. Dalenc, F. Courbon, M. Record, M. Poirot, and S. Silvente-Poirot. 2011. Importance of cholesterol and oxysterols metabolism in the pharmacology of tamoxifen and other AEBs ligands. *Chem. Phys. Lipids.* 164:432-437.

de Medina, P., B.L. Payré, J. Bernad, I. Bossier, B. Pipy, S. Silvente-Poirot, G. Favre, J.-C. Faye, and M. Poirot. 2004. Tamoxifen Is a Potent Inhibitor of Cholesterol Esterification and Prevents the Formation of Foam Cells. *Journal of Pharmacology and Experimental Therapeutics.* 308:1165 -1173.

- de Medina, P., S. Silvente-Poirot, and M. Poirot. 2009. Tamoxifen and AEBS ligands induced apoptosis and autophagy in breast cancer cells through the stimulation of sterol accumulation. *Autophagy*. 5:1066-1067.
- Meier, P., N. Genoud, M. Prinz, M. Maissen, T. Rülcke, A. Zurbriggen, A.J. Raeber, and A. Aguzzi. 2003. Soluble dimeric prion protein binds PrP(Sc) in vivo and antagonizes prion disease. *Cell*. 113:49-60.
- Merz, P.A., R.A. Somerville, H.M. Wisniewski, and K. Iqbal. 1981. Abnormal fibrils from scrapie-infected brain. *Acta Neuropathologica*. 54:63-74.
- Mijaljica, D., M. Prescott, and R.J. Devenish. 2011. Microautophagy in mammalian cells: Revisiting a 40-year-old conundrum. *Autophagy*. 7:673-682.
- Milhavet, O., and S. Lehmann. 2002. Oxidative stress and the prion protein in transmissible spongiform encephalopathies. *Brain Res. Brain Res. Rev.* 38:328-339.
- Mironov, A., D. Latawiec, H. Wille, E. Bouzamondo-Bernstein, G. Legname, R.A. Williamson, D. Burton, S.J. DeArmond, S.B. Prusiner, and P.J. Peters. 2003. Cytosolic Prion Protein in Neurons. *The Journal of Neuroscience*. 23:7183 - 7193.
- Mizushima, N., and T. Yoshimori. 2007. How to interpret LC3 immunoblotting. *Autophagy*. 3:542-545.
- Mizushima, N., B. Levine, A.M. Cuervo, and D.J. Klionsky. 2008. Autophagy fights disease through cellular self-digestion. *Nature*. 451:1069-1075.
- Montrasio, F., R. Frigg, M. Glatzel, M.A. Klein, F. Mackay, A. Aguzzi, and C. Weissmann. 2000. Impaired prion replication in spleens of mice lacking functional follicular dendritic cells. *Science*. 288:1257-1259.
- Moore, R.C., I.Y. Lee, G.L. Silverman, P.M. Harrison, R. Strome, C. Heinrich, A. Karunaratne, S.H. Pasternak, M.A. Chishti, Y. Liang, P. Mastrangelo, K. Wang, A.F. Smit, S. Katamine, G.A. Carlson, F.E. Cohen, S.B. Prusiner, D.W. Melton, P. Tremblay, L.E. Hood, and D. Westaway. 1999. Ataxia in prion protein (PrP)-deficient mice is associated with upregulation of the novel PrP-like protein doppel. *J. Mol. Biol.* 292:797-817.
- Mouillet-Richard, S., M. Ermonval, C. Chebassier, J.L. Laplanche, S. Lehmann, J.M. Launay, and O. Kellermann. 2000. Signal Transduction Through Prion Protein. *Science*. 289:1925 -1928.
- Mousavi, S.A., R. Kjekens, T.O. Berg, P.O. Seglen, T. Berg, and A. Brech. 2001. Effects of inhibitors of the vacuolar proton pump on hepatic heterophagy and autophagy. *Biochimica et Biophysica Acta (BBA) - Biomembranes*. 1510:243-257.

Naslavsky, N., R. Stein, A. Yanai, G. Friedlander, and A. Taraboulos. 1997a. Characterization of Detergent-insoluble Complexes Containing the Cellular Prion Protein and Its Scrapie Isoform. *Journal of Biological Chemistry*. 272:6324 -6331.

Naslavsky, N., R. Stein, A. Yanai, G. Friedlander, and A. Taraboulos. 1997b. Characterization of Detergent-insoluble Complexes Containing the Cellular Prion Protein and Its Scrapie Isoform. *Journal of Biological Chemistry*. 272:6324 -6331.

Nathanson, N., J. Wilesmith, and C. Griot. 1997. Bovine Spongiform Encephalopathy (BSE): Causes and Consequences of a Common Source Epidemic. *American Journal of Epidemiology*. 145:959 -969.

Neutra, M.R., A. Frey, and J.P. Kraehenbuhl. 1996. Epithelial M cells: gateways for mucosal infection and immunization. *Cell*. 86:345-348.

Nicolas, O., R. Gavín, and J.A. del Río. 2009. New insights into cellular prion protein (PrP<sup>c</sup>) functions: the “ying and yang” of a relevant protein. *Brain Res Rev*. 61:170-184.

Noda, T., and Y. Ohsumi. 1998. Tor, a Phosphatidylinositol Kinase Homologue, Controls Autophagy in Yeast. *Journal of Biological Chemistry*. 273:3963 -3966.

Nunziante, M., K. Ackermann, K. Dietrich, H. Wolf, L. Gädtke, S. Gilch, I. Vorberg, M. Groschup, and H.M. Schätzl. 2011. Proteasomal dysfunction and endoplasmic reticulum stress enhance trafficking of prion protein aggregates through the secretory pathway and increase accumulation of pathologic prion protein. *J. Biol. Chem*. 286:33942-33953.

Oesch, B., D. Westaway, M. Wälchli, M.P. McKinley, S.B. Kent, R. Aebersold, R.A. Barry, P. Tempst, D.B. Teplow, and L.E. Hood. 1985. A cellular gene encodes scrapie PrP 27-30 protein. *Cell*. 40:735-746.

Oldstone, M.B.A., R. Race, D. Thomas, H. Lewicki, D. Homann, S. Smelt, A. Holz, P. Koni, D. Lo, B. Chesebro, and R. Flavell. 2002. Lymphotoxin-alpha- and lymphotoxin-beta-deficient mice differ in susceptibility to scrapie: evidence against dendritic cell involvement in neuroinvasion. *J. Virol*. 76:4357-4363.

Oliver, T.N., J.S. Berg, and R.E. Cheney. 1999. Tails of unconventional myosins. *Cell. Mol. Life Sci*. 56:243-257.

Onfelt, B., S. Nedvetzki, R.K.P. Benninger, M.A. Purbhoo, S. Sowinski, A.N. Hume, M.C. Seabra, M.A.A. Neil, P.M.W. French, and D.M. Davis. 2006. Structurally distinct membrane nanotubes between human macrophages support long-distance vesicular traffic or surfing of bacteria. *J. Immunol*. 177:8476-8483.

- Onfelt, B., S. Nedvetzki, K. Yanagi, and D.M. Davis. 2004. Cutting edge: Membrane nanotubes connect immune cells. *J. Immunol.* 173:1511-1513.
- Owen, F., M. Poulter, R. Lofthouse, J. Collinge, T.J. Crow, D. Risby, H.F. Baker, R.M. Ridley, K. Hsiao, and S.B. Prusiner. 1989. Insertion in prion protein gene in familial Creutzfeldt-Jakob disease. *Lancet.* 1:51-52.
- Pan, K.M., M. Baldwin, J. Nguyen, M. Gasset, A. Serban, D. Groth, I. Mehlhorn, Z. Huang, R.J. Fletterick, and F.E. Cohen. 1993a. Conversion of alpha-helices into beta-sheets features in the formation of the scrapie prion proteins. *Proc Natl Acad Sci U S A.* 90:10962-10966.
- Pan, K.M., M. Baldwin, J. Nguyen, M. Gasset, A. Serban, D. Groth, I. Mehlhorn, Z. Huang, R.J. Fletterick, and F.E. Cohen. 1993b. Conversion of alpha-helices into beta-sheets features in the formation of the scrapie prion proteins. *Proc Natl Acad Sci U S A.* 90:10962-10966.
- Paquet, S., C. Langevin, J. Chapuis, G.S. Jackson, H. Laude, and D. Vilette. 2007. Efficient dissemination of prions through preferential transmission to nearby cells. *Journal of General Virology.* 88:706 -713.
- Parchi, P., A. Giese, S. Capellari, P. Brown, W. Schulz-Schaeffer, O. Windl, I. Zerr, H. Budka, N. Kopp, P. Piccardo, S. Poser, A. Rojiani, N. Streichemberger, J. Julien, C. Vital, B. Ghetti, P. Gambetti, and H. Kretzschmar. 1999. Classification of sporadic Creutzfeldt-Jakob disease based on molecular and phenotypic analysis of 300 subjects. *Ann. Neurol.* 46:224-233.
- Parizek, P., C. Roeckl, J. Weber, E. Flechsig, A. Aguzzi, and A.J. Raeber. 2001. Similar Turnover and Shedding of the Cellular Prion Protein in Primary Lymphoid and Neuronal Cells. *Journal of Biological Chemistry.* 276:44627 -44632.
- Parkyn, C.J., E.G.M. Vermeulen, R.C. Mootoosamy, C. Sunyach, C. Jacobsen, C. Oxvig, S. Moestrup, Q. Liu, G. Bu, A. Jen, and R.J. Morris. 2008. LRP1 controls biosynthetic and endocytic trafficking of neuronal prion protein. *J. Cell. Sci.* 121:773-783.
- Parry, H.B. 1979. Elimination of natural scrapie in sheep by sire genotype selection. *Nature.* 277:127-129.
- PATTISON, I.H., and G.C. MILLSON. 1961. Scrapie produced experimentally in goats with special reference to the clinical syndrome. *J. Comp. Pathol.* 71:101-109.
- Pauly, P.C., and D.A. Harris. 1998. Copper stimulates endocytosis of the prion protein. *J. Biol. Chem.* 273:33107-33110.

- Pearson, M.A., D. Reczek, A. Bretscher, and P.A. Karplus. 2000. Structure of the ERM protein moesin reveals the FERM domain fold masked by an extended actin binding tail domain. *Cell*. 101:259-270.
- Peters, P.J., A. Mironov, D. Peretz, E. van Donselaar, E. Leclerc, S. Erpel, S.J. DeArmond, D.R. Burton, R.A. Williamson, M. Vey, and S.B. Prusiner. 2003. Trafficking of prion proteins through a caveolae-mediated endosomal pathway. *The Journal of Cell Biology*. 162:703 -717.
- Pimpinelli, F., S. Lehmann, and I. Maridonneau-Parini. 2005. The scrapie prion protein is present in flotillin-1-positive vesicles in central- but not peripheral-derived neuronal cell lines. *Eur. J. Neurosci*. 21:2063-2072.
- Plantard, L., A. Arjonen, J.G. Lock, G. Nurani, J. Ivaska, and S. Strömlad. 2010. PtdIns(3,4,5)P<sub>3</sub> is a regulator of myosin-X localization and filopodia formation. *J. Cell. Sci*. 123:3525-3534.
- Plotnikov, E.Y., T.G. Khryapenkova, S.I. Galkina, G.T. Sukhikh, and D.B. Zorov. 2010. Cytoplasm and organelle transfer between mesenchymal multipotent stromal cells and renal tubular cells in co-culture. *Exp. Cell Res*. 316:2447-2455.
- Prusiner, S.B. 1982. Novel proteinaceous infectious particles cause scrapie. *Science*. 216:136-144.
- Prusiner, S.B. 1998. Prions. *Proc Natl Acad Sci U S A*. 95:13363-13383.
- Prusiner, S.B., M.P. McKinley, K.A. Bowman, D.C. Bolton, P.E. Bendheim, D.F. Groth, and G.G. Glenner. 1983. Scrapie prions aggregate to form amyloid-like birefringent rods. *Cell*. 35:349-358.
- Prusiner, S.B., M. Scott, D. Foster, K.M. Pan, D. Groth, C. Mirinda, M. Torchia, S.L. Yang, D. Serban, and G.A. Carlson. 1990a. Transgenic studies implicate interactions between homologous PrP isoforms in scrapie prion replication. *Cell*. 63:673-686.
- Prusiner, S.B., M. Scott, D. Foster, K.M. Pan, D. Groth, C. Mirinda, M. Torchia, S.L. Yang, D. Serban, and G.A. Carlson. 1990b. Transgenic studies implicate interactions between homologous PrP isoforms in scrapie prion replication. *Cell*. 63:673-686.
- Qi, Y., J.K.T. Wang, M. McMillan, and D.M. Chikaraishi. 1997. Characterization of a CNS Cell Line, CAD, in which Morphological Differentiation Is Initiated by Serum Deprivation. *The Journal of Neuroscience*. 17:1217 -1225.
- Race, R., K. Meade-White, A. Raines, G.J. Raymond, B. Caughey, and B. Chesebro. 2002. Subclinical scrapie infection in a resistant species:

persistence, replication, and adaptation of infectivity during four passages. *J. Infect. Dis.* 186 Suppl 2:S166-170.

Race, R., M. Oldstone, and B. Chesebro. 2000. Entry versus blockade of brain infection following oral or intraperitoneal scrapie administration: role of prion protein expression in peripheral nerves and spleen. *J. Virol.* 74:828-833.

Ratajczak, J., M. Wysoczynski, F. Hayek, A. Janowska-Wieczorek, and M.Z. Ratajczak. 2006. Membrane-derived microvesicles: important and underappreciated mediators of cell-to-cell communication. *Leukemia.* 20:1487-1495.

Raymond, C.R., P. Aucouturier, and N.A. Mabbott. 2007. In vivo depletion of CD11c+ cells impairs scrapie agent neuroinvasion from the intestine. *J. Immunol.* 179:7758-7766.

Reggiori, F., and D.J. Klionsky. 2002. Autophagy in the Eukaryotic Cell. *Eukaryot Cell.* 1:11-21.

Rescigno, M., M. Urbano, B. Valzasina, M. Francolini, G. Rotta, R. Bonasio, F. Granucci, J.-P. Kraehenbuhl, and P. Ricciardi-Castagnoli. 2001. Dendritic cells express tight junction proteins and penetrate gut epithelial monolayers to sample bacteria. *Nat Immunol.* 2:361-367.

Riesner, D. 2003. Biochemistry and structure of PrPC and PrPSc. *British Medical Bulletin.* 66:21 -33.

Rubinsztein, D.C., J.E. Gestwicki, L.O. Murphy, and D.J. Klionsky. 2007a. Potential therapeutic applications of autophagy. *Nat Rev Drug Discov.* 6:304-312.

Rubinsztein, D.C., J.E. Gestwicki, L.O. Murphy, and D.J. Klionsky. 2007b. Potential therapeutic applications of autophagy. *Nat Rev Drug Discov.* 6:304-312.

Rustom, A., R. Saffrich, I. Markovic, P. Walther, and H.-H. Gerdes. 2004. Nanotubular highways for intercellular organelle transport. *Science.* 303:1007-1010.

Sakaguchi, S., S. Katamine, N. Nishida, R. Moriuchi, K. Shigematsu, T. Sugimoto, A. Nakatani, Y. Kataoka, T. Houtani, S. Shirabe, H. Okada, S. Hasegawa, T. Miyamoto, and T. Noda. 1996. Loss of cerebellar Purkinje cells in aged mice homozygous for a disrupted PrP gene. *Nature.* 380:528-531.

Sarnataro, D., V. Campana, S. Paladino, M. Stornaiuolo, L. Nitsch, and C. Zurzolo. 2004. PrPC Association with Lipid Rafts in the Early Secretory Pathway Stabilizes Its Cellular Conformation. *Mol Biol Cell.* 15:4031-4042.

- Schätzl, H.M., L. Laszlo, D.M. Holtzman, J. Tatzelt, S.J. DeArmond, R.I. Weiner, W.C. Mobley, and S.B. Prusiner. 1997. A hypothalamic neuronal cell line persistently infected with scrapie prions exhibits apoptosis. *J Virol.* 71:8821-8831.
- Schrock, Y., G.P. Solis, and C.A.O. Stuermer. 2009. Regulation of focal adhesion formation and filopodia extension by the cellular prion protein (PrPC). *FEBS Letters.* 583:389-393.
- Scott, M., D. Foster, C. Mirenda, D. Serban, F. Coufal, M. Wälchli, M. Torchia, D. Groth, G. Carlson, S.J. DeArmond, D. Westaway, and S.B. Prusiner. 1989. Transgenic mice expressing hamster prion protein produce species-specific scrapie infectivity and amyloid plaques. *Cell.* 59:847-857.
- Sellers, J.R. 2000. Myosins: a diverse superfamily. *Biochim. Biophys. Acta.* 1496:3-22.
- Shortman, K., and Y.-J. Liu. 2002. Mouse and human dendritic cell subtypes. *Nat Rev Immunol.* 2:151-161.
- Shyng, S.L., J.E. Heuser, and D.A. Harris. 1994. A glycolipid-anchored prion protein is endocytosed via clathrin-coated pits. *J. Cell Biol.* 125:1239-1250.
- Sigurdson, C.J., and M.W. Miller. 2003. Other animal prion diseases. *Br. Med. Bull.* 66:199-212.
- Sikorska, B., P.P. Liberski, P. Giraud, N. Kopp, and P. Brown. 2004. Autophagy is a part of ultrastructural synaptic pathology in Creutzfeldt-Jakob disease: a brain biopsy study. *The International Journal of Biochemistry & Cell Biology.* 36:2563-2573.
- Silveira, J.R., G.J. Raymond, A.G. Hughson, R.E. Race, V.L. Sim, S.F. Hayes, and B. Caughey. 2005. The most infectious prion protein particles. *Nature.* 437:257-261.
- Simons, M., and G. Raposo. 2009. Exosomes--vesicular carriers for intercellular communication. *Curr. Opin. Cell Biol.* 21:575-581.
- Singh, S.K., R. Kurfurst, C. Nizard, S. Schnebert, E. Perrier, and D.J. Tobin. 2010. Melanin transfer in human skin cells is mediated by filopodia—a model for homotypic and heterotypic lysosome-related organelle transfer. *The FASEB Journal.* 24:3756 -3769.
- Sklaviadis, T., R. Dreyer, and L. Manuelidis. 1992. Analysis of Creutzfeldt-Jakob disease infectious fractions by gel permeation chromatography and sedimentation field flow fractionation. *Virus Res.* 26:241-254.

- Smith, I.F., J. Shuai, and I. Parker. 2011. Active generation and propagation of Ca<sup>2+</sup> signals within tunneling membrane nanotubes. *Biophys. J.* 100:L37-39.
- Solforosi, L., J.R. Criado, D.B. McGavern, S. Wirz, M. Sánchez-Alavez, S. Sugama, L.A. DeGiorgio, B.T. Volpe, E. Wiseman, G. Abalos, E. Masliah, D. Gilden, M.B. Oldstone, B. Conti, and R.A. Williamson. 2004. Cross-linking cellular prion protein triggers neuronal apoptosis in vivo. *Science.* 303:1514-1516.
- Soto, C., L. Estrada, and J. Castilla. 2006. Amyloids, prions and the inherent infectious nature of misfolded protein aggregates. *Trends in Biochemical Sciences.* 31:150-155.
- Soto, C., G.P. Saborio, and L. Anderes. 2002. Cyclic amplification of protein misfolding: application to prion-related disorders and beyond. *Trends in Neurosciences.* 25:390-394.
- Sousa, A.D., and R.E. Cheney. 2005. Myosin-X: a molecular motor at the cell's fingertips. *Trends Cell Biol.* 15:533-539.
- Sousa, A.D., J.S. Berg, B.W. Robertson, R.B. Meeker, and R.E. Cheney. 2006. Myo10 in brain: developmental regulation, identification of a headless isoform and dynamics in neurons. *J. Cell. Sci.* 119:184-194.
- Sowinski, S., C. Jolly, O. Berninghausen, M.A. Purbhoo, A. Chauveau, K. Köhler, S. Oddos, P. Eissmann, F.M. Brodsky, C. Hopkins, B. Onfelt, Q. Sattentau, and D.M. Davis. 2008. Membrane nanotubes physically connect T cells over long distances presenting a novel route for HIV-1 transmission. *Nat. Cell Biol.* 10:211-219.
- Spero, M., and I. Lazibat. 2010. Creutzfeldt-Jakob disease: case report and review of the literature. *Acta Clin Croat.* 49:181-187.
- Spraker, T.R., R.R. Zink, B.A. Cummings, C.J. Sigurdson, M.W. Miller, and K.I. O'Rourke. 2002. Distribution of protease-resistant prion protein and spongiform encephalopathy in free-ranging mule deer (*Odocoileus hemionus*) with chronic wasting disease. *Vet. Pathol.* 39:546-556.
- Stahl, N., M.A. Baldwin, A.L. Burlingame, and S.B. Prusiner. 1990. Identification of glycoinositol phospholipid linked and truncated forms of the scrapie prion protein. *Biochemistry.* 29:8879-8884.
- Stahl, N., D.R. Borchelt, K. Hsiao, and S.B. Prusiner. 1987. Scrapie prion protein contains a phosphatidylinositol glycolipid. *Cell.* 51:229-240.
- Stekel, D.J., M.A. Nowak, and T.R.E. Southwood. 1996. Prediction of future BSE spread. *Nature.* 381:119.

Suárez, Y., C. Fernández, D. Gómez-Coronado, A.J. Ferruelo, A. Dávalos, J. Martínez-Botas, and M.A. Lasunción. 2004. Synergistic upregulation of low-density lipoprotein receptor activity by tamoxifen and lovastatin. *Cardiovasc. Res.* 64:346-355.

Sunyach, C., A. Jen, J. Deng, K.T. Fitzgerald, Y. Frobert, J. Grassi, M.W. McCaffrey, and R. Morris. 2003. The mechanism of internalization of glycosylphosphatidylinositol-anchored prion protein. *EMBO J.* 22:3591-3601.

Tagliavini, F., F. Prelli, M. Porro, M. Salmona, O. Bugiani, and B. Frangione. 1992. A soluble form of prion protein in human cerebrospinal fluid: implications for prion-related encephalopathies. *Biochem. Biophys. Res. Commun.* 184:1398-1404.

Tanabe, K., I. Bonilla, J.A. Winkles, and S.M. Strittmatter. 2003. Fibroblast growth factor-inducible-14 is induced in axotomized neurons and promotes neurite outgrowth. *J. Neurosci.* 23:9675-9686.

Taraboulos, A., M. Scott, A. Semenov, D. Avrahami, L. Laszlo, S.B. Prusiner, and D. Avraham. 1995a. Cholesterol depletion and modification of COOH-terminal targeting sequence of the prion protein inhibit formation of the scrapie isoform. *J. Cell Biol.* 129:121-132.

Taraboulos, A., M. Scott, A. Semenov, D. Avrahami, L. Laszlo, S.B. Prusiner, and D. Avraham. 1995b. Cholesterol depletion and modification of COOH-terminal targeting sequence of the prion protein inhibit formation of the scrapie isoform. *J. Cell Biol.* 129:121-132.

Taraboulos, A., D. Serban, and S.B. Prusiner. 1990. Scrapie prion proteins accumulate in the cytoplasm of persistently infected cultured cells. *J. Cell Biol.* 110:2117-2132.

Tateishi, J., T. Kitamoto, M.Z. Hoque, and H. Furukawa. 1996. Experimental transmission of Creutzfeldt-Jakob disease and related diseases to rodents. *Neurology.* 46:532 -537.

Tattum, M.H., S. Cohen-Krausz, A. Khalili-Shirazi, G.S. Jackson, E.V. Orlova, J. Collinge, A.R. Clarke, and H.R. Saibil. 2006. Elongated Oligomers Assemble into Mammalian PrP Amyloid Fibrils. *Journal of Molecular Biology.* 357:975-985.

Taylor, D.R., and N.M. Hooper. 2006. The prion protein and lipid rafts. *Mol. Membr. Biol.* 23:89-99.

Taylor, D.R., and N.M. Hooper. 2007. The low-density lipoprotein receptor-related protein 1 (LRP1) mediates the endocytosis of the cellular prion protein. *Biochem J.* 402:17-23.

Taylor, D.R., N.T. Watt, W.S.S. Perera, and N.M. Hooper. 2005. Assigning functions to distinct regions of the N-terminus of the prion protein that are involved in its copper-stimulated, clathrin-dependent endocytosis. *Journal of Cell Science*. 118:5141 -5153.

Taylor, D.R., I.J. Whitehouse, and N.M. Hooper. 2009. Glypican-1 Mediates Both Prion Protein Lipid Raft Association and Disease Isoform Formation. *PLoS Pathog*. 5:e1000666.

Telling, G.C., M. Scott, K.K. Hsiao, D. Foster, S.L. Yang, M. Torchia, K.C. Sidle, J. Collinge, S.J. DeArmond, and S.B. Prusiner. 1994. Transmission of Creutzfeldt-Jakob disease from humans to transgenic mice expressing chimeric human-mouse prion protein. *Proceedings of the National Academy of Sciences*. 91:9936 -9940.

Telling, G.C., M. Scott, J. Mastrianni, R. Gabizon, M. Torchia, F.E. Cohen, S.J. DeArmond, and S.B. Prusiner. 1995. Prion propagation in mice expressing human and chimeric PrP transgenes implicates the interaction of cellular PrP with another protein. *Cell*. 83:79-90.

Tokuo, H., and M. Ikebe. 2004. Myosin X transports Mena/VASP to the tip of filopodia. *Biochemical and Biophysical Research Communications*. 319:214-220.

Tooze, S.A., and T. Yoshimori. 2010. The origin of the autophagosomal membrane. *Nat Cell Biol*. 12:831-835.

Toyoshima, F., and E. Nishida. 2007. Integrin-mediated adhesion orients the spindle parallel to the substratum in an EB1- and myosin X-dependent manner. *EMBO J*. 26:1487-1498.

Turk, E., D.B. Teplow, L.E. Hood, and S.B. Prusiner. 1988. Purification and properties of the cellular and scrapie hamster prion proteins. *Eur. J. Biochem*. 176:21-30.

Umeki, N., H.S. Jung, T. Sakai, O. Sato, R. Ikebe, and M. Ikebe. 2011. Phospholipid-dependent regulation of the motor activity of myosin X. *Nat. Struct. Mol. Biol*. 18:783-788.

Vassallo, N., and J. Herms. 2003. Cellular prion protein function in copper homeostasis and redox signalling at the synapse. *J. Neurochem*. 86:538-544.

Veith, N.M., H. Plattner, C.A.O. Stuermer, W.J. Schulz-Schaeffer, and A. Bürkle. 2009. Immunolocalisation of PrP<sup>Sc</sup> in scrapie-infected N2a mouse neuroblastoma cells by light and electron microscopy. *Eur. J. Cell Biol*. 88:45-63.

- Vella, L.J., R.A. Sharples, V.A. Lawson, C.L. Masters, R. Cappai, and A.F. Hill. 2007. Packaging of prions into exosomes is associated with a novel pathway of PrP processing. *J. Pathol.* 211:582-590.
- Veranic, P., M. Lokar, G.J. Schütz, J. Weghuber, S. Wieser, H. Hägerstrand, V. Kralj-Iglic, and A. Iglic. 2008. Different types of cell-to-cell connections mediated by nanotubular structures. *Biophys. J.* 95:4416-4425.
- Vetrugno, V., A. Cardinale, I. Filesi, S. Mattei, M.-S. Sy, M. Pocchiari, and S. Biocca. 2005. KDEL-tagged anti-prion intrabodies impair PrP lysosomal degradation and inhibit scrapie infectivity. *Biochem. Biophys. Res. Commun.* 338:1791-1797.
- Vey, M., S. Pilkuhn, H. Wille, R. Nixon, S.J. DeArmond, E.J. Smart, R.G.W. Anderson, A. Taraboulos, and S.B. Prusiner. 1996. Subcellular colocalization of the cellular and scrapie prion proteins in caveolae-like membranous domains. *Proceedings of the National Academy of Sciences.* 93:14945 -14949.
- Wadsworth, J.D.F., E.A. Asante, M. Desbruslais, J.M. Linehan, S. Joiner, I. Gowland, J. Welch, L. Stone, S.E. Lloyd, A.F. Hill, S. Brandner, and J. Collinge. 2004. Human Prion Protein with Valine 129 Prevents Expression of Variant CJD Phenotype. *Science.* 306:1793 -1796.
- Walmsley, A.R., F. Zeng, and N.M. Hooper. 2003. The N-terminal Region of the Prion Protein Ectodomain Contains a Lipid Raft Targeting Determinant. *Journal of Biological Chemistry.* 278:37241 -37248.
- Wang, Y., J. Cui, X. Sun, and Y. Zhang. 2011. Tunneling-nanotube development in astrocytes depends on p53 activation. *Cell Death Differ.* 18:732-742.
- Warner, R.G., C. Hundt, S. Weiss, and J.E. Turnbull. 2002. Identification of the Heparan Sulfate Binding Sites in the Cellular Prion Protein. *Journal of Biological Chemistry.* 277:18421 -18430.
- Watkins, S.C., and R.D. Salter. 2005. Functional connectivity between immune cells mediated by tunneling nanotubules. *Immunity.* 23:309-318.
- Watt, N.T., and N.M. Hooper. 2003. The prion protein and neuronal zinc homeostasis. *Trends in Biochemical Sciences.* 28:406-410.
- Watts, J.C., and D. Westaway. 2007. The prion protein family: diversity, rivalry, and dysfunction. *Biochim. Biophys. Acta.* 1772:654-672.
- Weber, K.L., A.M. Sokac, J.S. Berg, R.E. Cheney, and W.M. Bement. 2004. A microtubule-binding myosin required for nuclear anchoring and spindle assembly. *Nature.* 431:325-329.

- Wei, Z., J. Yan, Q. Lu, L. Pan, and M. Zhang. 2011. Cargo recognition mechanism of myosin X revealed by the structure of its tail MyTH4-FERM tandem in complex with the DCC P3 domain. *Proc. Natl. Acad. Sci. U.S.A.* 108:3572-3577.
- Westaway, D., P.A. Goodman, C.A. Miranda, M.P. McKinley, G.A. Carlson, and S.B. Prusiner. 1987. Distinct prion proteins in short and long scrapie incubation period mice. *Cell.* 51:651-662.
- Wilesmith, J., J. Ryan, and M. Atkinson. 1991. Bovine spongiform encephalopathy: epidemiological studies on the origin. *Veterinary Record.* 128:199 -203.
- Will, R.G., J.W. Ironside, M. Zeidler, S.N. Cousens, K. Estibeiro, A. Alperovitch, S. Poser, M. Pocchiari, A. Hofman, and P.G. Smith. 1996a. A new variant of Creutzfeldt-Jakob disease in the UK. *Lancet.* 347:921-925.
- Will, R.G., J.W. Ironside, M. Zeidler, S.N. Cousens, K. Estibeiro, A. Alperovitch, S. Poser, M. Pocchiari, A. Hofman, and P.G. Smith. 1996b. A new variant of Creutzfeldt-Jakob disease in the UK. *Lancet.* 347:921-925.
- Williams, E.S., and M.W. Miller. 2002. Chronic wasting disease in deer and elk in North America. *Rev. - Off. Int. Epizoot.* 21:305-316.
- Williams, E.S., and M.W. Miller. 2003. Transmissible spongiform encephalopathies in non-domestic animals: origin, transmission and risk factors. *Rev. - Off. Int. Epizoot.* 22:145-156.
- Williams, E.S., and S. Young. 1980. Chronic wasting disease of captive mule deer: a spongiform encephalopathy. *J. Wildl. Dis.* 16:89-98.
- Wong, E., and A.M. Cuervo. 2010. Autophagy gone awry in neurodegenerative diseases. *Nat Neurosci.* 13:805-811.
- Woolner, S., L.L. O'Brien, C. Wiese, and W.M. Bement. 2008. Myosin-10 and actin filaments are essential for mitotic spindle function. *The Journal of Cell Biology.* 182:77 -88.
- Wüstner, D., A. Herrmann, M. Hao, and F.R. Maxfield. 2002. Rapid nonvesicular transport of sterol between the plasma membrane domains of polarized hepatic cells. *J. Biol. Chem.* 277:30325-30336.
- Wyatt, J.M., G.R. Pearson, T.N. Smerdon, T.J. Gruffydd-Jones, G.A. Wells, and J.W. Wilesmith. 1991. Naturally occurring scrapie-like spongiform encephalopathy in five domestic cats. *Vet. Rec.* 129:233-236.
- Xie, Z., and D.J. Klionsky. 2007. Autophagosome formation: core machinery and adaptations. *Nat Cell Biol.* 9:1102-1109.

- Yamamoto, A., Y. Tagawa, T. Yoshimori, Y. Moriyama, R. Masaki, and Y. Tashiro. 1998. Bafilomycin A1 Prevents Maturation of Autophagic Vacuoles by Inhibiting Fusion between Autophagosomes and Lysosomes in Rat Hepatoma Cell Line, H-4-II-E Cells. *Cell Structure and Function*. 23:33-42.
- Yang, Z., and D.J. Klionsky. 2009a. An overview of the molecular mechanism of autophagy. *Curr. Top. Microbiol. Immunol.* 335:1-32.
- Yang, Z., and D.J. Klionsky. 2009b. An overview of the molecular mechanism of autophagy. *Curr. Top. Microbiol. Immunol.* 335:1-32.
- Yasuda, K., A. Khandare, L. Burianovskyy, S. Maruyama, F. Zhang, A. Nasjletti, and M.S. Goligorsky. 2011. Tunneling nanotubes mediate rescue of prematurely senescent endothelial cells by endothelial progenitors: exchange of lysosomal pool. *Aging (Albany NY)*. 3:597-608.
- Yasuda, K., H.-C. Park, B. Ratliff, F. Addabbo, A.K. Hatzopoulos, P. Chander, and M.S. Goligorsky. 2010. Adriamycin Nephropathy. *Am J Pathol*. 176:1685-1695.
- Yedidia, Y., L. Horonchik, S. Tzaban, A. Yanai, and A. Taraboulos. 2001. Proteasomes and ubiquitin are involved in the turnover of the wild-type prion protein. *EMBO J*. 20:5383-5391.
- Zafar, S., N. von Ahsen, M. Oellerich, I. Zerr, W.J. Schulz-Schaeffer, V.W. Armstrong, and A.R. Asif. 2011. Proteomics approach to identify the interacting partners of cellular prion protein and characterization of Rab7a interaction in neuronal cells. *J. Proteome Res*. 10:3123-3135.
- Zerial, M., and H. McBride. 2001. Rab proteins as membrane organizers. *Nat. Rev. Mol. Cell Biol*. 2:107-117.
- Zhang, H., J.S. Berg, Z. Li, Y. Wang, P. Lång, A.D. Sousa, A. Bhaskar, R.E. Cheney, and S. Strömblad. 2004. Myosin-X provides a motor-based link between integrins and the cytoskeleton. *Nat. Cell Biol*. 6:523-531.
- Zhu, X.-J., C.-Z. Wang, P.-G. Dai, Y. Xie, N.-N. Song, Y. Liu, Q.-S. Du, L. Mei, Y.-Q. Ding, and W.-C. Xiong. 2007. Myosin X regulates netrin receptors and functions in axonal path-finding. *Nat Cell Biol*. 9:184-192.

## ANNEXE 2:

Review in preparation for “Frontiers in Membrane Physiology and Biophysics”

### **Multifaceted role of tunneling nanotubes in intercellular communications**

Karine Gousset<sup>§1</sup>, Ludovica Marzo<sup>§1,2</sup> and Chiara Zurzolo<sup>1,2</sup>

1, Institut Pasteur, Unité de trafic membranaire et pathogenèse, 25 rue du docteur roux, 75015 Paris;

2, Dipartimento di Biologia e Patologia Cellulare e Molecolare, Università Federico II, Napoli, Italy

\*Corresponding author:

Chiara Zurzolo, Unité de trafic membranaire et pathogenèse

Institut Pasteur, 25 rue du docteur Roux

75074 Paris CEDEX 15, Paris, France

tel: +33145688277

fax: +33140613238;

[chiara.zurzolo@pasteur.fr](mailto:chiara.zurzolo@pasteur.fr)

<sup>§</sup> These authors contributed equally to this work

## **Abstract**

Cell-to-cell communication and exchanges of materials are vital processes in multicellular organisms during cell development, cell repair and cell survival. In neuronal and immunological cells, intercellular transmission between neighboring cells occurs via different complex junctions or synapses. Recently, long distance intercellular connections in mammalian cells called tunneling nanotubes (TNTs) have been described. These structures have been found in numerous cell types and shown to transfer signals and cytosolic materials between distant cells suggesting that they might play a prominent role in intercellular trafficking. However, these cellular connections are very heterogeneous in both structure and function, giving rise to more questions than answers as to their nature and role as intercellular conduits. To better understand and characterize the functions of TNTs, we have highlighted here the latest discoveries regarding the formation, structure and the role of TNTs in cell-to-cell spreading of various signals and materials. We first gathered information regarding their formation with an emphasis on the triggering mechanisms observed, such as stress and potentially important proteins and/or signaling pathways. We then describe the various types of transfer mechanisms, in relation to signals and cargoes that have been shown recently to take advantage of these structures for intercellular transfer. Because a number of pathogens were shown to use these membrane bridges to spread between cells we also draw attention to specific studies that point toward a role for TNTs in pathogen spreading. In particular we discuss the possible role that TNTs might play in prion spreading, and speculate on their role in neurological diseases in general.

## **Introduction**

The ability of cells to communicate with each other is essential for the life of a multicellular organism and is evolutionarily conserved between species (Alberts book ref). Without cell-to-cell communication, processes such as remodeling of tissues and organs, differentiation during development, growth, cell division and responses to stimuli could not take place. Therefore, a great number of cellular genes and their products are implicated in intercellular communication and their deregulation leads to the establishment of pathological conditions associated with many diseases (ref).

Chemical signaling by secretion of small molecules towards distant cells is the classical form of cell-to-cell communication and do not involve physical contact. It includes chemical mediators with a paracrine effect on cells nearby (ref), release of synaptic vesicles containing neurotransmitters between neurons (chemical synapses) (ref) and hormones, which travel in the blood stream after their release and can reach and stimulate distant target cells (ref).

In cases of close proximity, cells can interact with each other through gap junctions or synapses. Gap junctions connect the cytoplasm of two neighboring cells by clustering tens to thousands of intercellular channels, allowing the transfer of small, hydrosoluble molecules (Maeda and Tsukihara 2011). They

mediate electrical and metabolic coupling of cells and are implicated in a wide range of biological processes such as muscle contraction (ref) or electrical synapses in neurons (ref). Immunological synapses, established at the interface between a T-cell and an antigen-presenting cell (APC), are rather mediated by membrane receptors (Rechavi et al 2007, Tarakanov and Goncharova 2009) and are essential for the adaptive immune response (Dustin et al 2010; Thauland and Parker 2010). Structurally similar to the immunological synapse are the virological synapses. These supramolecular structures are cytoskeleton-dependent adhesive junctions induced by virus-infected cells and used by these pathogens to directly transfer to non-infected cells (Jolly and Sattentau 2004). Human immunodeficiency virus type 1 (HIV-1) and human T-cell leukemia virus type 1 (HTLV-1) can spread using virological synapses between T-cells (Tarakanov and Goncharova 2009).

Recently, long-range forms of intercellular communication consisting of different types of membrane bridges have been described in a wide variety of cell types in *in vitro* cell culture systems (ref). Similar connections have also been found *in vivo* (Wolpert and Gustafson 1961; Ramirez and Kornberg 1999; Miller et al 2004; Demontis et al 2007; Chinnery et al 2008). The discovery of these new types of communication highways has opened up new ways of viewing how cells interact with one another, leading to the reconsideration of the traditional view of the cell as a basic unit of structure, function and organization originally postulated by Schleiden and Schwann (1839).

Tunneling nanotubes (TNTs), initially described by *Rustom* and co-workers (2004), are long thin actin-containing bridges connecting PC12 cells in culture that do not contact the substratum, extending up to 100  $\mu\text{m}$  in length with diameters ranging from 50-200 nm. Since then, TNTs have been found in many cell types in culture, from immune to neuronal cells and primary cells, acting as conduits for cytosolic and membrane-bound molecules, organelles and spreading of pathogens (ref).

Filopodial bridges, also called viral cytonemes for their similarity with cytonemes, filopodial protrusions described in *Drosophila* imaginal discs (Ramirez and Kornberg 1999), are instead cellular extensions observed in different cell types (ie: Cos-1, HEK293, DFJ8, XC cells) and induced by some retroviruses before their entry into the cell (Sherer et al 2007). It has been shown that murine leukemia virus (MLV) and HIV-1 can be unidirectionally transported on the surface of these structures, using them for cell-cell transmission and spreading (Lehmann et al 2005; Sherer et al 2007; Mothes et al 2010). Vesicular clusters containing VP16, a structural protein of herpes simplex virus (HSV), and US3 kinase of the pseudorabies virus have been found in similar cellular projections, mainly at the contact site with neighboring cells, respectively in Vero cells (La Boissiere et al 2004) and RK13 cells (Favoreel et al 2005).

In addition, *Zani* and colleagues (2010a) have described two different types of cellular bridges (I and II), called epithelial bridges (EP bridges) that connect primary human bronchial epithelial cells. Differently from TNTs, EP bridges are more stable, longer (from 25 $\mu\text{m}$  up to 1 mm) and with a diameter ranging from 1 to 20  $\mu\text{m}$ . Structurally, they contain both F-actin and microtubules, like a type of TNTs found in primary human macrophages (Onfelt et al 2006), rat cardiac myoblast cells (He et al 2010) and cardiomyocytes/cardiofibroblasts co-culture

systems (He et al 2011). While type I EP bridges seamlessly allow the bi-directional transfer of different cellular components (e.g., lysosomes and Golgi), the type II structures might represent a new way of cell migration since it can transfer an entire cell from one multi-cellular EP island another (Zani et al 2010b).

The discovery of mammalian bridges is more recent compared to plant conduits, called plasmodesmata (PDs), because they are more fragile and more difficult to observe. For example, they are sensitive to prolonged light excitation, mechanical stress and chemical fixation and are close to the optical limit of resolution (Hurtig et al 2010). PDs share some structural characteristics with TNTs. They are thin membrane structures with a diameter around 50 nm but are shorter than TNTs as their length is determined by the thickness of the cell walls between neighboring cells (Rustom 2009). Moreover, PDs allow an actin-mediated transfer of small molecules, transcription factors and also spreading of viruses, creating a sort of continuity between symplasts of connected cells (Lucas et al 2009). Even more similarities between the mammalian TNTs and the plant PDs are found regarding the mechanisms of formation and transfer (e.g., passive diffusion of small molecules and gated-mechanisms for bigger components) although the nature of the transported molecules can vary (Rustom 2009). This highlights a possible common origin during evolution of TNTs and PDs that can allow a better understanding of the newly discovered mammalian bridges by comparing them with the better-known PDs.

Interestingly, along the same line of thinking, recent findings of bacterial networks and parasite protrusions make us wonder how evolutionally conserved these kinds of intercellular communications can be. Indeed, *Dubey and Ben-Yehuda* (2011) have recently shown that *Bacillus subtilis* grown on a solid surface can establish nanotube-mediated networks with neighboring bacteria of the same or different species, as *Staphylococcus aureus* or *Escherichia coli*, pointing towards a common way of communication shared between more phylogenetically distant bacterial species. These linking structures, their mammalian or plant counterparts, facilitate transfer of cytoplasmic components and non-conjugative plasmids, allowing the exchange of hereditary traits for the acquisition of new features between connected bacteria.

Sometimes in nature similarities in structure do not reflect related functions. This could be the case of the cell-to-cell connections formed by the malaria pathogen during reproduction in the mosquito midgut (Rupp et al 2011). In this paper, the authors have described the presence of filamentous structures containing F-actin, that they called “filaments of gametes”, (FiGs), in the activated gametocytes. Multiple FiGs are generated on the surface of the cell within few minutes after activation and can extend up to 180  $\mu\text{m}$ . A closer look at these structures revealed that they possess closed-ends and they do not transfer material. Interestingly, FiGs exhibit adhesion molecules on their surface that can instead mediate contact and recognition with the right mating partners for the *Plasmodium*, allowing clustering of gametocytes and facilitating the process of reproduction.

This and the other examples of intercellular contacts established by different type of cells reported here reveal a high heterogeneity in both structure and functions of these fascinating new routes of communication that need a further characterization and classification.

This review will focus on mammalian tunneling nanotubes, their possible mechanism of formation and their various functions, giving particular attention to their implication in prion spreading.

## **Mechanisms of TNT formation and proteins involved**

In two-dimensional cultures, TNT-like structures were first discriminated from filopodia from their structural space. Contrary to filopodia, they formed long bridges between cells and were not attached to the substratum (Rustom et al., 2004). In addition to their spatial differences, TNTs and filopodia appear to serve different purposes. While filopodia act as important environmental sensors and play key roles in cell motility, the main role of TNTs appears to be as a direct conduit for cell-to-cell communication, specifically in the transport of material from one cell to another. As stated above, numerous membrane bridges have been described in a multitude of cell types. Even within TNT-like structures, it became quickly evident that these various structures were distinct from one another both in their structures and functions.

### *TNT formation and structural components*

TNT-like structures were first described in PC12 neuronal cells (Rustom et al., 2004). In these cells, de novo actin-driven formation of TNTs was observed. Further examination of PC12 cells and TNT formation suggested that while the majority of tubes formed via de novo formation, from directed filopodia-like protrusions, a small subset (7%) were also able to form after cells detached from one another (Bukoretshliev et al., 2009). In the mouse neuronal CAD cell line, we were also able to observe both types of TNT formation (Figure? Or data not shown?). However, the significance and the differences between these various structures remain unclear. Similar to other cell types, we observed a high degree of heterogeneity in the diameters of TNT-like structures (Gousset et al., 2009). Furthermore, as previously described in PC12 cells (Rustom et al., 2004), neuronal TNTs formed between CAD cells contained actin filaments but no microtubules, even in the tubes with much larger diameters (Gousset et al., 2009). The fact that most TNTs in neuronal cells arise from the extension of filopodia-like protrusions toward neighboring cells suggested that actin polymerization plays an important role in this type of TNT formation. Rustom and colleagues demonstrated that using the F-actin depolymerizing drug latrunculin, no TNTs were detected in PC12 treated cells (Rustom et al., 2004). This type of treatment could thus be used to selectively block TNT formation and look at the effect of the presence or absence of nanotubes in various cultures. In our lab, we took advantage of this treatment to highlight the importance of the presence of TNTs in the transfer of infectious prion aggregates in neuronal cells (Gousset et al., 2009). Using nanomolar concentrations of Cytochalasin D (CytoD), another actin-depolymerizing drug, Bukoretshliev and colleagues went further and examined the effects of this drug during the lifetime of TNTs (Bukoretshliev et al., 2009). They showed that as expected, low levels of CytoD abrogated both filopodia formation and TNT formation. Interestingly, they also demonstrated that once formed, CytoD had little effects neither on the stability of

these tubes and their ability to transfer material from one cell to another. Thus, most neuronal TNTs arise from filopodia-like structures, detached from the substratum. Once formed however, they are no longer sensitive to low levels of actin-depolymerizing drugs, demonstrating that functional TNTs are distinct from filopodia in both structure and function. Interestingly, recent experiments with primary rat astrocytes and neurons also showed actin to be the major cytoskeleton component of TNTs formed between these cells (Wang et al, 2010). In addition, they showed that treatment with latrunculin or CytoD abrogated their formation, thus further validating the use of neuronal cell lines as neuronal models.

TNT-like structures have also been described in immune cells, such as B-cells, Natural killer cells and macrophages (Onfelt et al., 2004). In macrophages, two types of nanotubes were also described (Onfelt, 2006). The thin nanotubes were found to contain actin filament only, whereas thicker nanotubes, with diameters larger than 0.7  $\mu\text{m}$ , contained both F-actin and microtubules. These different structures also had distinct functions, with the thicker structures being able to transport in a bi-directional manner vesicles and various organelles in a microtubule dependent mechanism. Similarly, long nanotube connections between Jurkat T-cells and primary T cells were also described (Sowinski et al., 2008). In these cells, F-actin but no microtubules were detected in TNTs. In addition, while these tubes were not open-ended, they still allowed for the transfer of HIV-1 via a receptor-dependent mechanism. Finally, numerous networks of TNT-like structures were observed between dendritic cells and THP-1 monocytes (Watkins and Salter, 2005). These connections varied greatly in length and diameter but were able to quickly transfer calcium fluxes and small dyes to interconnected cells.

Thus, while numerous TNT-like structures have been described in immune cells, these tubes are clearly distinct from one another both in their structural components as well as in their means of transfer. The one characteristic consistent for all types of immune cells is their formation, that appears to rely primarily on cell-to-cell attachment and formation of immunological synapses prior to cell separation and tube formation.

In Urothelial cell lines, two types of TNT-like structures were described (Veranic, 2008). The shorter but more dynamic structures, described as Type I nanotubes, were found to contain actin. These structures did not collapse after micromolar concentrations of CytoD. On another hand, the longer and more stable structures, or type II nanotubes, no longer had actin filaments and were composed instead of cytokeratin filaments. In these cells, the formation and function of these types of tubes were affected by the different cytoskeletal components.

These examples show the disparity in the various cytoskeleton requirements and formation mechanisms in naturally occurring TNT-like structures in neuronal, immunological or epithelial cells. The type of formation however (de novo actin-driven vs cell-to-cell contact) might arise from the nature and role that these cells play in vivo. Indeed, mobile cells, which can more easily come into contact with other cells, might be more prone to form tubes from a previous cell-to-cell contact, whereas more immobile cells might be more adept at creating and extending tubes de novo toward distant cells.

### *Signals and molecules involved in TNT formation*

In order to better understand the role that TNTs may play in intracellular transfer of materials, a better characterization of the initiation steps of TNT formation, the signals that guide the extension of these structures toward a neighboring cell and the mechanisms of binding and fusion need to be elucidated.

Recently, the effects of stress on TNT formation have been analyzed in different cell types (Wang et al, 2010; Yasuda et al., 2010; Yasuda et al., 2011).

In their studies, Wang and colleagues have shown that stress induced by hydrogen peroxide (H<sub>2</sub>O<sub>2</sub>) treatment led to an increase in TNT formation in both astrocyte and neurons. They also observed the transfer of various organelles, such as ER, Golgi, endosomes and mitochondria via TNTs in astrocytes cultures. For both astrocytes and neurons, it was always the cells undergoing stress that developed TNTs and transferred cellular materials in a uni-directional fashion to the non-activated cells. Thus, suggesting that TNT formation might be directly induced by stress.

Next, Wang and colleagues looked at potentially important signaling proteins involved in TNT formation. They found that p53 activation, which is critical in apoptosis, led to an increase in TNT formation independently of stress stimulation, and that down regulation of p53 blocked TNT formation. Subsequently, they determined EGF receptor up-regulation was also necessary for TNT initiation using different conditioned media and that the initiation of TNT formation was likely dependent on the initiating cells and not the receiving cell. Finally, since the EGF receptor can activate the Akt/PI3K/mTOR pathway, they used various mutants and inhibitors to selectively block or activate each protein and found that this pathway was indeed up regulated in H<sub>2</sub>O<sub>2</sub> activated cells leading to an increase in TNT development. In another study, looking at a macrophage cell line and HeLa cells, it was demonstrated that the interaction between m-Sec and the Ral/exocyst complex was also critical for TNT formation (Hase et al; 2009). Thus, to see if m-Sec might also be important for TNT formation in astrocytes, Wang and colleagues looked by RT-PCR at the levels of mSec in astrocytes and found a positive relationship between H<sub>2</sub>O<sub>2</sub> treatment and the levels of m-Sec expression (Wang et al, 2010). They concluded that m-Sec might be regulated by p53 activation. Thus, the authors suggest that the initiating cells control TNT formation in a p53 and Akt/PI3K/mTOR pathway activation-dependent manner, but they do not exclude that some guidance cues might be originating from the receptor cells.

Interestingly, in another study Yasuda and colleagues analyzed the transfer of mitotracker labeled vesicles via TNTs between endothelial progenitor cells (EPC) and human umbilical vein endothelial cells (HUVEC) (Yasuda et al., 2010). They observed both TNT formation between the two cell types and transfer of mitochondrial material from the EPC to the HUVEC. Upon treatment of the HUVEC with adriamycin, they observed a large increase in the transfer of mitotracker particles from the non-stressed EPC to the adriamycin-stressed HUVEC. In addition, the transfer was uni-directional since the reverse loading and transfer experiments were not significant. While it was not clear in these experiments which cell type initiated the formation of the nanotubes, contrary to

what was found in neuronal and astrocyte cultures (Wang et al, 2010), the transfer of material occurred from the non-stressed cells to the stressed cells. These experiments raised the question of how these cells initiated TNTs. Further characterization in these co-cultures could determine whether the stressed cells might release some signals that might attract filopodia-like protrusions from the EPC to the HUVEC or whether the HUVEC might initiate formation and allow for a reverse transfer of material from the receptor cell to the initiator cell. This is exactly what the authors next set out to demonstrate. Indeed, in a follow-up study, they looked more precisely at the TNT formation mechanisms between these cells (Yasuda et al., 2011). First the authors showed that co-cultures of EPC with collagen I (GC)-stressed HUVEC led to a rescue of HUVEC viability. However, when the EPC were pre-treated with nanomolar levels of CytoD to block TNT formation prior to co-culture with the HUVEC, the rescue effects were almost entirely abrogated, pointing toward the importance of TNT formation from EPC to HUVEC for cell survival. Using both fluorescence microscopy and FACS analyses they showed the existence of basal levels of transfer of lysosomes between the two cell types in a bi-directional manner under non-stressed conditions. However, the transfer was much more efficient as it increased in speed and frequency and was found preferentially between non-stressed EPC and GC-stressed HUVEC, suggesting that the stressed-cells were able to signal and guide filopodia-like protrusions for the formation of de novo TNTs to occur. Further examinations suggested that surface-exposed phosphatidylserines (PS) in HUVEC might be able to guide TNT formation from the EPC to the stressed- HUVEC. Indeed, when PS on HUVEC were blocked by binding of Annexin V, the selective TNT formation and transfer from EPC to HUVEC was also blocked.

Overall, these studies suggest that transfer of materials via TNTs in most cell types occurred from the cell type that initiated TNT formation to the receptor cell. However, while certain stress conditions might increase the formation of TNTs between cells, it doesn't affect all cells the same way. Indeed, while in astrocytes and neurons, stress appears to increase TNT formation in the stressed cells leading to an increase in transfer of material, in endothelial cells stress increase the guidance signals from the stressed cells leading to an increased formation of TNTs from the non-stressed cells. Thus, once more the analysis of these two studies brings forward the disparities that exist in formation and nature of TNTs between different cell types. It suggests that even within an identical type of TNT formation (i.e., de novo extension of filopodia-like protrusions) the mechanisms might be very distinct from one another (activation of attractive guidance signals versus activation of initiation of filopodia-like protrusions). However, these studies open up the doors for more general signaling pathways by pointing key elements critical for TNT formation. For example, the role of m-Sec, which was found to be important in macrophages, HeLa cells and astrocytes could be of general importance in TNT formation, independently of cell type. In addition, since filopodia-like protrusions are critical for TNT formation in neuronal cells (Bukoretshliev et al., 2009), our lab, has turned its attention to the role that the actin molecular motor protein, Myosin-X might play in both the formation of TNT-like structures and its function in transfer of materials in neuronal cells. We found that over-expression of Myosin -X increased the number of TNTs observed in our cell

cultures. In addition, similar to what Wang and colleagues have found with stress signals, we observed a uni-directional transfer of vesicles occurring from the cells over-expressing Myo-X to acceptor cells (data not shown).

In addition, the search for guidance signals and the role that lipids might play in TNT formation might also bring up a better consensus in TNT formation in general.

### *Mechanisms involved in open-endedness of TNTs*

As previously stated, in T cells no membrane continuity or transfer of cytosolic material were observed (Sowinski et al., 2008), suggesting different types of tubular structures between T-cells and other cell types that allowed for the transfer of cytosolic materials such as neuronal cells, astrocytes, myeloid cells or endothelial cells. Recently, however, Arkwright and colleagues have shown that specific stimulation could lead to an increase of TNTs in T-cells along with the transfer of cytosolic material (Arkwright et al., 2010). First, they showed that FAS activation resulted in an increase in TNT formation and that both toxin B of *Clostridium difficile* (an inhibitor of actin Rho-GTPases) and secramine A (an inhibitor of CDC42) specifically blocked FAS stimulated TNT formation in T cells. They also looked at the bi-directional exchange of labeled membranes in T-cells, co-cultures. As expected, they only found a negligible number of TNTs with both markers, whereas upon FAS stimulation they observed a 20-fold increase in the number of TNTs labeled with both membrane markers. The transfer of cytosolic materials, including fluorescent cytosolic proteins as well as labeled vesicles, was also observed upon FAS-stimulation between T cells. These experiments demonstrated that the nanotubular structures initiated by FAS-stimulation were different from the TNTs previously described in none activated T-cells (Sowinski et al., 2008). These connections were similar to the connections observed in other cell types and demonstrate the complexity and dynamism of the various TNT-like structures that have been described to date. While this study demonstrates that within the same cells, different activation can quickly lead to the formation of different types of TNTs with distinct functions; the mechanisms involved in the gating of these tubular structures remain undetermined. Overall, these recent studies on TNTs have shown the diversity of these structures but also their ability to transfer numerous signals upon specific activation.

### **TNT-mediated transfer: How to explain selective transfer between cells?**

Tunneling nanotubes have revealed a high degree of heterogeneity also from a functional point of view, as different components seems to be selectively transferred by different cell types.

First, further investigation is needed to understand why some cargoes are unidirectionally or bidirectionally transported. Uni-lateral transfer occurs in the case where a donor cell transfers material to an acceptor cell, whereas bi-lateral transfer happens when both cells mutually exchange materials. The reasons for these different transport mechanisms can depend on the structural components (actin-only vs actin+microtubules containing TNTs) or on specific signals that

stimulate nanotube formation and are responsible for directing the traffic in one or two ways.

As already mentioned above, bidirectional transfer is found when both actin and microtubules are present (He et al 2011; Arkwright et al 2010; He et al 2010; Onfelt et al 2006), while it appears to be unidirectional when TNTs contain actin only (Koyanagi et al 2005; Rustom et al 2004; Gurke et al 2008; Eugenin et al 2009; Domhan et al 2011; Gousset et al 2009). A recent work by Plotnikov and coworkers (2010) shows that unidirectional transfer from rat renal tubular cells (RTC) to bone marrow multipotent mesenchymal stromal cells (MMSC) was observed in this co-culture system. However, passage of molecules in the opposite direction was also detected, albeit at a lower rate. Additionally, it has been shown that lysosome exchange (Lysotracker-labelled) between endothelial progenitor cells (EPC) and endothelial cells (HUVEC) in co-cultures occurs at a basal level and that this transfer selectively increases in one direction, from EPC to HUVEC cells, upon injury of the latter (Yasuda et al 2010). These studies suggest that the shift from a bidirectional basal level of transfer between cells, to a selective uni-directional transfer towards a specific cell population takes place upon specific treatment, as is the case for differentiation signal flow towards MMSC cells (Plotnikov et al 2010) and stress deriving from damaged organelles (Yasuda et al 2010). What remains to be determined is how transfer occurs within TNTs and whether common molecular motors might be involved during this process.

### *Signal transfer*

Up to now several reports have shown that calcium signals could propagate between remote cells through tunneling nanotubes (ref). This is especially important for remote cells that are unable to propagate calcium-mediated signalling to cells in close proximity using gap junctions (Wang and Gerdes, 2011 *in press*). Initially, Watkins and Salter (2005) demonstrated that myeloid cells can respond to stimulation through soluble factors or mechanical stress and are able to amplify the cellular response by calcium signalling through membrane connections. Since then, propagation of calcium flux has been shown in many other cell types able to make connections between each other. More recently, the transfer of IP3 receptor (IP3R) and endoplasmic reticulum has been described along TNTs in SH-SY5Y neuroblastoma and HEK cell lines (Smith et al 2011). The authors made a comparison between the current produced at the end of a TNT (typically 30  $\mu\text{m}$  in length and 200 nm in diameter) and single inositol trisphosphate receptor (IP3R)-channel. While the first produces a current  $< 1\text{fA}$ , corresponding to calcium flux propagated from an activated cell, the opening of a single channel results in  $\sim 100\text{ fA}$ . Considering that a single opened IP3R-channel generally fails to induce  $\text{Ca}^{2+}$  signaling, the passive diffusion of  $\text{Ca}^{2+}$  within TNTs appears quite inefficient. However, since IP3R is able to transfer along TNTs, it could overcome the limit of passive diffusion of calcium by amplifying calcium signalling within a population.

Overall, calcium spreading through nanotubes appears to be a good option for different type of cells to quickly spread calcium signalization under physiological conditions, leading to fast responses in connected neighboring cells.

Particularly fascinating and newly discovered is the spreading of death

signals by nanotubes occurring in Jurkat and primary T cells (Arkwright et al 2010). Fas-mediated signalling is important for peripheral deletion of activated T lymphocytes (Green et al 2003). Mutations in the cytoplasmic domain of the Fas receptor are responsible for a rare genetic disease, the autoimmune lymphoproliferative syndrome (the type Ia ALPS) (Martin et al 1999; Rieux-Laucat et al 1999). As stated previously, Arkwright and coworkers have shown that stimulation of the Fas receptor leads to an increase in the number of TNT-connected cells and this is critically dependent on Rho GTPase activation. Accordingly, the authors also demonstrated that primary T-cells deriving from ALPS patients were not able to form networks of TNTs. This points towards a pivotal role of the Fas-mediated pathway in promoting TNT formation and transfer in T-cells. Additionally, transfer of both membrane (detected by CD59 and CD81 staining) and cytoplasmic components was detected in Fas-induced TNTs.

Interestingly, FasL and active caspase-3 passage from Fas-activated cells in neighboring non-activated ones was detected, thus resulting in the spreading of apoptosis through fratricide, highlighting that this might be an efficient way to shut down cellular responses (Arkwright et al 2010). Moreover, it has been reported that FasL is upregulated in cancer cells (ref) and this could confer a double advantage to these cells in 'counterattacking' against the immune system and stimulating their own proliferation (ref). In this light, tunneling nanotubes could act as conduits for diverse signals between tumor cells (for their own survival) and from tumor cells to immune cells (for death) leading to opposite effects.

Finally, Chauveau and colleagues (2010) have also recently shown that Natural Killer immune cells (NK cells) can easily form intercellular nanotubes, particularly upon activation. NK cells are important immune cells implicated in defense against a range of infections (ref). The authors have shown that human primary NK cells can connect with different cell types by intercellular bridges and use them to mediate cytotoxicity. They are able to help lyse remote target cells leading to cell death (Chauveau et al 2010).

### *Organelle transfer*

Tunneling nanotubes can be in certain cases be highways for diverse organelle transfer. Labelling with membrane-specific dyes, markers of the endo-lysosomal pathway, or other dyes specific to organelles such as mitochondria, has revealed sub-cellular organelles traveling between cells along these connections (put just a review). Mitochondria are essential for eukaryotic cells playing a role in a range of different functions (Spees et al 2005). A range of cell types, including T-cells, macrophages, NRK, stem cells, epithelial cells, myocardial cells have exhibited transfer of mitochondria (ref). Differentiation of embryonic epithelial progenitor cells (EPC) in myocyte-like phenotype was observed when EPC were co-cultured with neonatal rat cardiomyocytes suggesting that TNTs-mediated transfer of mitochondria could have a reprogramming function in these cells (Koyanagi et al 2005). Moreover, Spees and colleagues (2005) have reported the passage of mitochondria from adult non-hematopoietic stem cells (from human bone marrow hMSCs) or skin fibroblasts to A549  $\rho^0$  cells that were defective or deleted in mtDNA rescue

aerobic respiration. However, the authors could only hypothesize an involvement of tubular connections between the two cell types without demonstrating it. A closer look at some recent work involving the use of co-culture systems shows that TNT-mediated mitochondrial transfer could indeed rescue injured cells for pathological conditions (ref). For example, Cselenyak and coworkers (2010) set up a co-culture system of H9c2 cardiomyoblasts and mesenchymal stem cells (MSC) mimicking ischemic damage in H9c2 cells by using oxygen glucose deprivation (OGD). They were able to show passage of functionally active mitochondria (labelled with Mitotracker dye) in the damaged cells specifically when nanotubular connections between the cells were present. In addition, selective bi-directional transfer of mitochondria in between connected rat ventricular cardiomyocytes (CMs) and cardiofibroblasts (FBs) was observed in tubular structures (He et al 2011). These connections were enriched in actin and microtubules and allowed for the traffic of soluble cytosolic dyes as well, demonstrating continuity between the membranes. Interestingly, the authors could also support a physiological significance of the nanotubular structures found in CMs-FBs co-culture system *in vitro* by culturing mouse heart tissue slices. By labelling CMs and FBs with WGA and other specific markers, the authors were able to detect thin structures between the two cell types, reminiscent of the connections observed *in vitro* (He et al 2011).

A rescue function of TNT-mediated organelle transfer might be associated with other cell types that undergo injuries as well. Accordingly, cell-to-cell contacts established between renal tubular cells and MMSC along with the exchange of cytoplasmic and organelle components could be implicated in restoring functions of damaged cells following acute renal failure (Plotnikov et al 2010). Finally, endothelial cells presenting lysosomal dysfunction after exposure to AGE-modified collagen I (Yasuda et al 2010) were rescued by transferring normal lysosomal pool from endothelial progenitors to stressed cells (Yasuda et al 2011), supporting a role for organelle TNT-mediated transfer in restoring functions and tissue repair.

Smaller particles, named nanoparticles, have also been shown to travel within nanotubes (He et al 2010). Particularly, Streptavidin-coated CdSe/ZnS Quantum Dots (QDs) were transported along membrane nanotubes of rat cardiac myoblast cells (H9c2) at a speed compatible with movement of DiD-labelled vesicles associated with dynein/kinesin motors walking on microtubules (Onfelt et al 2006), thus suggesting that nanoparticles can be transported inside vesicles within these structures. In fact, when WGA was used to label membrane vesicles, QDs colocalized with it inside TNTs, confirming the vesicular transport of these molecules. Moreover, like thicker TNTs described in macrophages (Onfelt et al 2006) the nanotubes of H9c2 cells contained both actin and microtubules and allowed a bi-directional transfer of membrane vesicles (He et al 2010). Use of nanoparticles, such as QDs, is an emerging research field for diverse medical applications, such as therapies and diagnostics (Youns et al 2011). For example, these small compounds could be used to selectively delivery drugs to cancer cells or for other infectious diseases (Singh and Nalwa 2011). The fact that cells can establish membrane nanotubes together with the new finding that nanoparticles could pass from one cell to another by these means of communication open up new ways for diffusing small therapeutics inside target "cell communities".

## *Pathogen spreading*

Tunneling nanotubes could be either actively hijacked from different pathogens or transport them as “Trojan horses”, along the membrane or inside, leading to the spreading of infection. Hijacking of these structures can be preceded by induction of TNT formation, thus optimizing pathogen transfer, as has been shown for HIV particles spreading, both surfing on or inside TNTs in primary macrophages (Eugenin et al 2009). The HIV virus can use these highways to spread as an alternative to the other means already mentioned above.

Recently, a more detailed characterization of HIV-carriers mediating the transfer of the virus along TNTs bridging macrophages has been made (Kadiu et al 2011a). In this work, the authors first observed an increase in the number of connections in macrophages, as previously described (Sowinski et al 2008). They then identified the composition of TNTs by proteomic analysis following isolation from cell bodies. Interestingly they found several organelle markers including endo-lysosomal compartment (14%), ER (9%) and Golgi (4%) inside TNTs the majority of which were regulators of different steps within the HIV life cycle. They also demonstrated by confocal microscopy that 72% of Golgi and 32% of ER colocalize in TNTs with the viral protein Env; similar results were also obtained for the viral protein Gag, confirming a role for these intracellular compartments in HIV intracellular behavior (Kadiu et al 2011a). Indeed, Golgi and ER represent sorting stations for the virus prior to reaching endosomal vesicles and before spreading. Additionally, they observed that Golgi and ER undergo morphological changes upon HIV infection (Kadiu et al 2011a). Overall these observations shed light on a new role for the Golgi and ER in TNT-mediated transfer of diverse cellular components and their regulation mechanisms.

Additional investigations on the trafficking of HIV have shown that HIV specifically traffics in TNTs associated with endocytic compartments and so these organelles could be responsible for viral spread between macrophages (Kadiu et al 2011b). Moreover, the acto-myosin machinery used by the cell to move virus-containing cargoes within TNTs is 25 times faster than the surfing process seen for HIV and other retroviruses on filopodial protrusions (Sherer et al 2007). In particular, HIV preferentially associates in TNTs with recycling endosomes and MVB (Kadiu et al 2011b). Whether viral particles spreading in vesicles through bridging conduits results in a productive infection of a recipient cell and how the flow of these carriers is regulated and intersects with the intracellular pathway remain to be investigated. Comparing intra- and inter-cellular trafficking with our current knowledge in the HIV field could improve our understanding and help in characterizing intercellular spreading of other pathogens that manipulate host intracellular components for their own survival, leading to progressive loss of cellular identity.

One of the best known mechanisms of cell-to-cell spread, common in some pathogenic bacteria such as *Listeria*, *Shigella* and *Salmonella*, is their ability to polymerize the host actin cytoskeleton to escape the host and keep infecting new targeted cells (ref). While little was known about other atypical cytoplasmic bacteria spreading, recently, new “unusual” ways of bacterial spreading have been observed. For example, it has recently been shown that *Cryptococcus*

*neoformans* is able to laterally transfer from an infected macrophage to an uninfected one allowing a latent persistency in the host for long periods before causing meningoencephalitis in the central nervous system (Ma et al 2007). The authors observed an actin-dependent transfer of the bacterium in both immortalized cell lines and human primary macrophages by a mechanism not yet understood. More recently, it has been reported that the obligate intracellular bacterium *Ehrlichia chaffeensis* associates with filopodia of infected DH82 monocytes and increases their numbers and lengths (Thomas et al 2010). The authors hypothesized that the transport of *Ehrlichia* through filopodia could be a potential mechanism for the pathogen to pass from one cell to another without contacting the extracellular environment. Another unusual way of spreading recently highlighted by Hagerdon *et al.* (2009) is the formation of an actin barrel, the “ejectosome”, induced by *Mycobacterium marinum* and used by it to pass within infected *Dictyostelium discoideum* amoeba as host. This mechanism is an alternative to the formation of a protrusion containing the pathogen created by actin polymerization that is then engulfed by adjacent cells (Carlsson and Brown 2009).

Onfelt and colleagues (2006) have shown that *M. bovis* BCG or clusters of several bacteria can surf on thin membrane nanotubes between macrophages before being internalized by receptor-mediated endocytosis, pointing towards a possible role of these structures in bacterial infection by concentrating the pathogen on the entry site for a more efficient invasion.

Additionally, one could also envisage a role for these newly discovered highways in the spreading of some obligatory intracellular bacteria, unable to surf along TNTs membranes that could use them to escape from the immune response. As already mentioned above, different sub-cellular organelles are found to shuttle in between cells by TNTs. Bacteria can use different endocytic compartments and modulate them to escape lysosomal degradation (ref). In particular, vacuoles-containing bacteria deriving from fusion of the pathogen with intracellular organelles were found to be positive for several endosomal proteins (ref). A problem for nanotubes in transporting these bigger cargoes along their tracks could be overcome by the presence of expansions along the tunnel, known as gondolas (Hurtig et al 2010). Veranic *et al.* (2008) have shown that these dilatations of the membrane can move for 5 to 15  $\mu\text{m}$  with an average speed of 40 nm/s. This “pearling” phenomenon seen along some TNT structures is probably due to the redistribution of lipids and cytoskeleton components localized in discrete areas and could be compatible with a vesicular transport of pathogen as well.

### **Prion spreading and other neurodegenerative diseases**

The mechanisms of prion spreading from the periphery to the central nervous system (CNS), and subsequently within the CNS, remain questionable. A number of mechanisms, such as cell-to-cell contact, exosomes and GPI-painting, have been proposed (Kanu et al., 2002; Fevrier et al., 2004; and Baron et al., 2006). We have recently demonstrated the presence of TNTs in neuronal CAD cell cultures (Gousset et al., 2009). In addition, we showed that these TNTs were able to transfer lysosomal organelles, the cellular GPI-anchor prion protein PrP<sup>C</sup>, as well as fluorescently labeled infectious prion particles, PrP<sup>Sc</sup>. Using various

co-culture conditions, we showed that these infectious particles were efficiently transferred to non-infected cells only in the presence of TNTs.

Since the prion protein is a GPI-anchored protein, it has the possibility of traveling via TNTs either at the surface or within vesicular structures. We have recently further analyzed the presence of PrP<sup>Sc</sup> and various organelles inside TNTs. Overall, we found that similar to what can be found in the cell body, PrP<sup>Sc</sup> can travel in TNTs in early endosomes and lysosomes but it is preferentially enriched in recycling compartments (Figure ? or data not shown?). Additionally, increasing the number of TNTs formed, by over-expression of Myosin-X, can increase the spreading of PrP<sup>Sc</sup> to non-infected cells. These data further demonstrate how efficient these structures are in allowing the passage of infectious prions from one cell to another.

Finally, we have also demonstrated that the transfer via TNTs of infectious prion particles resulted in the transfer of infectivity to the recipient cell. This transfer was not confined to neuronal co-cultures but was also efficiently transferred between loaded Bone-Marrow dendritic cells and primary neurons (Gousset et al., 2009; Langevin et al., 2010). Thus, our studies suggested that TNTs might play a critical role *in vivo* in the spreading of prions within the central nervous system (CNS) and at the periphery.

*In vivo*, the players involved in the spreading of prions from the gastrointestinal tract, to the lymphoid system and to the peripheral nervous system (PNS) are still unclear. Dendritic cells could bring infectious prion particles from the gut to Follicular dendritic cells, and subsequently pick up prions particles from FDCs and deliver them to the PNS. Thus, analyzing the interactions between these two cell types might reveal important clues about prion spreading in general. We have started to address these issues. By co-culturing DCs and FDC cell lines (Nishikawa et al., 2006), we were able to detect formation of TNT-like structures between the two-cell types. In addition, preliminary experiments by flow-cytometry suggested that loaded DCs were able to transfer labeled vesicles to FDCs in a manner consistent with transfer via TNTs (data not shown).

Overall, our studies suggest that TNTs might play a pivotal role in the spreading of prion diseases. Like prion diseases, neurodegenerative diseases such as Alzheimer, Parkinson and Huntington appear as the result of protein misfolding and aggregation, it is tempting to wonder whether these diseases might share some common spreading mechanisms. Recently, Wang and colleagues have analyzed whether intracellular A $\beta$  particles could spread through TNTs in astrocytes and neurons (Wang et al, 2010). Microinjection experiments demonstrated that intracellular A $\beta$ -fusion proteins were indeed able to quickly spread from cell-to-cell via TNTs. In addition, they looked at the transfer of A $\beta$  toxicity in co-cultures of infected astrocytes and neurons. They showed that increasing the number of TNTs between the cells by H2O2 treatment led to an increase in neuronal cell death in co-cultures with infected astrocytes compared to the control GFP or non-stressed cells. Thus suggesting that A $\beta$  particle spreading via TNTs within the cultures resulted in an increase in neuronal toxicity leading to cell death. Such observations are very similar to what we found with PrP<sup>Sc</sup> and infectivity and suggest that prion diseases and other neurological diseases might use TNTs as a spreading mechanism. If these types of studies can be further extended to Parkinson or Huntington, they might

open up new ways of looking at these diseases and could lead to new strategies to fight them.

### **Concluding remarks**

Since their discovery in 2004, an enormous amount of work has been done on the characterization of tunneling nanotubes in a multitude of cell types. Here, we have reviewed recent studies to look at the advances that have been made more specifically with respect to TNT formation, the role of specific molecules and signaling pathways, as well as their different physiological roles in the spreading of various molecules, signals and pathogens.

What has become evident from these studies is that long distance intercellular connections between cells are not artifacts, as they were first perceived. Indeed, they have become common features found in most cell types examined. Although discovered only recently, TNT-like structures are becoming more and more a part of mainstream cell biology. The biggest hurdle however, might be the enormous heterogeneity that exists within these structures. This is in part due to their high dynamicity. Indeed, TNTs can form quickly and have short lifetimes. They can be induced by different signals leading to different transport mechanisms. Thus, as more molecules and signaling pathways are being described as important players in both TNT formation and/or function, it will be necessary to determine whether a general mechanism might exist for most cell types or whether each cell system might have evolved its own set of mechanisms for TNT formation, stability and function. However, because of the disparity in the requirements of specific cytoskeleton components or specific proteins, more attention might have to be put on the role of specific lipids or lipid pathways. Indeed, while most naturally occurring nanotubes required some type of cytoskeleton components, artificially made nanotubes can be pulled from synthetic vesicles. Thus, the lipid environments and their subsequent interactions with specific proteins might bridge some of the differences observed between each cell type. For example, the determination that PI3K might play a role in TNT formation suggests that phosphoinositides such as PIP2 and PIP3 might play important roles. It might become necessary to look at more biophysical ways and work done with model membranes to determine the role that certain lipids might play in the membrane flexibility and ability to curve. We might need to analyze whether common membrane domains enriched in specific lipids and proteins might bring important components at the base and within TNTs for both formation and transfer.